THEORY

UNIFIED DISPERSION MODEL

DATE: December 2023

The Unified Dispersion Model (UDM) models jet, dense, buoyant and passive dispersion including droplet rainout and re-evaporation. The model allows for continuous, instantaneous, constant finite-duration, and general time-varying releases.

Reference to part of this report which may lead to misinterpretation is not permissible.

No.	Date	Reason for Issue	Prepared by	Verified by	Approved by
1	1999	PHAST 6.0	Witlox	Holt, Fanneløp, Webber, Woodward, Selmer-Olsen	
2	Jan 2006	SAFETI 6.5	Witlox	Harper	
3	Nov 2009	Phast (Risk) 6.6	Harper		
4	June 2011	Phast (Risk) 6.7	Harper & Witlox	Witlox & Harper	
5	August 2016	UDM AWD 8.0	Witlox	Harper	
6	Sep 2017	Phast 8.0	Witlox	Harper	
7	Sep 2018	Safeti-NL 8.12	Harper	Witlox	
8	May 2019	Safeti 8.21	Harper	Fernandez	
9	Oct 2021	Safeti 8.6	Harper	Hart	
10	June 2023	Added gas blanket modelling	Harper		

Date: December 2023

Prepared by: Digital Solutions at DNV

© DNV AS. All rights reserved

This publication or parts thereof may not be reproduced or transmitted in any form or by any means, including copying or recording, without the prior written consent of DNV AS.

ABSTRACT

This report describes the theory of the Unified Dispersion Model (UDM) implemented into the consequence modelling package Phast and the risk analysis package Phast Risk. The UDM models the dispersion following a ground-level or elevated two-phase pressurised release. It effectively consists of the following linked modules:

- jet dispersion
- droplet evaporation and rainout, touchdown
- pool spread and vaporisation
- heavy gas dispersion
- passive dispersion

These modules are linked in the UDM in such a way as to eliminate first-order discontinuities in cloud properties as transitions are made between models. This is achieved by using a single form of concentration profile to cover all stages of a release. This profile is extremely flexible and allows for anything from a sharp-edged profile in the initial stages of a jet release through to the diffuse Gaussian profile that would be expected in the final passive stage of spreading.

The UDM also includes the effects of droplet vaporisation using a more realistic non-equilibrium model. Rainout produces a pool which spreads and vaporises. Vapour is added back into the plume and allowance is made for this additional vapour flow to vary with time. In addition to the non-equilibrium droplet thermodynamics model, UDM also allows for an equilibrium model. This equilibrium model includes special treatment for releases of pure CO_2 (including modelling of solid CO_2 effects) and pure HF (including effects of polymerisation).

The UDM allows for variation in wind speed, air temperature, air pressure and atmospheric density with height above the ground by incorporating various vertical profiles for these variables.

Another feature of the UDM is possible plume lift-off, where a grounded cloud becomes buoyant and rises into the air. Rising clouds may be constrained to the mixing layer if it is reached.

The UDM allows for continuous, instantaneous and constant finite-duration releases. In addition the UDM model allows for general time-varying releases, enabling, for example effective modelling of a leak as blow-down proceeds.

UDM model coefficients have been obtained directly from established data in the literature (based on experiments), rather than doing UDM simulations and fitting the UDM results to the experimental data.

Table of contents

ABSTRACT I

1. INTRODUCTION 1

2. OVERVIEW OF UDM MODEL 3
2.1 UDM source-term input data (discharge or pool data) 3
2.2 Dispersion formulation (stages, thermodynamics, equations) 4
2.3 Dispersion models for range of scenarios 5
2.3.1 Steady-state release without rainout 5
2.3.2 Instantaneous release without rainout 5
2.3.3 Finite-duration release (no rainout) 6
2.3.4 Time-varying dispersion (time-varying release, rainout, or dispersion from pool) 6

3. UDM MODEL FOR STEADY-STATE OR UNPRESSURISED INSTANTANEOUS RELEASE (NO RAINOUT) 11
3.1 Similarity concentration profile; cloud geometry 11
3.1.1 Steady-state release 11
3.1.2 Instantaneous release 15
3.2 Dispersion variables and equations 19
3.3 Phases in cloud dispersion; transitions 25
3.4 Air entrainment 28
3.4.1 Jet entrainment 28
3.4.2 Cross-wind entrainment 30
3.4.3 Near-field passive entrainment 31
3.4.4 Heavy-gas entrainment 32
3.4.5 Far-field passive entrainment 34
3.5 Momentum equations 37
3.5.1 Airborne drag 38
3.5.2 Ground impact force 39
3.5.3 Ground drag 40
3.6 Cross-wind spreading 42
3.6.1 Jet spreading 42
3.6.2 Heavy-gas spreading 42
3.6.3 Passive spreading 43
3.6.4 Transition to passive 44
3.7 Averaging-time effects 46
3.7.1 Averaging time effect because of wind meander 46
3.7.2 Averaging time effect because of time-varying release rate 47

4. UDM DISPERSION MODEL FOR FINITE-DURATION RELEASE (NO RAINOUT) 48
4.1 Quasi-instantaneous model 48
4.2 Finite-duration correction 51

5. UDM DISPERSION MODEL FOR TIME-VARYING RELEASE (RAINOUT AND POOLS) 55
5.1 Introduction 55
5.2 Overall algorithm 57
5.2.1 Phast source-term calculations (prior to UDM calculations) 57
5.2.2 Release observers: set observer release location and observer release times 57
5.2.3 UDM calculations for each observer 57
5.2.4 Mass Conservation and Correction 58
5.2.5 Gas blanket modelling for buried pipelines 63
5.2.6 Inclusion of effects of along-wind diffusion 64
5.3 Details of observer dispersion calculations 66
5.3.1 Two-phase release: UDM observer primary variables 66
5.3.2 Detailed algorithm and two-phase dispersion equations 67

6. UDM DISPERSION MODEL FOR PRESSURISED INSTANTANEOUS TWO-PHASE RELEASE 79
6.1 New INEX model 79
6.2 Old INEX model 81
6.2.1 Experimental basis for model 81
6.2.2 Theoretical basis of model 81
6.3 The purple book method 84

7. UDM MODEL COEFFICIENTS 85

8. FUTURE DEVELOPMENTS 87

APPENDICES 88
Appendix A. Evaluation of ambient data 88
A.1 Atmospheric Profiles 88
A.2 Vertical wind profiles 89
A.3 Temperature 91
A.4 Pressure 92
A.5 Other Atmospheric Variables 93
Appendix B. Literature review of entrainment formulations 94
B.1 Entrainment Formulations 94
Ooms formulation for elevated plumes (Gaussian profile, airborne drag) 94
TECJET formulation for elevated plumes (Gaussian profile, airborne drag 95
HMP formulation for airborne plume (top-hat profile, no airborne drag) 95
AEROPLUME formulation for airborne plume (top-hat profile, no airborne drag) 95
Morton (crosswind extended) 97
Appendix C. Observer release times 100
C.1 Time-varying release without rainout 100
C.2 Liquid spill (immediate rainout) 101
C.3 Elevated release with rainout 102
C.4 Instantaneous release without or with rainout 102
Appendix D. Cloud shape correction for downwind gravity spreading 104
D.1 Global cloud formulation (not implemented) 104
D.2 Incremental cloud formulation (implemented in UDM) 105
Appendix E. Differential observer-velocity cloud mass correction 107
E.1 Time shifting for approaching observers 107
E.2 Rigorous correction to observer variables stepping forward in time (not implemented) 108
Appendix F. Guidance on input and output for UDM dispersion model 109
F.1 Input data 109
F.2 Model run and output data 127
F.3 Detailed information on UDM errors and warnings 132
Appendix G. SUNDIALS Differential-Algebraic Solver Licensing 134

FIGURES 135

NOMENCLATURE 150

REFERENCES 154

Table of figures

Figure 1. Droplet evaporation and rainout 1
Figure 2. UDM time-varying dispersion – observer method including AWD 6
Figure 3. UDM dispersion stages for time-varying release with rainout 10
Figure 4. Ground impact force acting on impinging cloud 39
Figure 5. UDM FDC correction for finite-duration releases 51
Figure 6. UDM time-varying dispersion – old multi-segment method excluding along-wind diffusion 55
Figure 7. Cloud mass correction: conserve mass (area under material rate curve) 60
Figure 8. UDM dispersion stages for instantaneous release with rainout 65
Figure 9. Vapour pick-up from pool while observer is moving over the pool 73
Figure 10. INEX dispersion phases for two-phase instantaneous release 80
Figure 11. Evaluation of 'release observer' data based on equal-mass release segments 100
Figure 12. Evaluation of 'pool observer' data based on equal-mass pool segments 101
Figure 13. UDM modelling of crosswind and along-wind gravity spreading 104
Figure 14. Cloud-shape gravity correction: conserve cloud area 104
Figure 15. Cloud-shape gravity correction: conserve observer interval cloud area 105
Figure 16. Observer time-shifting prior to Observer Mass Correction 107
Figure 17. UDM input data - Part I: input data always to be specified 109
Figure 18. UDM input data - Part II: input parameters 126
Figure 19. UDM output data 127
Figure 20. UDM plume geometry for continuous release (notation, stages of dispersion) 135
Figure 21. UDM cloud geometry for instantaneous release (notation, stages of dispersion) 136
Figure 22. Steady-state source 137
Figure 23. Instantaneous source 137
Figure 24 UDM models for finite-duration release 138
Figure 25. Vertical and horizontal concentration profiles 139
Figure 26. Correlation for the exponent m used in the horizontal profile 140
Figure 27. Correlation for the exponent n used in the vertical profile 141
Figure 28. Cloud profile during touching down 142
Figure 29. Phases in UDM cloud dispersion for range of scenarios 144
Figure 30. Normalised entrainment velocities 145
Figure 31. The development of a quasi-instantaneous release 146
Figure 32. Finite-duration source 147
Figure 33. Monin-Obukhov length 148
Figure 34. Wind power-law exponent 149

List of tables

Table 1. UDM time-averaging and post-processing options for range of scenarios 10
Table 2. List of primary plume variables (no rainout) 19
Table 3. Phases during cloud dispersion (continuous and instantaneous releases) 27
Table 4. List of UDM primary plume variables (including rainout) 67
Table 5. Purple book correlation for liquid fraction after energetic expansion phase 84
Table 6. UDM model coefficients 86
Table 7. Atmospheric temperature profile: variables α (K/m) and H_o (W/m^2) 91
Table 8. Comparison of integral plume models 98
Table 9. Selection of stability class 113
Table 10. Recommended values for surface roughness 117

1. INTRODUCTION

A greater hazard is generally posed by accidental discharges of toxic or flammable materials as pressurised liquids than as gases or vapours. This is because pressurised liquids tend to form an aerosol cloud which has considerably greater density and thus source strength than vapour or gas clouds. It is important to be able to predict the mass fraction of liquid which evaporates or remains suspended as aerosol droplets, or, conversely, the fraction which rains out. The rained out fraction will form a pool on the ground or on water and subsequently re-evaporate or partially dissolve in the water. Rainout generally results in weakening the original cloud but extending the duration of the hazardous event because of evaporation of the rained out liquid.

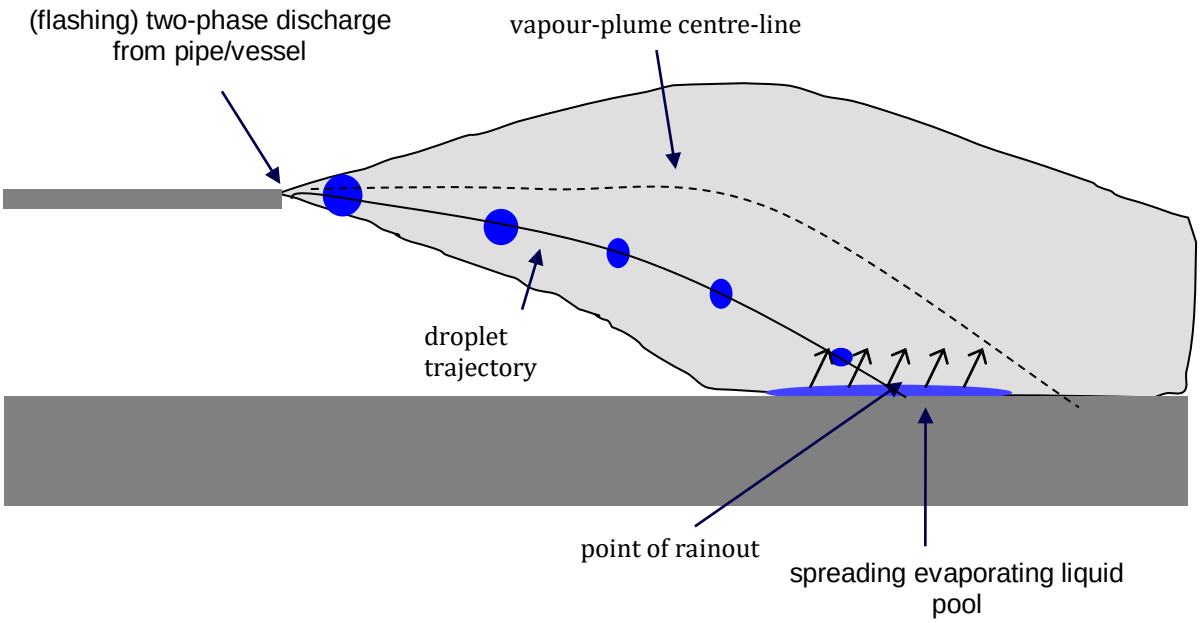

Figure 1. **Droplet evaporation and rainout**
After elevated two-phase discharge, evaporating droplets move away from the plume centre-line. If droplets reach the substrate, complete rainout is assumes to occur leading to the formation of a spreading liquid pool which provides a secondary source of vapour.

An integrated model must predict the following (see Figure 1):

- discharge data: release rate, aerosol flash fraction and Sauter mean drop diameter
- jet dispersion: air entrainment, vapour plume centre-line (particularly to touchdown)
- thermodynamics: droplet evaporation, droplet trajectories, rainout
- pool data: spreading, evaporation,
- heavy gas dispersion: air entrainment, gravity spreading
- possible plume lift-off
- passive dispersion

This report describes a model that integrates the above prediction modules, called the Unified Dispersion Model (UDM). The current version of the UDM (Version 3) as included in Phast and Safeti supersedes earlier versions

In experiments sponsored by the Center for Chemical Process Safety (CCPS) of the American Institute of Chemical Engineers (AIChE), measurements were made of the fraction of liquid captured after rainout from aerosol discharges.[1] The UDM uses a drop size correlation adjusted to match UDM rainout predictions to the CCPS test data. There are a number of other correlations required by the UDM for predicting such variables as the heat and mass transfer coefficients to the evaporating drops and the drag on the drops which affects their trajectories. Each of these correlations are established standards from the chemical engineering technical literature.

The original version of the UDM is described by papers by Cook and Woodward, i.e. papers on the droplet thermodynamics model[2,3], papers presenting an overview of the model[4,5,6,7]. The current version described here represents a significant revision and extension for all parts of the model. This has been carried out in conjunction with a detailed literature review, verification and validation of the model. A joint industry project was carried out to further refine the droplet size correlation (resulting in a 'modified CPSS' correlation) and to validate initial droplet

size and rainout against an extensive set of experimental data[8]. A new numerical UDM solver was developed to solve accurately and more rigorously a single set of droplet and plume-dispersion variables using a differential-algebraic solver from the Sundials suite[10] (see Appendix G).

The reader is referred to separate documentation[9] for details on

- the discharge calculations and droplet size correlations (which do not form part of the UDM model)
- the adopted thermodynamics model THRM and droplet equations
- the pool spread/evaporation model PVAP,

The plan of this report is as follows:

- In Section 2 a brief overview of the overall UDM model is given.
- In Section 3 the dispersion model for a continuous release or instantaneous unpressurised release is described. First the concentration similarity profile is given. Subsequently the unknown dispersion variables are listed and the governing equations are described. The mechanisms for entrainment and cloud spreading are given for the subsequent phases of jet dispersion, heavy-gas dispersion, and passive dispersion.
- Section 4 discusses the dispersion model for a finite-duration release with a constant release rate. This model accounts for effects of along-wind-diffusion (passive air entrainment at upwind and downwind edges of the cloud) reducing the cloud concentration. Two models are considered, i.e. the Quasi-Instantaneous (QI) model and the Finite-Duration Correction (FDC) model.
- In Section 5 the new model for time-dependent dispersion is discussed, whereby the time-dependency of the dispersion results from either pool evaporation or a time-dependent release. The several scenarios of rainout and evaporation are discussed, and the coupling between the dispersion model and the pool-evaporation model is described. Previously modelling of time-dependent dispersion was carried out using multi-segment logic, which excluded effects of along-wind-diffusion resulting in too narrow clouds with too high concentrations. In the new model effects of along-wind diffusion are included using the so-called ‘observer’ concept.
- In Section 6 the model for pressurised instantaneous releases is described.
- In Section 7 it is shown how the model coefficients are determined from experimental data.
- Section 8 finally contains a list of proposed future developments.

2. OVERVIEW OF UDM MODEL

The UDM model is designed for use in consequence and risk studies. Following the flashing for a two-phase pressurised release, it calculates the dispersion in the downwind direction (all phases between near-field and far-field dispersion) including possible touchdown, rainout (and subsequent pool formation and re-evaporation). It is applicable for toxic and flammable releases. Following touchdown, it assumes dispersion over flat terrain with uniform surface roughness.

The UDM includes possible plume lift-off, where a grounded cloud becomes buoyant and rises into the air. Rising clouds may be constrained to the mixing layer if required. The UDM allows for continuous, instantaneous, constant finite-duration, and general time-varying releases. For low wind-speed releases, effects of downwind gravity spreading effects are taken into account. For time-varying releases effects of downwind diffusion can be taken into account. In case of multi-component dispersion, the model currently adopts pseudo-component properties. In case rainout does not need to be modelled, the model also allows alternative more rigorous multi-component modelling.

The UDM assumes constant ambient conditions with the ambient wind speed, pressure and temperature being a function of height. Thus profiles are assumed for these variables as function of the vertical height (see Appendix A).

Figure 21 (steady-state dispersion) and Figure 22 (instantaneous dispersion) show the movement of the cloud in the downwind direction. The Cartesian co-ordinates x, y, z correspond to the downwind, cross-wind (lateral horizontal) and vertical directions, respectively; x=0 corresponds to the point of release, y = 0 to the plume centre-line and z = 0 to ground-level. In addition to these Cartesian co-ordinates use is made of the 'cloud' co-ordinates s and ζ. Here s is the arc length measured along the plume centre, with s=0 corresponding to the point of release.

In case of steady-state dispersion, the co-ordinate ζ indicates the direction perpendicular to the plume centre-line and perpendicular to the y-direction. The angle between the plume centre-line and the horizontal is denoted by $\theta = \theta(s)$, and the vertical plume height above the ground by $z_{cld} = z_{cld}(s)$. Thus z and ζ are related to each other by $z = z_{cld} + \zeta \cos(\theta)$.

In case of instantaneous dispersion, the co-ordinate ζ indicates the vertical distance above the plume centre-line and perpendicular to the y-direction. The angle between the plume centre-line and the horizontal is denoted by θ, and the vertical plume height above the ground by z_{cld}. Thus z and ζ are related to each other by $z = z_{cld} + \zeta$.

2.1 UDM source-term input data (discharge or pool data)

The pressurised release of the pollutant is at x=0, y=0, s=0 and at a release height $z = z_R$ (m). The release direction is in the plane y=0. For a continuous release, the model allows for an arbitrary release angle θ_R with the horizontal ($-90^o \leq \theta_R \leq 90^o$)[i]. The discharge data provided as input to the UDM model may be derived from a discharge model. The discharge parameters are as follows:

- release height z_R (m),
- thermodynamics data: release temperature (single phase) or liquid mass fraction (two-phase), initial drop size
- other data:
  - for instantaneous release: mass of released pollutant (kg), expansion energy (J)
  - for continuous release: release angle θ_R (^{o})[ii], rate of released pollutant (kg/s), release velocity (m/s), release duration (s)[iii]

As an alternative to the standard discharge models, time-varying source term data input to the UDM may be obtained from the pool model (see the PVAP theory document for full details[9]). In this case the rate of released pollutant (kg/s), release velocity (m/s), release temperature (vapour phase) and release duration (s) are all calculated by the pool model. In addition it is assumed that the release height $z_R = 0$ m (ground level).

[i] UDM (PHAST) also allows for a vertical downward jet impinging onto the ground. However the model for this is oversimplified and results should therefore treated with care. The UDM model is not valid for upwind releases. It is valid for downward releases, as long as the jet does 'gently' touch the ground. Turbulent air entrainment into the jet resulting from the jet impinging on the ground is not included, and therefore the model may not be valid if the jet hits the ground with a strong impact.

[ii] The angle is capped at +/- 89^o. Angles approaching 90 can generate instabilities in the solution or post-processing that can reduce performance or cause failures.

[iii] For continuous releases (i.e. not time-varying or instantaneous) the UDM imposes a minimum release duration of 1 second and gives a warning (UDM3 1135). This is to prevent mass conservation difficulties caused by observers moving relative to each other.

2.2 Dispersion formulation (stages, thermodynamics, equations)

Cloud movement, touchdown and lift-off; jet, heavy-gas and passive dispersion

Following the discharge, an elevated, heavy vapour/aerosol release is modelled as a circular cross section which tends to flatten into an ellipse as the cloud settles (see Figure 21 and Figure 22). Upon touching down momentum is conserved, and the cross section becomes a truncated ellipse; the cloud levels off as the vertical component of momentum is converted into downwind and cross-wind momentum. The cloud cross sectional ellipse remains truncated until the bottom edge of the ellipse rises above the ground. The plume may become buoyant and lift off and rise until constrained by the mixing layer.

The UDM provides a smooth model of touchdown and lift-off, and concentration profiles which become more diffuse farther downwind. In the near-field the jet speed is significantly larger than the ambient speed, and the major mechanism for cloud dilution is jet entrainment. The centreline velocity decays until either the heavy gas or the passive dispersion mechanisms become dominant. For a low-momentum release, the jet dispersion mode may never be dominant.

Droplet evaporation, rainout, and pool spreading/evaporation

A module for modelling droplet evaporation for an aerosol jet combined with entrainment and plume trajectory prediction has been used; see Figure 1. This model uses non-equilibrium heat and mass transfer correlations, and typically the liquid temperature decreases below the vapour temperature. Since evaporation then takes place at a lower vapour pressure, larger mass fractions rain out than are predicted by models which assume that thermal equilibrium is achieved with entrained air.

The progress of the drops is modelled and rainout occurs when the drops hit the ground or the bund wall. The location of the rainout is used to determine if the pool will be inside or outside the bund. Rainout produces a pool which spreads and vaporises. The rained out liquid is then modelled as a spreading, circular pool until it reaches both bund walls (if relevant), or until it reaches a steady-state pool size at the minimum pool thickness for which the rate of evaporation and dissolution matches the rate of inflow of mass to the pool. The vapour from the pool is added back to the plume, as a function of time.

Heat and water-vapour transfer from substrate

Following touchdown, heat transfer between the cloud and the substrate is taken into account. In case of dispersion over water, also water–vapour transfer from the substrate is taken into account.

Dispersion variables and solution to dispersion equations

The mathematical dispersion model is expressed in terms of differential and algebraic equations for the droplets and the plume. The droplet equations describe the droplet trajectories, droplet evaporation and droplet energy balance. The major basic plume dispersion variables can be considered to be the mass of wet air added to the cloud, the plume position, the plume momentum, the plume temperature, heat and water-vapour added from the substrate, and plume cross-wind radius. These variables are determined by imposing conservation of mass (entrainment of air into the cloud), conservation of momentum, the relation between cloud speed and cloud position, conservation of energy, substrate heat and water-vapour transfer relations, and cross-wind spreading equation.

The droplet and cloud differential and algebraic equations are solved simultaneously as a single linked set of equations using a differential-algebraic solver from the Sundials suite10, which provides an accurate and robust solution.

Downwind gravity spreading correction

The above differential equations do not account for downwind gravity spreading in case of a non-instantaneous release. This may be significant during the heavy-gas regime in case the plume crosswind gravity-spreading velocity is sufficiently large relative to the downwind plume velocity. Therefore in the latter case, the cloud width is reduced and the cloud downwind incremental length increased such that the downwind gravity spreading equals the crosswind gravity spreading; see Appendix D for details.

2.3 Dispersion models for range of scenarios

This section outlines the UDM methodology in case of steady-state releases, instantaneous releases, quasi-instantaneous releases, and time-varying releases.

2.3.1 Steady-state release without rainout

This model evaluates the dispersion variables as a function of downwind distance x. The basic variables are

- air mass flow (passing through vertical plane at x) added to the cloud (kg/s)
- excess horizontal and vertical momentum (kg m/s^2)
- downwind horizontal and vertical position (m)
- heat added from the substrate (J/s)
- water vapour added from the substrate (kg/s)
- cloud width (m)

which are determined by solving a set of ordinary differential equations forward in the downwind direction (starting from a jet release). These equations express air entrainment into the cloud, conservation of momentum, relation between cloud speed and cloud position, a substrate heat-transfer relation, a substrate water-vapour transfer relation, and a cross-wind spreading equation. The vapour temperature of the cloud is set in the UDM thermodynamics module by imposing conservation of cloud enthalpy.

The droplet data are determined from the thermodynamics model. The droplet variables are the mass, speed, position, and temperature. These variables are found by solving equations expressing droplet evaporation rate, conservation of droplet momentum, relation between droplet speed and position, and conservation of droplet energy.

The concentration c is given by a similarity profile c = c(x,y,ζ), with exponential decay in y, ζ described by means of cross-wind and vertical dispersion coefficients σ_y, σ_z, and with near-field top-hat profile (e.g. sharp-edge jet) developing into a Gaussian profile in the far field. The cloud area is obtained by integration over y, ζ.

Figure 23 displays the centre-line ground-level concentration and cloud width as function of downwind distance (case of a ground-level release).

2.3.2 Instantaneous release without rainout

The initial phase of the pressurised instantaneous release is radial energetic expansion during which the pressure reduces to the ambient pressure. Following this the cloud moves in the downwind direction. It moves upwards or downwards if the cloud is heavier or lighter than air.

This model evaluates the dispersion variables as a function of downwind travel time. The basic dispersion variables are

- mass of wet air added to the cloud (kg)
- excess horizontal and vertical momentum (kg m/s)
- downwind horizontal and vertical position (m)
- heat added from the substrate (J)
- water vapour added from the substrate (kg)
- cloud width (m)

which are determined by solving a set of ordinary differential equations forward in the time. The equations express air entrainment into the cloud, conservation of momentum, relation between cloud speed and cloud position, a heat-transfer relation, a water-vapour transfer relation, and a cross-wind spreading equation. The vapour temperature of the cloud is set in the UDM thermodynamics module by imposing conservation of cloud enthalpy.

The concentration c is given by a similarity profile c = c(x,y,ζ,t), with exponential decay in x,y,ζ described by means of ('passive') dispersion coefficients $\sigma_x = \sigma_y$, σ_z, and with near-field top-hat profile (e.g. sharp-edge jet) developing into a Gaussian profile in the far field. The cloud volume is obtained by integration over x,y,ζ.

Figure 24 illustrates the movement of the instantaneous cloud (case of a ground-level release). while the cloud travels downwind, the cloud dilutes and becomes larger.

2.3.3 Finite-duration release (no rainout)

The UDM contains two models for the case of a finite-duration release, i.e. the 'quasi-instantaneous' model (QI) and the 'finite-duration-correction' model (FDC).

The quasi-instantaneous model models the initial phase as a continuous source (neglect of downwind gravity spreading and downwind diffusion). When the cloud width becomes 'large' with respect to the cloud length, the cloud is replaced by an 'equivalent' circular cloud, and the subsequent phase is modelled as an 'instantaneous' circular cloud; see Figure 25a.

The 'finite-duration-correction' model is based on the HGSYSTEM formulation derived from that adopted in the SLAB dispersion model. It has a better scientific basis and is derived from an analytical solution of the Gaussian plume passive-dispersion equations. It takes the effects of downwind diffusion gradually into account including effects of both turbulent spread and vertical wind shear. A limitation of this model is however that it is strictly speaking only applicable to ground-level non-pressurised releases without significant rainout. Moreover it produces predictions of the maximum (centre-line ground-level) concentrations only (see Figure 25b).

2.3.4 Time-varying dispersion (time-varying release, rainout, or dispersion from pool)

In Phast prior to the UDM dispersion calculations, discharge calculations are carried out (for release from a hole of a vessel or a pipeline) to determine the UDM source-term data, i.e. the time-varying discharge data after expansion to atmospheric pressure and prior to air entrainment [flow rate, velocity, temperature, liquid mass fraction, droplet size (SMD – Sauter Mean Diameter)].

Observer calculations (prior to inclusion of effects of along-wind diffusion)

Subsequently 'observers' are released from the release location at intervals which can be chosen to correspond to equal-mass increments (see Figure 2 for the case of 6 release observers). These observers will follow the trajectory of the UDM cloud centre-line. For each observer steady-state calculations based on the observed source data are carried out to evaluate the observer concentration prior to including effects of along-wind diffusion; see Figure 2. These steady-state calculations involve a number of differential equations for the so called 'primary' variables, which are solved numerically stepping forward in the time.

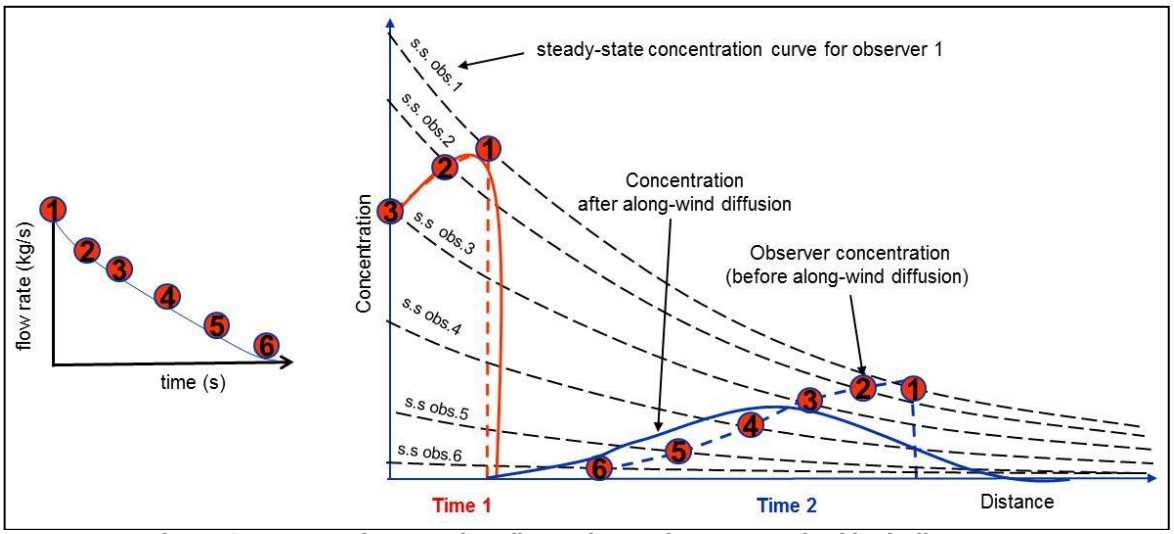

Figure 2. UDM time-varying dispersion – observer method including AWD

Elevated time-varying releases without rainout

In the absence of rainout, primary variables and associated differential equations are as follows

- Mass of moist air added to the cloud (kg/s) – air entrainment law describing turbulent mixing of air with the cloud, accounting for jet entrainment, crosswind entrainment, heavy-gas entrainment and/or passive entrainment
- Excess downwind cloud momentum and cloud vertical momentum (kg m/s^2) – conservation of cloud momentum accounting for gravity forces, ground impact forces and ground drag
- Downwind and vertical position of cloud centreline (m) – relation between cloud position and speed
- Heat conduction from substrate (J/s) – heat transfer equation between substrate and cloud
- Water evaporated from water substrate (kg/s) – water-vapour transfer equation between water substrate and cloud
- Cloud width (m) - empirical spreading law in case of heavy-gas dispersion and based on formula for ambient crosswind dispersion coefficient in case of passive dispersion

Additional equations are solved to derive the so-called 'secondary' variables from the 'primary' variables, which includes nonlinear equations for cloud thermodynamics (isenthalpic equation to evaluate cloud temperature) and cloud geometry. Furthermore an empirical concentration profile at each calculated downwind distance x is adopted to evaluate the observer concentration C as function of crosswind distance y, and vertical height z.

Elevated releases with rainout

In this case, the following steps are carried out consecutively:

- First calculations are carried out for all observers until the point of rainout to provide the time-varying spill data (rainout rate, rainout time, and rainout location) input to PVAP, with linear interpolation presumed between consecutive rainout times.
- PVAP calculations are carried out to determine the time-varying pool radius, pool evaporation rate, and downwind distance of pool centre.
- Calculations are redone for the above "release observers". While each observer moves above the pool, the observer dispersion equations (conservation of cloud mass and momentum conservation, cloud crosswind gravity spreading, heat transfer from the substrate, etc.) are modified to account for the pool vapour added back to the cloud. Additional "pool observers" (corresponding to equal pool-mass segments) are released upwind of the pool after the release plume has left the plume behind, or if the pool spreads upwind of the release point.

The above steps are illustrated by Figure 3, where the first "release observers" (1,2,3,4) start from the release point and subsequent "pool observers" (5, 6) start from the upwind edge of the pool:

- Figure 3a illustrates dispersion prior to rainout of the first observer 1, during which time no effects of pools need to be taken into account.
- Figure 3b illustrates rainout of the first observer 1, which requires adjustment of the variables of observer 1 at the rainout location.
- In Figure 3c observer 1 containing residual vapour is located downwind of the spreading pool. Observer 2 has crossed the upwind edge of the pool and picks up vapour from the pool and the final release observer 4 is released
- In Figure 3d observer 2 has rained out and has left the pool behind. Observer 3 moves above the pool and observer 4 is located upwind of the pool.
- In Figure 3e the first pool observer 5 is released from the upwind edge of the pool after all release observers 1, 2, 3, 4 have passed the upwind edge of the pool.
- In Figure 3f the original cloud (downwind pool edge marked by last release observer 4) starts to leave the pool behind, and a separate cloud develops from the pool (given by pool observers 5, 6).

Dispersion directly from ground-level pool or ground-level vapour area source

In this case spill rate data are directly input to the model, and PVAP calculations are carried out to determine the time-varying pool radius and evaporation rate. Subsequently "pool observers" corresponding to equal pool-mass segments are released at the upwind edge of the pool, and observer dispersion calculations are carried out as indicated above.

Alternatively pool source or vapour area source data can be supplied directly to the UDM in the same way as for a normal release, except the source radius is given instead of release velocity. This option is limited to a finite-duration ground-level source, with constant source data which do not vary with time.

<u>Differential observer-velocity cloud mass correction</u>

The above method for a non-instantaneous release is based on a quasi steady-state approach based on a steady-state solution for each observer. However, if observers move with substantially different velocities (different curves for observer downwind distance versus observer travel time) the mass of released material is not conserved by simply interpolating between these steady state solutions. Therefore a correction is applied to the observer concentrations to ensure mass conservation. It reduces observer concentrations when observers drift apart, and increases concentrations when they move to each other.

Inclusion of effects of along-wind diffusion

At a given time, the actual plume concentration including effects of along-wind-diffusion is calculated by means of Gaussian integration of the observer concentrations. Figure 2 depicts the pre-AWD and post-AWD observer concentrations at a short time after the release (time 1; limited AWD effects), and at a larger time after the release (time 2; larger AWD effects).

Averaging time effect because of time-varying release rate

In addition to the averaging time effect of wind meander, the user can optionally apply additional time-averaging of time-dependent concentrations. These can result from finite-duration releases, time-varying releases and/or time-varying pool evaporation.

Table 1 provides an overview of UDM time-averaging and post-processing options for the full range of release scenarios as described above.

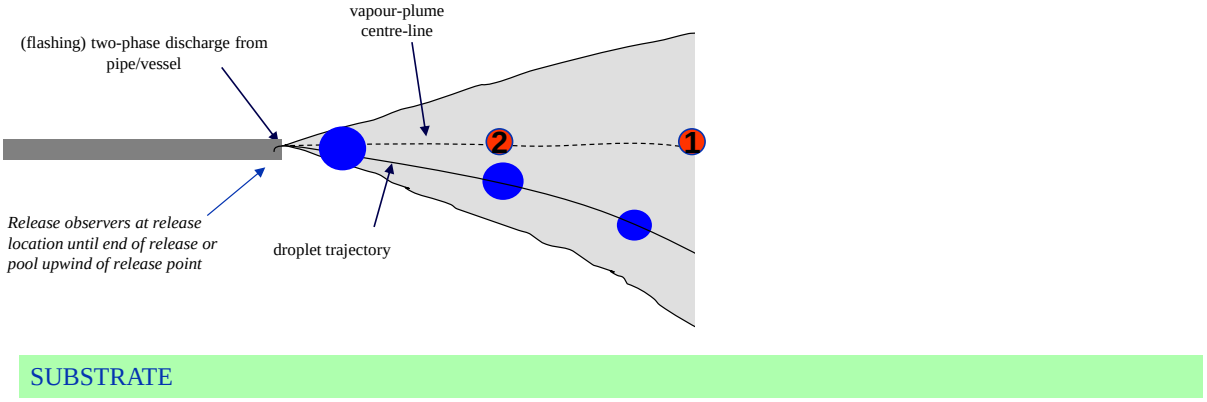

(a) Dispersion before rainout (release observers from release location – no pool effects)

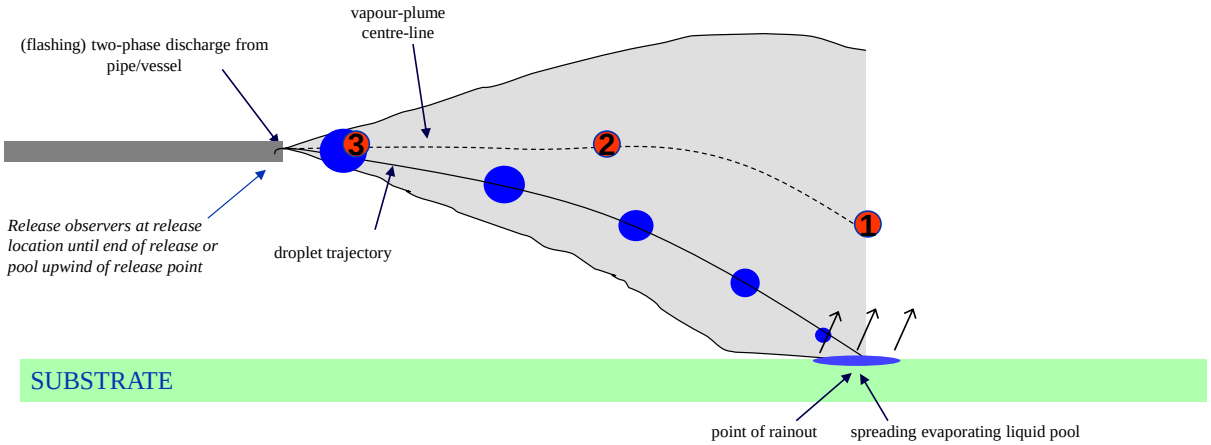

(b) Rainout (adjust observer variables at rainout location; solve pool equations afterwards)

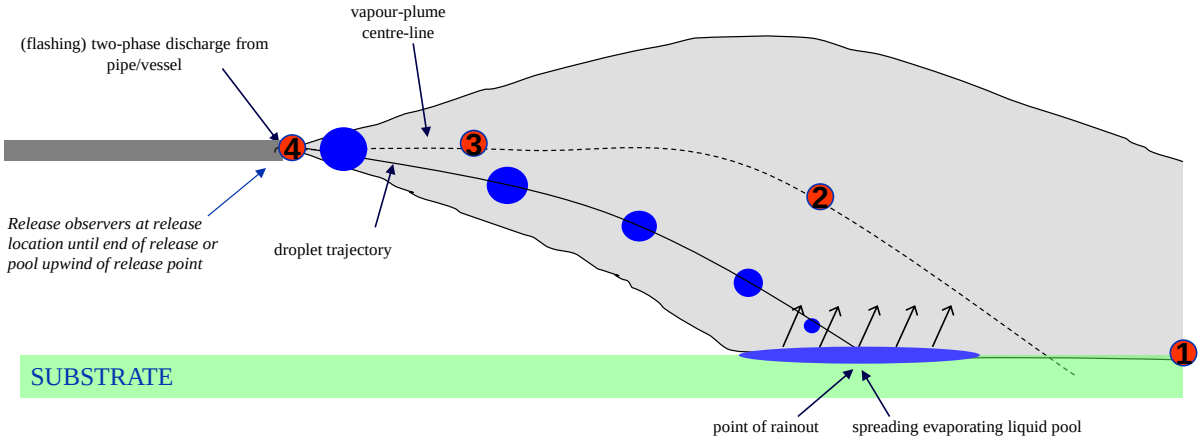

(c) Dispersion after rainout (account for pool vapour pick-up by cloud for observer calculations)

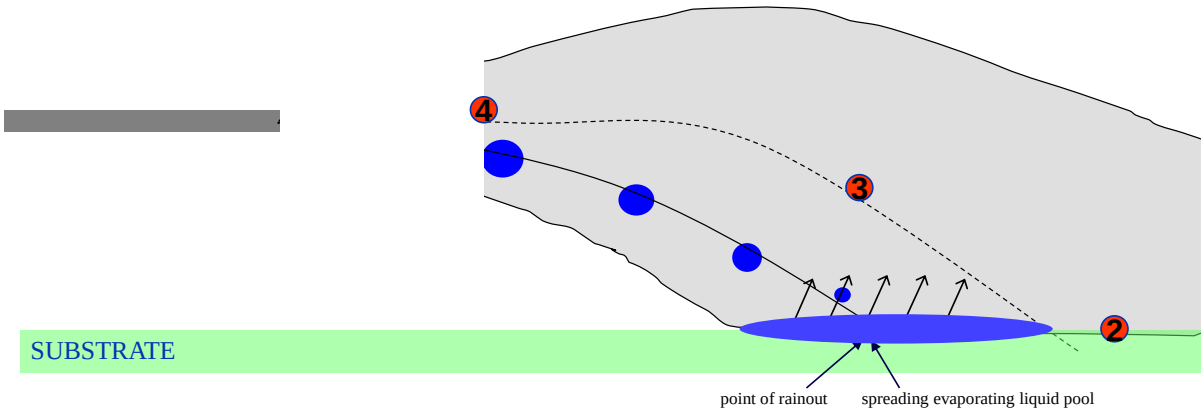

(d) Downwind movement of upwind edge of cloud towards pool (after end of release)

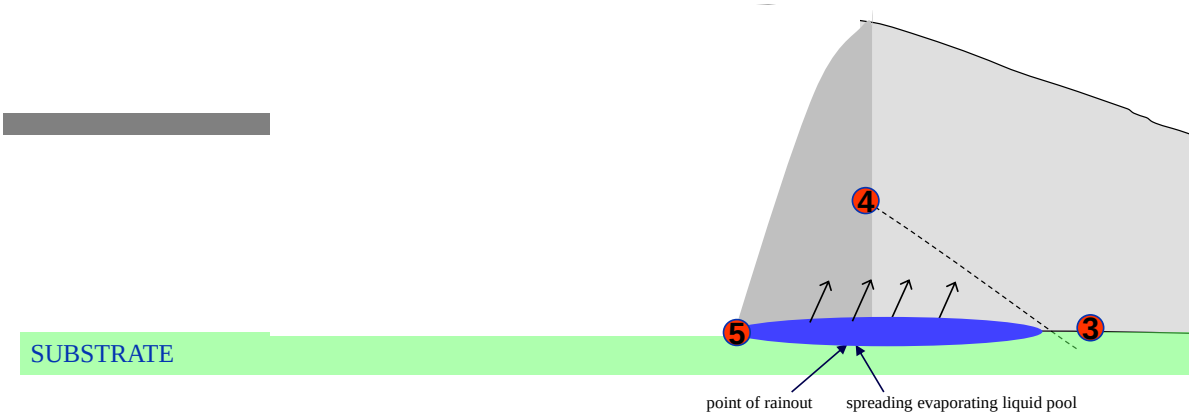

(e) Release observers upwind of pool (after 'release observers' all downwind of upwind pool edge)

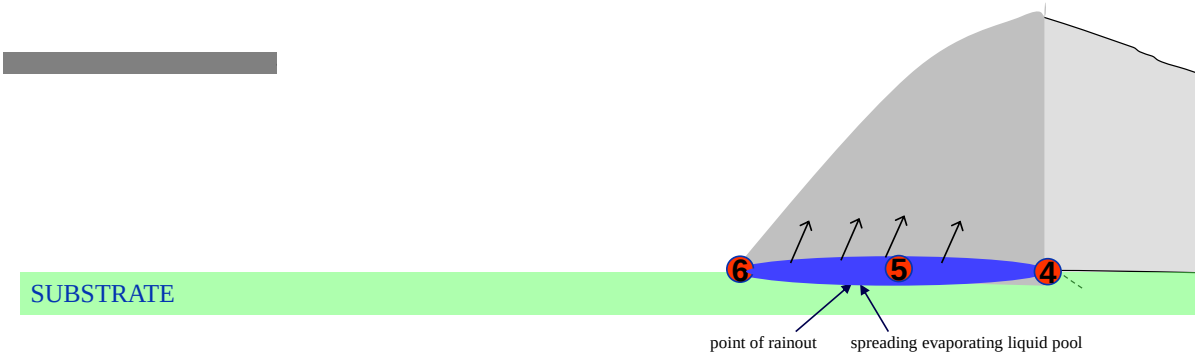

(f) Dispersion directly from pool, with residual cloud moving away from pool

Figure 3. UDM dispersion stages for time-varying release with rainout

	OBSERVER CALCULATIONS	POST-PROCESSING OPTIONS			
Release type	**Averaging-time wind-meander effect**	**Along-wind gravity spreading (GSC = gravity-shape correction)**	**Differential observer-velocity mass correction**	**Along-wind diffusion**	**Averaging-time time-varying release /pool effect**
steady-state without rainout	yes	optional GSC	no (n/a)	no (n/a)	no (n/a)
instantaneous without rainout	yes	yes	n/aq	yes	optional via integration
finite-duration, QI	yes	optional GSC for pre-QI results yes after QI	no (n/a)	optional before QI yes after QI (limitation $\sigma_x=\sigma_y$)	optional via integration
finite-duration, FDC	yes	optional GSC (prior to FDC)	no (n/a)	yes via multiplication factor F [max. conc. only]	optional via multiplication factor D [max. conc. only]
instantaneous (rainout)	yes	yes for instantaneous observer optional GSC after rainout for non-instantaneous observer	n/a for instantaneous observer optional after rainout other observers	yes for instantaneous observer (limitation $\sigma_x=\sigma_y$) optional after rainout via Gaussian integration for other observers	optional via integration
time-varying, rainout & pools, AWD	yes	optional GSC	optional	optional via Gaussian integration	optional via integration

Table 1. UDM time-averaging and post-processing options for range of scenarios

3. UDM MODEL FOR STEADY-STATE OR UNPRESSURISED INSTANTANEOUS RELEASE (NO RAINOUT)

The current chapter considers both cases of a steady-state release or an unpressurised release, where it is assumed that no rainout occurs. The cases of finite-duration releases, cases with rainout, of dispersion from (time-varying) ground-level pool sources will be dealt with in subsequent chapters.

3.1 Similarity concentration profile; cloud geometry

The Unified Dispersion Model is an advanced similarity model capable of describing a wide range of types of accidental releases. The main characteristic of similarity models is that profiles for concentration, velocity, and temperature are assumed. The Unified Dispersion Model uses a particularly flexible form for the concentration profile, allowing for sharp-edged profiles which become more diffuse downwind. The vertical cross section is in general, an ellipse while elevated, and a truncated ellipse while touching the ground[iv].

3.1.1 Steady-state release

The continuous release profile extends from the source downwind. An example of a general case continuous release is shown in Figure 21. An elevated, heavy vapour/aerosol release starts out with a circular cross section. Upon touching down, the cross section becomes a truncated ellipse, and the cloud levels off as the vertical component of momentum is converted into downwind and cross-wind momentum. Aerosol droplets may rain out shortly after touchdown. Rain-out produces a pool which spreads and vaporises. If spilled onto water, part of the material may also dissolve. The vapour from the pool is added back to the plume, as a function of time. The plume can become buoyant after evaporating all aerosol droplets and picking up heat by ground conduction, or by condensing water picked up over a wet surface. A buoyant plume lifts off and rises until constrained by the mixing layer.

The profile form assumed here generalises on the original concepts of Ooms et al. (1974)[11] as suggested by Webber et al. (1992)[12]. The concentration profile is given by

$$c(x,y,\zeta) = c_o(x) F_v(\zeta) F_h(y) \quad (1)$$

$$F_v(\zeta) = \exp\left\{ -\left| \frac{\zeta}{R_z(x)} \right|^{n(x)} \right\} \quad (2)$$

$$F_h(y) = \exp\left\{ -\left| \frac{y}{R_y(x)} \right|^{m(x)} \right\} \quad (3)$$

The scaling coefficients in the above equations are:

$$R_y = \sqrt{2}\,\sigma_y \quad (4)$$

$$R_z = \sqrt{2}\,\sigma_z \quad (5)$$

When m = n = 2, Equations (2), (3) reduce to the Gaussian form, and σ_y and σ_z reduce to the standard deviations (Gaussian vertical and cross-wind dispersion coefficients). For larger values, say m = 50, profiles are predicted by Equations (2), (3) to be very nearly sharp-edged as Figure 26 illustrates. This formulation allows modelling of a sharp-edged jet, as occurs from a smooth-edged nozzle, dispersing to a plume with a more nearly Gaussian profile farther downwind.

[iv] JUSTIFY. The model currently assumes that the cloud is not truncated during capping by the mixing layer. The mixing layer logic in the model needs further investigation.

The exponent m is correlated as a function of the normalised density difference $(\rho_{cld}-\rho_a)/\rho_a$ which goes into the calculation of buoyancy, as shown in Figure 27[v].

The correlation for n is similar to the correlations for atmospheric flux gradients proposed by Businger et al. (1971)[13], or Dyer and Hicks (1970)[14] as discussed by Lo and McBean (1978)[15]. Figure 28 illustrates the correlation for various stability classes as a function of $z_f = H_{eff}/|L|$ where H_{eff} is the effective height of the cloud defined below, and L is the Monin-Obukhov length (< 0 for unstable atmospheres)[vi].

Effective cloud data

At each downwind position x the UDM cloud can be characterised by a 'equivalent' cloud with effective height $H_{eff}(x)$, an effective cloud half-width W_{eff}, and cloud speed u_{cld}, and equivalent top-hat concentration equal to the centre-line concentration c_o[vii]. Using Equations (1), (2), (3), the effective cloud data can be expressed as follows,

$$H_{eff} = \frac{1}{c(x,y,0)} \int_0^\infty c(x,y,\zeta)\,d\zeta = \int_0^\infty F_v(\zeta)\,d\zeta = \Gamma\left(1+\frac{1}{n}\right) R_z(x) \qquad (6)$$

$$W_{eff} = \frac{1}{c(x,0,\zeta)} \int_0^\infty c(x,y,\zeta)\,dy = \int_0^\infty F_h(y)\,dy = \Gamma\left(1+\frac{1}{m}\right) R_y(x) \qquad (7)$$

where the gamma function $\Gamma(z)$ is defined by

$$\Gamma(z) = \int_0^\infty t^{z-1} e^{-t}\,dt \qquad (8)$$

The physical interpretation of the effective width and length is that the concentration profiles are "squared off", so the dimensions H_{eff} and W_{eff} define an ellipse-shaped cross section of a top hat model which contains all the mass in the cloud having the diffuse concentration profile given by Equations (1), (2), (3). This general similarity model, therefore, retains all the simplicity and convenience of a top-hat model, but at the same time allows quite general concentration profiles.

To clarify, consider Figure 29 which plots three alternative curves to define a cloud cross-section corresponding to an iso-concentration contour:

- The middle iso-concentration curve with semi-axes R_y, R_z plots

$$\left(\frac{y}{R_y}\right)^m + \left(\frac{\zeta}{R_z}\right)^n = 1$$

  According to Equation (1) it corresponds to the concentration contour level $c(x,y,\zeta) = e^{-1}\,c_o(x)$.

- The outer iso-concentration curve plots the concentration profile (1) at three standard deviations, i.e. it uses the ellipse semi-axes $3\sigma_y = 3R_y/2^{1/2}$, $3\sigma_z = 3R_z/2^{1/2}$. For the Gaussian case m=n=2 this corresponds to the contour level $c(x,y,\zeta) = e^{-4.5}\,c_o(x) = 0.011 c_o(x)$.

- Likewise the inner curve uses the semi-axes W_{eff} and H_{eff}. For the Gaussian case $W_{eff} = 0.5\,\pi^{1/2} R_y$, $H_{eff} = 0.5\,\pi^{1/2} R_z$ with the contour level $c(x,y,\zeta) = e^{-\pi/4}\,c_o(x)$.

[v] JUSTIFY. The adopted formula for m is similar to that adopted in the DRIFT model, but DRIFT adopts the more appropriate Richardson number Ri_* instead of the relative density difference. Large Richardson number means that gravitational potential energy dominates turbulence, while small Ri_* means that turbulent energy is dominating. Thus $m(Ri_*)$ embodies the idea that turbulence erodes a sharp edge.

[vi] JUSTIFY. The adopted formula for n needs further investigation against the quoted references. A single correlation (as function of H_{eff}/L) valid for all stability classes may be more appropriate.

[vii] The UDM cloud speed u_{cld} is assumed to be the speed at the cloud-centroid height z_c. Other models often adopt the effective cloud speed u_{eff} [e.g. HEGADAS, DEGADIS; see Equation (9)].

For a ground-level cloud moving with the ambient wind speed u_a, the so-called effective cloud velocity u_{eff} is given by

$$u_{eff}(x) = \frac{\int_0^\infty u_a(z)\,c(x,y,z)\,dz}{\int_0^\infty c(x,y,z)\,dz} \qquad (9)$$

which with the profiles (1), (2), (3) and the ambient profile $u_a(z) = u_a(z_{ref})\,(z/z_{ref})^p$ gives:

$$u_{eff} = \frac{u_a(z_{ref})}{(p+1)}\left(\frac{R_z}{z_{ref}}\right)^p \Gamma\left(1+\frac{p+1}{n}\right) / \Gamma\left(1+\frac{1}{n}\right) \qquad (10)$$

Plume cross-section area

A further simplification is to retain the elliptical cloud cross section as the cloud position changes from elevated to touching down to grounded.

Figure 29 illustrates this point for a cloud which is touching down or lifting off.

Only that portion of the cross section which is above ground is physical (contains aerosol). The vertical distance $z_{cld}(x)$ between the ground and the geometric centre of the cloud's elliptical cross section is related to the fraction $h_d(x)$ of the area in the bottom half of the ellipse which is above ground. Note that $\zeta = -z_{cld} / \cos(\theta)$ at the ground.

The cross section shown in Figure 29 can be considered as that of a continuous release. Integrating to find the cloud area via:

$$A_{cld}(x) = 2\int_{-z_{cld}/\cos(\theta)}^{\infty}\int_0^\infty \exp\left\{-\left|\frac{\zeta}{R_z}\right|^n\right\}\exp\left\{-\left|\frac{y}{R_y}\right|^m\right\} dy\,d\zeta \qquad (11)$$

giving:

$$A_{cld} = 2\,W_{eff}\,H_{eff}\,(1+h_d) \qquad (12)$$

where H_{eff}, W_{eff} are given by Equations (6), (7) and

$$h_d = P\left[\frac{1}{n}, \left(\frac{z_{cld}/\cos(\theta)}{R_z}\right)^n\right] \qquad (13)$$

Here the partial gamma function P(a,b) is defined by

$$P(a,b) = \frac{1}{\Gamma(a)}\int_0^b t^{a-1}e^{-t}\,dt \qquad (14)$$

with the limiting values: $P(a,0) = 0$, $P(a,\infty) = 1$. Note that for a plume aloft $z_{cld}/R_z >> 1$ applies; therefore $h_d = 1$ and the plume cross section is a full ellipse. For a grounded plume $z_{cld} = 0$ applies; therefore $h_d = 0$ and the plume cross section is a semi ellipse. For a plume partially touching down, H_{eff} is the effective cloud height above the ground centreline (centre to both the real and the "imaginary" portions).

The rectangular cross-sectional area A_{cld} defined by Equation (12) [width $2\,W_{eff}$, depth $H_{eff}(1+h_d)$] could be considered to contain all the cloud mass m_{cld} compressed to a concentrated, top hat form [equivalent top-hat concentration = c_o].

For the special case when n = m = 2, the Gaussian case, the results reduce to:

$$h_d = erf\left(\frac{z_{cld}}{R_z \cos(\theta)}\right) \quad (15)$$

$$A_{cld}(x) = \frac{1}{2}(1+h_d)\,\pi\,R_y\,R_z \quad (16)$$

where the error function erf(z) is defined by

$$erf(z) = \frac{2}{\sqrt{\pi}}\int_0^z e^{-t^2}\,dt \quad (17)$$

Plume centroid

The distance ζ_c perpendicular to the plume centre-line of the plume centroid is defined by

$$\zeta_c = \frac{\int_{-z_{cld}/\cos(\theta)}^{\infty} \zeta\; c(x,y,\zeta)\; d\zeta}{\int_{-z_{cld}/\cos(\theta)}^{\infty} c(x,y,\zeta)\; d\zeta} \quad (18)$$

Inserting Equations (1), (2), (5), (6) into the above equation leads to

$$\begin{aligned}
\zeta_c &= \frac{\int_{-z_{cld}/\cos(\theta)}^{\infty} \zeta\; F_v(\zeta)\,d\zeta}{\int_{-z_{cld}/\cos(\theta)}^{\infty} F_v(\zeta)\; d\zeta} = \frac{\int_{-z_{cld}/\cos(\theta)}^{\infty} \zeta\; \exp\left[-\left(\frac{\zeta}{R_z(x)}\right)^n\right] d\zeta}{H_{eff}\,(1+h_d)} \\
&= \frac{R_z^{\,2}}{n\,H_{eff}\,(1+h_d)}\left\{\Gamma\left(\frac{2}{n}\right) - \Gamma\left(\frac{2}{n}\right) P\left[\frac{2}{n}, \left(\frac{z_{cld}}{R_z\cos(\theta)}\right)^n\right]\right\} \\
&= \frac{\sigma_z}{(1+h_d)\sqrt{2}}\,\frac{\Gamma\left(1+\frac{2}{n}\right)}{\Gamma\left(1+\frac{1}{n}\right)}\left\{1 - P\left[\frac{2}{n}, \left(\frac{z_{cld}}{R_z\cos(\theta)}\right)^n\right]\right\}
\end{aligned} \quad (19)$$

Thus the vertical height of the centroid above the ground is given by $z_c = z_{cld} + \zeta_c \cos(\theta)$

For the special Gaussian case n=2, the above result reduces to

$$\zeta_c = \frac{2\,\sigma_z}{(1+h_d)\sqrt{2\pi}}\exp\left(-\left[\frac{z_{cld}}{R_z\cos(\theta)}\right]^2\right)$$

Plume perimeter above the ground

Consider the middle ellipse $(y/R_y)^m+(\zeta/R_z)^n=1$ with ellipse semi-axes R_y, R_z corresponding to the contour level $e^{-1}c_o(x)$. The perimeter P_{above} (m) of the nominal elliptical cross-section of the cloud above the ground is approximated as

$$P_{above} = 4\,[0.5(1+h_d)] \int_0^{R_y} \sqrt{1+\left(\frac{d\zeta}{dy}\right)^2}\, dy \qquad (20)$$

This is exact for an aloft plume (h_d=1; P_{above} is the perimeter of the full ellipse) and for a grounded plume (h_d=0; P_{above} is the perimeter of the upper half of the ellipse); it is approximate during touchdown (0<h_d<1). Setting $d\zeta/dy$ from $(y/R_y)^m+(\zeta/R_z)^n=1$ and subsequent inserting in the above equation it follows that

$$P_{above} = 2\,(1+h_d)\,R_y \int_0^1 \left\{ 1 + \left(\frac{mR_z}{nR_y}\right)^2 t^{2m-2}\left(1-t^m\right)^{2/n-2} \right\}^{1/2} dt$$

Using m=n=2[viii] it follows that the above integral reduces to

$$\begin{aligned} P_{above} &= 2\,(1+h_d)\,R_y \int_0^1 \left[1-t^2\right]^{-1/2} \left\{1-\left[1-\left(R_z/R_y\right)^2\right]t^2\right\}^{1/2} dt \\ &= 2\,(1+h_d)\;R_y \;\; E\left[1-\left(R_z/R_y\right)^2\right] \end{aligned} \qquad (21)$$

where $E[1-(R_z/R_y)^2]$ is the complete elliptic integral of the second kind. Note the following special cases for an aloft plume:

- $R_z = R_y$ (ellipse is circle): $E[1-(R_z/R_y)^2]=E[0]=\pi/2$, $P_{above} = 2\pi R_z$
- $R_z << R_y$ (wide, very thin): $E[1-(R_z/R_y)^2] \approx E[1] = 1$ $P_{above} = 4R_y$
- $R_z >> R_y$ (high, very narrow): $E[1-(R_z/R_y)^2] \approx R_z/R_y$ $P_{above} = 4R_z$

Width of part of cloud touching the ground

Consider the middle ellipse $(y/R_y)^m+[\zeta/R_z)^n=1$ with ellipse semi-axes R_y, R_z. The ground-level corresponds to z = 0 = z_{cld} + ζ cos(θ), i.e. ζ = -z_{cld} / cos(θ). Thus the half-width W_{gnd} of the part of the cloud touching the ground is found from $(W_{gnd}/R_y)^m+[z_{cld}/R_z\,\cos\theta]^n=1$, i.e.

$$\begin{aligned} W_{gnd} &= R_y \left\{1 - \left(\frac{z_{cld}}{R_z\,\cos(\theta)}\right)^n\right\}^{1/m} , \quad for\;\; 0 \le z_{cld} < R_z\cos(\theta) \\ &= 0 \quad , \qquad\qquad\qquad\qquad for\;\; z_{cld} \ge R_z\cos(\theta) \end{aligned} \qquad (22)$$

Note that the touchdown criterion (onset of touching down) is defined by z = 0 = z_{cld} - R_z cos(θ), i.e. z_{cld} = R_z cos(θ).

3.1.2 Instantaneous release

An instantaneous release profile is a volume defined by revolving the vertical cross section around the vertical axis. For instantaneous profiles the concentration profile is given by:

$$c(x,y,\zeta;t) = c_o(t)\,F_v(\zeta)\,F_h(x,y) \qquad (23)$$

with ζ = z – z_{cld}(t), $F_v(\zeta)$ defined by Equation (2), and $F_h(x,y)$ is given by [cf. Equation (3)]

$$F_h(x,y) = \exp\left\{ -\left[\left(\frac{x - x_{cld}(t)}{R_x(t)}\right)^2 + \left(\frac{y}{R_y(t)}\right)^2\right]^{m/2} \right\}, \;\; with \;\; R_x = R_y \qquad (24)$$

[viii] It would be more accurate to set P_{above} from general formula $(y/R_y)^m+(\zeta/R_z)^n=1$, while not assuming m=n=2. However this would imply either the accurate evaluation of the integral or the derivation of an analytical expression (or approximate fit of the solution to the integral). This may be an item of further work.

Furthermore $x_{cld}(t)$ is the downwind distance of the centre of the cloud at time t, and $c_o(t)$ is the concentration at the cloud centre at time t. At the core averaging time[ix] the along-wind dispersion is assumed to be identical to the cross-wind dispersion, i.e. $R_x = R_y$. A possible improvement would be to allow the along-wind dispersion to be different from the cross-wind dispersion, consistent with our use of along-wind dispersion in both the 'finite-duration-correction' model for continuous releases (see Section 4.2) and the model for time-varying releases (see Chapter 5). This extension would produce a ground-level footprint which is an ellipse. The present model keeps this ground-level footprint a circle. This also implies that $F_h(x,y) = F_h(r)$, with $F_h(r)$ defined by Equation (3) and the axisymmetric circle radius $r = [(x-x_{cld})^2+y^2]^{1/2}$.

Plume cross-section area and effective cloud data

The cross section shown in Figure 29 can be considered as either that of a continuous or an instantaneous release. For an instantaneous release settling as an oblate spheroid, $R_y > R_z$. Integrating to find the cloud volume via:

$$V_{cld} = \int_{-z_{cld}}^{\infty} \int_{-\infty}^{\infty} \int_{-\infty}^{\infty} \exp\left(-\left[\frac{\zeta}{R_z}\right]^n\right) \exp\left[-\left(\left[\frac{x-x_{cld}}{R_y}\right]^2 + \left[\frac{y}{R_y}\right]^2\right)^{\frac{m}{2}}\right] d\zeta \; dx\, dy \qquad (25)$$

and making use of $[(x-x_{cld})^2+y^2] = r^2$ gives:

$$V_{cld} = \pi W_{eff}^2 \; H_{eff}(1+h_d) \qquad (26)$$

Here H_{eff} is the effective cloud height H_{eff}, and the effective cloud radius W_{eff} is determined from the 'effective' circular horizontal cross-section $A_{eff} = \pi W_{eff}^2$; H_{eff}, A_{eff}, W_{eff} and h_d are defined by

$$H_{eff} = \frac{1}{c(x,y,0)} \int_0^{\infty} c(x,y,\zeta) d\zeta = \int_0^{\infty} F_v(\zeta) d\zeta = \Gamma\left(1+\frac{1}{n}\right) R_z \qquad (27)$$

$$A_{eff} = \frac{1}{c(x_{cld},0,\zeta)} \int_{-\infty}^{\infty} \int_{-\infty}^{\infty} c(x,y,\zeta)\, dx\, dy = 2\pi \int_0^{\infty} \exp\left(-\left[\frac{r}{R_y}\right]^m\right) r\, dr = \pi R_y^2 \Gamma\left(1+\frac{2}{m}\right) \qquad (28)$$

$$W_{eff} = \frac{1}{\pi}\sqrt{A_{eff}} = \sqrt{\Gamma\left(1+\frac{2}{m}\right)}\; R_y$$

$$h_d = P\left[\frac{1}{n}, \left(\frac{z_{cld}}{R_z}\right)^n\right] \qquad (29)$$

Thus at each time t, the UDM instantaneous cloud can be characterised by an 'equivalent' cylindrical cloud with effective radius W_{eff} and effective depth $H_{eff}(1+h_d)$. This equivalent cloud is taken to move with the cloud speed u_{cld} and to have an equivalent top-hat concentration equal to the centre-line concentration c_o.

For the special case when n = m = 2, the Gaussian case, the results reduce to:

$$H_{eff} = \frac{1}{2}\sqrt{\pi}\; R_z\,, \qquad W_{eff} = R_y\,, \qquad h_d = erf\left(\frac{z_{cld}}{R_z}\right) \qquad (30)$$

$$V_{cld}(x) = \frac{1}{2}(1+h_d)\pi^{3/2} R_z \; R_y^2 \qquad (31)$$

[ix] Passive along-wind diffusion is caused by both wind shear and turbulent spread, while passive cross-wind diffusion is caused by turbulent spread only. Thus for no time averaging (t_{av} = 18.75s) the instantaneous passive plume will be longer in the downwind direction than in the cross-wind direction, i.e. $\sigma_{xa} > \sigma_{ya}(t_{av}=18.75)$. See Section 3.7 for further details. Note that the assumption $R_x=R_y$ is also always adopted by the UDM post-processor.

where z_{cld} is the height of the cloud centreline above the ground.

Plume centroid

The formula for the plume centroid is derived analogous to that for the continuous release:

$$\zeta_c = \frac{\int_{-z_{cld}}^{\infty} \zeta\ c(x,y,\zeta)\ d\zeta}{\int_{-z_{cld}}^{\infty} c(x,y,\zeta)\ d\zeta} = \frac{\sigma_z}{(1+h_d)\sqrt{2}} \frac{\Gamma\left(1+\frac{2}{n}\right)}{\Gamma\left(1+\frac{1}{n}\right)} \left\{1 - P\left[\frac{2}{n}, \left(\frac{z_{cld}}{R_z}\right)^n\right]\right\} \quad (32)$$

Thus the vertical height of the centroid above the ground is given by $z_c = z_{cld} + \zeta_c$. For the special Gaussian case n=2, the above result reduces to

$$\zeta_c = \frac{2\ \sigma_z}{(1+h_d)\sqrt{2\pi}} \exp\left(-\left[\frac{z_{cld}}{R_z}\right]^2\right)$$

Cloud surface area above the ground

The cloud surface area S_{above} above the ground for an instantaneous plume is calculated in an analogous way to the calculation of the cloud perimeter for a steady plume.

Consider the ellipsoid $(r/R_y)^m + (\zeta/R_z)^n = 1$ with ellipsoid semi-axes R_y, R_z corresponding to the contour level $e^{-1}c_o(t)$ and with the radius $r = [(x-x_{cld})^2+y^2]^{1/2}$. The cloud surface area S_{above} (m^2) of the surface of the ellipsoid above the ground is approximated as

$$S_{above} = 4\pi\,[0.5(1+h_d)] \int_0^{R_y} \sqrt{1+\left(\frac{d\zeta}{dr}\right)^2}\ r\ dr \quad (33)$$

This is exact for an aloft plume (h_d=1; S_{above} is the surface area of the full ellipsoid) and for a grounded plume (h_d=0; S_{above} is the surface area of the upper half of the ellipsoid); it is approximate during touchdown ($0<h_d<1$). Setting $d\zeta/dr$ from $(r/R_y)^m+(\zeta/R_z)^n=1$, subsequent insertion in the above equation, and using the substitution $t = r/R_y$ it follows that

$$S_{above} = 2\pi\,(1+h_d)\,R_y^{\,2} \int_0^1 \left\{1 + \left(\frac{mR_z}{nR_y}\right)^2 t^{2m-2}\left(1-t^m\right)^{2/n-2}\right\}^{1/2} t\ dt$$

Using $m=n=2^x$ and substituting $u=1-t^2$ it follows that the above integral reduces to

$$S_{above} = 2\pi\,(1+h_d)\,R_y^{\,2} \int_0^1 \left[1-t^2\right]^{-1/2} \left\{1-\left[1-\left(R_z/R_y\right)^2\right]t^2\right\}^{1/2} t\ dt$$

$$= \pi\,(1+h_d)\,R_y R_z \int_0^1 u^{-1/2} \left\{1 + \left[(R_y/R_z)^2-1\right]u\right\}^{1/2} du$$

$$= 2\pi\,(1+h_d)\,R_y R_z\ F\left[-\frac{1}{2}, \frac{1}{2}; \frac{3}{2}; 1-(R_y/R_z)^2\right]$$

[x] It would be more accurate to set S_{above} from the general formula $(r/R_y)^m+(\zeta/R_z)^n=1$, while not assuming m=n=2. However this would imply either the accurate evaluation of the integral or the derivation of an analytical expression (or approximate fit of the solution to the integral). This may be an item of further work.

(34)

where F is the hypergeometric function[16,17] defined by the integral representation[xi]

$$F(a,b;c;z) \quad = \quad \frac{\Gamma(c)}{\Gamma(b)\Gamma(c-b)} \int_0^1 u^{b-1}(1-u)^{c-b-1}(1-u\,z)^{-a}\,du$$

Note the following special cases for an aloft plume (h_d=1):

- $R_z = R_y$ (ellipsoid is sphere): $S_{above} = 4\pi R_z^2$
- $R_z << R_y$ (wide, very thin cylinder): $S_{above} = 2\pi R_y^2$
- $R_z >> R_y$ (high, very narrow plume): $S_{above} = \pi^2 R_y R_z$

Area of part of cloud touching the ground

Again consider the ellipsoid $(r/R_y)^m+[\zeta/R_z)^n=1$ with ellipse semi-axes R_y, R_z. The ground-level corresponds to z = 0 = z_{cld} + ζ, i.e. ζ = -z_{cld}. Thus the radius W_{gnd} of the part of the cloud touching the ground is found from $(W_{gnd}/R_y)^m+[z_{cld}/R_z]^n=1$, i.e.

(35)

$$W_{gnd} \quad = \quad R_y \left\{1 - \left(\frac{z_{cld}}{R_z}\right)^n\right\}^{1/m} \quad , \quad for \;\; 0 \le z_{cld} < R_z$$

$$= \quad 0 \quad , \qquad\qquad for \;\; z_{cld} \ge R_z$$

Note that the touchdown criterion (onset of touching down) is defined by z = 0 = z_{cld} - R_z, i.e. $z_{cld} = R_z$.

From the above it follows that the area of the cloud touching the ground is given by

(36)

$$S_{gnd} \;=\; \pi \; W_{gnd}^{\;2}$$

[xi] This compares to the formula of the cloud perimeter for continuous dispersion: $P_{above} = 2(1+h_d)R_y\,E[1-(R_z/R_y)^2] = \pi(1+h_d)R_y\,F[-1/2,1/2;1;1-(R_z/R_y)^2]$. The hypergeometric function in Equation (34) has been evaluated by means of (a) a series expansion for $-0.5 < 1-(R_y/R_z)^2 < 0.5$, (b) a least-square fit of the numerical solution otherwise. The fit is a polynomial fit in $z = 1-(R_y/R_z)^2-0.5$ for $0.5 < 1-(R_y/R_z)^2 < 1$, and a polynomial fit in $z = \log(|1-(R_y/R_z)^2|+0.5)$ for $-\infty < 1-(R_y/R_z)^2 < -0.5$. See Abramowitz et al.[16] and Press et al.[17] for further details for the series expansion and the numerical solution for the hypergeometric function.

3.2 Dispersion variables and equations

The Unified Dispersion Model is formulated as an integral model. A set of differential equations is integrated to give the key variables as a function of distance or time. A number of algebraic equations are then solved to obtain other variables describing the dispersing cloud. The set of differential equations are basically the same for instantaneous and continuous releases, although they are integrated with respect to time in the first case and with respect to distance in the latter. The same differential equations apply throughout all phases of dispersion (e.g. jet, dense, passive), although the exact terms on the right hand side may vary as the cloud passes from one phase to the next.

The Unified Dispersion Model uses the similarity profiles [Equations (1), (2), (3) for continuous or (23), (24) for instantaneous], generalising an approach first developed by Ooms et. al. (1972)[18], and modified by Emerson (1986, 1987)[19,20,21]. The two sets of ordinary differential equations are integrated by either the synchronised or rigorous solution methods as described in Section 2.2. The first set, describing the overall cloud behaviour, is described in this section; the second set, describing droplet evaporation and trajectories, is described in a separate UDM thermodynamics report.

For each set of equations, we first write the balances as time derivatives, which apply with an instantaneous release. For a continuous release, the time derivatives are transformed to spatial derivatives via[xii]:

$$\frac{d(\ )}{ds} = \frac{d(\ )}{dt}\frac{1}{u_{cld}} \qquad (37)$$

Plume variables

The plume variables which are integrated are indicated in the table below

plume variable	Symbol	unit (instant.)	unit (cont.)
mass of wet air added to the cloud	m_{wa}	kg	kg/s
excess downwind momentum	$I_{x2} = I_x - m_{cld}u_a(z_c) = m_{cld}u_x - m_{cld}u_a(z_c) \quad = I_x - m_{cld}u_w = m_{cld}u_x - m_{cld}u_w$	kg m/s	kg m/s^2
vertical momentum	$I_z = m_{cld}\, u_z \quad = m_{cld}\, u_z$	kg m/s	kg m/s^2
downwind position	x_{cld}	m	m
vertical position	z_{cld}	m	m
heat conduction from substrate	q_{gnd}	J	J/s
water evaporated from substrate	m_{wv}^{gnd}	kg	kg/s
cross-wind radius[xiii]	$R_y = 2^{1/2}\sigma_y \quad = 2^{1/2}\sigma_y$	m	m

Table 2. List of primary plume variables (no rainout)

In the above table the first of the pair of units is for instantaneous releases and the second for continuous releases; $m_{cld} = m_c+m_{wa}+m_{wv}^{gnd}$ is the cloud mass (kg, instantaneous release), or the mass flow passing through a vertical plane (kg/s, continuous releases). Here m_c is the released component mass (kg) or mass flow (kg/s). Furthermore u_x and u_z are the horizontal and vertical components of the cloud speed and $u_a(z_c)$ is the ambient wind speed at plume-centroid height z_c.

The initial values of the above primary variables at the point of release are set as follows:

1. Initial air (at ambient temperature) added to the cloud: $m_{wa} = m_{wa}^o$ (kg or kg/s). For most Phast scenarios the UDM input variable $m_{wa}^o = 0$, except for modelling outdoor dispersion following an in-building release or a "vent from vapour space".[xiv]

2. The initial cloud position is the release position[xv]: $x_{cld} = 0$, $z_{cld} = z_R$

3. There is no initial heat and water vapour transfer: $q_{gnd} = 0$ (J or J/s), $m_{wv}^{gnd}=0$ (kg or kg/s)

[xii] In fact in the current UDM numerical model always the time is used as an independent variable, where Equation (37) is used to switch between independent variable s (arc length) and independent variable t (time).

[xiii] A differential equation is not used for the jet phase (circular jet assumed), but for the heavy and passive phase only.

[xiv] IMPROVE. Currently the model mixes in a minimum mass of air (mass fraction = 10^{-6}) to circumvent problems in the HF thermodynamic calculations This should be removed for non-HF.

[xv] FUTURE. One could consider to apply an expansion length or liquid break-up length L_{exp} upwind of which no entrainment is assumed to occur, i.e. the initial position is set as $x_{cld} = L_{exp}\cos(\theta_R)$, $z_{cld} = L_{exp}\sin(\theta_R)$. Here L_{exp} could be derived from an atmospheric expansion model. See Phase III JIP reports for discussion.

4. Initial cloud speed:

   - For an instantaneous release, the initial cloud speed is zero (prior to energetic expansion; $u_x=u_z=0$)[xvi]
   - For a continuous release, the initial cloud speed is derived from the release speed u_R and the release angle θ_R to the horizontal (specified or set from the discharge model): $u_x = u_R \cos(\theta_R)$, $u_z = u_R \sin(\theta_R)$.

5. The initial momentum of the cloud depends upon its source:

   - For a non pool source, the velocity of any initial added air is assumed to be the same as the release velocity of the released component. The cloud momentum is subsequently set as[xvii] $I_{x2} = m_{cld}[u_x-u_a(z_R)]$, $I_z = m_{cld}u_z$.
   - For a release from a pool source (see section 2.1), the velocity of any initial added air is assumed to be the same as the windspeed ($u_a(z_R)$). The cloud momentum, in this case, is set as $I_{x2} = m_c[u_x-u_a(z_R)]$[xviii], $I_z = 0$ (since pool sources are by definition grounded).

6. Initial cloud radius,

   - For a continuous release, the initial cloud area A_{cld} is set from the initial cloud mass m_{cld}, initial density ρ_{cld} and initial speed u_R: $A_{cld} = m_{cld}/[u_R\rho_{cld}]$. The initial cloud radius R_y is subsequently derived from Equation (12) with $R_y=R_z$.
   - For an instantaneous release, the initial cloud volume is likewise set as $V_{cld} = m_{cld}/\rho_{cld}$. The initial cloud radius R_y is subsequently derived from Equation (26) with $R_x=R_y=R_z$.

After initialisation, the variables are determined from numerically solving the dispersion equations in the downwind direction. These equations impose air entrainment, conservation of momentum, the relation between cloud speed and cloud position, a heat-transfer relation, a water-vapour transfer relation, and a cross-wind spreading relation. The equations are described in detail below.

For each integration step the above variables are evaluated, while the thermodynamic data are set separately from the thermodynamics equations (liquid temperature, droplet temperature, droplet position and speed, droplet mass). The cloud vapour temperature is determined by imposing conservation of cloud energy. See the separate UDM thermodynamics report for further details.

Subsequently the cloud density ρ_{cld} is set from the mixture composition, pressure and temperature (see the separate UDM thermodynamics report).

For a continuous release the cloud area is set as $A_{cld} = m_{cld} / [u_{cld}\ \rho_{cld}]$, the effective cloud height H_{eff} is set from Equation (12), and the maximum concentration c_o from imposing pollutant mass conservation $m_c = c_o A_{cld}\ u_{cld}$ [m_c = component release rate, kg/s].

For an instantaneous release, the cloud volume is set as $V_{cld} = m_{cld}/\rho_{cld}$, the effective cloud height H_{eff} from Equation (26), and the maximum concentration c_o is set from imposing pollutant mass conservation, $m_c = c_o V_{cld}$ [m_c = component released mass, kg].

Plume equations

The model equations for the overall behaviour of the dispersing cloud are as follows:

- *Air entrainment law*

$$\frac{d\, m_{wa}}{ds} = E_{tot}, \text{ steady-state}$$
$$\frac{d\, m_{wa}}{dt} = E_{tot}, \text{ instantaneous}$$

(38)

[xvi] The UDM applies a cut-off velocity for the initial cloud velocity u_{cld} of 0.1 m/s for both continuous and instantaneous releases.

[xvii] For partial spills (where liquid in the release immediately forms a pool leaving only vapour) the momentum of the liquid does not contribute to the cloud.

[xviii] $u_x = 0$ for a pool source. In fact currently I_{x2} is set as zero. As the initial mass is negligible for pool sources this will not be a significant difference, and it eliminates a couple of solver failures.

The above equation describes entrainment of air into the cloud. The total air entrainment is E_{tot} (kg/s for instantaneous cloud, and kg/m/s for steady-state cloud). Air entrainment into a plume may be caused by a range of mechanisms:

- 'jet' entrainment E_{jet} is caused by turbulence resulting from the difference between the plume speed and the ambient wind speed; thus it is present both for a jet (plume speed larger than ambient wind speed) and a plume which moves lest fast than the wind.
- cross-wind entrainment E_{cross} in response to the deflection of the plume by the wind
- passive entrainment is caused by ambient turbulence; it is present both in the near-field (E_{pas}^{nf}) and the far-field (E_{pas}^{ff}).
- heavy-gas entrainment E_{hvy} is included for a grounded heavy-gas plume

Jet entrainment and crosswind entrainment are dominant in the near field after a high-pressure continuous release. During the jet dispersion phase, the centreline velocity decays until either the heavy gas or the passive dispersion mechanisms become dominant. For a low-energy release, the jet dispersion mode may never be dominant. A transition is made to passive dispersion if the cloud density is sufficiently close to the ambient density, the cloud speed is sufficiently close to the ambient speed and the contribution of non-passive entrainment is sufficiently small.

See Section 3.4 for full details on the evaluation of the total air entrainment E_{tot}.

- *Conservation of excess horizontal and vertical component of momentum*

The adopted momentum equations (vector notation) are as follows for continuous dispersion [cloud area $A_{cld} = m_{cld} / (\rho_{cld} u_{cld})$],

$$\begin{bmatrix} \frac{dI_{x2}}{ds} \\ \frac{dI_z}{ds} \end{bmatrix} = F_{drag}^{air} \begin{bmatrix} |\sin\theta| \\ -\cos\theta \frac{\sin\theta}{|\sin\theta|} \end{bmatrix} + F_{impact}^{ground} \begin{bmatrix} -\sin\theta \\ 0 \\ \cos\theta \end{bmatrix} + F_{drag}^{ground} \begin{bmatrix} 1 \\ 0 \end{bmatrix} + A_{cld}(\rho_{cld} - \rho_a) g \begin{bmatrix} 0 \\ -1 \end{bmatrix} \quad \textbf{(39)}$$

and for instantaneous dispersion [cloud volume $V_{cld} = m_{cld} / \rho_{cld}$],

$$\begin{bmatrix} \frac{dI_{x2}}{dt} \\ \frac{dI_z}{dt} \end{bmatrix} = F_{drag}^{air} \begin{bmatrix} |\sin\theta| \\ -\cos\theta \frac{\sin\theta}{|\sin\theta|} \end{bmatrix} + F_{impact}^{ground} \begin{bmatrix} -\sin\theta \\ 0 \\ \cos\theta \end{bmatrix} + F_{drag}^{ground} \begin{bmatrix} 1 \\ 0 \end{bmatrix} + V_{cld}(\rho_{cld} - \rho_a) g \begin{bmatrix} 0 \\ -1 \end{bmatrix} \quad \textbf{(40)}$$

The terms in the right-hand side represent forces on the plume. They are respectively:

- the air-borne drag force F_{drag}^{air} (N/m or N). This force is perpendicular to the plume centre line, with a positive downwind x-component.
- the ground impact force F_{impact}^{ground} (N/m or N) resulting from plume collision with the ground. This force is perpendicular to the plume centre line, and is added during touching down only.
- the horizontal ground drag force F_{drag}^{ground} (N/m or N). This force is added after onset of touchdown only.
- the vertical buoyancy force (N/m or N). This force is proportional to the gravitational acceleration g (= 9.81 m^2/s) and the density difference between the plume and the air.

Note that the vertical momentum equation is not used when the cloud is grounded or capped at the mixing layer (constant plume height).

Expressions for each of the forces above are derived in Section 3.5. Note that airborne drag is currently ignored, while the formulas for the ground drag and ground impact forces are partly taken from McFarlane[22].

- *Horizontal and vertical position:*

$$\frac{dx_{cld}}{dt} = u_x = u_{cld}\cos\theta \qquad (41)$$

$$\frac{dz_{cld}}{dt} = u_z = u_{cld}\sin\theta \qquad (42)$$

- *Rate of heat convection from the substrate*

The heat convection from the substrate to the cloud is described by the following differential equation,

$$\frac{d\,q_{gnd}}{ds} = Q_{gnd}\ [2W_{gnd}], \quad in\ W/m \quad \text{(continuous)} \qquad (43)$$

$$\frac{d\,q_{gnd}}{dt} = Q_{gnd}\ S_{gnd}\ , \quad in\ W \quad \text{(instantaneous)} \qquad (44)$$

where Q_{gnd} is the heat conduction flux (W/m^2) transferred from the substrate to the cloud.

In case of continuous releases, dq_{gnd}/ds (J/m/s) is the heat transferred from the substrate per second and per unit of downwind direction and W_{gnd} is the half-width of the cloud in contact with the substrate [see Equation (22)].

In case of instantaneous releases q_{gnd} is the total heat (J) transferred from the substrate to the cloud and S_{gnd} is the area of the cloud in contact with the substrate [see Equation (36)].

The heat conduction flux Q_{gnd} (W/m^2) transferred from the substrate to the cloud is given by

$$\begin{aligned} Q_{gnd} &= \max\left\{Q_{gnd}{}^{n}, Q_{gnd}{}^{f}\right\}, \quad T_{gnd} > T_{vap} \\ &= Q_{gnd}{}^{f}, \quad T_{gnd} \le T_{vap} \end{aligned} \qquad (45)$$

where $Q_{gnd}{}^{n}$ and $Q_{gnd}{}^{f}$ are the natural and forced convection flux from the substrate to the vapour cloud (W/m^2).

The natural convection flux $Q_{gnd}{}^{n} = 0$ if the substrate is cooler than the vapour cloud ($T_{gnd} \le T_{vap}$). Otherwise it is given by the following expression introduced by McAdams (1954)[23]:

$$Q_{gnd}{}^{n} = \frac{0.14\left(D_{ac}^2\, g\right)^{1/3} \rho_{cld}\, C_p{}^{cld}\, (T_{gnd} - T_{vap})^{4/3}}{\left(\mu_{ac}\, T_{vap} / \rho_{cld}\right)^{1/3}}, \quad T_{gnd} > T_{vap} \qquad (46)$$

Here the specific vapour heat of the cloud $C_p{}^{cld}$ (J/kg/K), the thermal diffusivity of the material in air D_{ac} (m^2/s), and the dynamic viscosity of the material in air μ_{ac} (kg/m/s) are taken at the vapour-cloud temperature T_{vap}.

The forced convection rate is given by the following expression introduced by Holman (1981)[24,xix]

[xix] The original Holman model adopts in the denominator the cloud velocity u_{cld}. For larger cloud speeds this means reduced forced heat transfer. HEGADAS adopts the ambient wind speed at 10 m, $u_a(10m)$ instead of u_{cld}. As a result $\max[u_{cld}, u_a(10m)]$ is adopted. This needs further checking against Holman article etc.

$$Q_{gnd}{}^{f} = \left(\frac{D_{ac}\,\rho_{cld}}{\mu_{ac}} \right)^{2/3} \frac{u_*^2\,\rho_{cld}\,C_p{}^{cld}\,(T_{gnd} - T_{vap})}{\max\,[u_{cld}, u_a(10m)]} \qquad (47)$$

where C_p^{cld} is taken at the vapour temperature T_{vap}[xx].

- *Water-vapour transfer from the substrate*

Water vapour can be transferred from a water surface into the cloud when the vapour temperature of the cloud is less than that of the water surface. This has been included in the Unified Dispersion Model following the approach of the Colenbrander and Puttock described by Witlox[25] which relates the rate of water vapour pick-up to the rate of heat convection from the water surface:

$$\frac{dm_{wv}^{gnd}}{ds} = \frac{5\left[\,P_v{}^{w}(T_{gnd}) - P_v{}^{w}(T_{vap})\,\right]}{C_p{}^{cld}\,T_{gnd}\,P_a}\,\frac{dq_{gnd}}{ds}\,, \quad T_{gnd} > T_{vap} \quad \text{(continuous)} \qquad (48)$$

$$\frac{dm_{wv}^{gnd}}{dt} = \frac{5\left[\,P_v{}^{w}(T_{gnd}) - P_v{}^{w}(T_{vap})\,\right]}{C_p{}^{cld}\,T_{gnd}\,P_a}\,\frac{dq_{gnd}}{dt}\,, \quad T_{gnd} > T_{vap} \quad \text{(instantaneous)} \qquad (49)$$

where P_v^w is the saturated vapour pressure of the water. If $T_{gnd} < T_{vap}$ or $T_{gnd} < 0^oC$ (substrate is ice) or if the cloud is passing over dry ground, $dm_{wv}^{gnd}/ds = 0$ (continuous) or $dm_{wv}^{gnd}/dt = 0$ (instantaneous).

- *Crosswind spreading*

In general cross-wind spreading consists of the following three subsequent phases.

1. Near-field ('jet') spreading. The cloud is assumed to remain circular until the passive transition or (after onset of touching down) until the spread rate reduces to the heavy-gas spread rate, i.e.

$$R_y = R_z$$

2. Heavy-gas spreading. The heavy spread rate is applied until the passive transition. For instantaneous dispersion it is given by

$$\frac{d\,R_y}{dt} = \frac{C_E}{C_m}\sqrt{\frac{g\left\{\max\left[0,\,\rho_{cld} - \rho_a(z = z_{cld})\right]\right\}\,H_{eff}\,(1+h_d)}{\rho_{cld}}}\,,\; C_m = \left[\Gamma\left(1+\frac{2}{m}\right)\right]^{1/2}$$

and for continuous dispersion by

$$\frac{d\,R_y}{dx} = \frac{C_E}{u_x C_m}\sqrt{\frac{g\left\{\max\left[0,\,\rho_{cld} - \rho_a(z = z_{cld})\right]\right\}\,H_{eff}\,(1+h_d)}{\rho_{cld}}}\,,\; C_m = \Gamma\left[1+\frac{1}{m}\right]$$

where $C_E = 1.15$ is the Van Ulden[26] cross-wind spreading parameter[xxi].

[xx] See Appendix B in UDM thermodynamics theory for evaluation of C_p^{cld}, the dynamic viscosity μ_{ac} and the diffusivity D_{ac}.

[xxi] IMPROVE. In the literature, models either assume ρ_{cld} or ρ_a in the denominator for the spreading law [HEGADAS, DEGADIS assume ρ_{cld}; most instantaneous models assume ρ_a; see the UDM verification manual for further details and discussion]. The 'gravity' force $g\,H_{eff}(1+h_d)\,(\rho_{cld}-\rho_a)$ compares to the resistance force of $\rho_a[dW_{eff}/dt]^2$. This leads to dW_{eff}/dt = constant * $[g\,H_{eff}(1+h_d)\,(\rho_{cld}-\rho_a)/\rho_a]^{1/2}$. Thus using ρ_a instead of ρ_{cld} may be more appropriate. However for most cases using ρ_{cld} instead of ρ_a will not make significant difference.

3. Passive spreading. After the passive transition the passive spread rate is applied [$\sigma_{ya}(x)$ = ambient passive dispersion coefficient; $x_0 = 0$ presently]

$$\frac{dR_y}{dx}[at\ x] = 2^{0.5}\frac{d\,\sigma_{ya}}{dx}[at\ \ x - x_o], \quad \text{continuous}$$

$$\frac{dR_y}{dt}[at\ \ x] = u_x\,2^{0.5}\frac{d\,\sigma_{ya}}{dx}[at\ \ x - x_o], \quad \text{instantaneous}$$

See Section 3.6 for full details.

3.3 Phases in cloud dispersion; transitions

The subsequent phases of cloud dispersion are determined by elevated dispersion, touchdown (impact), transition from jet to heavy dispersion, and transition from jet/heavy to passive dispersion. In addition the plume may lift-off or capped by the mixing layer. Figure 30 illustrates the subsequent phases of dispersion for a range of scenarios:

(a) Elevated jet/plume, which does not touch down or hits the mixing layer
(b) Elevated jet/plume, which becomes passive during touching down [no full touchdown; centre-line remains above the ground]
(c) Elevated jet/plume, which becomes passive after full touchdown
(d) Ground-level plume, which becomes buoyant and lifts off
(e) Jet/plume, which hits the mixing layer

The subsequent phases of cloud dispersion for a continuous or instantaneous cloud are as follows:

1. Energetic instantaneous expansion (instantaneous cloud only)
   1.1. Elevated jet/plume: before touchdown/capping, and before passive criterion is met
   1.2. [ends with touching down, or passive criterion met]
   1.3. Elevated passive cloud: before touchdown/capping, and after passive criterion is met [including transition to passive]
2. Touching down: after edge touch down, and before cloud centre-line reaches ground [during touching down possible transitions from 'jet' to 'heavy', 'passive', or lift-off]
   2.1. Grounded 'jet': after touchdown, before spread rate reduces to heavy-gas spread rate, before passive criterion is met and before lift-off
   2.2. Grounded dense plume: after touchdown, after transition jet to heavy, before passive criterion is met and before lift-off
3. Grounded passive plume: after touchdown, after passive criterion is met, before lift-off
4. Lifting off: after lift-off criterion has been met, before aloft (edge lift-off)
5. Aloft after lifting off
6. Becomes dense after beginning lift-off
7. Edge touching down again
8. Capping at mixing layer
9. Capped at mixing layer

The following is assumed in the present UDM version [xxii] :

Plume entrainment
- $E_{tot} = E_{jet}+E_{cross}+E_{pas}^{nf}$, elevated 'jet' before passive-transition and touchdown and before capping
- $E_{tot} = E_{pas}^{nf} + \max(E_{jet}+ E_{cross},E_{hvy})$ after touching down or after capping; E_{cross} , E_{pas}^{nf} are phased out during touching down and E_{hvy} is phased in during touchdown; E_{cross} is is phased out during capping
- along transition zone to passive: phase out total near-field entrainment and phase in far-field passive entrainment E_{pas}^{ff}
- downwind of passive-transition zone: $E_{tot} = E_{pas}^{ff}$

Forces acting on plume:
- ground drag force is applied for grounded plume, phased in during touching down, phased out during lifting
- plume impact force is applied during touching down

Plume spreading:
- circular plume until passive transition or (for grounded plume) spread rate reduces to heavy-spread rate
- otherwise before passive transition, heavy spread rate
- along transition zone to passive: phase out near-field spread rate and phase in passive spread rate
- downwind of passive-transition zone: passive spread rate $d\sigma_{ya}/dx$

Table 3 illustrates the controlling mechanisms during the phases of dispersion.

Transition zone from near-field dispersion to far-field passive dispersion

[xxii] IMPROVE - The heavy spread rate should not be applied after lifting off. The logic after lift-off needs further investigation.

The transition distance x_{tr}^{pas} is the downwind distance at the onset of transition to passive, and $r_{tr}^{pas}\, x_{tr}^{pas}$ is the downwind distance at the end of transition to passive. Along the transition zone $x_{tr}^{pas} < x < r_{tr}^{pas}\, x_{tr}^{pas}$, the near-field entrainment E_{tot}^{nf} and spread rate $(dR_y/ds)^{nf}$ are phased out, while the far-field passive entrainment E_{pas}^{ff} and passive spread rate $(dR_y/ds)^{ff} = d\sigma_{ya}/dx$ are phased in:

$$\begin{aligned} dR_y/ds &= [1-f(x)]\ (dR_y/ds)_{nf} + [f(x)]\ 2^{1/2}(d\sigma_{ya}/ds) \\ E_{tot} &= [1-f(x)]\ E_{tot}^{nf} + [f(x)]\ E_{pas}^{ff} \end{aligned} \qquad \textbf{(50)}$$

where the linear smoothing function f(x) is given by $f(x) = [x - x_{tr}^{pas}]/[r_{tr}^{pas}\, x_{tr}^{pas} - x_{tr}^{pas}]$. The above transition is needed to avoid discontinuous entrainments and discontinuous spread rates. This will smoothen curves, but retains the disadvantage of a rather arbitrary transition distance.[xxiii]

The distance x_{tr}^{pas} is defined by the first distance at which both the cloud speed is sufficiently close to the wind speed, the cloud density sufficiently close to the ambient density, the 'passive-type of entrainment to be close to the total entrainment, and (after touchdown) the Richardson number Ri_* to be sufficiently small

$$|u_{cld}/u_a(z_c)-1| < r_u^{pas},\ \ |\rho_{cld}/\rho_a(z_{cld})-1| < r_\rho^{pas}$$

$[1 - (E_{pas}^{nf})/E_{tot}] < r_E^{pas}$ (elevated), $[1-(E_{pas}^{nf} + E_{hvy})/E_{tot}] < r_E^{pas}$ (during lifting or touchdown) or $[1 - E_{hvy}/E_{tot}] < r_E^{pas}$ (after touchdown)

$Ri_* < Ri_*^{cr}$ (for ground-level plume only)

Note that in general transition to passive may occur during all stages, i.e. elevated dispersion, touching down, after touchdown, lifting, capping and capped; and from 'jet' to passive and from dense to passive.

Recommended values of the above transition parameters are:

- $r_u^{pas} = 0.1$, $r_E^{pas} = 0.3$. These values are in line with HGSYSTEM assumptions[27].
- $r_\rho^{pas} = 0.015$. This value is in line with the former UDM assumption. Note that CCPS guidelines quotes a range $0.001 < r_\rho^{pas} = 0.01$. The DEGADIS model adopts 0.001. Since averaging time effects will not be included as long as the transition criterion is not achieved, the larger UDM value is maintained
- $Ri_*^{pas} = 15$. This value assures that $\Phi(Ri_*) < \Phi(Ri_*^{pas}) \approx 2$, and therefore the heavy-gas top-entrainment velocity $u_{top} = \kappa u_*/\Phi(Ri_*)$ at transition is not more than twice as small as its passive limit $u_{top} = \kappa u_*/\Phi(0)$. Again since averaging time effects will not be included as long as the transition criterion is not achieved, a rather large value of the critical Richardson number Ri_*^{pas} is selected[xxiii].
- $r_{tr}^{pas} = 2$. This value should be sufficiently large to smoothen the discontinuities between the near-field and far-field passive entrainment and spread-rates.

[xxiii] IMPROVE. In future removal of the rather arbitrary transition zone should be considered. Also the density criterion may need to be fully replaced by a Richardson number criterion. Finally the transition parameter Ri_*^{pas} may need reduced to ensure that heavy-gas entrainment is more close to its passive limit. See the transition chapter in the UDM verification manual for a detailed discussion.

Phase	E_{jet}	E_{cross}	E_{pas}^{nf}	E_{hvy}	E_{pas}^{ff}	F_{drag}^{ground}	F_{impact}^{ground}	F_{drag}^{air}	spreading differential equation	time averaging
0. energetic inst. expansion	n.a.	n.a.	n.a.	n.a.	n.a.	n.a.	n.a.	n.a.	special module (instantaneous only)	-
1a. elevated jet	x	x	x	-	-	-	-	x	$R_y = R_z$ (circular)	-
1b. elevated trans.to pass.	ph.out	ph.out	ph.out	-	ph.in	-	-	x	phase in passive rate	ph. in
elevated passive	-	-	-	-	x	-	-	-	passive rate	x
2. touching down, jet	x	x	x	ph.in	-	ph.in	x	x	$R_y = R_z$	-
touching down, dense	-	-	-	ph.in	-	ph.in	x	x	heavy rate	-
touching d. tr.to pass.	ph.out	ph.out	ph.out	ph.out	ph.in	ph.in	x	x	phase in passive rate	ph. in
touching down, passive	-	-	-	-	x	ph.in	x	-	passive rate	x
3a. grounded jet	x	-	-	x	-	x	-	-	$R_y = R_z$	-
3b. grounded dense	-	-	-	x	-	x	-	-	heavy rate	-
4. grounded trans.to pass.	ph.out	-	ph.out	ph.out	ph.in	x	-	-	phase in passive rate	ph. in
grounded passive	-	-	-	-	x	-	-	-	passive rate	x
5. lifting off, bef. passive	x	x	x	ph. out	-	ph.out	-	x	heavy rate[xxiv] before passive transition	-
6 aloft after lift-off, bef.pa.	x	x	x	-	-	-	-	x	heavy rate[xxiv] before passive transition	-
7. dense after lift-off,b.pa.	x	x	x	-	-	-	-	x	heavy rate[xxiv] before passive transition	-
8. edge touchdown,bef.pas.	x	x	x	ph. in	-	-	x	x	heavy rate[xxiv] before passive transition	-
9. capping, before passive	x	x	x	-	-	-	-	x	no previous touchd.: $R_y=R_z$, before pas.tr. previous touchd.: heavy rate[xxiv] before pas.tr.	-
10. capped, before passive	x	-	x	-	-	-	-	-	no previous touchd.: $R_y=R_z$, before pas.tr. previous touchd.: heavy rate[xxiv] before pas.tr.	-

Table 3. Phases during cloud dispersion (continuous and instantaneous releases)

[xxiv] $R_y=R_z$ if transition has not yet taken place from jet to heavy spreading rate; transition may take place from jet to heavy, prior to transition to passive

3.4 Air entrainment

Air entrainment into a plume may be caused by a range of mechanisms:

- 'jet' entrainment is caused by turbulence resulting from the difference between the jet speed and the ambient wind speed
- cross-wind entrainment in response to the deflection of the plume by the wind
- passive entrainment is caused by ambient turbulence
- heavy-gas entrainment is the reduced air entrainment included for a grounded heavy-gas plume

Thus the total air entrainment E_{tot} (kg/m/s) is taken for an elevated 'jet' as[xxv]

$$\begin{aligned} E_{tot} &= E_{jet} + E_{cross} + E_{pas}^{nf}, && x < x_{tr}^{pas} \\ &= f(x)\,[E_{jet} + E_{cross} + E_{pas}^{nf}] + [1-f(x)]\,E_{pas}^{ff}, && x_{tr}^{pas} < x < r_{tr}^{pas}\, x_{tr}^{pas} \\ &= E_{pas}^{ff} && x > r_{tr}^{pas}\, x_{tr}^{pas} \end{aligned} \qquad \textbf{(51)}$$

and for a grounded 'jet' as

$$\begin{aligned} E_{tot} &= \max\{E_{jet} + E_{cross}, E_{hvy}\} + E_{pas}^{nf}, && x < x_{tr}^{pas} \\ &= f(x)\,[\max\{E_{jet} + E_{cross}, E_{hvy}\} + E_{pas}^{nf}] + [1-f(x)]\,E_{pas}^{ff}, && x_{tr}^{pas} < x < r_{tr}^{pas}\, x_{tr}^{pas} \\ &= E_{pas}^{ff} && x > r_{tr}^{pas}\, x_{tr}^{pas} \end{aligned} \qquad \textbf{(52)}$$

Here E_{jet}, E_{cross}, E_{pas}^{nf}, E_{hvy}, E_{pas}^{ff}, are respectively the jet entrainment, the cross-wind entrainment, the near-field passive entrainment, the heavy-gas entrainment[xxvi] and the far-field passive entrainment.

Many reviews exist on jet dispersion and entrainment relations. Recent reviews include Lees (1996)[28], the TNO yellow book (1997)[29], and Section 5.2 in the CCPS guidelines (1996)[30]. Appendix B contains the results of a literature review of entrainment formulations, which provides a basis for the selection of the formulations of the above UDM entrainment terms. In the remainder of this section, the adopted expressions for the jet entrainment E_{jet}, the cross-wind entrainment E_{cross}, the near-field passive entrainment E_{pas}^{nf}, the heavy-gas entrainment E_{hvy}, and the far-field passive entrainment E_{pas} are given.

3.4.1 Jet entrainment

'Jet' entrainment results from the difference between the jet speed and the ambient wind speed. Thus it is present both for a jet (plume speed larger than ambient wind speed) and a plume which moves less fast than the wind.

Formulations for free turbulent momentum jets in stagnant air have been formulated by Ricou and Spalding (1961)[31] and Morton, Taylor and Turner (1956)[32]. In these formulations circular jets were considered ($P_{above} = 2\pi R$ with R the jet radius), with $\rho_{cld} = \rho_{air}$.

[xxv] JUSTIFY. In the code the total entrainment is adjusted as $E_{tot} = E_{tot} * \max(0.01, 1 - \eta_{cL})$, if the cloud is 'slumping', i.e. if the cloud is instantaneous and the spreading velocity $U_{spd} = \sqrt{\max(g \times H_{eff}\,(1+h_d) \times \frac{\rho_{cld} - \rho_a(z_c)}{\rho_a(z_c)}, 0)}$ is larger than the expansion velocity $U_{exp} = (2E_{exp})^{0.5}$.

[xxvi] For heavy-gas ground-level non-jet plumes, concentrations will be too high if the transition is too early (at which passive entrainment is larger than heavy), but in the far-field E_{hvy} should approach E_{pas} [provided cloud density is close to the ambient density]

Formulations for the jet-entrainment E_{jet} (kg/m/s) in most continuous dispersion models are based on extensions of the above formulations for non-zero wind speed u_a, densities different from air, and possibly non-circular jets.

$$E_{jet} = \alpha_1 \left[m_{cld} \rho_a | u_{cld} - u_a \cos\theta | \right]^{1/2} \quad \text{(I – Ricou-Spalding)}$$

$$E_{jet} = e_{jet} \; P_{above} \; \rho_a \; | u_{cld} - u_a \cos\theta | \quad \text{(II – Morton-Taylor-Turner)}$$

Here I_{x2} is the excess horizontal momentum. The values of the coefficients may depend on the model assumptions, i.e. on the adopted wind-speed and concentration profiles [UDM 'Drift' profile, Gaussian profile or top-hat profile].

Ricou and Spalding formulation

Ricou and Spalding formulation $E_{jet} = \alpha_1[\rho_a I_{x2}]^{0.5}$ was used for non-zero wind speeds. Formulation (I) is an extension of Ricou-Spalding's formulation, which is used by Emerson[20] in the Technica model TECJET. Note that this formulation can be rewritten as

$$E_{jet} = \alpha_1 \rho_a u_{cld} \left[A_{cld} \frac{\rho_{cld}}{\rho_a} \left| 1 - \frac{u_a}{u_{cld}} \cos\theta \right| \right]^{1/2}$$

which for a circular jet reduces to ($A_{cld} = \pi R^2$, $P_{above} = 2\pi R$)

$$E_{jet} = e_{jet} P_{above} \rho_a u_{cld} \left[\frac{\rho_{cld}}{\rho_a} \left| 1 - \frac{u_a}{u_{cld}} \cos\theta \right| \right]^{1/2} \quad \text{(I*)}$$

Thus formulation (I) is identical to (II) in case of a circular jet, with u_a=0 and $\rho_{cld} = \rho_a$. Thus formulation (I*) is identical to (II) in case of u_a=0 and $\rho_{cld} = \rho_a$ (also after touchdown).

The formulation (I*) is considered to be preferable to the formulation (I), since it's proportional to P_{above}. For a plume touched down the formulation (I) assumes the same jet entrainment rate which seems to be wrong.

Comparison of formulations

Following comparison with experimental data, Wheatley (1987)[33] concluded the formulation (I,I*) is not valid when the density is significantly different from the ambient density, and formulation (II) is preferable.

A generalised formulation for two-phase jet dispersion is given by Webber and Kukkonen (1990)[34], who also consider both the Morton-Taylor-Turner and Ricou-Spalding models. They observe from sensitivity analyses that the different models do not have a larger direct effect than about 10% in the concentration values.

Evaluation of jet-entrainment coefficient α_1

Assuming a top-hat profile (jet of uniform density), Ricou-Spalding[31] determined from experiments $\alpha_1 = \pi^{0.5}\tan(\beta_\infty) = 0.282$, where β_∞=9.1° is the empirical value of the asymptotic half-angle of the jet.; this corresponds to $e_{jet} = 0.5 \tan(\beta_\infty) = 0.08$. The latter value is adopted in the HGSYSTEM top-hat program AEROPLUME.

Different ratios are quoted in the literature for conversion between top-hat profiles and Gaussian profiles, i.e. relations between top-hat concentration c_{pl} and maximum concentration c_o and top-hat radius R_{pl} and Gaussian radius R:

- Post[35] quotes that in Spalding's experiments the maximum concentrations were 70% higher: c_0/c_{pl} = 1.7
- Chen quoted by Lees[28]: c_0/c_{pl} = 1.6
- Long quoted by Lees[28]: c_0/c_{pl} = 2.0
- Roberts included in the HGSYSTEM program PROFILE conversion from AEROPLUME top-hat profile to Gaussian profile: c_0/c_{pl} = 1.481 (quoted to be the theoretical value), $R/R_{pl} = 1.481^{-0.5} = 0.82$. Thus $R_{pl}^2 c_{pl} = R^2 c_o$ and mass conservation $R_{pl}^2 c_{pl} u_{pl} = R^2 c_o u_{cld}$ applies if $u_{pl} = u_{cld}$.

As a result of the above c_0/c_{pl} = 1.7 is taken. Using the analytical solution for the UDM equations, this implies that the chosen UDM value equals α_1 = 0.282/1.7=0.17. Notice that this value corresponds to the value of Ooms, who also adopts a Gaussian profile. It is also close to the TECJET value of 0.142, who adopts the same type of excess-momentum equation.

In the UDM the continuous plume is replaced with an equivalent plume of maximum concentration c_0 and radius R [cloud mass $m_{cld} = \pi R^2 \rho_{cld} u_{cld}$]. Thus the visible plume (with averaged concentrations) is larger. Therefore the top-hat radius R_{pl} is larger than that the UDM radius R. In addition the top-hat cloud mass will be larger [$=\pi R_{pl}^2 \rho_{pl} u_{pl}$].

Therefore the analytical solution used for the UDM equations, adopt a smaller value of the cloud half-angle β [smaller value for α_1], a smaller Gaussian radius R, and a small cloud mass $m_{cld} = \pi R^2 \rho_{cld} u_{cld}$, than the top-hat profile. Since the top-hat cloud mass is larger than the UDM cloud mass, the entrainment coefficient is larger.

Conclusion

Following the above reasons, the recommended formulation implemented in the new UDM is the Morton-Taylor formulation

$$E_{jet} = e_{jet} \quad P_{above} \, \rho_a \, | u_{cld} - u_a \cos\theta | \quad \text{in} \quad \text{kg/m/s} \qquad \text{(continuous)} \tag{53}$$

with $e_{jet} = 0.5 \, \pi^{-0.5} \, \alpha_1$, and α_1 = 0.17.

Note that for the continuous plume E_{jet} is the cloud entrainment per unit of cloud axis length (kg/m/s), and P_{above} is the perimeter of the plume above the ground. For an instantaneous cloud, the 'jet' entrainment E_{jet} is the total air entrainment into the cloud (kg/s) and it is therefore natural to replace in the above equation the continuous plume perimeter P_{above} by the instantaneous equivalent S_{above} (cloud area above the ground). Thus the following formula is adopted for the instantaneous jet entrainment:

$$E_{jet} = e_{jet} \quad S_{above} \, \rho_a \, | u_{cld} - u_a \cos\theta | \quad \text{in} \quad \text{kg/s} \qquad \text{(instantaneous)} \tag{54}$$

3.4.2 Cross-wind entrainment

Morton

Cross-wind entrainment is associated with the formation in the wake of a rising or falling plume of trailing vortices in response to the deflection by the release plume of ambient air. Following Morton et al.[32] the cross-wind entrainment (kg/m/s) for continuous dispersion can be expressed as

$$E_{cross} = \alpha_2 \, \rho_a \, P_{above} \, | u_a \sin\theta |$$

Briggs (1984)[36] states that the best current value is α_2 = 0.60 for buoyant plumes and α_2 = 0.40+1.2/R for a jet [R = ratio of initial jet speed and ambient speed]. As for the jet entrainment, it appears to be that these values are applicable for a top-hat profile[xxvii].

Therefore analogous to the case of jet-entrainment, the value of the cross-wind coefficient α_2 = 0.6/1.7=0.35 can be applied to convert from the Briggs recommended top-hat value of 0.6 [used in HGSYSTEM] to the Gaussian profile. The formulation is intended to be used with a drag coefficient of zero.

Morton extended and near-field suppression (default)

Experimental data suggests the Morton model over-predicts entrainment in the near-field for low velocity releases. Based on a review of the literature and a comparison with published experiments, we have extended the Morton formulation to include an empirical near-field correction term. Based on the work of Kamotani & Greber[37] and Yuan & Street[38] we define a distances L_{core} and L_{supp} as:

[xxvii] JUSTIFY - Ideally to be further checked.

$$L_{core} = \frac{6.4D}{1 + (4.6/R)} L_{supp} = \left(1 + \sqrt{\frac{\rho_0}{\rho_\infty}}\right) L_{core} \qquad (55)$$

L_{core} is the region over which crosswind entrainment is completely suppressed, and L_{supp} the distance over which the Morton predicted values are eventually restored. Associated with this is a near-field non-zero crosswind air drag term C_D (see Section 3.5.1). Further details of the model are given in Appendix B.1

Conclusion

The adopted formula for cross-wind entrainment is a modified form of Morton's model:

$$E_{cross} = f\alpha_2 \rho_a P_{above} |u_a \sin\theta| \quad \text{in kg/m/s} \quad \text{(continuous)} \qquad (56)$$

with $\alpha_2 = 0.35$. The fraction f is defined by:

$$f(x) = \begin{cases} 0, & s < L_{core} \\ \left(\frac{s - L_{core}}{L_{supp} - L_{core}}\right), & L_{core} \le s < L_{supp} \\ 1, & s \ge L_{supp} \end{cases}$$

As for jet entrainment, the formula applicable for instantaneous dispersion is derived from the above formula for continuous dispersion by replacing the cloud perimeter P_{above} with the cloud area S_{above}. We retain the original Morton form and omit the f term:

$$E_{cross} = \alpha_2 \rho_a S_{above} |u_a \sin\theta| \quad \text{in kg/s} \quad \text{(instantaneous)} \qquad (57)$$

The original Morton model, and the Ooms model are also included as non-default options – see Appendix B for further details.

3.4.3 Near-field passive entrainment

Continuous dispersion

Passive entrainment is caused by ambient turbulence. The near-field passive entrainment formulation is taken from McFarlane[22] based on experiments by Disselhorst (1987)[39]. The near-field entrainment is defined by

$$E_{pas}^{nf} = \left[1 - \frac{W_{gnd}}{R_y}\right] \pi \rho_a e_{pas} \varepsilon^{1/3} \left(l_y^{4/3} + l_z^{4/3}\right) \quad \text{in kg/m/s} \quad \text{(continuous)} \qquad (58)$$

Here the coefficient $e_{pas} = 1$; the turbulent (transverse horizontal, vertical) eddy length scales l_y, l_z, and the dissipation rate of kinetic energy ε are given by

$l_y = \min\{R_y, 0.88(z_c+z_0)L_y(Z)\}$, $l_z = \min\{R_y, 0.88(z_c+z_0)L_z(Z)\}$
$\varepsilon = E(Z)\, u_*^3/[\kappa(z_c+z_0)]$

where $Z = (z_c+z_0)/L$, z_c the centroid height, z_0 the surface roughness length, L the Monin-Obukhov length L, u_* the friction velocity, κ the Von Karman constant. The functions $L_y(Z)$, $L_z(Z)$ and $E(Z)$ are defined as a function of stability class by

$L_y(Z) = L_z(Z) = (1-7.4\kappa Z)/E(Z)$, $E(Z) = 1 - 5\kappa Z$,	stability class = A,B,C
$L_y(Z) = L_z(Z) = E(Z) = 1$	stability class = D
$L_y(Z) = 1 / (1+0.1Z)$, $L_z(Z) = 1/ E(Z)$, $E(Z) = 1 + 4Z$,	stability class = E,F

Note that the near-field passive entrainment is phased out during touchdown.[xxviii]

Extension to instantaneous dispersion

The above formulation is applicable to continuous dispersion only. For sufficiently high continuous cloud $l_y=l_z=R_y=R_z$ and $W_{gnd}=0$. Thus $E_{pas}^{nf} = e_{pas}\rho_{air}\,[2\pi R_y]\,(\varepsilon R_y)^{1/3}$, where $e_{pas} = 1$ and $u'=(\varepsilon R_y)^{1/3}$ is the air entrainment velocity (m/s). This formulation corresponds to the formulation adopted by Ooms (see Appendix B).

Therefore (similarly to the jet and cross-wind entrainment formulations) a natural extension for an instantaneous spherical plume with surface area $4\pi R_y^2$ is: $E_{pas}^{nf} = e_{pas}\rho_a\,[4\pi R_y^2]\,(\varepsilon R_y)^{1/3}$. Assuming $l_x=l_y$ (in line with $R_x=R_y$ assumption) , this suggests the following instantaneous formulation

$$E_{pas}^{nf} = \left[1-\frac{W_{gnd}}{R_y}\right]\frac{4\pi}{3}\,\rho_a\; e_{pas}\,\varepsilon^{1/3}\left(l_x^{\,7/3}+l_y^{\,7/3}+l_z^{\,7/3}\right) \qquad \text{in kg/s (instantaneous)} \qquad (59)$$

This assumption is consistent to the continuous formulation. For stability classes A,B,C,D moreover $l_x=l_y=l_z$ and for sufficiently high cloud $W_{gnd}=0$, $l_x=l_y=l_z=R_y$ and E_{pas}^{nf} reduces to the above expression $E_{pas}^{nf} = e_{pas}\rho_a\,[4\pi R_y^2]\,(\varepsilon R_y)^{1/3}$.

3.4.4 Heavy-gas entrainment

Dense gas and aerosol clouds are known to suppress dispersion below that obtained by ambient turbulence (passive dispersion) in the surrounding atmosphere. This phenomenon is described in the UDM by making the dominant (top) entrainment velocity depend on the layer Richardson number, an indicator of cloud buoyancy.

Heavy-gas entrainment for instantaneous plume

For an instantaneous release the heavy gas entrainment rate E_{hvy} (kg/s) is given by

$$E_{hvy} = \left[\frac{W_{gnd}}{R_y}\right]\left\{u_{side}A_{side}+u_{top}A_{top}\right\}\rho_a \qquad (60)$$

where u_{side} is the horizontal air-entrainment velocity through the plume side-area A_{side}, u_{top} is the vertical air-entrainment velocity through the plume top-area A_{top}. The side area A_{side} and the top area A_{top} correspond to an instantaneous plume of cylindrical shape with height $H_{eff}(1+h_d)$ and radius W_{eff},

$$A_{side} = 2\pi\, W_{eff}\, H_{eff}\,(1+h_d)\;, \qquad A_{top} = \pi\, W_{eff}^2 \qquad (61)$$

Note that the term $[W_{gnd}/R_y]$ in Equation (60) ensures that the heavy-gas entrainment is not applied for an elevated plume, is phased in during touching down and phased out during lifting-off.

Heavy-gas entrainment for continuous plume

For a continuous cloud the heavy gas entrainment rate E_{hvy} (kg per second per unit of downwind length of the plume) at a given downwind distance is given by

$$E_{hvy} = \left[\frac{W_{gnd}}{R_y}\right]\left\{u_{side}H_{eff}\,(1+h_d)+u_{top}(2W_{eff})\right\}\rho_a \qquad (62)$$

[xxviii] The passive-entrainment formula is taken to be compatible with those adopted by Ooms and HGSYSTEM (based on Disselhorst experiments). It may need to be further refined, in order to ensure full convergence to the passive formula in the far field automatically. This may involve considering the use of an alternative formula for the near-field and/or far-field passive entrainment.

where the cloud width and height are chosen to correspond to the effective cloud width $2W_{eff}$ and the effective cloud height $H_{eff}(1+h_d)$.

Side entrainment velocity

The side surface entrainment velocity is taken to be proportional to the spread rate or

$$u_{side} = \gamma \frac{dW_{eff}}{dt} \quad (63)$$

where γ is an edge-entrainment coefficient. For a continuous release the side entrainment is ignored [γ=0].

Top entrainment velocity

The top surface entrainment generally dominates over the side entrainment except very near the source. The top surface entrainment velocity u_{top} is formulated to have the same functionality as the vertical dispersion coefficient, K_z. That is, for a vertical wind profile in a power law form:

$$u_a(z) = u_a(z_{ref}) \left(\frac{z}{z_{ref}} \right)^p \quad (64)$$

K_z satisfies the two-dimensional dispersion relationship:

$$u_a(z) \frac{\partial c}{\partial x} = \frac{\partial}{\partial z} \left(K_z \frac{\partial c}{\partial z} \right) \quad (65)$$

with a functional form given by:

$$K_z = \frac{\kappa u_* z}{\Phi(Ri_*)} \quad (66)$$

where κ=0.4 is the Von Karman constant, and Φ the entrainment function of the Richardson number Ri_*.

To retain this form, the top-entrainment velocity u_{top} is defined by:

$$u_{top} = \frac{\kappa u_*}{\Phi(Ri_*)} \quad (67)$$

Richardson number, entrainment function

The layer Richardson Number is defined by[xxix]:

$$Ri_* = \frac{g \left[\rho_{cld} - \rho_a(z = z_{cld}) \right] H_{eff}(1+h_d)}{\rho_a u_*^2} \quad (68)$$

where z_{cld} is the centre-line height.

The entrainment function $\phi(Ri_*)$ represents the phenomenon that heavy gases (Ri_*>0) tend to suppress turbulent mixing within a cloud below that of ambient turbulence. On the other hand, positively buoyant clouds (Ri_*<0) lifting off are known to have enhanced turbulence. The entrainment function is given as follows,

[xxix] Note that HEGADAS uses the definition $Ri_* = g[\rho_{cld}-\rho_a(z=H_{eff})]H_{eff} / [\rho_a(z=0)u_T^2]$ with the friction velocity u_T modified for heat transfer. In the old UDM $Ri_* = g[\rho_{cld}-\rho_a(z=z_c)]H_{eff} / [\rho_{cld}u_*^2]$

$$\Phi(Ri_*) = \frac{1}{1+0.65\,|\,Ri_*|^{0.6}}\ , \qquad Ri_* < 0$$

$$= 1 \qquad 0 < Ri_* < 2.3625$$

$$= (1 + 0.8\ Ri_*)^{1/2}/1.7 \qquad 2.3635 < Ri_* < 14.72$$

$$= Ri_* / 7 \qquad Ri_* > 14.72$$

(69)

For $Ri_* < 0$, the above formula is taken from the correlation adopted by Havens and Spicer for the model DEGADIS[40].

For $Ri_* > 0$, the formulation adopted by Witlox (1989)[41] is adopted. The latter formulation is based on an entrainment function proposed by Britter (1988)[42]. It is close to those adopted by DEGADIS and the HGSYSTEM model AEROPLUME[43]. In addition the above function does accurately fit experimental data for a wide range of Richardson numbers.

Figure 31a plots the original UDM 5.2 curve for $Ri_*>0$ in comparison with data by McQuaid (1976)[44] and by Kranenburg (1984)[45]. Kranenburg's data were measured using a straight water channel with wind-induced flow of water over a salt solution. His data have a distinct dependence on $Ri_*^{-1/2}$. Also shown in Figure 31a for comparison are data by Scranton and Lindberg (1983)[46] and Kantha, Phillips, and Azad (1977)[47]. The data of Scranton and Lindberg are substantially overlapped by those of Kato and Phillips (1969)[48]. These latter data are all taken with an annular water tank. A shear wheel moved the upper water surface which mixed with a lower salt water layer. Scranton and Lindberg point out that radial profiles are set up in an annular tank which makes these data less applicable to an unconstrained heavy gas cloud. Furthermore, Deardorf and Willis (1982)[49], using an annular tank, confirm the Richardson Number dependence to the -1/2 power, and reconcile why the annular tank data drop below the straight channel data. They attribute it to variability in the velocity profile, which contributes an additional undesirable entrainment mechanism.

Figure 31b plots the new original UDM 5.2 curve for $Ri_*>0$ in comparison with data by McQuaid (1976)[44], Kantha et al. (1977) [47] and Lofquist (1960)[50]. The new UDM 6.0 curve is more in line with the Ri_*^{-1} dependence as used by Havens and Spicer (1990)[51], Cox and Carpenter (1980)[52], and a number of others.

3.4.5 Far-field passive entrainment

Passive dispersion is represented by correlations for the ambient horizontal (σ_{ya}) and vertical (σ_{za}) dispersion coefficients. The correlations used in the Unified Dispersion Model are taken from McMullen (1975)[53] for σ_{ya} and from Hosker (1973)[54] for σ_{za}. These correlations depend upon the stability class and distance from the release point. For σ_{ya} it also depends on the averaging time t_{av} and for σ_{za} it also depends on the surface roughness length z_0.

Ambient cross-wind dispersion coefficient

The ambient cross-wind dispersion coefficient σ_{ya} is based on a formula by McMullen (1975) for downwind distance x larger than L, and is assumed to vary linearly for x<L,

$$\sigma_{ya}(x) = \left(\frac{t_{av}}{600}\right)^{0.2} e^{I + J[\ln(x/1000)] + K[\ln(x/1000)]^2}\ , \quad x > L$$

$$= \frac{x}{L}\ \sigma_{ya}(L) \qquad , \quad x < L$$

(70)

Here x is the downwind distance from the source (m), and t_{av} the averaging time t_{av} (s); the coefficients I, J, K, L (with L in m) are given as a function of stability class by[xxx]

[xxx] Values of I,J,K at stability classes A,B,C,D,E,F from McMullen (1975). Values for intermediate stabilitiy classes obtained from interpolation. Unknown origin for chosen values for L as function of stability class.

stab.cl.	A	A/B	B	B/C	C	C/D	D	E	F	G
I	5.357	5.208	5.058	4.855	4.651	4.441	4.230	3.922	3.533	3.144
J	0.8828	0.8926	0.9024	0.9103	0.9181	0.9202	0.9222	0.9222	0.9181	0.9024
K	-0.0076	-0.0080	-0.0096	-0.0080	-0.0076	-0.0080	-0.0087	-0.0064	-0.0070	-0.0070
L (m)	0.4481	1.2156	6.1992	3.6748	4.5704	6.8227	11.433	2.2925	2.8799	0.9383

Ambient vertical dispersion coefficient

The ambient vertical dispersion coefficient σ_{za} is based on a formula by Hosker (1973)[54] for downwind distances larger than 100 m, and is assumed to vary linearly for downwind distance less than 100m. It is a function of the downwind distance x (m), the stability class, and the surface roughness z_0 (m),

$$\sigma_{za}(x) = F(z_0;x)\ g(x), \quad x > 100 \text{ m}$$
$$= \frac{x}{100}\sigma_{za}(100), \quad x < 100 \text{ m} \qquad (71)$$

Here the function g(x) is the vertical dispersion coefficient for surface roughness 0.1m and is given by

$$g(x) = \frac{a_1 x^{b_1}}{1 + a_2 x^{b_2}} \qquad (72)$$

with the coefficients a_1, b_1, a_2, b_2 defined as a function of stability class by[xxxi]

stab.cl.	A	A/B	B	B/C	C	C/D	D	E	F	G
a_1	0.112	0.121	0.130	0.121	0.112	0.105	0.098	0.0609	0.0638	0.065
b_1	1.06	1.01	0.950	0.935	0.920	0.905	0.889	0.895	0.783	0.671
a_2	5.38E-4	5.95E-4	6.52E-4	7.79E-4	9.05E-4	1.13E-3	1.35E-3	1.96E-3	1.36E-3	9.05E-4
b_2	0.815	0.783	0.750	0.734	0.718	0.703	0.688	0.684	0.672	0.660

The function $F(z_0,x)$ applies the effect of the surface roughness z_o and is given by

$$F(z_0;x) = \ln\left\{\frac{c_1 x^{d_1}}{1 + c_2 x^{d_2}}\right\}, \quad z_o < 0.1 \text{ m}$$
$$= \ln\left\{c_1 x^{d_1}\left[1 + \frac{1}{c_2 x^{d_2}}\right]\right\}, \quad z_o > 0.1 \text{ m} \qquad (73)$$

where the coefficients c_1, d_1, c_2, d_2 are given for the various roughness lengths by

surface roughness (m)	c_1	d_1	c_2	d_2
0.01	1.56	0.0480	6.25E-4	0.45
0.04	2.02	0.0269	7.76E-4	0.37
0.1	e[xxxii]	0	0	0
0.4	5.16	-0.098	18.6	-0. 225
1	7.37	-0.0957	4.29E3	-0.60
4	11.7	-0.128	4.59E4	-0.78

Let $0.01<z_o<4$, then the values for $F(z_o,x)$ are obtained from the above via interpolation between the surrounding surface roughness lengths z_{oa}, z_{ob} (e.g. for $z_o = 0.08$, $z_{oa} = 0.04$ and $z_{ob} = 0.1$),

[xxxi] Values at stability classes A,B,C,D,E,F from Hosker (1973). Others obtained from interpolation.

[xxxii] e = 2.71828… is the base of the natural logarithm (ln).

$$F(z_o, x) = F(z_{oa}, x) + \frac{\log(z_o) - \log(z_{oa})}{\log(z_{ob}) - \log(z_{oa})}\left[F(z_{ob}, x) - F(z_{oa}, x)\right] \quad (74)$$

For $z_o < 0.01$ m, the value at 0.01 m is assumed: $F(z_o,x) = F(0.01,x)$.
Likewise for $z_o > 4$ m, the value at 4 m is assumed: $F(z_o,x) = F(4,x)$.

Discussion

Different dispersion coefficients have been found for urban and rural data. One approach to reconciling these differences was suggested by Hosker (1973), and is currently incorporated in the Unified Dispersion Model. This attributes the differences between urban and rural σ_z curves to the surface roughness length. Essentially, weighted average coefficients are found between the values for urban conditions given by McElroy and Pooler (1968)[55] and those for rural conditions given by Turner (1969)[56] and Smith (1968)[57].

An alternative approach has been suggested by McFarlane et. al (1990)[43], citing Hanna et al. (1982)[58] and Pasquill and Smith (1983)[59], who attributes the differences between urban and rural σ_z to differences in the averaging time of the measurements. By applying an averaging time correction, the two sets of data are resolved into one, without the need to invoke a surface roughness effect on σ_z.

Passive-dispersion entrainment

For a continuous cloud, the entrainment rate by the far-field passive dispersion mechanism, E_{pas}^{ff} (kg/m/s) is given by[xxxiii]:

$$E_{pas}^{ff} = A_{cld}(x)\left[\frac{1}{\sigma_y}\frac{d\sigma_{ya}}{dx} + \frac{1}{\sigma_z}\frac{d\sigma_{za}}{dx}\right]\rho_a(z = z_{cld})\;\; u_a(z = z_c) \quad (75)$$

while for an instantaneous cloud E_{pas}^{ff} is given by (kg/s)

$$E_{pas}^{ff} = V_{cld}(x)\left[\frac{2}{\sigma_y}\frac{d\sigma_{ya}}{dx} + \frac{1}{\sigma_z}\frac{d\sigma_{za}}{dx}\right]\rho_a(z = z_{cld})\;\; u_a(z = z_c) \quad (76)$$

[xxxiii] JUSTIFY - In the above equations $d\sigma_{ya}/dx$ and $d\sigma_{za}/dx$ were originally evaluated at $x - x_o$ with x_o a virtual source distance such that spread rate is continuous. However the use of x_o in code has been eliminated (why?), and instead the continuous spread rate is obtained via a more arbitrary smoothing algorithm. Note that strictly speaking for continuous, $E_{pas} = \rho_a u_a\,[\partial A_{cld}/\partial x] = \rho_a u_a\;\partial/\partial x[4\Gamma(1+n^{-1})\,\Gamma(1+m^{-1})(1+h_d)\sigma_y\sigma_z]$. This leads to Equation (76) ignoring downwind variations of n,m,h_d and assuming $\partial\sigma_y/\partial x = \partial\sigma_{ya}/\partial x$, $\partial\sigma_z/\partial x = \partial\sigma_{za}/\partial x$. Likewise for instantaneous: $E_{pas} = \rho_a u_a\,[\partial V_{cld}/\partial x] = \rho_a u_a\;\partial/\partial x[\pi\Gamma(1+s^{-1})\,\Gamma(1+2m^{-1})\,\sigma_y^2\sigma_z]$.

3.5 Momentum equations

The adopted momentum equations (vector notation) are as follows for continuous dispersion [cloud area $A_{cld} = m_{cld} / (\rho_{cld} u_{cld})$], [xxxiv]

$$\begin{bmatrix} \frac{dI_{x2}}{ds} \\ \frac{dI_z}{ds} \end{bmatrix} = F_{drag}^{air} \begin{bmatrix} |\sin\theta| \\ -\cos\theta \frac{\sin\theta}{|\sin\theta|} \end{bmatrix} + F_{impact}^{ground} \begin{bmatrix} -\sin\theta \\ 0 \\ \cos\theta \end{bmatrix} + F_{drag}^{ground} \begin{bmatrix} 1 \\ 0 \end{bmatrix} + A_{cld}(\rho_{cld} - \rho_a) g \begin{bmatrix} 0 \\ -1 \end{bmatrix} \quad (77)$$

and for time-dependent dispersion [cloud volume $V_{cld} = m_{cld} / \rho_{cld}$] [xxxv],

$$\begin{bmatrix} \frac{dI_{x2}}{dt} \\ \frac{dI_z}{dt} \end{bmatrix} = F_{drag}^{air} \begin{bmatrix} |\sin\theta| \\ -\cos\theta \frac{\sin\theta}{|\sin\theta|} \end{bmatrix} + F_{impact}^{ground} \begin{bmatrix} -\sin\theta \\ 0 \\ \cos\theta \end{bmatrix} + F_{drag}^{ground} \begin{bmatrix} 1 \\ 0 \end{bmatrix} + V_{cld} (\rho_{cld} - \rho_a) g \begin{bmatrix} 0 \\ -1 \end{bmatrix} \quad (78)$$

The terms in the right-hand side represent forces on the plume. They are respectively:

- the air-borne drag force F_{drag}^{air} (N/m or N). This force is perpendicular to the plume centre line, with a positive downwind x-component. It is proportional to the airborne drag coefficient C_{Da}. The force is currently ignored by setting C_{Da}=0.
- the ground impact force F_{impact}^{ground} (N/m or N) resulting from plume collision with the ground. This force is perpendicular to the plume centre line, and is added during touching down only.
- the horizontal ground drag force F_{drag}^{ground} (N/m or N). This force is added after onset of touchdown only.
- the vertical buoyancy force (N/m or N). This force is proportional to the gravitational acceleration g (= 9.81 m^2/s) and the density difference between the plume and the air. It is directed downwards for a dense plume.

Expressions for the airborne drag force, the ground impact force, and the ground drag force are derived in the Sections 3.5.1,3.5.2, and 3.5.3 below.

During touchdown the plume impact force reduces vertical momentum, and after touchdown the vertical momentum equals zero. A grounded plume may lift off from the ground if the buoyancy forces exceed the turbulent forces within the ambient boundary layer. The UDM lift-off criterion for a grounded plume is taken from Briggs[60],

$$Ri_* = \frac{g\left[\rho_{cld} - \rho_a(z = z_{cld})\right] H_{eff}}{\rho_a u_*^2} < -20 \quad (79)$$

where Ri_* is the Richardson number (see Equation (68)). Note that the above criterion implies that lift-off will never occur for a heavy cloud. For a buoyant cloud (ρ_{cld}-ρ_a < 0), the above criterion implies that lift-off will occur if the windspeed u_a is sufficiently small [small $u_a(z)$ implies small friction velocity u_*]. In addition we

[xxxiv] JUSTIFY – Note that McFarlane[22] includes for airborne plume also the horizontal shear force associated with the vertical gradient of the wind speed = $(dm_{cld}/dt) \sin(\theta) du_w/dz$.

[xxxv] Note that instantaneous equation is only used after energetic expansion, at which excess momentum probably has become negligible.

stipulate that the criterion be continuously met for a time, t_{lo}. This is defined as the time required for the buoyancy force to displace the cloud upwards by a characteristic vertical distance D

$$D = 0.5\sqrt{W_{eff}H_{eff}}$$

This leads to

$$t_{lo}^2 = \frac{\rho_a\sqrt{W_{eff}H_{eff}}}{g(\rho_{cld} - \rho_a)}$$

As described in the above excess momentum equations, the cloud will not rise higher than the mixing layer height[xxxvi].

Note from the above that the vertical momentum equation is not used when the cloud is grounded or capped at the mixing layer (constant plume height).

3.5.1 Airborne drag

The formula for the airborne drag force F_{drag}^{air} is taken from Ooms[11,18]

$$F_{drag}^{air} = C_{Da}\,P_{abov}\,\rho_a\,(u_a \sin\theta)^2 \quad , \text{ continuous} \qquad \textbf{(80)}$$

It is reported by Li, Leijdens and Ooms[61] and Havens[62] to be a successful predictor not only of buoyant and neutral plumes, but of dense emissions as well. Note that it is proportional to the perimeter P_{above} (m) of the nominal elliptical cross-section of the cloud above the ground, and the square of the component $u_a\sin\theta$ of the wind speed normal to the plume. The proportional factor is the drag coefficient C_{Da} of the plume in the air. The value of C_{Da}=0.15m is derived by Ooms, Mahieu and Zelis[11] from comparison of theoretically predicted plume properties against one experiment. However this was used in conjunction with a different cross-wind entrainment formulation. It is shown in the verification and sensitivity manual that neglect of airborne drag C_{Da} = 0 leads to the best results. Note that this is also in line with the assumption adopted by the HGSYSTEM model.

The extended Morton crosswind entrainment model however (Section 3.4.2) replaces drag lost due to supressing near-field entrainment with an increased C_D over a similar distance scale ($3L_{supp}$):

$$C_{Da} = C_D^{init}\left(1 - \max\left[\frac{s}{3L_{supp}}, 1\right]\right)$$

The initial value C_D^{init} is 0.39.

In the case of instantaneous dispersion, the airborne drag force (N) is taken to be proportional to the cloud area above the ground S_{above},

$$F_{drag}^{air} = C_{Da}\,S_{above}\,\rho_a\,(u_a \sin\theta)^2 \quad , \quad \text{instantaneous} \qquad \textbf{(81)}$$

[xxxvi] IMPROVE. Default values are 1300, 1080, 920, 880, 840, 820, 800, 400, 100, 100 m for stability class A, A/B, B, B/C, C, C/D, C, E, F, G respectively with unknown reference for these data|. For SAFETI-NL the defaults are taken as 1500, 1500, 1500, 1250, 1000, 750, 500, 230, 50, 50 m for stability class A, A/B, B, B/C, C, C/D, C, E, F, G. These values correspond to those recommended by Table 4.7 in Part I of the Yellow Book[29], where the values correspond to the geographical location specific to the Netherlands and where for neutral and stable conditions a value of 0.3 of the surface roughness is assumed. In the future a more detailed literature review may be carried out. This could apply the mixing layer heights as function of surface roughness and wind-speed at 10m height, with windspeed profile taken form the UDM profile and the UDM values for the Monin-Obukhov length (rather than applying the Yellow Book profiles). Furthermore further aspects of the mixing layer logic may be improved in conjunction with this as mentioned elsewhere in this theory manual.

3.5.2 Ground impact force

The ground impact force F_{impact}^{ground} (N/m or N) results from collision of the plume with the ground. This force is added during touching down only. A new ground-impact-force formulation is implemented into PHAST 6.0, which is based on the formulation proposed by McFarlane[22] for the HGSYSTEM program AEROPLUME.

The assumption of elastic collision is applied to the plume as a whole. This requires that the impact pressure force $\underline{F}_{impact}$ is at right angles to the momentary orientation of the centre-line, which ensures conservation of kinetic energy (i.e. absolute velocity remains constant during plume impact); see Figure 4. .

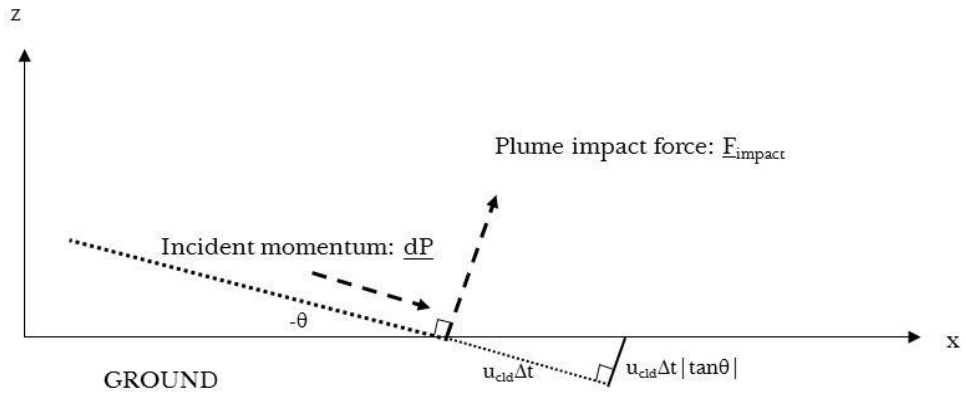

Figure 4. Ground impact force acting on impinging cloud

Continuous releases

According to the figure above, the cross-sectional plume area dA_{abs} (perpendicular to plume axis) 'absorbed' into the ground surface during a time step dt is given by a rectangle with as width the cloud ground width $2W_{gnd}$ and as length $\{u_{cld}\ dt\ |\tan\theta|\}$. Thus the absorbed area equals $dA_{abs} = \{2W_{gnd}\}\{u_{cld}\ dt\ |\tan\theta|\}$. The cloud momentum per unit of axis length $\underline{dP}$ [kg(m/s)/m] impinging on the ground during a time step dt, is directed along the plume centre-line axis and is given by

$$\underline{dP} \;=\; dA_{abs}\ \rho_{cld} \begin{bmatrix} u_x \\ 0 \\ u_z \end{bmatrix} \;=\; dA_{abs}\ \rho_{cld}\ u_{cld} \begin{bmatrix} \cos\theta \\ 0 \\ \sin\theta \end{bmatrix}$$

The ground impact force $\underline{F}_{impact}^{ground}$ is the force exerted by the ground onto the plume per meter of plume axis length (N/m). Using the assumption of elastic collision mentioned above, it follows that its absolute value equals $F_{impact}^{ground} = |\underline{dP}/dt|$, and that its direction is perpendicular to $\underline{dP}/dt$. Thus

$$\underline{F}_{impact}^{ground} \;=\; F_{impact}^{ground} \begin{bmatrix} -\sin\theta \\ 0 \\ \cos\theta \end{bmatrix} \quad , \quad with\ F_{impact}^{ground} = \frac{dA_{abs}}{dt}\ \rho_{cld}\ u_{cld} = \left\{2W_{gnd}\right\}\left\{u_{cld}\ \max[\,0, \tan(-\theta)]\right\}\rho_{cld} u_{cld}$$

Note that $F_{impact}^{ground} \neq 0$ during touching down only (i.e. for $W_{gnd} > 0$ and $\theta < 0$). For $\theta \downarrow -\pi/2$ (vertical downward impinging plume), $F_{impact}^{ground} \uparrow \infty$ since an infinite force per unit of axis length needs to be applied.

Note that McFarlane suggested that the above formulation should be applied for $\theta > -\pi/4$ only (incident angles less than 45 degrees).

Instantaneous releases

According to the above figure, the cross-sectional plume volume dV_{abs} (perpendicular to plume axis) 'absorbed' into the ground surface during a time step dt is given by a tilted cylinder with as basis the cloud ground surface area S_{gnd}, a height $u_{cld}\Delta t$, and a tilt angle $-\theta$. Thus the absorbed volume equals $dV_{abs} = \{S_{gnd}\}\{u_{cld}\ dt\ |\sin\theta|\}$. The cloud momentum $\underline{dP}$ (kg*m/s) impinging on the ground during a time step dt, is directed along the plume centre-line axis and is given by

$$\underline{dP} \;=\; dV_{abs}\ \rho_{cld} \begin{bmatrix} u_x \\ 0 \\ u_z \end{bmatrix} \;=\; dV_{abs}\ \rho_{cld}\ u_{cld} \begin{bmatrix} \cos\theta \\ 0 \\ \sin\theta \end{bmatrix}$$

The impact force $\underline{F}_{impact}^{ground}$ is the force exerted by the ground onto the plume (N). Using the assumption of elastic collision mentioned above, it follows that its absolute value equals $F_{impact}^{ground} = |\underline{dP}/dt|$, and that its direction is perpendicular to $\underline{dP}/dt$. Thus

$$\underline{F}_{impact}^{ground} \;=\; F_{impact}^{ground} \begin{bmatrix} -\sin\theta \\ 0 \\ \cos\theta \end{bmatrix} \quad , \qquad with\ F_{impact}^{ground} = \frac{dV_{abs}}{dt}\ \rho_{cld}\ u_{cld} = \{S_{gnd}\}\{u_{cld}\ \max[\,0, \sin(-\theta)]\}\ \rho_{cld} u_{cld}$$

Note that $F_{impact}^{ground} \neq 0$ during touching down only (i.e. for $W_{gnd} > 0$ and $\theta < 0$). Note that for $\theta = -\pi/2$ (vertical downward impinging plume), the impact force is directed vertical upwards and $F_{impact}^{ground} = \{S_{gnd} u_{cld}\}\ \rho_{cld} u_{cld}$.

3.5.3 Ground drag

The horizontal ground drag force F_{drag}^{ground} is added after the onset of touchdown. For a slumping plume, this term represents the drag force exerted at the ground surface by a slumped plume. This force results from differences in the mean horizontal and undisturbed wind speeds in the neighbourhood of the ground surface.

HGSYSTEM formulation

McFarlane[22] recommends a formulation proportional to the footprint width $2\ W_{gnd}$ (for continuous release),

$$F_{drag}^{ground} \;=\; 2\,W_{gnd}\ \rho_a(z = z_{cld})\ u_*^{\,2} \left[1 - \left(\frac{\rho_{cld}}{\rho_a(z = z_{cld})} \right) \left(\frac{u_{cld}\cos\theta}{u_a} \right)^2 \right]$$

Note that $\rho_a u_*^2$ is the surface stress associated with the ambient wind profile. Thus the above formula states the following:

- For a non-moving cloud the ground-drag force (N / m of downwind distance) is proportional to the surface stress and the part of the cloud touching the ground: $F_{ground}^{drag} = 2\, W_{gnd}\, \rho_a u_*^2$.
- The ground drag force is zero for a horizontal cloud speed equal to the ambient wind speed and a cloud density equal to the ambient density.
- The ground drag force is larger for a dense cloud

The author is not aware of validation of the above ground drag formulation.

UDM formulation

The above formulation has the disadvantage that the drag force does NOT reduce to zero for cloud speed equal to the wind speed, which is considered to be undesirable. As a result it is suggested to deviate from McFarlane assumption and ignore the ρ_{cld}/ρ_a term. This ensures that cloud will not be slowed down for a heavy cloud moving with the ambient speed (although the McFarlane formulation may be more accurate for a heavy ground-level jet).

Thus the following UDM formulation has been adopted

$$F_{drag}^{ground} = 2\, W_{gnd}\, \rho_a(z = z_{cld})\, u_*^2 \left[1 - \left(\frac{u_{cld}\cos\theta}{u_a}\right)^2\right], \quad \text{in N/m} \quad \text{(continuous)} \tag{82}$$

In the case of instantaneous dispersion, the ground drag force (N) is taken to be proportional to the area of the cloud touching the substrate, S_{gnd}

$$F_{drag}^{ground} = S_{gnd}\, \rho_a(z = z_{cld})\, u_*^2 \left[1 - \left(\frac{u_{cld}\cos\theta}{u_a}\right)^2\right], \quad \text{in N} \quad \text{(instantaneous)} \tag{83}$$

3.6 Cross-wind spreading

3.6.1 Jet spreading

The cloud is assumed to remain circular until the passive transition or (after onset of touching down) until the spread rate reduces to the heavy-gas spread rate, i.e.

$$R_y = R_z \quad (84)$$

3.6.2 Heavy-gas spreading

The lateral spread rate in the heavy gas entrainment regime is given by[xxxvii]:

$$\frac{dW_{eff}}{dt} = C_E \sqrt{\frac{g\{\max[0, \rho_{cld} - \rho_a(z = z_{cld})]\} H_{eff}(1+h_d)}{\rho_{cld}}} \quad (85)$$

Thus the adopted equation for instantaneous releases is

$$\frac{d R_y}{dt} = \frac{1}{C_m}\frac{dW_{eff}}{dt} = \frac{C_E}{C_m}\sqrt{\frac{g\{\max[0, \rho_{cld} - \rho_a(z = z_{cld})]\} H_{eff}(1+h_d)}{\rho_{cld}}} \quad (86)$$

and

$$\frac{d R_y}{dx} = \frac{1}{u_x C_m}\frac{dW_{eff}}{dt} = \frac{C_E}{u_x C_m}\sqrt{\frac{g\{\max[0, \rho_{cld} - \rho_a(z = z_{cld})]\} H_{eff}(1+h_d)}{\rho_{cld}}} \quad (87)$$

for continuous releases. Here the factor C_m is defined by

$$C_m = \sqrt{\Gamma\left(1+\frac{2}{m}\right)}, \quad \text{instantaneous} \quad (88)$$

$$C_m = \Gamma\left(1+\frac{1}{m}\right), \quad \text{continuous} \quad (89)$$

Transition from the jet-spreading regime to the heavy-spreading regime is chosen to take place as soon as dR_y/ds from the circular spreading rate drops below the above heavy-spread rate. Thus the heavy spread rate is applied after the circular spread rate has reduced to the heavy spread rate, and before the passive transition.

Light gases can enter the heavy gas regime due to low temperature or the presence of a liquid phase. In such cases its density will fall to below ambient as the temperature rises or the liquid rains out or evaporates. The lateral spread rates as defined in Eq.(86) and Eq. (87) become zero and heavy spreading rates are no longer appropriate.

[xxxvii] Note that more up-to-date ideas for cloud entrainment are given by Billeter,L. and Fanneløp, T.K.,"Concentration measurements in dense isothermal gas clouds with different starting conditions", Atm. Env. Vol. 31, No. 5, pp.755-771 (1997).

Instead across the heavy spreading regime the spread rate used is the maximum of the heavy, jet and passive spread rates:

$$\frac{dR_y}{dx} = Max\left(\left.\frac{dR_y}{dx}\right|_{hvy}, \left.\frac{dR_y}{dx}\right|_{jet}, \left.\frac{dR_y}{dx}\right|_{pass}\right) \quad (90)$$

Gravity collapse

Once in the heavy gas spreading regime, clouds will continue to entrain air and spread laterally. However eventually heavy-gas spreading can break down due to boundary layer or other turbulence[63]. To mitigate excessive spreading for non-instantaneous[xxxviii] clouds the UDM includes a model for adapted from HEGADAS[64]. It is controlled by a transition criterion which requires the volume of air added due to top entrainment exceeds its growth due to lateral spreading[xxxix]:

$$\frac{u_{top}}{u_g}\frac{W_{eff}}{H_{eff}} \geq 1 \quad (91)$$

u_{top} is the top entrainment velocity from Eq (62). u_g is the cloud spreading velocity dW_{eff}/dt which, expressed in terms of Ri_* can be written

$$u_g = C_E u_* \left(\frac{Ri_* \rho_a}{\rho}\right)^{1/2}$$

In addition we require that the pool has been left behind and rainout has finished, and that Ri* must exceed a threshold of 35 continuously for a period t_g in order that we can say gravity spreading has become established[xl]

$$t_g = \frac{W_{eff}}{u_g}$$

Once gravity-collapse has occurred, the reduced spread rate is given by:

$$\frac{dW_{eff}}{dt} = \frac{u_* Ri\, \Phi(Ri_*)}{3\kappa C_D}\frac{H_{eff}}{W_{eff}} \quad (92)$$

3.6.3 Passive spreading

The lateral spread rate in the passive entrainment regime is given by[xli]

$$\frac{dR_y}{dx}[at\ x] = 2^{0.5}\frac{d\,\sigma_{ya}}{dx}[at\ \ x - x_o], \quad \text{continuous} \quad (93)$$

$$\frac{dR_y}{dt}[at\ \ x] = u_x\, 2^{0.5}\frac{d\,\sigma_{ya}}{dx}[at\ \ x - x_o], \quad \text{instantaneous} \quad (94)$$

where x_o is the virtual source distance (currently not used, $x_o = 0$) and where $\sigma_{ya}(x)$ is the empirical formula for the passive dispersion coefficient.

[xxxviii] 2D-spreading for instantaneous clouds results is less extreme and the extension is therefore not applied

[xxxix] An earlier implementation of gravity spreading collapse was included in the Flashing JIP Phase III (Witlox and Harper, 2008) but never included in a commercial release

[xl] This reduces the likelihood transiently heavy buoyant materials (such as evaporating LNG pools) trigger the transition. As Ri* only accounts for atmospheric turbulence, this condition also excludes other potentially turbulent regimes such as evaporating pools or jets.

[xli] UDM applies the differential equation for dR_y/ds instead of dR_y/dx. This difference is neglible because $dx/ds = \cos\theta \approx 1$ for passive dispersion. Likewise in the differential equation for dR_y/dt, u_{cld} is adopted instead of u_x and $u_{cld} \approx u_x$.

3.6.4 Transition to passive

Along the transition zone $x_{tr}^{pas} < x < r_{tr}$ x_{tr}^{pas} the near-field spread rate $(dR_y/ds)^{nf}$ is phased out, while the far-field passive spread rate $(dR_y/ds)^{ff}$ is phased in

$$dR_y/ds = [1-f(x)]\,(dR_y/ds)_{nf} + [f(x)]\,2^{1/2}(d\sigma_{ya}/ds)$$

For heavy-gas spreading the near-field spread rate $(dR_y/ds)_{nf}$ is given by the heavy-gas spread rate [see Equations (86),(87)]. For the near-field jet spreading $R_y = R_z$, and an method needs to be developed to evaluate $(dR_y/ds)_{nf}$. This is described below for continuous and instantaneous dispersion, respectively.

Continuous dispersion

For continuous dispersion the following applies:

$A_{cld} = 2W_{eff}H_{eff}(1+h_d)$, $W_{eff}=C_mR_y$, $H_{eff} = C_nR_z$ with $C_n = \Gamma(1+1/n)$, $C_m = \Gamma(1+1/m)$
$m_{cld} = \rho_{cld}u_{cld}A_{cld} = 2C_nC_mR_yR_z(1+h_d)\rho_{cld}u_{cld}$

Assuming at the transition point negligible $dC_s/ds, dC_m/ds, du_{cld}/ds$, $d\rho_{cld}/ds$, it follows

$$\frac{1}{m_{cld}}\frac{dm_{cld}}{ds} \approx \frac{1}{A_{cld}}\frac{dA_{cld}}{ds} = \frac{1}{R_y}\frac{dR_y}{ds} + \frac{1}{R_z}\frac{dR_z}{ds} + \frac{1}{1+h_d}\frac{dh_d}{ds}$$

Using the formula for h_d,

$$h_d = P\left[\frac{1}{n}, \left(\frac{z_{cld}}{R_z\cos(\theta)}\right)^n\right], \quad \text{with } P(a,b) = \frac{1}{\Gamma(a)}\int_0^b t^{a-1}e^{-t}\,dt \qquad \textbf{(95)}$$

dh_d/ds can be calculated. Assuming negligible dh/ds, $d\theta/ds$, the above equation thus reduces to

$$\frac{1}{m_{cld}}\frac{dm_{cld}}{ds} \approx \frac{1}{R_y}\frac{dR_y}{ds} + \frac{1}{R_z}\frac{dR_z}{ds}\left[1 - \frac{1}{(1+h_d)\Gamma\left(1+\frac{1}{n}\right)}\left(\frac{z_{cld}}{R_z\cos\theta}\right)e^{-\left(\frac{z_{cld}}{R_z\cos\theta}\right)^n}\right]$$

If the plume is circular prior to the transition, $R_y=R_z$, and the above equation may be solved for dR_y/ds. Note that the above equation compares to the far-field equation as

$$\frac{1}{\rho_a u_a A_{cld}}E_{pas} = \frac{1}{\sigma_y}\frac{d\sigma_{ya}}{dx} + \frac{1}{\sigma_z}\frac{d\sigma_{za}}{dx}$$

Instantaneous dispersion

For instantaneous dispersion, an analogous derivation can be made, summarised as

$V_{cld} = \pi W_{eff}^2 H_{eff}(1+h_d)$, $W_{eff}=C_mR_y$, $H_{eff} = C_nR_z$
$m_{cld} = \rho_{cld}V_{cld} = \pi C_nC_mR_y^2R_z(1+h_d)\rho_{cld}$

$$\frac{1}{m_{cld}}\frac{dm_{cld}}{ds} \approx \frac{1}{V_{cld}}\frac{dV_{cld}}{ds} = \frac{2}{R_y}\frac{dR_y}{ds} + \frac{1}{R_z}\frac{dR_z}{ds} + \frac{1}{1+h_d}\frac{dh_d}{ds}$$

$$\frac{1}{m_{cld}}\frac{dm_{cld}}{ds} \approx \frac{2}{R_y}\frac{dR_y}{ds} + \frac{1}{R_z}\frac{dR_z}{ds}\left[1 - \frac{1}{(1+h_d)\Gamma\left(1+\frac{1}{n}\right)}\left(\frac{z_{cld}}{R_z}\right)e^{-\left(\frac{z_{cld}}{R_z}\right)^n}\right]$$

Using the above equation, again $(dR_y/ds)_{nf}$ can be evaluated. Note that the above equation compares to the far-field equation as

$$\frac{1}{\rho_a u_a V_{cld}} E_{pas} = \frac{2}{\sigma_y}\frac{d\sigma_{ya}}{dx} + \frac{1}{\sigma_z}\frac{d\sigma_{za}}{dx}$$

3.7 Averaging-time effects

This section discusses the effects of time averaging on the cloud concentrations and cloud shape. Time averaging may include the following two effects:

- the effect of wind meander, resulting in wider less dense clouds for large averaging times (for both continuous and time-varying dispersion). This effect occurs for both continuous and time-varying dispersion. It is only relevant after the transition to passive dispersion, i.e. when the cloud moves passively with the wind.

- Additional time-averaging at a specific position, resulting from time-dependent concentrations at this point (as a result of the effect of varying release rate).

3.7.1 Averaging time effect because of wind meander

The effect of wind meander results in a wider and more dilute cloud for a larger averaging time. The dispersion coefficient σ_{ya} from McMullen (1975) corresponds to an averaging time of 600 seconds. It is converted to an average time of t_{av} seconds using:

$$\sigma_{ya}(t_{av}) = \sigma_{ya}(600)\left(\frac{t_{av}}{600}\right)^{0.2} \qquad (96)$$

For toxic releases, the adopted averaging time t_{av} is usually chosen to be equal to 600 seconds. For flammable clouds and calculation of flammable zones, one needs to calculate non-averaged instantaneous values of the concentrations. The instantaneous value of σ_{ya} is approximately half the 10-minutes value (see TNO yellow book[65] and CCPS guidelines[30]). Using the above equation, it follows that this corresponds to the instantaneous averaging time t_{av}^{ins} = 18.75 seconds[xlii] [$(18.75/600)^{0.2}$=0.5]. Thus the following recommended averaging times apply for toxic and flammable releases,

$$\begin{aligned} t_{av} &= 600 \ \text{seconds}, \quad \textit{toxic releases} \\ t_{av} &= 18.75 \ \text{seconds}, \quad \textit{flammable releases} \end{aligned} \qquad (97)$$

For the purposes of acute toxic risk, the averaging time should generally be equal to or shorter than either the release duration or the cloud duration. It should also reflect the exposure time associated with the toxic exposure guideline of interest [see the EPA guidelines[66]] i.e. 60 minutes for the Emergency Response Planing Guideline (ERPG), 30 minutes for the Immediately Dangerous to Life and Health Level (IDLH), and 15 minutes for the Short Term Exposure Limit (STEL).

Averaging time for instantaneous dispersion

Passive along-wind diffusion is caused by both wind shear and turbulent spread [see Equation(107)], while passive cross-wind diffusion is caused by turbulent spread only. Thus for no time averaging (t_{av} = 18.75s) the instantaneous passive plume will be longer in the downwind direction than in the cross-wind direction, i.e. $\sigma_{xa} > \sigma_{ya}(t_{av}=18.75)$.

However as described in Section 3.1.2, a circular horizontal cross-section is assumed ($R_x=R_y$) for the UDM calculations in the case of instantaneous dispersion. Thus the downwind passive dispersion coefficient σ_{xa} is assumed to be equal to the crosswind passive dispersion coefficient $\sigma_{ya}(x;t_{av})$, and therefore erroneously also depends on the averaging time. This is not satisfactory, and as indicated in Section 3.1.2 a future improvement would be to allow for $R_x \neq R_y$ and therefore to allow σ_{xa} to depend on x only and not the averaging time.

[xlii] Thus 18.75 seconds should not be considered as an 'actual averaging time', but as the value to be adopted in Equation (96) to ensure that the instantaneous concentration is half the value of that at 10 minutes. This approach is consistent with the TNO yellow book, the CCPS guidelines and HGSYSTEM.

3.7.2 Averaging time effect because of time-varying release rate

In addition to the averaging time effect of wind meander, the user can optionally apply additional time-averaging at a specific position $\underline{x}$, resulting from time-dependent concentrations at this point resulting from the effect of time-varying release rate or time-varying pool evaporation rate. The time-averaged concentration at time t is obtained by integration of the time-dependent concentration between times $t-t_{av}/2$ and $t+t_{av}/2$:

$$[c(\underline{x},t;t_{av})]_{avg} = \frac{1}{t_{av}} \int_{t-t_{av}/2}^{t+t_{av}/2} c(\underline{x},\tau;t_{av})\, d\tau \qquad \textbf{(98)}$$

Here $c(\underline{x},\tau;t_{av})$ is the concentration at position $\underline{x}$ for time τ, including averaging-time effects of wind meander only; $[c(\underline{x},t;t_{av})]_{avg}$ is the concentration at position $\underline{x}$ for time t including averaging-time effects of both wind meander and time-dependency of concentrations.

Using the above equation, the time-averaging effect is optionally applied to concentrations for time-varying dispersion. For uniform finite-duration releases it can be optionally applied by means of the finite-duration correction; see Chapter 4 for further details.

Table 1 includes the averaging-time effects and along-wind-diffusion effects that are included for the different types of model scenarios.

4. UDM DISPERSION MODEL FOR FINITE-DURATION RELEASE (NO RAINOUT)

In Section 2.3 an overview has been given for the UDM models for steady-state, instantaneous and finite-duration releases (see also Figure 23, Figure 24, and Figure 25). In Chapter 3 the dispersion model for steady-state releases (with infinite duration) and instantaneous releases has been discussed detail.

In this chapter the sub-models in the UDM for finite-duration releases are discussed. The release mass rate is assumed to be constant during the finite duration. The UDM contains two models for the case of a finite-duration release, i.e. the 'quasi-instantaneous' model and the 'finite-duration-correction' model.

The quasi-instantaneous model is described in Section 4.1. It models the initial phase as a continuous source (neglect of downwind gravity spreading and downwind diffusion). When the cloud width becomes 'large' with respect to the cloud length, the cloud is replaced by an 'equivalent' circular cloud, and the subsequent phase is modelled as an 'instantaneous' circular cloud; see Figure 25a and Figure 32.

The 'finite-duration-correction' model is described in Section 4.2. It is based on the HGSYSTEM formulation derived from that adopted in the SLAB dispersion model. It has a better scientific basis and is derived from an analytical solution of the Gaussian plume passive-dispersion equations. It takes the effects of downwind diffusion gradually into account including effects of both turbulent spread and vertical wind shear. A limitation of this model is however that it is strictly speaking only applicable to ground-level non-pressurised releases without significant rainout. Moreover it produces predictions of the maximum (centre-line ground-level) concentrations only (see Figure 25b).

4.1 Quasi-instantaneous model

Previous approaches to the modelling of a very short duration continuous release have tended to assume that if the duration falls below some minimum criterion the release should simply be modelled as an instantaneous release starting from the origin. However, this approach can give a rather strange description of the release when the duration in absolute terms is reasonably long, even if it is short compared to the time for the cloud to disperse. If a release is only say one minute long, the release will effectively be instantaneous from the point of view of far field effects. Yet the front edge of the release can have reached several hundred metres from the release point by the time the release finishes, so in the near field the release will appear to behave as a true continuous release. To model it as an instantaneous cloud centred on the release point will not correctly describe the behaviour in this area. At the very least this instantaneous release will show upwind effects and a wide area of effect near the release point which would not be present for the actual release.

Therefore a different approach has been taken which is to model it as a continuous release during the initial stages of the release and then at some point replace it with an equivalent instantaneous cloud for subsequent effects.

In the initial stages of the release [(a) through (d) in Figure 32] the effects from the continuous release are idealised as a section of the expected concentration profile for a long duration continuous release with the front and back boundaries of that section moving downwind. The separation between these is the duration of the release.

Criterion for transition from continuous to instantaneous plume

At some point, the shape of this truncated part of the continuous plume begins to look more like a short, fat cloud than a long, thin continuous plume. In the UDM model a test is applied to the ratio of the cloud width to its length. When this ratio becomes too large the cloud has become quasi-instantaneous, and is replaced with an equivalent instantaneous cloud [(e) in Figure 32].

Let the current downwind and upwind edges of the continuous plume be located at x_{dw} and x_{uw}. Then the cloud length equals $L_{cld} = x_{dw} - x_{uw}$, and the cloud width at the downwind edge equals $2W_{eff}(x_{dw})$. The transition is now made if the cloud width/length ratio $[2W_{eff}(x_{dw})]/L_{cld}$ exceeds the parameter $r_{quasi} = 0.8$.

Matching of data between continuous and instantaneous plume at transition point

The data for the new instantaneous cloud are chosen to correspond to the data for the truncated continuous cloud, i.e. by matching of cloud masses, momentum, energy, cloud centroid, and horizontal cross-section area. This is done by the following consecutive steps[xliii]:

[xliii] JUSTIFY. The droplet variables (M_d, u_{dz} , T_d , z_d , I_{dz}) are not transformed during the transition. However there appear to be considerable discontinuies in the gradients of these variables which look incorrect.

1. Matching of masses of cloud compounds [pollutant (m_c)[xliv], wet air (m_{wa}), added water from the ground (m_{wv}^{gnd})], horizontal excess momentum (I_{x2}), vertical momentum (I_z), and total cloud enthalpy (H_{cld}). This is carried out by the following transformation formula,

$$[S]_{inst} = \int_{x_{dw}}^{x_{uw}} \left[\frac{S(x)}{u_{cld}(x)}\right]_{cont} dx = \int_{t_{dw}}^{t_{uw}} [S]_{cont} dt, \quad for\ S = m_c, m_{wa}, m_{wv}^{gnd}, I_{x2}, I_z, H_{cld} \qquad (99)$$

where t_{uw} is the time at which the cloud reaches x_{uw} (time at which transition is made) and where t_{dw} is the time at which the cloud reaches x_{dw}. Thus, for example, the above formula determines the component mass $[m_c]_{inst}$, kg, of the instantaneous cloud by means of integration of the mass rate $[m_c]_{cont}$, kg/s, of the continuous cloud. The total mass of the instantaneous cloud is set as $[m_{cld}]_{inst} = [m_{wa}]_{inst} + [m_{wv}^{gnd}]_{inst} + [m_c]_{inst}$.

2. The instantaneous cloud centre co-ordinates $[x_{cld}]_{inst}$, $[z_{cld}]_{inst}$ are calculated by means of matching the cloud mass centroid,

$$[x_{cld}]_{inst} = \frac{\int_{t_{dw}}^{t_{uw}} [x_{cld}\ m_{cld}]_{cont}\ dt}{[m_{cld}]_{inst}}, \quad [z_{cld}]_{inst} = \frac{\int_{t_{dw}}^{t_{uw}} [z_{cld}\ m_{cld}]_{cont}\ dt}{[m_{cld}]_{inst}} \qquad (100)$$

3. Subsequently thermodynamic calculations are carried out (see Part II of the UDM Technical Reference Manual) based on the above-calculated instantaneous cloud composition, total cloud mass $[m_{cld}]_{inst}$ and total cloud enthalpy $[H_{cld}]_{inst}$[xlv]. These provide as output the instantaneous cloud temperature, the cloud density $[\rho_{cld}]_{inst}$, and the cloud volume $V_{cld} = [m_{cld}]_{inst}/[\rho_{cld}]$.

4. The effective cloud data are subsequently set as[xlvi,xlvii]

$$[H_{eff}]_{inst} = \frac{[V_{cld}]_{inst}}{\int_{x_{dw}}^{x_{uw}} 2\left[W_{eff}(x)\right]_{cont} dx}, \quad [W_{eff}]_{inst} = \sqrt{\frac{[V_{cld}]_{inst}}{\pi(1+h_d)[H_{eff}]_{inst}}} \qquad (101)$$

In the above equation for $[H_{eff}]_{inst}$ the denominator is the horizontal cross-section area of the truncated effective steady-state cloud. The equation for $[W_{eff}]_{inst}$ is derived from Equation (26). The primary variable R_y is then set from W_{eff}.

5. The heat transfer q_{gnd} is found from subtracting from the total cloud enthalpy the enthalpies of wet air, component and added water from the substrate[xlviii].

$$q_{gnd} = H_{cld} - m_{wa}h_{wa}(T_a) - m_c h_c(T_c) - m_{wv}^{gnd} h_{wv}(T_{gnd}) \qquad (102)$$

Subsequent calculation of dispersion and effects start from the above instantaneous cloud, which moves away while increasing in radius, [(f) inFigure 32]. There are bound to be small discontinuities in behaviour and effects at the transition point, but the aim has been to make these as small as possible. However, given the nature of the assumed distribution of concentration in space and time for instantaneous and continuous releases, the scheme as described here is the only way to give a reasonable picture of how the true situation will evolve.

Discussion

[xliv] For m_c^{inst} we simply set $m_c^{cont} \times (t_{dw} - t_{uw})$, as coarse output steps can results in inaccurate pollutant masses..

[xlv] The specific enthalpies of cloud components are unchanged from the continuous release; masses of pollutant, wet air and mass of water vapour from substrate are calculated by the integration. These are used to calculate H_{cld}.

[xlvi] h_d is initially assumed to be the same as that of the final continuous cloud.

[xlvii] If the continuous cloud is a jet, then so will the instantaneous and therefore these calculations are only necessary for heavy or passive clouds.

[xlviii] Note that as a result of the approximate assumptions during matching H_{cld} will not be exactly equal to $m_a h_{wa}(T_a)+m_c h_c(T_c)+m_{wv}^{gnd} h_{wv}(T_{gnd})$ if no heat transfer occurs from the substrate. Thus in this case q_{gnd} as calculated from Equation (102), is effectively a residual energy term that needs to be included in the enthalpy equation to ensure conservation of energy at the quasi-instantaneous transition. If heat transfer DOES occur from the substrate, q_{gnd} should be considered to be the sum of [this residual energy term] and [the heat transfer from the substrate to the instantaneous cloud].

This quasi-instantaneous approach is an improvement, compared to the very old approach of replacing the continuous plume with an instantaneous plume starting from the origin. However, it still has the disadvantages of an abrupt plume transition and, since it neglects the effects of downwind diffusion and downwind gravity spreading (before the transition), it may over-predict concentrations in the near-field. Furthermore it is limited to the assumption of a circular cloud after the instantaneous transition. As shown in the UDM verification manual, this may lead to too short clouds (too large concentrations) for stable conditions in conjunction with small averaging times, and to too long clouds (too small concentrations) for unstable conditions in conjunction with large averaging times.

4.2 Finite-duration correction

In this section the finite-duration correction algorithm is introduced, and a formulation for the governing mathematical model is given.

Background

Ermak[67,68] developed a simple analytical algorithm to calculate the centre-line ground-level concentration for finite-duration ground-level sources (no jet). He implemented this algorithm into the dispersion shallow-layer model SLAB. This algorithm was later on adjusted for use in HGSYSTEM by Witlox[69,43].

The finite-duration correction approach is recommended instead of the current UDM quasi-instantaneous approach described in the previous section. It has a better scientific basis and it is derived from an analytical solution of the Gaussian plume passive-dispersion equations. Moreover it takes the effects of downwind diffusion gradually into account including effects of both turbulent spread and vertical wind shear (see Figure below). This is contrary to the quasi-instantaneous model, for which an unrealistic abrupt transition occurs from the continuous cloud to the instantaneous cloud (see Figure 25a).

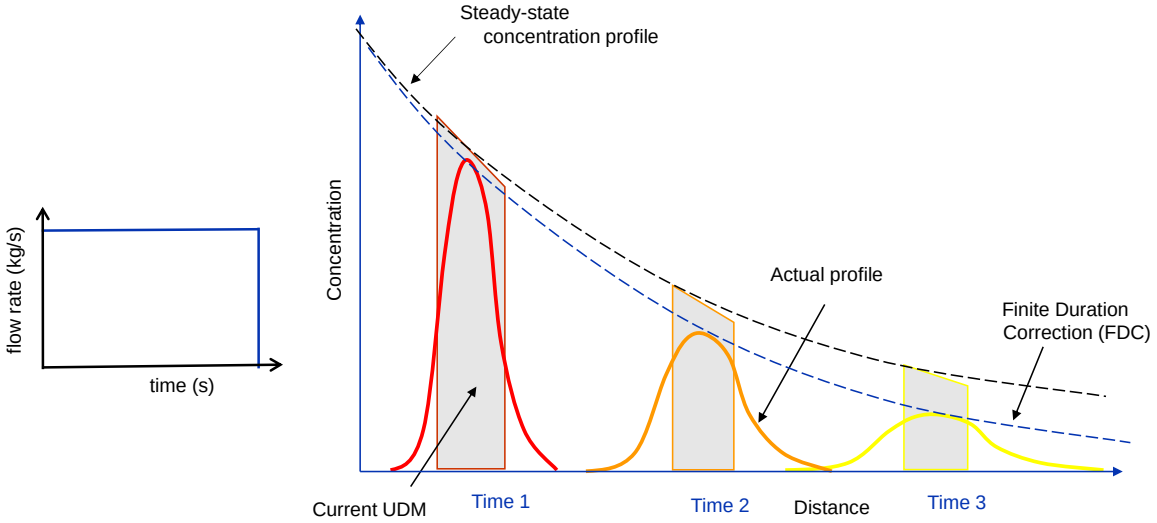

Figure 5. UDM FDC correction for finite-duration releases

Witlox[69] has shown that the finite-duration correction corresponds well with the more sophisticated HEGADAS-T time-dependent dispersion formulation, provided equivalent formulations are adopted for the downwind dispersion coefficient, etc. However the latter formulation also allows to impose more sophisticated and accurate downwind-dispersion formulations (e.g. prescribed downwind dispersion coefficients as a function of travel time, rather than as a function of downwind distance), and to provide more complete information of the concentrations, cloud widths, etc.

Mathematical model

The UDM finite-duration correction algorithm is based on the theory underlying the finite-duration correction originally applied in SLAB by Ermak[67,68], and later on adjusted for use in HGSYSTEM by Witlox; for full details, see Section 8.6.1 in the HGSYSTEM user's manual[69], and Equations (7.42) and (7.44) in the HGSYSTEM theory manual[43]. In HGSYSTEM, Ermak's algorithm is further adjusted to ensure compatibility of the UDM finite-duration correction with the dispersion coefficients adopted by the steady-state UDM model. Likewise in the UDM finite-duration correction algorithm given below, it is adjusted to ensure compatibility with the dispersion coefficients adopted by the steady-state UDM model. For further details and derivation of the equations below the reader is referred to the above references.

The equations are derived from an analytical solution of the Gaussian plume passive-dispersion equations. They assume the power-law $u_a(z) = u_a(z_{ref})\ [z/z_{ref})^p$ [see Equation (181)] for the ambient wind-speed profile, where u_{ref} is the wind speed at the reference height z_{ref} and p the exponent in the wind-speed power-profile.

The centre-line ground-level concentration $c^{fd}(x)$ for a constant release with duration t_{dur} is obtained from the steady-state centre-line ground-level concentration $c^{ss}(x)$ by applying a finite-duration correction:

$$c^{fd}(x) = F\ c^{ss}(x) \quad , \quad for\ ins\tan\tan eous\ concentrations$$
$$= F\ D\ c^{ss}(x) \quad , \quad for\ an\ averaging\ time\ t_{av} \qquad (103)$$

where the correction factors F and D are given by

$$F = erf\left[2^{-3/2}\frac{U_c t_{dur}}{\sigma_x}\right] \qquad (104)$$

$$D = \frac{\sqrt{2\pi}\ \sigma_x^t}{U_c t_{av}} erf\left[2^{-3/2}\frac{U_c t_{av}}{\sigma_x^t}\right] \quad , \quad with \quad \sigma_x^t = \sqrt{\sigma_x^2 + (U_c t_{dur})^2/(2\pi)} \qquad (105)$$

Here the error function erf is defined by (17), $\sigma_x = \sigma_x(x)$ is the downwind dispersion coefficient, and $U_c = U_c(x)$ the mean convection velocity of the cloud. The expressions for the latter two data are given below.

Downwind dispersion

The downwind dispersion coefficient $\sigma_x = \sigma_x(x)$ consists of two components,

$$\sigma_x(x) = \sqrt{\sigma_{xs}^2(x) + \sigma_{xt}^2(x)} \qquad (106)$$

where σ_{xs} is the downwind dispersion due to vertical wind shear,

$$\sigma_{xs}(x) = a_{xs}\ x \quad , \quad with \quad a_{xs} = 0.6\ p\left[\frac{0.48}{\gamma}\right]^p \qquad (107)$$

and σ_{xt} is the downwind dispersion due to turbulent spread caused by downwind velocity fluctuations. In UDM the formula for σ_{xt} is chosen to be equal to the UDM formula for the (time-averaged) ambient cross-wind dispersion coefficient σ_{ya} given by McMullen (1975)[53], i.e. $\sigma_{xt}(x) = \sigma_{ya}(x)$, with $\sigma_{ya}(x)$ given by Equation (70).

Cloud speed

The mean convection velocity of the cloud, $U_c = U_c(x)$, is given by

$$U_c(x) = u_{ref}\left[\gamma\frac{\sigma_z(x)}{z_{ref}}\right]^p, \ where\ \gamma = \sqrt{2}\left\{\frac{(1-p\,d)\,\Gamma(\frac{1}{2}p+\frac{1}{2})}{\sqrt{\pi}}\right\}^{1/p} \qquad (108)$$

Here the formula for the vertical dispersion coefficient $\sigma_z(x)$ is chosen equal to the UDM formula for the ambient vertical dispersion coefficient given Hosker (1973)[54], i.e. $\sigma_z(x) = \sigma_{za}(x)$, with $\sigma_{za}(x)$ given by Equation (71) as a stability-class dependent function of x and the surface roughness z_o. Furthermore $d = d_{sc} + d_{zo}$ is the exponent in the approximate[xlix] power-law fit $\sigma_z(x) = (c\ x^d)$. Here c and d_{sc} are a function of stability class, and d_{zo} a function of surface roughness:

c = 0.02, 0.12, 0.25, 0.38, 0.52, 0.28 for stability class A,B,C,D,E,F;

d_{sc} = 0.9021, 0.8354, 0.8031, 0.7614, 0.7322, 0.669 for stability class A,B,C,D,E,F

d_{zo} = 0.0523, 0.0255, 0, -0.0414, -0.0625, -0.079 for surface roughness z_o = 0.01,0.04,0.1,0.4,1,4 m.

[xlix] This power-law fit is determined by Panos Topalis to obtain a best fit for 100 m < x < 10000 m

Evaluation of FDC correction in limit cases

Using the above equations, the FDC correction can be analytically evaluated for the following limit cases:

A. Steady-state limit: for $U_c t_{dur} >> \sigma_x$ [negligible effects of along-wind diffusion: $F \approx 1$] and $t_{dur} >> t_{av}$ [negligible effect of time-averaging: $D \approx 1$]:

$$c^{fd} = FDc^{ss} \approx c^{ss}$$

B. Negligible effects of along-wind diffusion [$U_c t_{dur} >> \sigma_x$: $F \approx 1$] and significant dominant effects of time-averaging [$t_{dur} << t_{av}$: $D \approx t_{dur}/t_{av}$]:

$$c^{fd} = FDc^{ss} \approx [t_{dur}/t_{av}]\ c^{ss}$$

C. Significant dominant effects of along-wind diffusion [$U_c t_{dur} << \sigma_x$: $F \approx (2\pi)^{-1/2} U_c t_{dur}/\sigma_x$] and significant effects of time-averaging [$\sigma_x << U_c t_{av}$: $D \approx (2\pi)^{1/2} \sigma_x / U_c t_{av}$:

$$c^{fd} = FDc^{ss} \approx [t_{dur}/t_{av}]\ c^{ss} \approx 0$$

D. Significant dominant effects of along-wind diffusion [$U_c t_{dur} << \sigma_x$: $F \approx (2\pi)^{-1/2} U_c t_{dur}/\sigma_x$] and negligible effect of time-averaging [$U_c t_{av} << \sigma_x$: $D \approx 1$]

$$c^{fd} = FDc^{ss} \approx [(2\pi)^{-1/2} U_c t_{dur}/\sigma_x]\ c^{ss} << c^{ss}$$

It is interesting to compare the above extreme limit cases A-D for the FDC module against the quasi-instantaneous (QI) model with or without duration adjustment:

- Limit cases A and D corresponds to the QI model without duration adjustment. Limit case A corresponds to the dispersion before the QI transition; limit case D corresponds to the QI model after the QI transition in the far-field [but with the limiting assumption $\sigma_y = \sigma_x$].
- Limit case B corresponds to the dispersion before the QI transition for the QI model with duration adjustment.

Finite-duration correction module FDC (post-processing module to UDM)

The above FDC correction has been implemented as a sub-module of the separate post-processor module RPRO to the UDM. This module converts the steady-state UDM results for the centre-line ground-level concentrations $c_{ss}(x)$ into finite-duration results $c_{fd}(x)$ for the centre-line ground-level concentrations. The FDC has also been tested as a post-processor for the HGSYSTEM/SLAB steady-state results, and shown to lead to finite-duration results virtually identical to the latter programs, provided the dispersion coefficients were chosen to be consistent with the latter models.

The input parameters required by the FDC module include the stability class, the wind speed u_{ref} (m/s), the wind-speed reference height z_{ref} (m), the wind-speed power-law exponent p (-), the averaging time t_{av} (s), the release duration t_{dur} (s), and the surface roughness z_o.

Range of validity of the FDC module

Unlike the quasi-instantaneous model, the finite-duration-correction algorithm produces predictions for the centre-line ground-level concentrations only. Thus it is an improvement in the calculation of centreline concentrations compared with the quasi-instantaneous approach. Strictly speaking, the model applies to the following scenario only:

- ground-level non-pressurised release
- no significant rainout
- uniform release rate of a finite duration

It should be noted that the correction is negligible in the near-field (jet and heavy gas dispersion, possibly with liquid within the cloud). Therefore the FDC approach is not incorrect in the near-field, although it was initially derived from a passive-dispersion formulation.

For a high-speed jet release, the cloud speed may reduce to the ambient speed at a large downwind distance from the release point, say at $x = x_{tr}$. In this case, the FDC approach may be less accurate, in particular if the correction factors at $x = x_{tr}$ are significant. However it should still lead to good predictions at distances sufficient far from $x = x_{tr}$. Similarly, for elevated releases, the FDC approach will be accurate sufficiently far downwind from the point of touchdown (but may be inaccurate prior to touchdown and also after lift-off).

The FDC method is not applied in the case of rainout, where there is significant pool vaporisation. The FDC method should never be used for scenarios with a time-varying release rate (multi-segment scenarios).

FDC merely predicts centreline ground-level concentrations, although the calculated steady-state (uncorrected) values for cloud width may still be reasonable. It should be noted that the FDC does not calculate cloud lengths and therefore, currently, the FDC option cannot be used in QRA (in Safeti).

5. UDM DISPERSION MODEL FOR TIME-VARYING RELEASE (RAINOUT AND POOLS)

5.1 Introduction

Previous UDM model (Phast 6.7, 7.1): segment method excluding along-wind diffusion

For a time-varying release, Phast divided the calculated discharge mass into a user-specified number of equal-mass segments (Figure 6). Likewise in case of rainout or dispersion directly from an evaporating pool, the evaporated mass from the pool is divided into equal-mass segments. Subsequently the UDM model carries out steady-state dispersion calculations for each segment, and determines for successive times the concentration as a function of distance from these segment data as shown in Figure 6 by the dashed curves. Thus for time-varying releases or for dispersion after rainout, the previous UDM model did not apply along-wind-diffusion at the upwind and downwind edges of the cloud, or between segments, which may lead to significant over-prediction of concentration and under-prediction of duration in the far-field (see Figure 6 at time 2). This is particularly important for toxic releases, where dispersion calculations are required to be carried out to low concentrations such as ERPG levels. It is less important for flammable releases with calculations to relatively high concentration levels only, such as LFL or 0.5LFL.

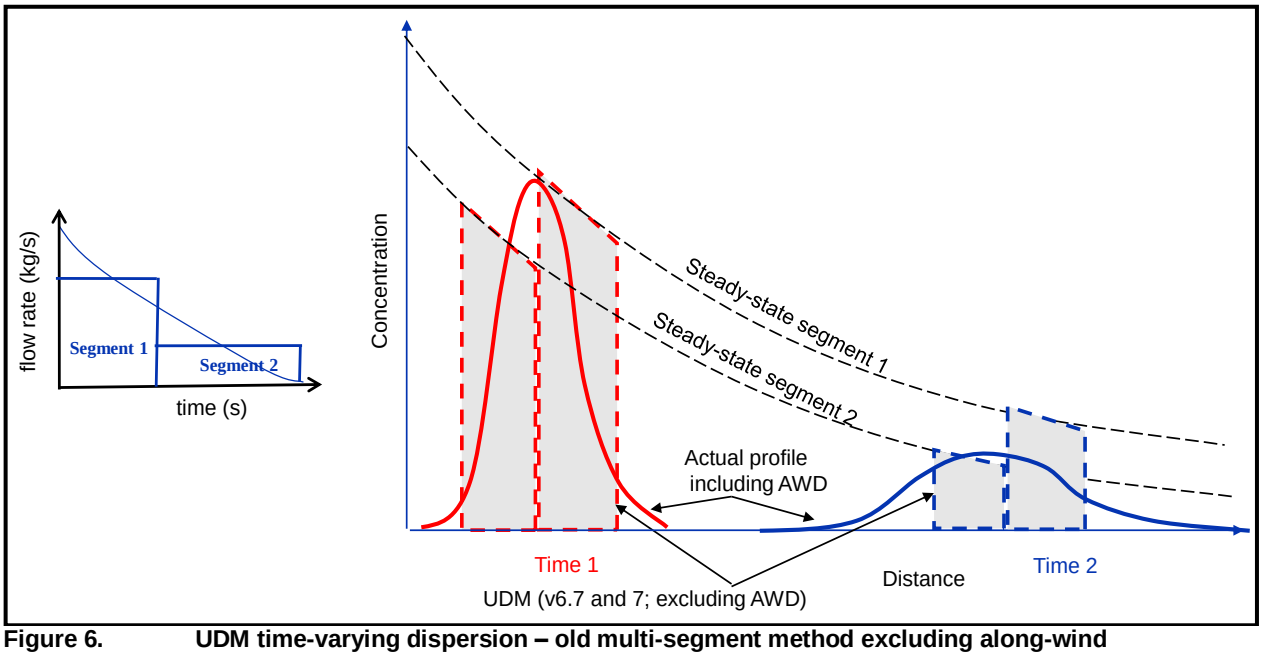

Figure 6. UDM time-varying dispersion – old multi-segment method excluding along-wind diffusion

HEGADAS heavy-gas-dispersion model: observer method including along-wind diffusion

The Shell consequence modelling package HGSYSTEM 3.0 (Post[85]) includes the time-dependent dispersion model HEGADAS-T (Witlox[70]) for modelling the time-dependent dispersion of a heavy-gas cloud moving with the wind. It can be used to model the dispersion downwind of either a time-dependent ground-level source (unpressurised release) or a vertical-plane transition (breakpoint) with a near-source jet model (pressurised release). The time-varying behaviour of the cloud is approximated by a quasi-steady-state description in which so-called “observers” are released at the source/transition-plane at a series of times. These observers travel with the wind. For each observer, the observed concentration is set from steady-state HEGADAS-S calculations using the observed source/transition data. Thus by calculating the position of each observer at a given time t, the concentration c is set for a number of downwind distances. Subsequently the actual concentration is set from Gaussian integration with respect to the downwind distance x of the above observer calculations. This involves a downwind dispersion coefficient σ_x, which allows along-wind diffusion to be taken into account.

New UDM model: observer method including along-wind-diffusion

The current chapter describes a new enhanced dispersion formulation accounting for time-varying effects resulting from a time-varying release.

The new UDM model generalises the above HEGADAS-T observer formulation both for ground-level unpressurised releases (e.g. evaporating pools) and for elevated two-phase pressurized releases including potential rainout.

- The release rate is no longer divided into a number of discontinuous release segments. Instead a number of 'release observers' are released from the release location until the release terminates and/or the upwind edge of the pool moves upwind of the release point. Observer steady-state calculations are carried out based on observed source-term data.
- Following rainout the new UDM model invokes pool spreading/evaporation equations using a PVAP model with a new robust numerical solver (see PVAP theory manual for details). Here unlike the former UDM model, the pool vapour is added back to the cloud without discontinuities in pool evaporation rate and/or pool radius. Thus there is a considerably improved link between cloud and pool. Moreover the pool centre is no longer fixed at the initial point of rainout, but it will move upwind or downwind in case of time-varying rainout or in case the pool reaches the bund.
- Additional 'pool observers' are then released from the upwind edge of the evaporating pool. This can occur after either the upwind edge of the pool has moved upwind of the release point, or the release has left the pool behind.
- The new model applies an added correction to the observer concentrations to ensure mass conservation in the cloud when observers move downwind with different velocities (different curves of observer downwind distance versus time). The former UDM model modelled the latter case by a number of discontinuous equal-mass release segments, where cloud segments could drift apart resulting in unrealistic gaps between segments and too high concentrations.
- As in HEGADAS-T, the new UDM model applies effects of along-wind diffusion at a given time by means of integration of observer concentrations along the downwind distance. As indicated above the former UDM model does not include effects of along-wind diffusion, apart from instantaneous clouds where spreading in the alongwind direction was already modelled.
- The new model allows the additional option of including time-averaging effects resulting from time-varying release rates and/or time-varying pool evaporation (see Section 3.7.2 for details).

The new model can be applied to the following cases:

- Finite-duration continuous release without rainout (optional, alternative QI or FDC)
- Time-varying release without rainout
- Dispersion starting from time-varying pool
- Finite-duration continuous release with rainout
- Time-varying release with rainout
- Instantaneous release with rainout

The reader is referred to Section 2.3.4 for a summary description of the overall new UDM model. Section 5.2 describes the overall algorithm for the new model, while Section 5.3 provides further details of the observer dispersion calculations.

5.2 Overall algorithm

5.2.1 Phast source-term calculations (prior to UDM calculations)

In Phast prior to the UDM dispersion calculations, first Phast discharge calculations are carried out (for release from a hole of a vessel or a pipeline) to determine the UDM source-term data, i.e. the time-varying discharge data after expansion to atmospheric pressure and prior to air entrainment [flow rate, velocity, temperature, liquid mass fraction, droplet size (SMD – Sauter Mean Diameter)].

5.2.2 Release observers: set observer release location and observer release times

Non-instantaneous release (see Figure 3)

First 'release observers' are released from the release point.

Secondly observers will be released from the upwind edge of the pool after the time that either (a) the upwind edge of the pool moves upwind of the release point, or (b) the release has stopped and all previously-released observers are located downwind of the downwind edge of the pool[l,li].

No more observers will be released after both the original release and the pool evaporation calculations have been terminated (i.e. time larger than release duration, and pool evaporation rate below minimum rate).

Release observers are released at intervals based on equal-mass discharge increments, while pool observers are released at intervals based on equal-mass pool-evaporation increments[lii].

Instantaneous release (see Figure 9)

The initial observer moves with the instantaneous cloud. Pools and instantaneous clouds can only co-exist after rainout. Following rainout, the instantaneous cloud will pick up vapour from the pool until the upwind edge of the instantaneous cloud has left the downwind edge of the pool behind[liii].

After the upwind edge of the instantaneous cloud has left the upwind edge of the pool behind (this may happen almost immediately if the cloud moves faster than the pool spreads), additional observers will be released from the upwind edge of the pool with equal PVAP mass evaporation segments as for non-instantaneous releases.

5.2.3 UDM calculations for each observer

The dispersion data are determined by means of UDM steady-state calculations for the 'steady-state' observers, and by means of UDM instantaneous dispersion calculations for the 'instantaneous' observer. For each observer, the observer dispersion data are set as function of downwind distance, while the observer is moving in the downwind direction. This also includes the downwind position of the observer as function of time. Calculations carried out are as follows:

- While the observer is upwind of the pool carry out UDM calculations as described in Chapter 3. Here the source-term data input to the observer correspond to the release source-term data at the time of the release of the observer.

[l] $x_{cld} > x_{pool} + R_{pool}$. A pool observer is released immediately after the pool has been left behind. This is because the cloud can be highly discontinuous at this point, and releasing a pool observer will better anchor the results.

[li] IMPROVE. Consider releasing pool observer immediately or shortly after the last release observer has passed the upwind edge of the pool. Delayed for now because of differential observer velocities issues (observers which are released close are more likely to overtake each other).

[lii] REFINE. Initial observers released from release point are to be provided by TVAV or UDM as for the case without rainout (GSPP, PBRK; not yet TVDI). To further specify logic to set release times for observers released from the pool. This may be based on existing PVAP pool segmentation logic (reducing observers in case of small difference between evaporation rates) or otherwise analogous to current TVAV logic for setting equal mass segments for discharge models.

[liii] That is if $x_{cld} - W_{eff} > x_{pool} + R_{pool}$

- While the observer is above the pool, account for added pool component mass/momentum etc. by applying appropriately modified equations.
- While the observer is downwind of the pool, carry out unmodified UDM dispersion equations as described in Chapter 3.

Observers released from the upwind edge of the pool may pass over the release location at x=0. If at this time the original release is still on-going, the observer data (primary variables) are adjusted to account for the added release term. If a pool has spread upwind of the release and is still evaporating when the release ends, then in order to better resolve the discontinuity in release rate at this time, two pool observers are released at almost co-incident times. The first pool observer is released at a time such that it passes x = 0 immediately[liv] before the release ends (thereby encountering the source term and corresponding to the upwind edge of the release), while the second observer is released at a time such that it passes x = 0 immediately[liv] after the release ends.

As part of the above equations, observer droplet rainout is applied at the time at which the observer droplet hits the ground or the bund wall. In case of observer rainout, the following calculations are carried out in sequence:

- Case of instantaneous release with rainout
    - First calculations are carried out for the instantaneous observer until the point of rainout to provide the instantaneous spill data input to the PVAP pool spreading/evaporation model (e.g. rainout location and spilled mass).
    - PVAP calculations are carried out to determine the time-varying pool radius, pool evaporation rate, etc.
    - Following rainout, the instantaneous cloud will pick up vapour from the pool until the upwind edge of the instantaneous cloud has left the downwind edge of the pool behind.
    - After the upwind edge of the instantaneous cloud has left the upwind edge of the pool behind (this may happen almost immediately if the cloud moves faster than the pool spreads), additional observers will be released from the upwind edge of the pool. One is released immediately, and others at intervals corresponding to equal mass increments being evaporated from the pool. This is illustrated by Figure 9, where observer 1 corresponds with the first 'instantaneous release observer, and observers 2,3 with subsequent "pool observers" starting from the upwind edge of the pool.
    - If there is a bund that fails, an additional observer is released that crosses the pool just before it overspills. This helps to capture a significant discontinuity in the results.

- Case of time-varying (non-instantaneous) elevated release with rainout
    - First calculations are carried out for all observers until the point of rainout to provide the time-varying spill data (rainout rate, rainout time, and rainout location) input to the PVAP pool spreading/evaporation model, with linear interpolation presumed between subsequent rainout times.
    - PVAP calculations are carried out to determine the time-varying pool radius, pool evaporation rate, and downwind distance of pool centre.
    - Calculations are redone for the above "release observers" form the time at which the reach the upwind pool edge. While each observer moves above the pool, the observer dispersion equations (conservation of cloud mass and momentum conservation, cloud crosswind gravity spreading, heat transfer from the substrate, etc.) are modified to account for the pool vapour added back to the cloud.
    - Additional "pool observers" (corresponding to equal pool-mass increments) are released from the upwind edge of the pool after the release plume has left the pool behind, or after the upwind pool edge has moved upwind of the release location. This is illustrated by Figure 3, where the first "release observers" (1,2,3,4) start from the release point and subsequent "pool observers" (5, 6) start from the upwind edge of the pool.
    - If there is a bund that fails, an additional observer is released that crosses the pool just before it overspills. This helps to capture a significant discontinuity in the results.

5.2.4 Mass Conservation and Correction

Mass Conservation Checking and Handling Lost Mass

[liv] 0.1 secs

Sometimes for large rainout rates and very rapidly spreading / evaporating pool mass is not conserved by observers passing over the pool – mainly this is due to observers not 'seeing' a significant fraction of the pool while evaporation rates are high. Checking has been implemented immediately downwind of the pool to ensure that:

$$M_{release} = M_{pool} + M_{obs} + M_{loss}$$

where

- $M_{release}$ is the total mass (kg) released by the source term
- M_{pool} is the mass left in the pool at the final time, at which the observer calculations are terminated
- M_{obs} is the integrated mass rate against time for all observers at the downwind edge of the pool[lv]
- M_{loss} is the evaporated mass from the pool when the evaporation rate is lower than the cut-off rate. This mass is not added back to the cloud and is 'lost' from the system[lvi].

If this check fails because release mass exceeds observer + pool mass by more than 25% one of two corrective approaches, described below, is used. A warning will be given to say if mass conservation problems have forced to use either method.

Instantaneous Over Pool

Often mass conservation errors occur due to the pool being highly dynamic and of very short duration compared to the transit times of observers over it. In such cases using an 'averaged pool' may underestimate near-field concentrations due to the removal of transient evaporation rate peaks.

The instantaneous over pool model models the case as an initially zero mass instantaneous cloud centred at the release point and fed by time-varying evaporation from the pool underneath. In all other respects it conforms to the modelling described in Section 5.3.2 for an instantaneous cloud with rainout, including determination of when the pool has been left behind by the instantaneous cloud and the release of any subsequent continuous observers.

By modelling the scenario as an instantaneous cloud centred over the pool (including any residual vapour), we ensure that the entire mass of the pool is captured whilst the dynamic nature of the pool is preserved.

This method is the first one attempted. However, if the scenario is such that the pool sees significant vaporisation after it is been left behind by the instantaneous observer, then this approach is likely to be less good than the equivalent pool (below), and we use that method instead.

Equivalent Pool

Here the time-varying pool is replaced with an equivalent finite-duration steady-state pool. The duration, d_{equiv}, of the equivalent pool is the time taken for 95% of the total mass evaporated (M_{evap}) to be vaporised[lvii]. The mass rate is M_{evap} / d_{equiv}. Other quantities (radius, temperature) are averaged over the duration of the original pool. This equivalent pool is then modelled as a pool source[lviii].

Any residual vapour – i.e. that fraction of material which did not originally rain out – is handled by increasing the equivalent pool evaporation rate. So, a case where residual vapour accounted for 10% of vaporised mass would have the equivalent pool evaporation rate increased by 1/0.9 to compensate.

Application of differential observer-velocity cloud mass correction

The above method for a non-instantaneous release is based on a quasi steady-state approach based on a steady-state solution for each observer. However, if observers move with substantially different velocities (different curves for observer downwind distance versus observer travel time) the mass of released material is not conserved by simply interpolating between these steady state solutions. Therefore a correction must be applied to ensure mass conservation.

[lv] At the downwind edge of the pool, observer mass will no longer change and a correct mass balance can be calculated.

[lvi] If it is significant a warning is given; see UDM3 warning 1136 in Appendix F.3.

[lvii] That is, the elapsed time between the 97.5 and 2.5 percentiles of evaporated mass

[lviii] If this method is adopted, warning UDM3 1128 will be reported.

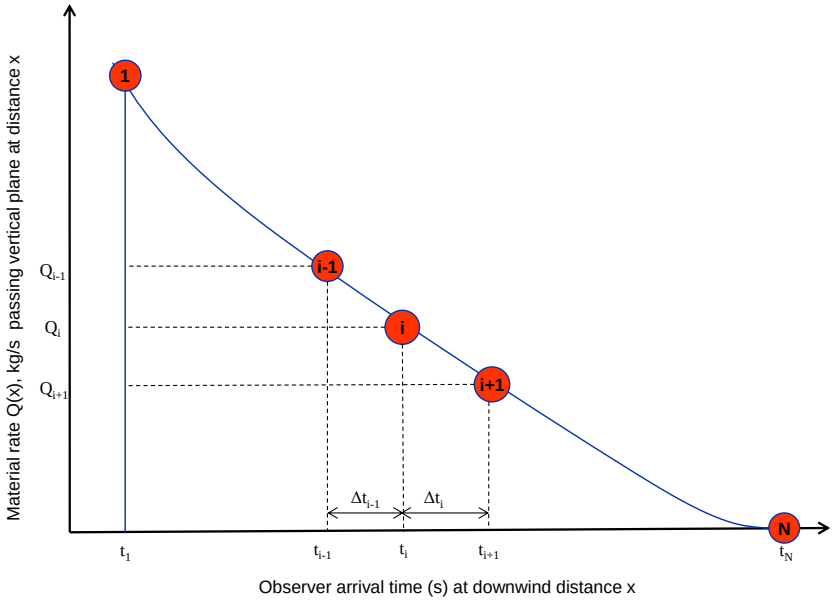

Figure 7. Cloud mass correction: conserve mass (area under material rate curve)

Let t be the time since the start of the release. Let N be the number of observers. For each observer i (i=1,…N) we define $t_i(x)$ as the time at which the observer reaches the downwind distance x [i.e. observer position $x_{cld,i}(t_i)=x$], and $Q_i(x)$ the observed amount of material mass rate (kg/s) passing through the vertical plane at distance x; see Figure 7. Let $\Delta t_i(x)$ be the time interval between arrival times of observers i and i+1: $\Delta t_i(x) = t_{i+1}(x)-t_i(x)$.

Thus in case of an elevated release without rainout, $t_i(0)$ is the release time of the observer, $Q_i(0)$ the observer release rate, and $\Delta t_i(0)$ the observer release interval. The above pseudo state-state formulation assumes that $Q_i(x)$ remains equal to the release rate $Q_i(0)$, while the correction accounts for a modification of $Q_i(x)$ as a result of observers moving with different velocities.

Evaluation of observer material rate $Q_i(x)$: case of no rainout

First the case is considered of either an elevated release without rainout (only presence of release observers, released from release location x=0), or dispersion from a ground-level area source (only presence of pool observers released from upwind edge of the pool).

It is presumed that the material mass rate through the vertical plane at x varies linearly with time between subsequent observer arrival times. Thus the total amount of mass passing through the plane x is given by

$$M_{tot}(x) = \sum_{i=1}^{N-1}\left\{\frac{Q_i(x)+Q_{i+1}(x)}{2}\Delta t_i(x)\right\} = \sum_{i=1}^{N} M_i(x) \qquad (109)$$

Here $M_i(x)$ can be considered to be the prescribed 'observer mass' associated with observer i:

$$M_1(x) = Q_1(x)\frac{\Delta t_1(x)}{2} \quad , \quad M_N(x) = Q_N(x)\frac{\Delta t_{N-1}(x)}{2} \qquad (110)$$

$$M_i(x) = Q_i(x)\frac{\Delta t_{i-1}(x)+\Delta t_i(x)}{2} \quad , \; i = 2,....N-1$$

Mass conservation requires that the above mass $M_{tot}(x)$ must be identical to the released mass for all values of x, i.e. $M_{tot}(x)=M_{tot}(x_o)$, for $x \geq x_o$. Here $x_o=0$ in case of an absence of a pool, and it equals the furthest downwind distance of the downwind edge of the pool in case of the presence of a pool·

Presuming that the release rate of an observer can only be affected by its adjacent observers, this leads to the requirement that the observer mass for each observer i cannot change with time and distance:

$$M_i(x) = M_i(x_o)\ , \qquad i = 1,....N \tag{111}$$

Thus M_i can be set at the start of the UDM calculations from the specified release rate. Use of Equation (111) into (110) leads to an equation which can be easily solved for $Q_i(x)$, i=1,…N:

$$Q_i(x) = f_i(x)Q_i(x_o), \ \ with \ \ f_1(x) = \frac{\Delta t_1(x_o)}{\Delta t_1(x)}\ , \ \ f_N(x) = \frac{\Delta t_{N-1}(x_o)}{\Delta t_{N-1}(x)} \tag{112}$$

$$f_i(x) = \frac{\Delta t_{i-1}(x_o) + \Delta t_i(x_o)}{\Delta t_{i-1}(x) + \Delta t_i(x)}\ , \ i = 2,....N-1$$

The above equation shows that no modification to the rate $Q_i(x)$ is applied if the observer time intervals do not change when the observers moves downwind, which is the case for a steady-state finite-duration release. It is reduced if the observer time intervals increase, while it is increased if the observer time intervals reduce.

Simplified implementation of observer mass correction

At present a simplistic version of the above correction is implemented. The correction is ignored for the initial observer steady-state calculations. No mass correction is applied for $x<x_o$. For $x>x_o$, subsequently Equation **Error! Reference source not found.** is applied by post-processing the UDM pre-AWD observer data. Let $N_{pol,i}$ b e the molar flow pollutant passing through a plane prior to the correction (kmol/s; independent of x), and let $N_{air,i}(x)$ be the molar of wet air (kmol/s). Thus after the observer mass correction (OMC), the molar flow of pollutant equals $f_i(x)$ $N_{pol,i}$. Thus the concentrations (mole fraction) before and after the observer mass correction are given as follows:

$$c_i(x) = \frac{N_{pol,i}}{N_{pol,i} + N_{air,i}(x)}\ , \ c_i{}^{OMC}(x) = \frac{f_i(x)N_{pol,i}}{f_i(x)N_{pol,i} + N_{air,i}(x)}\ , \ i = 0,....N \tag{113}$$

Thus the concentration after observer mass correction can be expressed in terms of the concentration prior to mass correction as follows:

$$c_i{}^{OMC}(x) = \left\{1 + \frac{1}{f_i(x)}\left[\frac{1}{c_i(x)} - 1\right]\right\}^{-1}\ , \ i = 0,....N \tag{114}$$

By ignoring the correction for the initial observer steady-state calculations, heavy-gas crosswind spreading and passive transition are not affected by the correction, which may lead to added inaccuracy. However in case of toxic releases, this new correction method still provides superior results to the old Phast (pre 8.0; involving possible gaps between subsequent segments, or overlapping segments) for the evaluation of the toxic load, while in case of the probit exponent n=1 it may provide more similar results to the old Phast.

Appendix E.1 describes a time-shifting algorithm, which is applied prior to the observer mass correction to avoid observers approaching each other too close. Appendix E.2 describes a more rigorous implementation of the observer-velocity cloud mass correction for potential future implementation.

Handling Discontinuities at the End of the Release

When the release ends, it can represent a large discontinuity in the simulation if there remains an evaporating pool. An additional pool observer is normally released very shortly afterwards to try and capture this, but the release and pool observers will typically travel at very different speeds (with the release travelling faster) and this is often not well handled by the mass correction method described above. Therefore, we add a duplicate of the final release observer[lix] but delayed by 0.001 secs, and with modified concentrations c' determined from

$$c(x)' = \frac{N_{pol} - N_{res}}{N_{pol}}\ c(x)$$

[lix] This can either be the final release observer, or the last pool observer that encounters the release

N_{pol} is the final molar flow of pollutant (i.e. once it has left the pool behind; kmol/s). N_{res} is the residual vapour flow rate, calculated as the release flow rate (kmol/s) minus the rainout flow rate (kmol/s).

The purpose of this added observer is to force an instantaneous transition (in time) from a high flow (release) regime to a lower flow (pool only) regime.

5.2.5 Gas blanket modelling for buried pipelines

This model describes the release of dense material from buried pipeline ruptures. Releases such as dense phase CO_2 from large diameter pipes have been observed to 'collapse' on themselves and spread upwind. They can produce much higher ground-level concentrations than those predicted by the UDM.

The model is an adaptation of the "Instantaneous Over Source" model discussed in the preceding section. It effectively substitutes the continuous or time-varying vertical jet with an instantaneous cloud fed continuously from underneath by the crater. This substitution gives a much better physical representation of the observed cloud behaviour.

It has been implemented alongside, and for use with, the "Defined area" crater model (see Crater Model Theory). The momentum reduction within the crater makes gas blanket behaviour much more likely to occur.

Formulation and Assumptions

The behaviour of collapsing plumes is highly complex in terms of momentum, entrainment and many other key variables. Rather than try and explicitly model this stage we make an up-front determination of whether the cloud will collapse. By modelling a collapsed cloud as a ground level instantaneous one, we ignore the spreading effects due to downwards momentum. We assume that ultimately the spreading of the cloud will instead be determined by heavy-gas type behaviour.

Activation

The first release observer is modelled as a normal vertical jet. The gas blanket modelling is activated if (a) the cloud centreline becomes grounded; and (b) the centreline angle between touchdown and becoming grounded ever drops below the critical angle (-45^o by default)

If this activation fails, the case is rerun as a normal continuous or time-varying vertical jet release.

Generally activation is more likely for large low velocity releases, lower windspeeds and very dense materials.

Initialisation

Upon activation, the case is modelled as an instantaneous cloud starting with zero mass and fed with release mass and entrained air flowrates from the crater, allowing the cloud to grow and spread in all directions (Figure 8a). This is entirely analogous to the instantaneous over source model, but with a point source rather than a pool (area) source.

Crater Left Behind

The crater is left behind once $x_{cld} - 0.5W_{gnd} > r_{src}$ where r_{src} is the source radius calculated by the Crater Model. If when this happens the crater source is still active, then additional continuous observers are run while the source is active (Figure 8b).

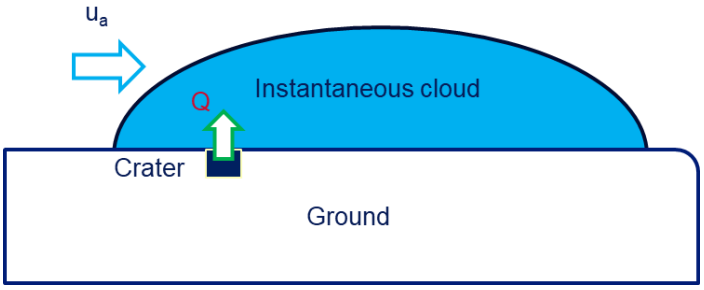

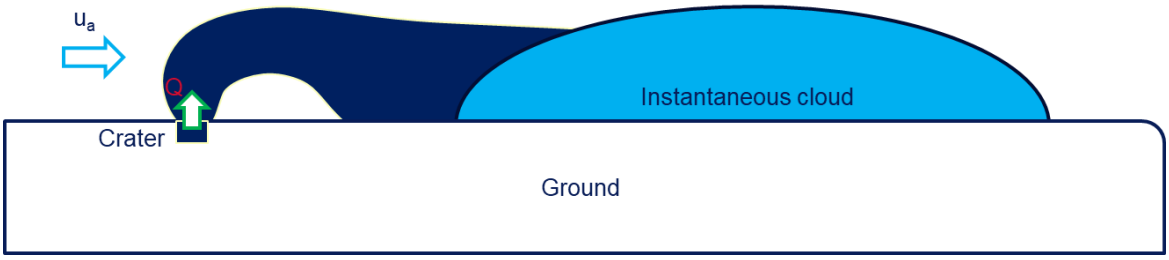

Figure 8. (a) An instantaneous cloud while over the crater; (b) subsequent continuous observers once the crater has been left behind

5.2.6 Inclusion of effects of along-wind diffusion

Time-varying release

The actual plume concentration c(x,y,z,t) including effects of along-wind-diffusion is a function of time t, x, y, and z; this function is calculated by means of Gaussian integration of the observer concentration C(ξ,y,z,t),

$$c(x,y,z,t) = \int_0^\infty \frac{C(\xi,y,z,t)}{(2\pi)^{1/2}\,\sigma_x(\xi)} \exp\left\{-\frac{(x-\xi)^2}{2\,\sigma_x^{\,2}(\xi)}\right\} d\xi \qquad \textbf{(115)}$$

In the above equation ξ is the downwind distance from the release point at time t of an observer travelling with the cloud in the downwind direction. At this position the observer sees the concentration C(ξ,y,z,t). In Equation (115) along-wind diffusion is taken into account by assuming that the concentration C(ξ,y,z,t) spreads out around ξ according to a Gaussian distribution with a downwind dispersion coefficient $\sigma_x = \sigma_x(\xi)$. Figure 2 depicts the pre-AWD observer concentration C and the post-AWD concentration c at a short time after the release (time 1; limited AWD effects), and at a larger time after the release (time 2; larger AWD effects).

The evaluation of the downwind dispersion coefficient $\sigma_x(\xi)$ is fully consistent with the UDM FDC model for the specific case of including AWD effects for finite-duration releases (see Section 4.2). In case of stability class D, the model also allows an alternative formulation proposed by Chatwin (1968)[71]where the along-wind diffusion coefficient $\sigma_x = \sigma_x(t_{obs}(\xi))$ is evaluated at the observer downwind distance ξ through the observer travel time since the time of observer release,

$$\sigma_x(t_{obs}) = 2\,u_*\,t_{obs} \quad , \quad for\ stability\ class\ D\ (Chatwin) \qquad \textbf{(116)}$$

where u_* is the friction velocity.

Instantaneous release

For an instantaneous release effects of along-wind diffusion have already been applied to the initial instantaneous observer, and therefore along-wind diffusion only needs to be further applied to the 'non-instantaneous' observers released from the upwind edge of the pool [using Gaussian integration as given by Equation (115)]. Afterwards the instantaneous concentration is added to obtain the overall concentration.

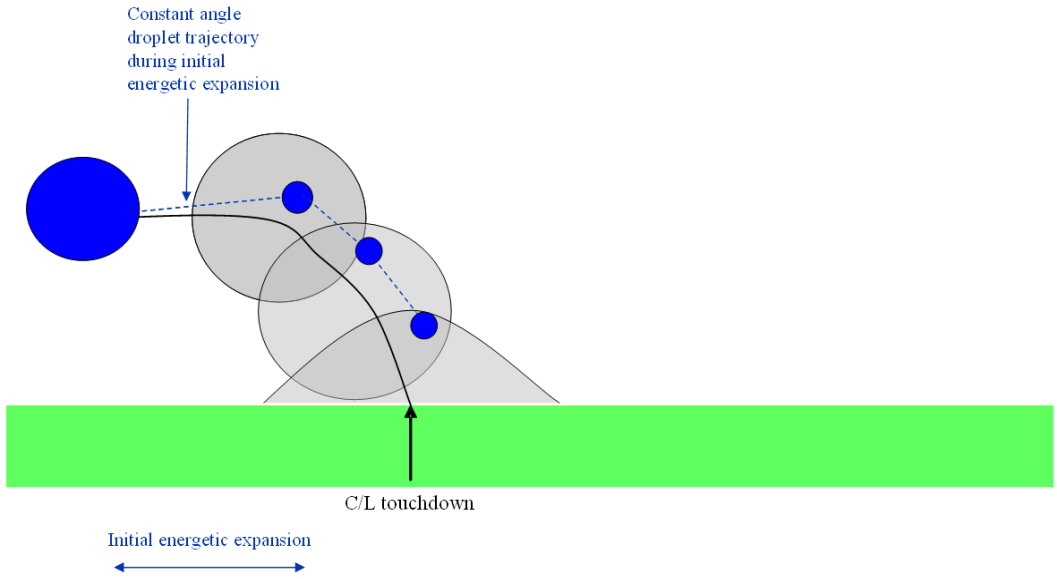

(a) Dispersion before rainout (single instantaneous observer 1 only)

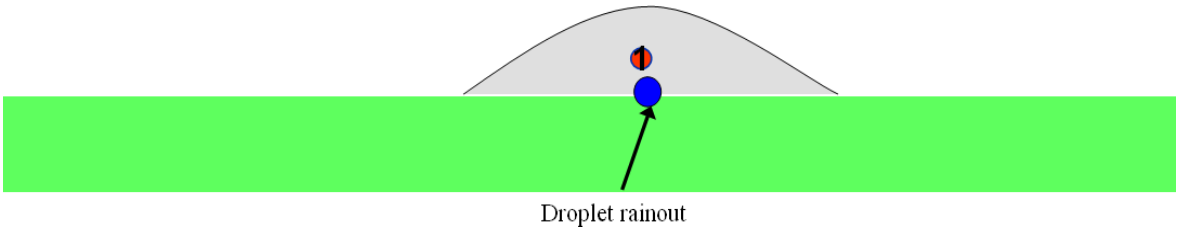

(b) Rainout (adjust observer variables at rainout location; solve pool equations afterwards)

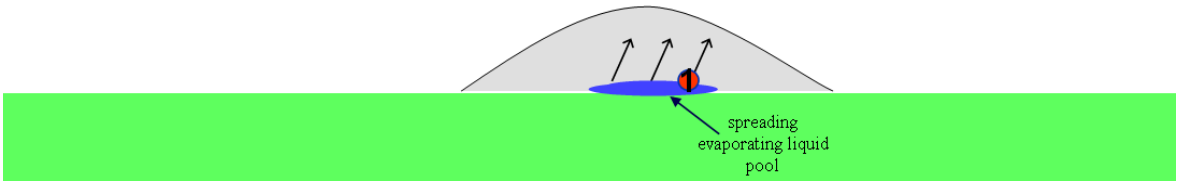

(c) Dispersion after rainout (account for pool vapour pick-up by instantaneous observer)

release pool observers at upwind edge of pool

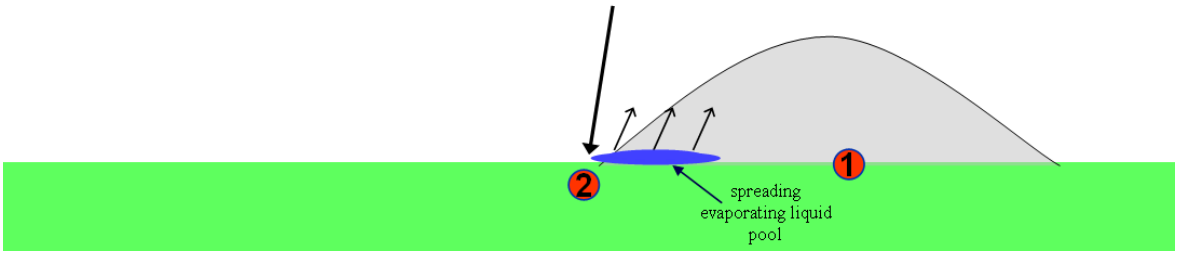

(d) Release 'pool observers' after upwind edge of instantaneous observer passes upwind pool edge

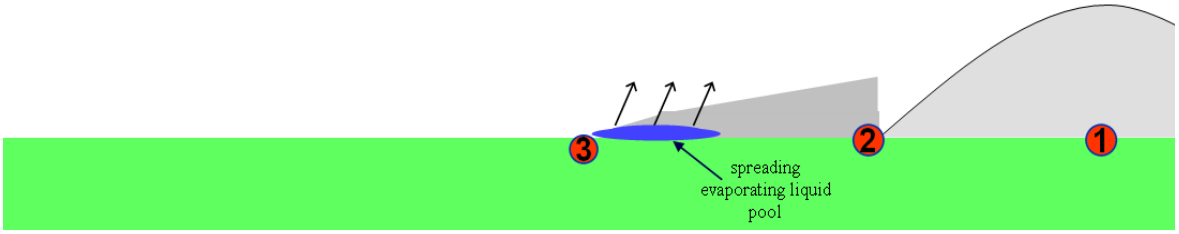

(e) Dispersion directly from pool, with original instantaneous cloud moving away from pool

Figure 9. UDM dispersion stages for instantaneous release with rainout

5.3 Details of observer dispersion calculations

5.3.1 Two-phase release: UDM observer primary variables

Two-phase release: rainout and pool evaporation

In case of a two-phase release, a single droplet size (SMD) is presumed. The initial droplet size (after expansion to the ambient pressure) is obtained from the ATEX atmospheric expansion model. Two-phase dispersion equations are solved in the downwind direction with droplets moving towards the ground (because of gravity effects). The UDM thermodynamics manual describes in detail the droplet thermodynamics model. The unknown droplet variables (position, velocity, mass and temperature) are found by relating the droplet speed to the droplet position, and imposing momentum, mass and heat balances for a single droplet.

The rainout location is determined from the point at which the droplets hit the ground or hit the bund wall (whichever happens first) and the liquid component mass is removed from the cloud. PVAP pool spreading and evaporation calculations are carried out until the termination criterion is satisfied, i.e. until the pool evaporation rate has dropped below a minimum specified flow rate.

The total evaporated mass is calculated (until termination), and the times corresponding to the evaporation of equal-mass increments are determined. The maximum number of equal-mass increments is input to the model but the actual observers released depends on the function of flow rate versus time; see Appendix C for full details on the algorithm for selection of observer release times.

Once the pool has been calculated, its influence on release observers is accounted for. While an observer is travelling over the pool, the observer equations are modified. For example mass is added from evaporation, conservation of momentum takes account of vertically evaporating vapour, heat and ground vapour transfer take account of the underlying pool. This also affects observer height, i.e. the observer would be very close to the ground in case mass from pool is very much larger than mass originally from release[lx].

After the pool has moved upwind of the release point, or the release has left the pool behind, observers are released from the upwind edge of the pool at these times. Whilst above the pool, these observers are influenced by its presence in the same way as described above for release observers.
The influence of the pool on any observer ends when that observer has left the pool behind (i.e. $x_{cld} > x_{pool} + R_{pool}$).

For non-instantaneous releases, it is presumed that those observers which do rain out, rain out successively, although some of the observers may not rainout. Let i = 0,1,…, NSEG be the observers, which are released at subsequent release times. Let j and k ($0 \leq j < k \leq$ NSEG) be two observers which are both raining out, then it is therefore always presumed that the rainout time t_{ro}^{k} for observer k is always larger than the rainout time t_{ro}^{j} for observer j.[lxi]

For instantaneous releases, the initial 'instantaneous' observer corresponds with the original instantaneous cloud. In case of rainout and after the upwind edge of the original instantaneous cloud has left behind the upwind edge of the pool, 'steady-state' observers are released from the upwind edge of the pool.

UDM observer primary variables

For each observer, differential equations are formulated for the unknown primary variables listed in the table below. Variables listed in italic are added primary variables compared to the UDM formulation described in Chapter 3 (steady-state or unpressurised instantaneous releases without rainout).

[lx] These differences can potentially affect the amount of rainout (normally it will increase). Ideally, the pool calculations and observer calculations should be rerun iteratively to convergence, but this is impractical. Instead we use the updated observer results, but do not rerun the pool. If total rainout increased by more than 25% (and evaporated mass is a significant component of the cloud) then a warning (UDM3 1134) is given as the pool evaporated mass may be too low.

[lxi] If this would not be the case, the UDM provides a fatal error.

UDM PRIMARY VARIABLE	SYMBOL	UNIT (inst.)	UNIT (cont.)
UDM downwind distance of pool centre	x_{pool} (secondary variable for inst. case)	m	m
PVAP POOL PRIMARY VARIABLES	Various; see PVAP theory manual	-	-
UDM PRIMARY VARIABLES (for each observer)			
component mass	m_c	kg	kg/s
component enthalpy	H_c	J	J/s
mass of wet air in the cloud	m_{wa}	kg	kg/s
excess downwind momentum	$I_{x2} = I_x - m_{cld}u_a(z_c) = m_{cld}u_x - m_{cld}u_a(z_c) = I_x - m_{cld}u_w = m_{cld}u_x - m_{cld}u_w$	kg m/s	kg m/s^2
vertical momentum	$I_z = m_{cld}\, u_z = m_{cld}\, u_z$	kg m/s	kg m/s^2
downwind position	x_{cld}	m	m
vertical position	z_{cld}	m	m
heat conduction from substrate	q_{gnd}	J	J/s
water evaporated from substrate	m_{wv}^{gnd}	kg	kg/s
cross-wind dispersion coefficient[lxii]	$R_y = 2^{1/2}\sigma_y = 2^{1/2}\sigma_y$	m	m
droplet primary variables	Various; see THRM theory manual	-	-

Table 4. List of UDM primary plume variables (including rainout)

In addition to the above differential equations for the UDM primary variables, non-linear algebraic cloud-geometry equations are formulated for two additional primary variables (based on theory from Section 3.1), i.e. the vertical concentration exponent n and centroid height z_c.[lxiii] Subsequently a number of expressions are formulated in terms of primary variables to evaluate the UDM secondary variables. For the new modified formulation this includes as added secondary variables the rainout rate $m_{ro}(t)$, the rainout distance $x_{ro}(t)$, and the liquid rainout temperature $T_{d,ro}$ as function of the time t. Furthermore it includes secondary variables for each observer.

The differential equations for the above primary variables[lxiv] are solved while stepping forward in the time t.

5.3.2 Detailed algorithm and two-phase dispersion equations

The detailed algorithm can now be described as follows.

A. Evaluate rainout data, downwind distance of pool centre, and pool calculations

For the purpose of pool spill calculations, the liquid rainout mass m_{ro} (spill rate; kg/s for non-instantaneous release and kg for instantaneous release), liquid rainout temperature $T_{d,ro}$ (K) and downwind distance x_{pool} of the pool centre are evaluated as a function of time. For each observer, the point of rainout x_{ro} is taken as the downwind distance at which the droplet hits the ground or bund wall (whichever happens first).

Non-instantaneous release

Calculations are carried out for all observers until the point of rainout to provide the time-varying spill data (rainout rate m_{ro}^i, rainout time t_{ro}^i, rainout temperature $T_{d,ro}^i$ and rainout location x_{ro}^i; i=0,…NSEG) input to the PVAP pool spreading/evaporation model. Herewith for all observer calculations it is assumed that no pool is present (no linking between cloud and pool), i.e. the presence of the pool does not affect the amount of rainout.

Zero rainout is presumed before the first observer rains out. Likewise zero rainout is presumed after the last observer rains out. Furthermore observer rainout cannot occur after the droplet sizes drops below the critical

[lxii] A differential equation is not used for the jet phase (circular jet assumed), but for the heavy and passive phase only.

[lxiii] FUTURE. To further remove internal UDM geometry iterations (alongside THRM iterations).

[lxiv] The PVAP pool equations and the observer UDM equations could be considered to be solved simultaneously enabling a rigorous solution while the observers move over the pool. This enables a rigorous link between the cloud and the pool for the case of non-instantaneous elevated releases with rainout. For the other cases this simultaneous solution would not provide added benefit. However it has been shown for a wide set of test cases that a separate solution for each observer (as discussed in the current chapter, decoupling the rainout calculations from the pool evaporation calculations) provides overall very accurate results. In case the presence of the pool would significantly affect the amount of rainout, the current model produces a warning (in case of more than 1% difference) or an error (in case of more than 10% difference). Moreover a separate solution more easily enables automation of observers (subsequent release of additional observers to enable convergence check and to improve accuracy until convergence criterion is achieved). Investigations have shown that if a simultaneous solution would be adopted, then estimating rainout rate as a function of time would be problematic.

droplet size. Linear interpolation is presumed between two subsequent rainout times[lxv][lxvi], i.e. for the time period $t_{ro}^{i-1} \le t \le t_{ro}^{i}$ between rainout of observer i-1 and observer (i = 1, …NSEG):

$$m_{ro}(t) = m_{ro}^{\,i-1} + \frac{t - t_{ro}^{\,i-1}}{t_{ro}^{\,i} - t_{ro}^{\,i-1}}(t)\,[m_{ro}^{\,i} - m_{ro}^{\,i-1}] \quad (117)$$

$$x_{ro}(t) = x_{ro}^{\,i-1} + \frac{t - t_{ro}^{\,i-1}}{t_{ro}^{\,i} - t_{ro}^{\,i-1}}(t)\,[x_{ro}^{\,i} - x_{ro}^{\,i-1}] \quad (118)$$

$$T_{d,ro}(t) = T_{d,ro}^{\,i-1} + \frac{t - t_{ro}^{\,i-1}}{t_{ro}^{\,i} - t_{ro}^{\,i-1}}(t)\,[T_{d,ro}^{\,i} - T_{d,ro}^{\,i-1}] \quad (119)$$

Based on the above spill data, PVAP calculations are carried out to determine the time-varying pool radius and pool evaporation rate. See the PVAP theory manual for the governing theory. Furthermore a new UDM differential equation is added for the new added primary variable x_{pool} (x_{pool} is downwind pool mass centroid distance, m; M_{pool} = pool mass, kg):

$$\frac{dx_{pool}}{dt}(t) = \frac{m_{ro}(t)}{M_{pool}(t)}\left[x_{ro}(t) - x_{pool}(t)\right] \quad (120)$$

In case of the presence of a circular bund (with bund radius R_{bund} and bund centre at release point x=0), the bund is assumed to be only included in case the first observer rains out inside the bund. All subsequent rainout is assumed to be inside the bund (with a warning given in case subsequent rainout occurs outside the bund). Moreover the bund will only be included before bund overflow. In case the bund is to be included, the above equation (120) is subject to the additional condition

$$x_{pool}(t) = \min\left[x_{pool}(t),\, R_{bund} - R_{pool}(t)\right] \quad (121)$$

Thus as long the downwind edge of the pool remains to touch the bund wall [i.e. $x_{pool}(t)=R_{bund}-R_{pool}(t)$], the following modified differential equation is applied instead of Eq. (120)[lxvii]:

$$\frac{dx_{pool}}{dt}(t) = \min\left[\frac{m_{ro}(t)}{M_{pool}(t)}\left[x_{ro}(t) - x_{pool}(t)\right], -\frac{dR_{pool}(t)}{dt}\right] \quad (122)$$

Instantaneous release

For a non-instantaneous release, the observer droplets are currently assumed to be located at the same downwind distance as the centre-line, i.e. $x_d = x_{cld}$. However for an instantaneous release there is a droplet lag distance $x_d^{lag} = x_d^{ro} - x_{cld}(t_d^{ro}) \neq 0$[lxviii]. For the initial instantaneous observer, the rainout mass m_{ro} (kg), the rainout distance x_{pool}, and the rainout temperature $T_{d,ro}$ are determined from the primary observer variables at the rainout time, i.e. at the time t_d^{ro} at which the instantaneous observer droplet reaches the ground or hits the bund wall.

At time t=0, the downwind distance of the centre of the pool will be equal to the rainout distance: $x_{pool} = x_d^{ro}$. The distance x_{pool} will be fixed in case rainout does not occur inside the bund; otherwise it is subject to the condition of Equation (121).

[lxv] In case rainout occurs, rainout is presumed to stop as soon as an observer does not rain out. In case subsequent rainout occurs, a warning message (UDMA 1113) is given

[lxvi] The difference in rainout time for consecutive observers can be greater than the difference in the observer release times. Given we use linear interpolation of rainout rate this can lead to much more mass raining out than is released (see D-12109). Mass conservation requires that rainout intervals for observers after the first are equal to observer release intervals. Thus for i > 0 we set $t_{ro}^{\,i} = t_{ro}^{\,0} + t_{rel}^{\,i}$.

[lxvii] FUTURE. This equation for time-varying rainout releases not yet implemented, since dR_{pool}/dt is unknown for all but pools spreading normally on land. Presently Eq. (121) is used all cases. Equation (122) is not used, since an analytical expression for dR_{pool}/dt is not available for cases spreading on water.

[lxviii] The droplet lag distance $x_d^{lag} = x_d^{ro} - x_{cld}(t_{ro}) \neq 0$ is caused by the starting position of the droplet at the edge of the instantaneous cloud [$x_d(t=0) = x_{cld}(t=0) + W_{eff}$], and for pressurised instantaneous releases also because during the initial energetic expansion the downwind droplet size velocity u_{dx} is different to the downwind cloud velocity u_x; see the THRM theory manual for further details. The instantaneous droplet logic is expected to change further following the INEX work.

B. Adjust observer data if observer passes release location with ongoing release

Observers released from the upwind edge of the pool will pass over the release location x=0, say at time t = t_s^i for pool observer i. If at this time the original release is still ongoing, i.e. $t_s^i \leq t_{dur}$ (never applicable for instantaneous releases), the observer data (primary variables) are adjusted to account for the added release term.

Immediately prior to the adjustment, we have two separate plumes, one possibly momentum-driven elevated plume ('release' plume) starting from the release height (with 100% concentration, not yet air entrainment), and a second heavy-gas ground-level plume ('pool' plume) with possibly already significant air entrainment. For purpose of UDM calculations after the adjustment, we need to combine these two plumes into an equivalent plume ('combined' plume). This combination should be both appropriate for material release rate much larger than the material flow rate in the 'pool' plume and vice versa. To ensure this we will not be able to always apply the more usual approach of adding the plumes together (e.g. adding amount of wet air, conserving mass of water and heat added from the substrate, etc.), but we apply a more appropriate averaging of the plume as further detailed below.

The adjustment of the primary variables is now as follows:

1. Unchanged primary variables (derived from original 'pool' plume):

   1.1. UDM downwind distance of pool centre, x_{pool}, and PVAP pool primary variables
   1.2. downwind position, x_{cld}

2. Conservation of component mass and component enthalpy. Adjust observer component mass $m_c^i(t_s^i)$ to add source release rate $Q(t_s^i)$, kg/s, and adjust component enthalpy to add source release enthalpy [release temperature = $T_c^R(t_s^i)$]

$$m_c^{\,i}(t_s^{\,i}) = m_c^{\,i}(t_s^{\,i}) + Q(t_s^{\,i}), \quad H_c^{\,i}(t_s^{\,i}) = H_c^{\,i}(t_s^{\,i}) + Q(t_s^{\,i})\, h_c\left(T_c^{\,R}(t_s^{\,i})\right) \qquad \textbf{(123)}$$

3. Since liquid is only released from the 'release plume', the initial values of the droplet variables for the 'combined' plume are immediately determined from the 'release' plume. Thus the droplet dispersion variables are initialised as described in Section 4.3 of the THRM theory manual:

   3.1. The initial droplet position $[x_d(t_s^i), z_d(t_s^i)]$ = release position of the jet = $[0, z_R]$
   3.2. The initial droplet speed equals the release speed of the jet[lxix]
   3.3. The initial droplet temperature equals the temperature of the jet
   3.4. The initial droplet mass is found from the initial droplet diameter (derived from ATEX) and the initial droplet density

4. The vertical momentum I_z is found by summing the vertical momentum of the original cloud (zero, since dispersion from pool) and the vertical momentum of the release (absolute release speed, u_R (m/s); release angle to horizontal, θ_R (radians)[xvii]:

$$I_z = Q(t_s^{\,i})\, u_R(t_s^{\,i}) \sin(\theta_R) \qquad \textbf{(124)}$$

5. The vertical cloud position, z_{cld}, the mass of wet air added to the cloud, m_{wa}, the water vapour transfer added from the substrate, m_{wv}^{gnd}, and the heat transfer added from the substrate are obtained by component material mass averaging[lxx] over the original 'pool' plume [component flow rate $m_c^i(t_{s^-}^i)$] and the 'release' plume [component release rate $Q(t_s^i)$]:

[lxix] This is not currently applied, since the horizontal droplet velocity must now be set equal to the plume velocity.

[lxx] Combining plumes by summing heat fluxes and wet air does NOT result in the correct behaviour, e.g. consider a pool with a tiny evaporation rate and a huge amount of added mass. This issue is overcome by mass averaging which gives the correct behaviour (including both extreme cases, pool rate << release rate and pool rate >> release rate).

$$z_{cld}(t_s^{\,i}) = \frac{Q(t_s^{\,i})\, z_R}{m_c(t_s^{\,i}{}_-) + Q(t_s^{\,i})} \quad , \qquad \textbf{(125)}$$

$$m_{wa}(t_s^{\,i}) = m_{wap}(t_s^{\,i}) + m_{waR}(t_s^{\,i}),\ with$$

$$m_{wap}(t_s^{\,i}) = \frac{m_c(t_s^{\,i}{}_-)\, m_{wa}(t_s^{\,i}{}_-)}{m_c(t_s^{\,i}{}_-) + Q(t_s^{\,i})},\ m_{waR}(t_s^{\,i}) = \frac{Q(t_s^{\,i})\, m_{wa}{}^{R}(t_s^{\,i})}{m_c(t_s^{\,i}{}_-) + Q(t_s^{\,i})}$$

$$m_{wv}{}^{gnd}(t_s^{\,i}) = \frac{m_c(t_s^{\,i}{}_-)\, m_{wv}{}^{gnd}(t_s^{\,i}{}_-)}{m_c(t_s^{\,i}{}_-) + Q(t_s^{\,i})},\ q^{gnd}(t_s^{\,i}) = \frac{m_c(t_s^{\,i}{}_-)\, q^{gnd}(t_s^{\,i}{}_-)}{m_c(t_s^{\,i}{}_-) + Q(t_s^{\,i})}$$

Here $m_{wa}{}^{R}(t_s{}^{i})$ is the initial mass of wet air of the release plume. The mass of wet air added to the cloud, m_{wa} is presumed above to consist of a mass of wet air m_{wap} from the original pool and a mass of wet air m_{waR} from the initial release plume.

6. The remaining primary variables are the excess downwind momentum I_{x2}, and the cross-wind dispersion coefficient R_y. These are set as follows

6.1. Set cloud effective width (secondary variable) using mass averaging as above[lxxi]

$$W_{eff}(t_s^{\,i}) = \frac{m_c(t_s^{\,i}{}_-)\, W_{eff}(t_s^{\,i}{}_-) + Q(t_s^{\,i}) W_{eff}{}^{R}}{m_c(t_s^{\,i}{}_-) + Q(t_s^{\,i})}, \qquad \textbf{(126)}$$

6.2. Set new total cloud mass (secondary variable)

$$m_{cld}{}^{i} \quad = \quad m_{wa}{}^{i} + m_c{}^{i} + m_{wv}{}^{gnd\,i} \qquad \textbf{(127)}$$

6.3. The horizontal velocity is now derived from conservation of horizontal momentum:

$$m_{cld}{}^{i}\, u_x(t_s^{\,i}) = \left[m_{wap}(t_s^{\,i}) + m_{wv}{}^{gnd}(t_s^{\,i}) + m_c(t_s^{\,i}{}_-)\right] u_{cld}(t_s^{\,i}{}_-) + \left[Q(t_s^{\,i}) + m_{waR}(t_s^{\,i})\right] u_R(t_s^{\,i}) \cos(\theta_R) \qquad \textbf{(128)}$$

6.4. The total plume velocity u_{cld} can now be derived from Equations (124), (128), and $I_z = m_{cld} u_z$, i.e. $u_{cld} = [u_x^2 + (I_z/m_{cld})]^{1/2}$.

6.5. Set cloud geometry

6.5.1. Carry out THRM calculations to set new cloud density ρ_{cld}; set new volumetric flow rate $A_{cld}u_{cld} = m_{cld}/\rho_{cld}$ [m^3/s]. Set exponent m from new ρ_{cld}.

6.5.2. Set C_m from m and set cloud radius $R_y = W_{eff} / C_m$. Also initially we assume we are again in the elevated jet phase.

6.5.3. Section 3.1.1 describes the geometry for a non-instantaneous cloud including an expression for n as function of H_{eff} (see Figure 28), H_{eff} as function of n and R_z [Equation (6)], and h_d as function of z_{cld}, R_z, θ and n [Equation (13)]. By insertion of these expressions into Equation (12) for A_{cld}, a non-linear equation for R_z can be formulated, which is solved iteratively for R_z.

6.5.4. Set centroid height z_c from the thus found values for R_z, h_d, H_{eff}, and n using Equation (19)

6.6. Set residual horizontal excess cloud momentum:

[lxxi] TO DO. Source width does not take account of added air.

$$I_{x2} = m_{cld}[u_x - u_a(z_c)], \quad \textbf{(129)}$$

C. Apply observer rainout at rainout time

Rainout is applied at the time $t=t_{ro}^i$ at which the observer vertical droplet coordinate reduces to zero $[y_d^i(t)=0]$ or when the observer hits the bund wall. The liquid component is removed from the cloud [only droplets above critical droplet size; mass $m_{ro}(t)$] to obtain primary and secondary variables for the "residual" cloud:

1. Set residual component mass m_c and residual enthalpy H_c by removing rained-out liquid

$$m_c^{\,i}(t_{ro}^{\,i}) = m_c^{\,i}(t_{ro}^{\,i}) - m_{ro}(t), \;\; H_c^{\,i}(t_{ro}^{\,i}) = H_c^{\,i}(t_{ro}^{\,i}) - m_{ro}(t_{ro}^{\,i})\, h_{cL}\left(T_{d,ro}^{\,i}\right) \quad \textbf{(130)}$$

2. The following primary variables are presumed to be unchanged: m_{wa}, x_{cld}, z_{cld}, q_{gnd}, m_{wv}^{gnd}. Also the cloud speed (u_x, u_z) is assumed to be unchanged. The remaining primary variables are set as follows[lxxii]:

2.1. Set residual total cloud mass (secondary variable)

$$m_{cld}^{\;\;i} \;\; = \;\; m_{wa}^{\;\;i} + m_c^{\,i} + m_{wv}^{\;\;gnd^i} \quad \textbf{(131)}$$

2.2. Set cloud geometry

2.2.1. Carry out THRM calculations to set residual cloud density ρ_{cld}; set residual cloud volume $V_{cld} = m_{cld}/\rho_{cld}$ [instantaneous, m^3] or residual volumetric flow rate $A_{cld}u_{cld} = m_{cld}/\rho_{cld}$ [m^3/s]. Set exponent m from new ρ_{cld}.

2.2.2. In case at time of rainout the transition from jet to heavy phase has taken place, R_y is a primary variable and it is presumed that W_{eff} is not changed during rainout: set C_m from m and set cloud radius $R_y = W_{eff} / C_m$.

2.2.3. Section 3.1 describes the UDM cloud geometry for both cases of a non-instantaneous release and an instantaneous release. This section includes an expression for n as function of H_{eff}, H_{eff} as function of n and R_z, and h_d as function of z_{cld}, R_z, θ and n. By insertion of these expressions into formulas for V_{cld} (instantaneous) or A_{cld} (continuous), a non-linear equation for R_z can be formulated, which is solved iteratively for R_z.

2.2.4. Set centroid height z_c from the thus found values for R_z, h_d, H_{eff}, and n.

2.3. Residual cloud momentum (assuming u_x and u_z remain unchanged at rainout as indicated above):

$$I_{x2} = m_{cld}[u_x - u_a], \; I_z = m_{cld}u_z, \quad \textbf{(132)}$$

3. Reset other secondary variables accordingly

D. Solution of dispersion equations for each observer

For each observer, carry out modified UDM observer dispersion equations accounting for pool evaporation while the observer moves over the pool (see Figure 10).

As described in above step B this accounts for the observer possibly passing the release location x=0 with a still active pool.

[lxxii] CHECK. Perhaps it would be more convenient to apply W_{eff} as a primary variable instead of R_y

As described in above step C this also accounts for rainout if the observer droplet hits the ground or the bund wall.

As described in above step A it sets the PVAP spill rate, the PVAP spill temperatures, the downwind distance x_{pool} of the pool, and it carries out the associated PVAP pool calculations. For non-instantaneous observers these are set as described in above step A in initial observer calculations (unaffected by the pool), while for the subsequent calculations the concentrations of the release observers will be affected by the pool.

For a non-instantaneous observer the observer will pick-up incrementally vapour from the pool while it is moving over the pool as shown in Figure 10a.

As soon as the upwind edge of the original instantaneous cloud reaches the upwind edge of the pool, i.e. as soon as $x_{cld}(t) - W_{gnd}(t) \geq x_{pool} - R_{pool}(t)$, non-instantaneous observers will be released from the upwind edge of the pool. Before this time, the entire pool vapour will be added back to the instantaneous cloud; see Figure 10b. The instantaneous cloud is considered to have left the pool behind if the 'upwind edge' of the instantaneous cloud reaches the downwind edge of the evaporating pool, i.e. when $x_{cld}(t) - W_{gnd}(t) = x_{pool} + R_{pool}(t)$; see Figure 10b. After this time, the original instantaneous plume moves away from the pool and no vapour is picked up from the pool[lxxiii].

[lxxiii] In 6.54 it was assumed that the instantaneous cloud picks up vapour from the entire pool before it leaves the pool behind, while no vapour pick up is assumed after the pool leaves the pool behind. Furthermore the instantaneous cloud was considered to have left the pool behind if the 'upwind edge' $x = x_{cld}(t) - W_{eff}(t)$ of the instantaneous cloud reaches the downwind edge of the evaporating pool, i.e. when $x_{cld}(t) - W_{eff}(t) = x_d^{ro} + R_{pool}(t)$. This results in a discontinuity. After this time, the original instantaneous plume moves away from the pool, and a new finite-duration continuous plume emanates from the pool. At this transition time, the downwind edge of the new plume is located at the downwind edge of the pool (=upwind edge of original instantaneous plume).

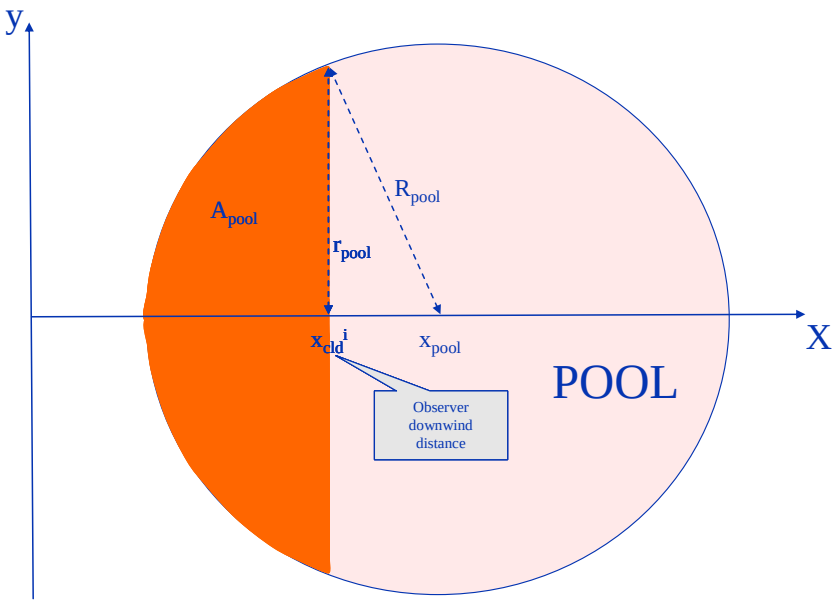

(a) non-instantaneous observer (incremental vapour pick-up while observer moves over pool)

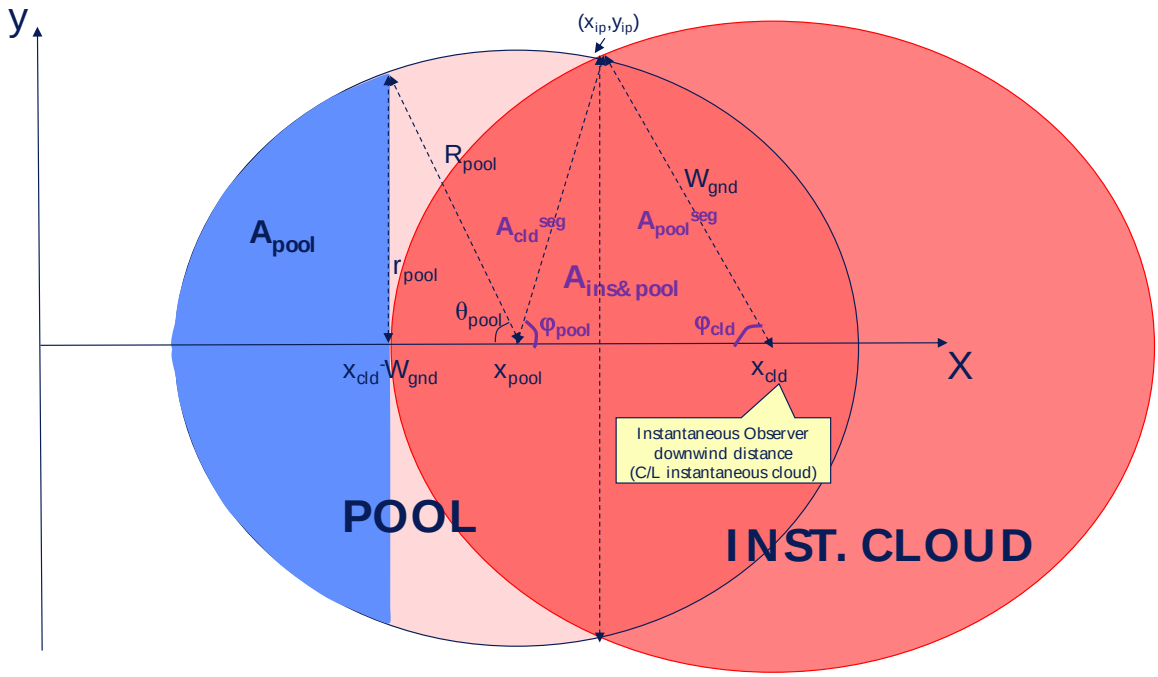

(b) instantaneous observer [vapour from pool area πR_{pool}^2-A_{pool} is added back to instantaneous cloud; W_{gnd} is radius of instantaneous cloud touching the ground; area of cross-section of pool and instantaneous cloud ground area is $A_{ins\&pool}=A_{cld}^{seg}+A_{pool}^{seg}$]

Figure 10. Vapour pick-up from pool while observer is moving over the pool

The UDM observer dispersion equations are as follows:

- *Mass balance for observer component mass m_c; enthalpy balance for observer component enthalpy H_c*

Non-instantaneous observer

If the observer moves over the pool [x_{pool}-R_{pool}< x_{pool}< x_{pool}+R_{pool}] the observer will pick up vapour from the pool. Let $r_{pool}^{i}(t)$ be the crosswind radius of the pool immediately below the observer i [at time t, when observer is located at downwind distance $x_{cld}^{i}(t)$], then (see Figure 10a)

$$r_{pool}^{\ i}(t) = \sqrt{\left[R_{pool}(t)\right]^2 - \left[x_{pool}(t) - x_{cld}^{\ i}(t)\right]^2} \qquad (133)$$

$$\frac{dm_c^{\ i}}{dt}(t) = \frac{dx_{cld}^{\ i}}{dt}\frac{dm_c^{\ i}}{dx_{cld}^{\ i}} = u_x^{\ i}(t)\left[2r_{pool}^{\ i}(t)\right]\frac{m_c^{\ pool}(t)}{\pi\left[R_{pool}(t)\right]^2} \qquad (134)$$

$$\frac{dH_c^{\ i}}{dt}(t) = \frac{dm_c^{\ i}}{dt}(t)\ \ h_{vc}(T_{pool}, P_a) \qquad (135)$$

If the observer does not move over the pool, the observer primary variables m_c^{i} and H_c^{i} remain constant (upwind or downwind of the pool).

Instantaneous observer (see Figure 10b)

Prior to rainout and after the instantaneous observer has left the pool behind, the observer primary variables m_c^{i} and H_c^{i} remain constant. When the instantaneous observer moves over the pool, it is assumed to pick up vapour from that part of the pool which lies downwind of x = x_{cld}-W_{gnd}. The vapour upwind of this part will be added back to subsequent non-instantaneous observers. Thus,

$$\frac{dm_c^{\ i}}{dt}(t) = \frac{\pi\left[R_{pool}(t)\right]^2 - A^{pool}(t)}{\pi\left[R_{pool}(t)\right]^2} m_c^{\ pool}(t) \qquad (136)$$

Here $A^{pool}(t)$ is the area of that part of the pool for which vapour is not added back to the instantaneous cloud[lxxiv].

For $x_{cld} - W_{gnd} \leq x_{pool} - R_{pool}$, the upwind edge of the instantaneous cloud is upwind of the upwind edge of the pool and $A_{pool} = 0$. For $x_{cld} - W_{gnd} \geq x_{pool} + R_{pool}$, the upwind edge of the instantaneous cloud is downwind of the downwind edge of the pool and $A_{pool} = \pi R_{pool}^2$. Otherwise, for $x_{pool} - R_{pool} \leq x_{cld} - W_{gnd} \leq x_{pool} + R_{pool}$, we define (see Figure 10b), $r_{pool} = R_{pool}\sin(\theta_{pool})$, $x_{pool} - (x_{cld} - W_{gnd}) = R_{pool}\cos(\theta_{pool})$ with the angle θ_{pool} ($0 \leq \theta_{pool} \leq \pi$),

$$\theta_{pool} = \arccos\left(\frac{x_{pool} - \left(x_{cld} - W_{gnd}\right)}{R_{pool}}\right) \qquad (137)$$

It can be derived that $A_{pool}(t)$ is given by

[lxxiv] This is slightly inconsistent with the formulation previously adopted for Phase III of the Droplet Modelling JIP (Report C2). Here the instantaneous cloud was assumed to leave the pool behind, when the upwind instantaneous-cloud $x_{cld}(t)$-$W_{eff}(t)$ reaches the downwind edge of the evaporating pool. In the current formulation we have used the more appropriate choice of W_{gnd} instead of $W_{eff}(t)$, since pool vapour pick-up should be affected by the ground.

$$A_{pool}(t) = R_{pool}^{\,2}\,\vartheta_{pool} - \left[x_{pool} - (x_{cld} - W_{gnd})\right] r^{pool}(t) \qquad (138)$$
$$= R_{pool}^{\,2}\left[\vartheta_{pool} - \cos(\vartheta_{pool})\sin(\vartheta_{pool})\right]$$
$$= \frac{R_{pool}^2}{2}\left[2\vartheta_{pool} - \sin(2\vartheta_{pool})\right]$$

Conservation of instantaneous observer enthalpy again yields:

$$\frac{dH_c^{\,i}}{dt}(t) = \frac{dm_c^{\,i}}{dt}(t)\;\; h_{vc}(T_{pool}, P_a) \qquad (139)$$

- *Conservation of observer mass of wet-air in cloud,* $m_{wa}^{\,i}$ (kg for instantaneous; kg/s for continuous)

$$\frac{dm_{wa}^{\,i}}{dt} = u_{cld}^{\,i} E_{tot}^{\,i} \qquad (\text{non-instantaneous}) \qquad (140)$$
$$\frac{dm_{wa}^{\,i}}{dt} = E_{tot}^{\,i} \qquad (\text{instantaneous})$$

Here $E_{tot}^{\,i}$ is the total wet air entrainment rate (kg/s for instantaneous; kg/m/s for continuous).

- *Conservation of observer excess horizontal and vertical component of momentum*

The horizontal momentum equation for excess downwind momentum $I_{x2} = I_x - m_{cld}u_a(z_c) = m_{cld}u_x - m_{cld}u_a(z_c)$, and the vertical momentum equation for vertical momentum $I_z = m_{cld}u_z$ are modified at observer rainout as described above. They are further modified to account for added momentum of pool vapour.

For a non-instantaneous observer, the modified equations are given by

$$\begin{bmatrix} \frac{dI_{x2}}{dt} \\ \frac{dI_z}{dt} \end{bmatrix} = u_{cld}\,F_{drag}^{air}\begin{bmatrix} |\sin\theta| \\ -\cos\theta\,\frac{\sin\theta}{|\sin\theta|} \end{bmatrix} + u_{cld}\,F_{impact}^{ground}\begin{bmatrix} -\sin\theta \\ \cos\theta \end{bmatrix} + \qquad (141)$$
$$u_{cld}\,F_{drag}^{ground}\begin{bmatrix} 1 \\ 0 \end{bmatrix} + u_{cld}\,A_{cld}\,(\rho_{cld} - \rho_a)g\begin{bmatrix} 0 \\ -1 \end{bmatrix} + \frac{dm_c^{\,i}}{dt}(t)\begin{bmatrix} -u_a(z_c) \\ u_z^{pool} \end{bmatrix}$$

Here the cloud area $A_{cld} = m_{cld} / (\rho_{cld}u_{cld})$, and u_z^{pool} is the vertical velocity of the component evaporating from the pool.

For an instantaneous observer, [cloud volume $V_{cld} = m_{cld} / \rho_{cld}$],

$$\begin{bmatrix} \frac{dI_{x2}}{dt} \\ \frac{dI_z}{dt} \end{bmatrix} = F_{drag}^{air}\begin{bmatrix} |\sin\theta| \\ -\cos\theta\,\frac{\sin\theta}{|\sin\theta|} \end{bmatrix} + F_{impact}^{ground}\begin{bmatrix} -\sin\theta \\ \cos\theta \end{bmatrix} + \qquad (142)$$
$$F_{drag}^{ground}\begin{bmatrix} 1 \\ 0 \end{bmatrix} + V_{cld}\,(\rho_{cld} - \rho_a)g\begin{bmatrix} 0 \\ -1 \end{bmatrix} + \frac{dm_c^{\,i}}{dt}(t)\begin{bmatrix} -u_a(z_c) \\ u_z^{pool} \end{bmatrix}$$

- *Observer horizontal and vertical position:*

The equation for horizontal position is unchanged,

$$\frac{dx_{cld}}{dt} = u_x = u_{cld}\cos\theta \qquad (143)$$

The equation for vertical position is modified to account for addition of pool mass at ground level z=0 instead at the C/L height z_{cld} (conservation of mass centroid height),

$$\frac{dz_{cld}}{dt} = u_z - \frac{z_{cld}}{m_{cld}}\frac{dm_c}{dt} = u_{cld}\sin\theta - \frac{z_{cld}}{m_{cld}}\frac{dm_c}{dt} \qquad (144)$$

- *Rate of heat convection from the substrate*

Heat transfer will take place from the pool to the cloud, but the amount of heat transfer will be different in case the cloud is not above the pool since the pool is at temperature T_{pool} and not at the substrate temperature T_{gnd}. Moreover part of the cloud could be above the pool and part above the substrate. Thus the following is assumed for the heat transfer from the substrate:

$$\frac{d\,q^{gnd^i}}{dt} = \frac{d\,q^{gnd,pool^i}}{dt} + \frac{d\,q^{gnd,gnd^i}}{dt} \qquad (145)$$

Here the first term represents the heat transfer from the pool to the cloud and the second term represents the heat transfer from the substrate to the cloud:

$$\frac{dq^{gnd,pool^i}}{dt} = 2u_{cld}{}^i Q_{gnd,T_{pool}} \min\left[W_{gnd}{}^i, r^{pool^i}(t)\right]$$
$$\frac{dq^{gnd,gnd^i}}{dt} = 2u_{cld}{}^i Q_{gnd,T_{gnd}}\left\{W_{gnd}{}^i - \min\left[W_{gnd}{}^i, r^{pool^i}(t)\right]\right\} \qquad (146)$$

in W/s, continuous

$$\frac{dq^{gnd,pool^i}}{dt} = Q_{gnd,T_{pool}} A_{ins\&pool}$$
$$\frac{dq^{gnd,gnd^i}}{dt} = Q_{gnd,T_{gnd}}\left\{S_{gnd}{}^i - A_{ins\&pool}\right\}$$

in W, instantaneous

Here $A_{ins\&pool,}$ is that part of the ground surface area of the instantaneous cloud which covers the pool (red-coloured area in Figure 10b).

The point (x_{ip}, y_{ip}) as depicted in Figure 10b is given by

$$x_{ip} = x_{pool} + \frac{\left(x_{cld} - x_{pool}\right)^2 + R_{pool}{}^2 - W_{gnd}{}^2}{2\left(x_{cld} - x_{pool}\right)} \qquad (147)$$
$$y_{ip} = \sqrt{R_{pool}{}^2 - \left(x_{pool} - x_{ip}\right)^2}$$

Equation (138) includes a formula for the pool-circle area segment A_{pool} defined by the angle θ_{pool} (x_{pool}-R_{pool}≤x≤x_{cld}-W_{gnd}). In case the instantaneous cloud partly covers the pool, one can similarly calculate the area $A_{ins\&pool}$ as the sum of area $A_{pool}{}^{seg}$ for the pool-circle area segment define by angle φ_{pool} (x_{ip}≤x≤x_{pool}+R_{pool}) in Figure 10b and the area $A_{cld}{}^{seg}$ for the cloud-circle area segment defined by angle φ_{cld} (x_{cld}-W_{gnd}≤x≤ x_{ip}) in Figure 10b, where

$$A_{pool}^{seg} = \frac{R_{pool}^2}{2}\left[2\varphi_{pool} - \sin\left(2\varphi_{pool}\right)\right],\ A_{cld}^{seg} = \frac{W_{gnd}^2}{2}\left[2\varphi_{cld} - \sin\left(2\varphi_{cld}\right)\right] \quad \textbf{(148)}$$

Thus:

$$\begin{aligned} A_{ins\&pool} &= 0, && (no\ \text{int}er\,\text{section}) \\ &= \pi R_{pool}^{\ 2}, && (entire\ pool\ \text{cov}ered) \\ &= \pi W_{gnd}^{\ 2}, && (entire\ cloud\ above\ pool) \\ &= A_{pool}^{seg} + A_{cld}^{seg}, && (else) \end{aligned} \quad \textbf{(149)}$$

The angles φ_{pool} and φ_{cld} in Figure 10b can be calculated as follows with the use of Equation (147):

$$\varphi_{pool} = \cos^{-1}\left(\frac{x_{ip} - x_{pool}}{R_{pool}}\right) = \cos^{-1}\left(\frac{R_{pool}^2 + \left(x_{cld} - x_{pool}\right)^2 - W_{gnd}^2}{2R_{pool}\left(x_{cld} - x_{pool}\right)}\right) \quad \textbf{(150)}$$

$$\varphi_{cld} = \cos^{-1}\left(\frac{x_{cld} - x_{ip}}{W_{gnd}}\right) = 2\cos^{-1}\left(\frac{W_{gnd}^2 + \left(x_{cld} - x_{pool}\right)^2 - R_{pool}^2}{2W_{gnd}\left(x_{cld} - x_{pool}\right)}\right)$$

- *Water-vapour transfer from the substrate*

Water vapour transfer from the substrate to the cloud will only take place for that part of the cloud above the water. As a result, the water vapour transfer from the substrate is now set identical as previously, however now using $dq^{gnd,gnd}/dt$ instead dq^{gnd}/dt, i.e.

$$\frac{dm_{wv}^{gnd}}{dt} = \frac{5\left[\ P_v^{\ w}(T_{gnd}) - P_v^{\ w}(T_{vap})\ \right]\frac{dq_{gnd,gnd}}{dt}}{C_p^{\ cld}\ T_{gnd}\ P_a}\ ,\quad T_{gnd} > T_{vap} \quad \textbf{(151)}$$

where P_v^w is the saturated vapour pressure of the water. If $T_{gnd} < T_{vap}$ or $T_{gnd} < 0$ºC (substrate is ice) or if the cloud is passing over dry ground, $dm_{wv}^{gnd}/dt = 0$.

- *Crosswind spreading*

In general cross-wind spreading consists of the following three subsequent phases.

1. Near-field ('jet') spreading *(unmodified).* The cloud is assumed to remain circular until the passive transition or (after onset of touching down) until the spread rate reduces to the heavy-gas spread rate, i.e. $R_y = R_z$

2. Heavy-gas spreading *(modified to account for added pool vapour)*. For a detailed discussion of the effects of pools on heavy-gas spreading Report C2 of Phase III of the modelling JIP[72] includes a detailed discussion and a range of options for modelling the effects of pools on heavy-gas spreading[lxxv]. The heavy-gas spread rate is applied until the passive transition. In case of the absence of a pool, according to Equations (86) and (87), the heavy gas spread rate can be written as

$$\frac{d\,R_y}{dt} = \frac{F_{CE}}{C_m}\ ,\quad with\ F_{CE} = C_E\sqrt{\frac{g\left\{\max\left[0,\ \rho_{cld} - \rho_a(z = z_{cld})\right]\right\}\ H_{eff}\,(1 + h_d)}{\rho_{cld}}} \quad \textbf{(152)}$$

Non-instantaneous observer

[lxxv] In this section mass averaging is considered over the component mass in the cloud m_c and the mass Δm_c added during a time step Δt. Instead one could consider mass averaging over the cloud mass m_{cld} and Δm_c. Furthermore r_{pool} is now compared with W_{eff}, while one could consider to compare r_{pool} with R_y. Note that in report C2 of Phase III of the modelling JIP a range of options have been discussed and compared. This also includes the option of possible implementation of the HEGADAS heavy-gas criterion including gravity-spreading collapse.

For an incremental step Δt of a non-instantaneous observer, the incremental spread is calculated based on mass averaging of the mass of component m_c in the cloud (kg/s) and the mass component added from the pool Δm_c (kg/s),

$$C_m \Delta R_y = \frac{m_c F_{CE} \Delta t + \Delta m_c \max\left[0, r_{pool}(t) - W_{eff}\right]}{m_c + \Delta m_c} \quad \textbf{(153)}$$

Here $r_{pool}(t)$ is the pool half-width in the crosswind direction (Figure 10a), while W_{eff} is the effective cloud half-width. The above equation reduces in differential form to:

$$\frac{d R_y}{dt} = \frac{1}{C_m}\left\{F_{CE} + \frac{1}{m_c}\frac{dm_c}{dt} \max\left[0, r_{pool}(t) - W_{eff}\right]\right\} \quad \textbf{(154)}$$

Instantaneous observer

For an incremental step Δt of an instantaneous observer, the incremental spread is calculated based on mass averaging of the component mass m_c in the cloud (kg) and the mass component added from the pool Δm_c (kg),

$$C_m \Delta R_y = \frac{m_c F_{CE} \Delta t + \Delta m_c C_m \max\left[0, \sqrt{\frac{A_{ins\&pool}}{\pi}} - W_{gnd}\right]}{m_c + \Delta m_c} \quad \textbf{(155)}$$

Here $A_{ins\&pool}$ (t) is the part of the pool which is covered by the instantaneous cloud, while W_{gnd} is the radius of the instantaneous cloud area at the ground (Figure 10b). The above equation reduces in differential form to:

$$\frac{d R_y}{dt} = \frac{F_{CE}}{C_m} + \frac{1}{m_c}\frac{dm_c}{dt} \max\left[0, \sqrt{\frac{A_{ins\&pool}}{\pi}} - W_{gnd}\right] \quad \textbf{(156)}$$

Thus in case the equivalent radius associated with $A_{ins\&pool}$ is larger than W_{gnd}, the above equation applies mass averaging over the cloud mass m_{cld} (kg) and the mass flow added from the pool dm_c/dt (kg/s).

3. Passive spreading *(modified to account for added pool vapour – however unlikely passive when observer still moving over the pool; possibly ignore this).* After the passive transition the passive spread rate is applied [$\sigma_{ya}(x)$ = ambient passive dispersion coefficient; $x_0 = 0$ presently]

$$\frac{dR_y}{dt}[at\ x] = \frac{1}{C_m}\left\{[r_{pool}(s) - W_{eff}]\frac{1}{m_c}\frac{dm_c}{dt}\right\} + u_x 2^{0.5}\frac{d\sigma_{ya}}{dx}[at\ \ x - x_o] \quad \textbf{(157)}$$

6. UDM DISPERSION MODEL FOR PRESSURISED INSTANTANEOUS TWO-PHASE RELEASE

For a pressurised instantaneous release (catastrophic vessel rupture), the Phast discharge model presumes isentropic expansion from the stagnation conditions to the atmospheric pressure without air entrainment. The initial UDM dispersion state is based on the post-expansion discharge results. The UDM dispersion model for instantaneous releases includes an initial phase of energetic rapid expansion (modelled by UDM sub-model INEX), and a subsequent phase of dispersion where equations are adopted applicable for unpressurized releases.

The UDM includes three separate, independent instantaneous energetic expansion models:

- Section 6.1 outlines the new improved INEX model (default model from 8.0).
- Section 6.2 describes the previous old INEX model (default model prior to 8.0).
- Section 6.3 describes a simplistic model labelled as the “Purple Book”[73] model.

The new INEX model includes improved modelling of time-varying dispersion including potential rainout using the observer concept as described in Chapter 5.

The old INEX model is a simplistic model for the calculation of the initial dispersion phase of energetic expansion for pressurized instantaneous releases. The main limitations of this model are that this sub-model does not account for gravity effects, and that it presumes a single droplet size moving along a fixed upward angle resulting in too little rainout. Moreover droplets currently start at the edge of the cloud and therefore may erroneously rainout beyond the bund wall, if present.

Overall the old model tends to under-predict the cloud radius and cloud speed versus time, while the new model more closely agrees with experimental data. Therefore the new model produces smaller concentrations and doses, and is less conservative. For two-phase releases the new model predicts an increased amount of rainout, which is more in line with the experimental data.

6.1 New INEX model

This section summarises the theory governing the new INEX model for the initial dispersion phase of energetic instantaneous expansion following a catastrophic vessel rupture. For full details of the theory, solution algorithm and model verification and validation the reader is referred to the detailed report by Witlox[74].

The new INEX model allows for both vapour and two-phase releases. In case of two-phase releases the model accounts for droplet dispersion and potential time-varying droplet rainout to form a spreading evaporating liquid pool.

During the initial UDM INEX stage of energetic expansion the air entrainment is dominated by a large radial expansion velocity. Figure 11 depicts the subsequent dispersion phases during the INEX stage. The cloud is modelled as a sphere while elevated, as a truncated sphere during touching down and as a hemisphere after full touchdown. In case of a 2-phase release, the liquid droplets are assumed to be uniformly distributed throughout the cloud volume during the INEX expansion and thus travelling radially at a speed proportional to their distance from the cloud centre. Therefore rainout starts when the lower edge of the cloud hits the ground while it ends at full touchdown (see Figure 11). A transition from INEX to the standard UDM model is applied, when the INEX air entrainment reduces to the UDM air entrainment, or if the INEX spread rate reduces to the UDM gravity spreading rate. Any remaining liquid will rainout at this transition if the cloud is grounded, or possibly at a later stage (using standard UDM droplet modelling) if elevated.

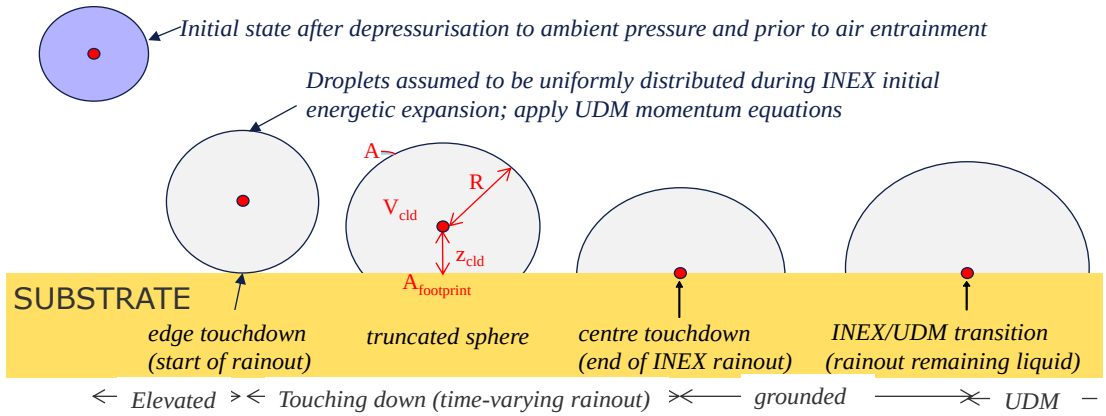

Figure 11. INEX dispersion phases for two-phase instantaneous release

From the above cloud geometry, the cloud volume V_{cld} can easily be expressed as a function of the cloud radius R and the cloud center-line height z_{cld}. The INEX radial momentum (kg m/s) is defined as $I_r = m_{cld} U$. Here the radial cloud expansion speed $U=dR/dt$, and the total cloud mass $m_{cld} = m_{cL} + m_{cv} + m_{wa}$, where m_{cL} is the chemical liquid mass, m_{cv} the chemical vapour mass and m_{wa} is the mass of wet ambient air added to the cloud. The key INEX assumption is that the radial momentum is constant, apart from the loss of momentum due to rainout. Thus the following differential equations are applied in INEX for the radial momentum I_r, the entrained mass of wet air m_{wa}, and the rained out liquid mass m_{cL}^{ro},

$$\frac{dI_r}{dt} = -\frac{dm_{cl}^{ro}}{dt} U \qquad (158)$$

$$\frac{dm_{wa}}{dt} = \rho_{wa} \frac{dV_{cld}}{dt} \qquad (159)$$

$$\frac{dm_{cL}^{ro}(t)}{dt} = 0 \quad , \quad if\ z_{cld} \geq R\,(cloud\ elevated)\ or\ if\ z_{cld} = 0\ (cloud\ grounded)$$

$$= \max\left\{ K_D \frac{m_{cL}}{V_{cld}} A_{footprint}\left[\frac{z_{cld}}{R} U - \frac{dz_{cld}}{dt}\right], 0\right\},\ if\ 0 < z_{cld} < R\ \ (cloud\ touching\ down) \qquad (160)$$

Here t is the time (s), and the change in cloud volume is set as

$$\frac{dV_{cld}}{dt} = AU\ , \qquad if\ z_{cld} \geq R\,(cloud\ elevated)\ or\ if\ z_{cld} = 0\ (cloud\ grounded)$$

$$= AU + A_{footprint} \frac{dz_{cld}}{dt}\ , \quad if\ 0 < z_{cld} < R\ \ (cloud\ touching\ down) \qquad (161)$$

where A is the cloud surface area above the ground, and $A_{footprint}$ is the cloud footprint area (see Figure 11).

The first term in the right-hand side of rainout equation (164) represents the rainout due to cloud expansion and the second term represents the rainout due to the cloud center-line height z_{cld} reducing. In the derivation of first term it is presumed that the radial cloud velocity linearly increases, and thus it can be derived that the vertical downward component at the footprint equals $(z_{cld}/R)\ U$. The maximum value of the parameter $K_D=1$, which presumes that all liquid hitting the ground will rainout.

The initial cloud speed $U(t=0)=U_o$ is set as $U_o=f_{kinetic}\ E_{exp}^{0.5}$. Here the specific expansion energy (J/kg) is set as $E_{exp} = h_{st} - h_f$, where h_{st} is the specific stagnation enthalpy and h_f is the specific final enthalpy after expansion to ambient pressure. Furthermore the fraction of total energy converted to kinetic energy is set to $f_{kinetic}=0.04$ following the recommendation of Pattison[75] based on a best fit to data from Schmidli[76].

In addition to the above equations, the standard UDM equations are applied during the INEX stage to evaluate the cloud centre location (from momentum equations including gravity effects), the cloud temperature, the cloud volume V_{cld} and the cloud phase distribution (from UDM two-phase thermodynamics equations). Following rainout, the model carries out pool spreading/evaporation calculations and the model accounts for pickup of vapour from the time-varying pool by the instantaneous cloud. For this purpose the so-called observer concept is applied to evaluate the time-varying dispersion in line with methodology described in Chapter 5.

6.2 Old INEX model

An analytic solution is developed for the initial stages of the expansion which begins after the initial cloud expansion by flashing, and is assumed to end when the radial expansion rate slows to dR/dt = 1 m/s. Thereafter the dispersion is modelled by numerically integrating the equations described in Section 3.2.

The model does not permit any initial dilution of air[lxxvi].

6.2.1 Experimental basis for model

Researchers at Air Products, Inc. (Landis, et. al, 1993)[77] experimented with sudden releases of a gas marked with micrometer-range solid tracer particles. The Air Products releases were from a horizontal, elevated cylinder. Using high-speed videotape, they obtained cloud dimensions as a function of time.

Our model is based upon experiments conducted on sudden decompression of pressurised liquid propylene by researchers at BASF (Maurer, Schneider, et. al.[78,79]). They used cylinders with length, diameter, and wall thickness in proportion to commercial cylinders used in rail transport. The BASF experiments heated pressurised containers of propylene until they burst. Bursting occurred in the range of 50 to 80 ^{o}C and 22 to 39 bar. They recorded the rapid hemispherical expansion of liquid and vapour on high speed film. By drawing representative radii through the highly turbulent profiles, Maurer et al. were able to deduce not only R(t) data, but also by numerical differentiation, dR(t)/dt data.

To correlate the data for all cylinder sizes, Maurer, et. al. plotted dR/dt against normalised time, $t/V_{Go}^{1/3}$. Their correlation of the data makes use of V_{Go} as a scaling parameter where V_{Go} is the initial volume of twice the initial mass ($2m_o$) evaluated at the density of propylene vapour at 1 atmosphere and 0^{o}C. The factor of two was invoked to extend the work to elevated releases forming a spherical volume rather than a hemisphere. We modified their approach by using the initial mass, m_o as the correlating parameter instead.

6.2.2 Theoretical basis of model

Instantaneous releases occurring from a pressurised container expand very quickly and reach a maximum cloud size upon dissipating their initial expansion energy. The expansion energy E_{exp} (J/kg) is defined by

$$E_{\exp} = \Delta U - P_a(v_0 - v_a) \qquad (162)$$

where ΔU is the internal energy (J/kg), P_a the ambient pressure (N/m^2), v_o the initial specific cloud volume (m^3/kg), and v_a the specific cloud volume after expansion to ambient pressure. The above equation can be approximated by:

$$E_{\exp} = \Delta H - (P_0 - P_a)v_0 \qquad (163)$$

where ΔH is the enthalpy change (J/kg) from the tank conditions (T_o, P_o) to the expansion zone conditions (T_2, P_a).

The above calculations are carried out by the discharge model, and the expansion energy is passed through as input to the UDM model.

[lxxvi] Silk 8539

Cloud radius and cloud expansion rate

According to turbulent transport theory, the cloud radius R is given as function of time t by

$$R(t) = K_c \sqrt{4\,\varepsilon\, t} \qquad (164)$$

Here K_c = 1.36 and the turbulent diffusivity ε (m^2/s) is given by Opschoor (1980)[80] in terms of the expansion energy E_{exp} by[lxxvii]

$$\varepsilon = K_1 E_{\exp}^{1/2} V_{GO}^{1/3} \left[\frac{t\, E_{\exp}^{1/2}}{V_{Go}^{1/3}} \right]^{-1/4} \qquad (165)$$

with K_1 = 0.0137.

We have replaced V_{Go} by m_o[lxxviii], and have subsequently verified this change against Maurer et. al.'s data.

Inserting Equation (165) into(164), and subsequent substitution into

$$V_{cld}(t) = \frac{4}{3}\pi\, R(t\ )^3 \qquad (166)$$

gives

$$V_{cld}(t) = V_0\, t^{9/8} \qquad (167)$$

with[lxxix]

$$V_0 = \frac{32}{3}\pi\, K_c^3 K_1^{3/2} E_{\exp}^{9/16} m_0^{5/8} \qquad (168)$$

$$= 0.135\, E_{\exp}^{9/16} m_0^{5/8}$$

or:

$$t = \left(\frac{V_{cld}}{V_o} \right)^{8/9} \qquad (169)$$

and:

$$R(t) = \left[\frac{3}{4\pi} V_{cld} \right]^{1/3} = R_o\, t^{3/8} \qquad (170)$$

from which:

$$\frac{dR}{dt} = \frac{3}{8} R_o\, t^{-5/8} \qquad (171)$$

Using Equation (168) to find R_o, and substituting this into Equation (171) gives expansion rate dR/dt at time t, and subsequent integration leads to the radius R of the cloud[lxxx],

[lxxvii] JUSTIFY - Inconsistent units, unless K_1 has dimension $m^{1/2}$!

[lxxviii] JUSTIFY - This is inconsistent with the definition of V_{Go} as described earlier! As stated it is claimed that following this change a good fit was obtained with dR/dt. If so, this should e.g. be demonstrated by a figure.

[lxxix] THEORY corrected. Replaced $(4/3)^{5/2}$ by (32/3)

[lxxx] THEORY corrected. Equation for R(t) is wrong in Loss Prevention Paper

$$\frac{dR}{dt} = \frac{3}{4} K_c K_1^{1/2} E_{\exp}^{3/16} \left(\frac{t}{m_o^{1/3}} \right)^{-5/8} \quad , \quad R(t) = 2 K_c K_1^{1/2} E_{\exp}^{3/16} m_o^{5/24} t^{3/8} \qquad (172)$$

With these assumptions, our modelling describes the experimental data better than the original correlations[lxxviii].

Time period for energetic cloud expansion

The high energy expansion phase begins after the initial cloud expansion by flashing. That is, upon depressurising to 1 atmosphere, a flashed mass fraction of vapour, x, is produced. The two-phase density ρ_{cld} is given by:

$$\frac{1}{\rho_{cld}} = \frac{x}{\rho_{vap}} + \frac{1-x}{\rho_{liq}} \qquad (173)$$

The initial cloud volume is, then:

$$V_{cinit} = \frac{m_{cld}}{\rho_{cld}} \qquad (174)$$

This actual volume is likely to be inconsistent with the theoretical volume V_0 given by Equation (168). Thus, we allow expansion from V_0 to V_{cinit} before starting the clock-time used in the analytic solution.

Substituting V_{cinit} into Equation (169) gives the starting time for energetic expansion as

$$t_o = \left(\frac{V_{cinit}}{V_o} \right)^{8/9} \qquad (175)$$

The energy expansion phase is assumed to end when the radial expansion rate slows to $(dR/dt)_{end}$ = 1 m/s[lxxxi]. The ending time for the energetic expansion mode, t_{end}, is given by Equation (171) as:

$$t_{end} = \left[\frac{\frac{3}{8} R_0}{\left[\frac{dR}{dt} \right]_{end}} \right]^{\frac{8}{5}} \qquad (176)$$

After $t > t_{end}$, the numerical solution described in Section 3.2 proceeds.

Droplet trajectories

Droplet trajectories in the energetic expansion period are taken as occurring along an average trajectory angle $\theta_{d,exp}$. This average angle is found as the angle which gives the average rain-out time $t_{d,exp}$ if, after the energetic expansion, drops fall at a constant terminal velocity, u_t.

The fallout time ranges from zero for drops with an initial angle θ=0 to R/u_t for drops with an angle of $\theta=0.5\pi/u_t$. The average fallout time is found by integration over θ

$$t_{d,\exp} = \frac{1}{\pi/2} \int_o^{\pi/2} \frac{R \sin\theta \, d\theta}{u_t} = \frac{2R}{\pi u_t} = \frac{R \sin(\theta_{d,\exp})}{u_t} \qquad (177)$$

where the 'average' drop-out angle is defined by[lxxxii]

[lxxxi] JUSTIFY this criterion

[lxxxii] JUSTIFY/DOC - Code uses formula $\theta_{d,exp} = \min\{E_1/E_{exp}, 1\} \arcsin(2/\pi)$, with E_1 = 690 J/kg being a parameter. Why?

$$\sin(\theta_{d,\exp}) = \arcsin\left(\frac{2}{\pi}\right) = 0.690\ radians = 39.5° \quad \textbf{(178)}$$

Air entrainment

As stated above, the cloud volume is expanded from the theoretical volume V_o to $V_{cinit} = V_o t_o^{9/8}$ at the start cloud time t_0 (V_{cinit} = the initial cloud volume after flashing). Thus at the start cloud-time for the UDM, the cloud volume equals: $V_{cld}(t=0) = V_{cinit}$. During the process of energetic expansion, the cloud volume increases to $V_{cld}(t) = Vo(t+t_o)^{9/8}$, and the mass of air entrainment is calculated as $\rho_a [V_{cld}(t) - V_{cinit}]$[lxxxiii].

6.3 The purple book method

The purple book method is a very simple correlation. It relates the liquid mass fraction in the cloud after the energetic expansion phase, η_{cL}, to the initial adiabatic[lxxxiv] liquid mass fraction, η_{cL}^0. This is the liquid fraction in the cloud following the initial cloud expansion by flashing from the storage conditions to atmospheric pressure. The adopted correlation, taken from table 4.8 of the purple book, is shown in the table below:

adiabatic liquid mass fraction, η_{cL}^0	Post expansion liquid mass fraction, η_{cL}
$\eta_{cL}^0 > 0.9$	$1 - 2\times(1-\eta_{cL}^0)$
$0.9 \geq \eta_{cL}^0 > 0.64$	$1 - [0.8\times(1-\eta_{cL}^0) - 0.028]/0.26$
$\eta_{cL}^0 \leq 0.64$	0

Table 5. Purple book correlation for liquid fraction after energetic expansion phase
This correlation relates the liquid fraction at the end of the energetic expansion phase to the initial adiabatic liquid mass fraction.

In implementing this correlation the following assumptions have been made:

1) The expansion phase occurs instantaneously and the cloud is situated at the release location (x=0, y=0 and z=z_R (m))
2) No air is entrained in to the cloud[lxxxv]
3) Any liquid remaining in the cloud following the expansion phase immediately rains out.

The purple book method takes no account of the energetic expansion phase for pure vapour releases.

[lxxxiii] JUSTIFY - Is this true? Note that a part of the volume increase will be caused by cloud depressurisation rather than air entrainment!

[lxxxiv] The initial flash fraction provided from the discharge model is calculated assuming an isentropic expansion from the storage conditions to atmospheric pressure i.e. adiabatic, reversible expansion

[lxxxv] IMPROVE. It should be possible to "reverse engineer" the thermodynamic calculations in order to obtain the amount of air that would be entrained to give the revised liquid fraction in the cloud following the expansion phase

7. UDM MODEL COEFFICIENTS

This section describes the evaluation of the model coefficients in the UDM. This has been significantly revised relative to the original UDM tuning process described by Cook and Woodward (1995)**Error! Bookmark not defined.**.

For the original UDM Cook and Woodward adopted a tuning process, where the tuning coefficients were obtained by comparison of UDM results against a relative large set of 'tuning experiments'. The problem with this approach was that several code errors and/or unrealistic model physics was 'tuned out'. This type of tuning has largely been eliminated as part of the current work. The model coefficients have now been obtained directly from established data in the literature (based on experiments), rather than doing UDM simulations and fitting the UDM results to the experimental data.

As described in this report, the UDM effectively links the following modelling modules:

- discharge rate prediction, aerosol flash fraction and Sauter mean drop size estimation
- jet entrainment and trajectories
- droplet evaporation and rainout
- pool spread, evaporation and dissolution, dilution of vapours across the pool surface
- heavy gas dispersion
- passive dispersion

This reader is referred to separate documentation[9,74] for details on the evaluation of model coefficients for the discharge calculations, droplet size correlations, pool spreading/evaporation, and the new INEX model (initial dispersion phase for pressurised instantaneous releases). A list of model coefficients for the droplet thermodynamics, jet dispersion, heavy gas dispersion, and passive dispersion is as follows:

- droplet thermodynamics:
  - correlation of drag coefficient C_{Dd} of the drop as function of Reynolds number
  - coefficients a,b in empirical correlations for Sherwood and Nusselt numbers describing droplet mass and heat transfer

- concentration profile:
  - correlation for exponent m in horizontal profile as function of $(\rho_{cld}-\rho_a)/\rho_a$
  - correlation for exponent s in vertical profile as function of $H_{eff}/|L|$ and stability class

- momentum and cross-wind spreading:
  - drag coefficient C_{Da} of plume in air (momentum equation)
  - correlation for cloud radius during energetic expansion of instantaneous cloud
  - parameter C_E for cross-wind gravity spreading
  - parameters r_u, r_E, r_ρ, Ri_*^{cr}, r_{tr}^{pas} defining onset of transition and transition distance from near-field to passive dispersion
  - correlations for ambient vertical, crosswind and downwind dispersion coefficients as function of downwind distance, surface roughness and stability class

- entrainment
  - jet-entrainment: parameters α_1, α_2
  - heavy-gas top entrainment: Von Karman constant κ, correlation of entrainment function $\phi(Ri_*)$ as function of Richardson number Ri_*
  - heavy-gas side entrainment: parameter γ

- interaction with substrate:
  - correlations for natural and forced convection heat transfer from substrate
  - correlation for water-vapour transfer from substrate

- atmospheric data:
  - mixing height as function of stability class
  - temperature: temperature gradient and surface heat flux as function of stability class
  - wind speed: Monin-Obukhov length as function of stability class

The table below lists the model coefficients. It excludes the coefficients that have been obtained via standard correlations. For each coefficient, the table gives the UDM value and the experiment by means of which the coefficient has been obtained.

Symbol	Tuning parameter	Value	Reference/experiment
a	term in correlation for droplet numbers Sh, Nu	1.0	Ranz and Marshall[81]
b	term in correlation for droplet numbers Sh, Nu	0.32	Ranz and Marshall[81]
r_{drop}^{exp}	ratio of drop to cloud velocity for initial energetic expansion of instantaneous cloud (old INEX model only)	0.8	Chosen value
C_{Da}	drag coefficient of plume in air	0	Ignored
α_1	term in jet entrainment	0.17	Ricou and Spalding[31]
α_2	term in cross-wind entrainment	0.35	Briggs correlation[36]
γ	term in heavy-gas side entrainment	0 (continuous) 0.3 (instantaneous)	Ignored Thorney Island
κ	Von Karman constant in heavy-gas top entrainment	0.4	established value
C_E	gravity-spreading parameter	1.15	Van Ulden[26]
r_ρ^{pas} r_u^{pas} r_E^{pas} Ri_*^{pas}	transition to passive if $\lvert\rho_{cld}-\rho_a\rvert/\rho_{cld}<\varepsilon_{tr}^{pas}$ and $\lvert u_{cld}-u_a\rvert/u_a<r_u^{pas}$ and $\lvert 1-(E_{pas}^{nf}+E_{hvy})\rvert<r_E^{pas}$ and (for grounded plume) $Ri_* < Ri_*^{pas}$	0.015 0.1 0.3 15	Chosen value HGSYSTEM consistent HGSYSTEM consistent Chosen value
r_{tr}^{pas}	distance multiple for transition from near-field to passive dispersion	2.0	Chosen value
r_{quasi}	quasi-instantaneous transition (width/length)	0.8	Chosen value

Table 6. UDM model coefficients

8. FUTURE DEVELOPMENTS

The following future developments are proposed (see the UDM verification manual for further details and a more complete list of further work).

1. Release conditions

   - A cross-wind release formulation could be developed. This requires extensions to the modelling of the initial phase for which the jet direction is not located in the vertical plane along the wind direction. Availability of experimental data should be ideally be investigated prior to attempt to model this feature.
   - Multiple heavy-gas or passive-gas sources

2. Type of pollutant and thermodynamics

   - Quality-assure and improve flash calculations to ensure that post-flash data input to UDM (post-flash velocity, droplet size) are accurate.
   - Improve current UDM droplet model (droplet trajectories for instantaneous clouds, distributed rainout, condensation and drop growth, validation), as a further follow-up of Phase IV of the droplet modelling JIP
   - More robust HF model (modular code, remove oscillations, more testing)
   - Extend multi-compound modelling: generalised multiple-aerosol rainout algorithm for time-varying cloud compositions
   - Allow for solid thermodynamics (for other chemicals than CO_2), possibly in combination with modelling of smoke dispersion
   - Allow general type of reaction for pollutant
   - For instantaneous or time-varying releases, improved modelling of heat transfer from the substrate to the cloud using the formulation of Kunsch and Fannelop[82]

3. Near-field (jet) dispersion

   - Additional validation for grounded jets to validate ground drag formulation and to validate transition from jet phase to heavy gas phase
   - Additional validation for elevated plumes/jets for further testing of entrainment formulations (jet entrainment, cross-wind entrainment and near-field passive entrainment)

4. Passive dispersion, averaging time, low wind speeds

   - Improvement of transition from near-field dispersion to far-field passive dispersion. A too late transition to far-field dispersion may lead to too conservative results. In conjunction with this, also potential experimental work is recommended to assist the improvement and validation of the model.
   - Reduce passive transition zone to transition point (e.g. by means of introducing virtual sour); further check compatibility between near-field and far-field passive dispersion. See also the UDM verification manual for a further discussion.
   - The UDM (as well as the HGSYSTEM and SLAB) formulas for passive dispersion and their averaging-time treatment may need to be further updated to reflect the latest progress, i.e. the work by Dave Wilson[83]. Crabol[84] noted that for very low wind speeds the Pasquill-Gifford dispersion coefficients may not be appropriate, and Doury coefficients should be adopted. This may result in a further considerable reduction of the peak concentration (check also against PERF).

5. Mixing layer logic following literature review:

   - Improvement of mixing-layer logic (amongst others the choice of the mixing-layer height); see also footnotes xxii and xxxvi for a further detailed discussion. A too low mixing layer height may lead to overly conservative results.

6. Instantaneous releases:

   - Verfiy current model for initial phase of gravity spreading for unpressurised instantaneous cloud, e.g. against HGSYSTEM model HEGABOX[85]

- Allow for downwind spreading different to cross-wind spreading (improved along-wind diffusion)
- Additional validation particularly for elevated clouds

7. Improved modelling of time-varying dispersion

   - A more advanced algorithm could be implemented to impose along-wind gravity-spreading; see Appendix D for details.
   - A more advanced algorithm could be implemented to impose mass conservation in case subsequent observers move with different velocities; see Appendix E for details.
   - The single-droplet size algorithm described in Section 5.3 presumes that observers rain out in sequence. This formulation could be generalised, to account for possible observers not to rain out in sequence.
   - Extension of observer algorithm to allow for distributed rainout
   - Automated choice of observer release times (in line with HGSYSTEM method)
   - Implementation of improved AWD coefficients following the Ph.D. thesis by Jessica Morris (Morris, 2018)[86]

8. Turbulent concentration fluctuations

   - Concentration fluctuations are proposed to be added applying possibly a method like implemented in HGSYSTEM85 or relating to the work by Wilson83.
   - In conjunction with this, it is recommended to carry out a further investigation in the appropriate method for lethality/dose calculations, including the appropriate associated choice of averaging time for wind meander, method for time-averaging over transient calculations, and accounting for concentration fluctuations.

9. Dynamic meteo:

   - The UDM dispersion model currently assumes dispersion over terrain (without obstacles) in a constant ambient turbulent flow field. Thus the mean values of ambient speed, pressure and temperature are assumed to be constant (defined by profiles as function of height). The model may be extended to allow for time-variations of the wind-speed and/or the wind direction.

10. Non-flat terrain:

    - Modelling of variable surface roughness (e.g. in line with HEGADAS logic)
    - modelling of dispersion for large surface-roughness (averaged height of obstacles is comparable with cloud height, e.g. dispersion within the urban canopy layer; cf. paper by Roberts and Hall[87])
    - Modelling of slopes and fences (cf. Webber et al.[88])
    - Modelling of canyon effects (e.g. HGSYSTEM logic[85])

APPENDICES

Appendix A. Evaluation of ambient data

A.1 Atmospheric Profiles

To begin the description of the Unified Dispersion Model, a summary of the profiles used to model the lower layer of the atmosphere in which the dispersion is assumed to take place is given.

The wind speed varies with height in the atmosphere, as does the atmospheric temperature, pressure, density, humidity, etc.. Simple relations are described here which are appropriate to the first few hundred metres of the atmosphere.

Two options are provided for the variation of wind speed with height:

- constant wind speed profile
- power-law wind profile (power-law fit of logarithmic profile)

and three options for the variation of atmospheric temperature and pressure with height:

- constant temperature and pressure profiles
- linear temperature and pressure profiles
- logarithmic temperature profile and linear pressure profile

These options may be selected independently of each other. It is recommended that logarithmic temperature, linear pressure, and power-law wind profiles are used since this will give the most realistic modelling.

Many of these profiles use the Monin-Obukhov length. This is calculated from Haven and Spicer's (1990)[51] formula and depends upon the stability class and surface roughness length z_0 as shown in Figure 34. For stability class D, L=∞ (flagged by large value L = 10^5 m) while for non-neutral conditions the following equation (L in m) is adopted

$$L = a_{Monin}\, z_0^{\,b_{Monin}} \qquad \textbf{(179)}$$

where the parameters a_{Monin} and b_{Monin} are given as function of stability class by:

stability class	*A*	*A/B*	*B*	*B/C*	*C*	*C/D*	*E*	*F*	*G*
a_{Monin}	-11.4	-17.2	-26.0	-56.5	-123.0	-425.0	123.0	26.0	11.4
b_{Monin}	0.1	0.135	0.17	0.235	0.3	0.375	0.30	0.17	0.1

A.2 Vertical wind profiles

The simplest vertical wind profile is one where the wind speed is constant with increasing height in the atmosphere. To provide more realistic modelling, UDM also provides a power law form[lxxxvi]:

$$u_a(z) = u_a(z_{ref})\left(\frac{z}{z_{ref}}\right)^p \qquad \textbf{(180)}$$

where	u_a	ambient wind speed	(m/s)
	z	height above the ground	(m)
	z_{ref}	reference height for measurement of wind speed	(m)
	p	wind profile power	(-)

The power law profile is an approximation to the logarithmic wind profile given by[lxxxvii]:

$$u_a(z) = \frac{u_*}{\kappa}\left[\ln\left(\frac{z+z_0}{z_0}\right) - \Psi\left(\frac{z}{L}\right)\right] \qquad \textbf{(181)}$$

where	u_*	friction velocity	(m/s)
	κ	Von Karman constant, 0.40	(-)
	z_0	surface roughness length	(m)
	L	Monin-Obukov length	(m)

The logarithmic profile accurately describes the variation of wind speed with height in the atmospheric boundary layer. The exponent p of the power law profile is given by[lxxxviii]:

[lxxxvi] UDM uses as default cut-off values at z_{min}= 1 m and z_{max} = 200 m. Thus for z < z_{min}, u(z) = u(z_{min}) and for z> z_{max}, u(z) = u(z_{max}).

[lxxxvii] Following the suggestion of Randerson[91] the term ln(z/z_0) has been replaced by ln[(z+z_0)/z_0] to avoid infinite shear at z=0. Alternatively ln(z/z_0) could be considered to be replaced by ln[max(z,z_0)/z_0].

[lxxxviii] JUSTIFY. Term Φ is of unknown origin

$$p = \frac{\Phi}{\ln\left(\frac{32.6}{z_0}\right) - \Psi\left(\frac{z}{L}\right)} \quad \textbf{(182)}$$

The Businger (1971)[13] relationship is used for the function Ψ(z/L), with different forms depending upon the stability category:

- unstable weather conditions:

$$\Psi = 2\ln\left(\frac{1+a}{2}\right) + \ln\left(\frac{1+a^2}{2}\right) - 2\tan^{-1}a + \frac{\pi}{2} \quad \textbf{(183)}$$

with[lxxxix]

$$a = \left(1 - 15\frac{32.6}{L}\right)^{1/4} \quad \textbf{(184)}$$

and

$$\Phi = \frac{1}{a} \quad \textbf{(185)}$$

- neutral stability:

$$\Psi = 0 \quad \textbf{(186)}$$
$$\Phi = 1$$

- stable weather conditions:

$$\Psi = -\beta\frac{z}{L} \quad \textbf{(187)}$$
$$\Phi = 1 - \Psi$$

where the value of β = 2.0 from Irwin (1979)[89] has been used rather than the usually cited value of β = 4.7, since it better fits experimental data.

The friction velocity u_* is found by evaluating the logarithmic wind speed profile at the height z = z_{ref}:

$$u_* = \frac{\kappa\, u_a(z_{ref})}{\left[\ln\left(\frac{z_{ref}+z_o}{z_0}\right) - \Psi\left(\frac{z_{ref}}{L}\right)\right]} \quad (99)$$

The power-law exponent p is calculated by fitting the slope of the power law profile to the slope of the logarithmic wind profile, averaged over the layer from 10 m to 100 m[xc]. Figure 35 shows the variation of the power-law exponent as a function of the surface roughness length and stability class calculated using this method. It is found that p is a strong function of stability class for stable conditions (E-G), but is insensitive to stability class for unstable conditions (A-C). Similarly, p is fairly insensitive to surface roughness length, z_0, at low values of z_0, but more sensitive at high values of z_0.

[lxxxix] ERROR. The constant of 32.6 here is that used in the equation for p, and is used instead of height z (as previously documented)

[xc] Theory used similarly to Irwin (1979)[89]; see also Hanna, Briggs and Hosker (1982). Note HEGADAS adopts least-square fit between z_0 and 10 z_o with z_o reference height for wind speed u_o. This may lead to more accurate predictions, in particular when the cloud centroid is significantly below 10 m.

A.3 Temperature

The simplest temperature profile is one where the atmospheric temperature is constant with height. The next most complicated is a linear profile given by[xci]:

$$T_a(z) = T_a(z_{ref}) + \alpha(z - z_{ref}) \quad \textbf{(188)}$$

where	T_a	atmospheric temperature	(K)
	z	height	(m)
	z_{ref}	reference height for temperature and pressure	(m)
	α	temperature gradient	(K/m)

Values of α for the various stability classes from Crutcher (1984)[90] are listed in Table 7, interpolated for the A/B, B/C and C/D mid-classes.

variable	*A*	*A/B*	*B*	*B/C*	*C*	*C/D*	*D*	*E*	*F*	*G*
α	-0.02	-0.019	-0.018	-0.017	-0.016	-0.013	-Γ[xcii]	0.005	0.028	0.040
H_0	250	180	150	125	90	45	0	-15	-5	-2.5

Table 7. Atmospheric temperature profile: variables α (K/m) and H_o (W/m^2)

A logarithmic temperature profile is obtained by integrating the temperature gradient given by Randerson (1984)[91], Pasquill and Smith (1983)[92], Panofsky and Dutton (1984)[93]:

$$\frac{\kappa z}{T_*}\left(\frac{dT_a}{dz} + \Gamma\right) = \phi_h\left(\frac{z}{L}\right) \quad \textbf{(189)}$$

where	κ	Von Karman constant, 0.40	(-)
	T*	scale temperature	(K)
	Γ	dry adiabatic lapse rate[xciii,xciv] = g/C_{pa} = 9.81/1004 = 0.00977	(K/m)
	L	Monin-Obukhov length	(m)

The function ϕ has different forms depending on the stability class:

- For unstable weather conditions:

$$\phi_h = a_1\left(1 - b_1\frac{z}{L}\right)^{-1/2}$$

- For neutral stability:

$$\phi_h = 0$$

- For stable weather conditions:

[xci] DOC - For the plume centre-line at the mixing height, different equation is used for the temperature T(z), (ATMOS). Check on equations and on references.

[xcii] The calculated dry adiabatic lapse rate.

[xciii] CORRECTED. In Phast 6.54 the heat capacity of moist air rather than dry air was used. In Phast 6.6 that of dry air is always used.

[xciv] For neutral conditions lapse rate is calculated, for others it is a constant. CORRECTED: In Phast 6.54 lapse rate was only calculated for the 1st case run and not subsequently recalculated.

$$\phi_h = \left(a_1 + b_2 \frac{z}{L} \right)$$

Different values of the constants a_1, b_1, and b_2 are assigned by different authors. Values from Businger et al (1971)[13] are used in the UDM model: $a_1 = 0.74$, $b_1=9.0$, $b_2=4.7$.

The above equations can be integrated to give the following temperature profile[xcv,xci]:

$$T_a(z) = T_a(z_{ref}) - \Gamma(z - z_{ref}) + \frac{a_1 T_*}{k} \left[\ln\left(\frac{z + z_0}{z_{ref} + z_0} \right) - \Psi_h\left(\frac{z}{L} \right) + \Psi_h\left(\frac{z_{ref}}{L} \right) \right] \quad \textbf{(190)}$$

Here the function Ψ_h is given by

$$\Psi_h(z/L) = 2\ln\left[\frac{1+y^2}{2} \right], \text{ with } y = \left(1 - b_1 \frac{z}{L} \right)^{1/4} \quad \text{if unstable (L<0)}$$

$$= 0 \quad \text{if neutral (L=}\infty\text{)}$$

$$= -(b_2/a_1)\left(\frac{z}{L} \right) \quad \text{if stable (L>0)}$$

and the scale temperature T_* is estimated from the surface heat flux H_0 using the following relation:

$$T_* = - \frac{H_0}{\rho_a C_{pa} u_*} \quad \textbf{(191)}$$

where	H_0	surface heat flux	(W/m^2)
	ρ_a	atmospheric density at reference height z_{ref}	(kg/m^3)
	C_{pa}	atmospheric specific heat capacity	(J/kg/K)
	u_*	friction velocity	(m/s)

Values of H_0 (see Table 7) for unstable and neutral weather categories have been taken from Clarke (1979)[94], while for stable classes values are used which give good agreement between the logarithmic and linear temperature profiles.

A.4 Pressure

UDM offers the choice of two atmospheric pressure profiles: one which is constant with height, and one where the pressure decreases linearly with height. The latter is obtained from the pressure gradient given by:

$$\frac{dP_a}{dz} = - \rho_a g \quad \textbf{(192)}$$

If it is assumed that ρ and g are constants then this can be integrated to give:

$$P_a(z) = P_a(z_{ref}) - \rho_a g (z - z_{ref}) \quad \textbf{(193)}$$

[xcv] Exact integration would lead to the term $\ln(z/z_{ref})$. This has been replaced by $\ln[(z+z_0)/(z_{ref}+z_0)]$ to avoid problems near/ at z=0, and to enable the specification of temperatures at ground level. Alternatively $\ln(z/z_{ref})$ could be considered to be replaced by $\ln[\max(z,z_0)/\max(z_0,z_{ref})]$.

where	$P_a(z_{ref})$	is the atmospheric pressure at reference height z_{ref}	(N/m^2)
	ρ_a	is the atmospheric density at reference height z_{ref}	(kg/m^3)
	g	is acceleration due to gravity, 9.81	(m/s^2)
	z	is the height above ground level	(m)

This is an approximation since ρ_a will vary with height as the temperature and pressure change. However this is a second order effect which is not important within the first few hundred metres of the atmosphere.

A.5 Other Atmospheric Variables

Humidity

The relative humidity r_h is assumed to be constant with height.

Density

The atmospheric density ρ_a at a height z is calculated from the atmospheric temperature T_a, pressure p_a and humidity r_h at that height[xcvi]. See the UDM thermodynamics theory for further details.

Composition

The composition and relative humidity of the atmosphere is assumed to be constant with height.

[xcvi] CORRECTED Phast 6.6. In Phast 6.54 the air was not updated with the correct pressure, temperature and composition before density was calculated.

Appendix B. Literature review of entrainment formulations

B.1 Entrainment Formulations

Ooms formulation for elevated plumes (Gaussian profile, airborne drag)

Ooms[11,18] applies the following entrainment equation

$$\frac{d}{ds}\left[\int_0^{2^{1/2}\lambda R} \rho\, u\, 2\pi r\, dr\right] = E_{tot}$$

Here the integral has been rather arbitrarily cut-off at r = $2^{1/2}\lambda$R, and Gaussian profiles are assumed for cloud velocity u, concentration c, and density ρ:

$$u = u_m + [u_m - u_a \cos\theta]e^{-\lambda^2 r^2/R^2}, \quad c = c_0 e^{-r^2/R^2} \quad \rho = \rho_a + [\rho_m - \rho_a]e^{-r^2/R^2}$$

Here u_m, c_o, ρ_m are the velocity, concentration and density at the centre-line, and λ=1.35$^{0.5}$ is the Schmidt number.

The total entrainment E_{tot} is assumed to consist of jet, cross-wind and passive entrainment,

E_{tot} = $E_{jet} + E_{cross}^{wind} + E_{pas}^{nf}$,

E_{jet} = a_1 [2πR/λ] ρ_{air} |u_m-$u_w$cos(θ)| , a_1 = 0.057 [$\alpha_1 = 2\pi^{0.5}a_1/\lambda$=0.17]

E_{cross} = a_2 [2πR/λ] ρ_{air} u_w |sin(θ)| cos(θ), a_2 = 0.5 [α_2 = 0.5/λ = 0.43]

E_{pas}^{nf} = a_3 ρ_{air} [2πR/λ] u', a_3 = 1.0

where u' is the entrainment velocity due to ambient turbulence. Note that Ooms applies the Morton formulation for jet entrainment. In comparison with the UDM, the cross-wind entrainment contains an additional term cos(θ). This cross-wind formulation was shown to give good agreement in conjunction with a non-zero airborne drag correlation.

The ambient entrainment velocity u' = (εR/λ)$^{1/3}$ in the inertial sub-range of the turbulence energy (ε = eddy energy dissipation), while for other cases u' equals the root-mean square value [$u_a'^2$]$^{0.5}$ of the wind velocity fluctuation due to turbulence.

The eddy dissipation rate ε is the rate at which on the small scale turbulence is dissipated into heat. Ooms does not include the definition, but following Lees[28] (Section 15.12.28),

$$\varepsilon = \frac{u_*^3}{\kappa z}\left[\varphi_m - \frac{z}{L}\right] = u_*^2\left[\frac{\partial U_a}{\partial z} - \frac{u_*}{\kappa L}\right]$$

where[xcvii]

ϕ_m = 1 - βz/L , stable (β = 2.0)

= 1 neutral

= $1 + \frac{15}{4L}\frac{1}{a^3}\left[\frac{1}{1+a} - \frac{a-2}{1+a^2}\right]$, *with* $a = \left(1 - 15\frac{z}{L}\right)^{1/4}$, unstable

Note that Ooms states that always including the complete passive term is a conservative assumption.

[xcvii] DOC. ϕ_m is (to be) given in Appendix A.2 [differentiate ψ, to double check]

TECJET formulation for elevated plumes (Gaussian profile, airborne drag

Emerson[20] developed the TECJET model, and is based on a further refinement of the Ooms model. The same Gaussian velocity, concentration and density profiles are assumed, but now with the Schmidt number taken to be $\lambda = 1.1^{0.5}$.

The mass M adopted by the integral in Ooms includes the air entrainment. As a result the integral needs to be 'cut off' by Ooms in order to avoid divergence of the integral. This problem is avoided by Emerson by defining an 'alternative mass M_2, defined (as in the UDM) as a term in the excess momentum $I_{x2} = M_2(v_o \cos\theta - u_a)$, where v_o is the absolute centre-line velocity. The entrainment equation is given by $dM_2/ds = E_{tot}$, with

$E_{tot} = E_{jet} + E_{cross}^{wind} + E_{pas}^{nf}$,

$E_{jet} = a_1 [\rho_{air} M_2 (v_o - u_a \cos\theta)]^{1/2}$, $a_1 = 0.141$ [$\alpha_1 = a_1 = 0.141$]

$E_{cross} = a_2 [2\pi R/\lambda] \rho_{air} u_w |\sin(\theta)|$, $a_2 = 0.17$[xcviii] [$\alpha_2 = a_2/\lambda = 0.16$]

$E_{pas}^{nf} = a_3 \rho_{air} [2\pi R/\lambda] u'$, $a_3 = 1.0$

In the limit of purely passive dispersion, M_2 reduces to $\rho_a u_a \pi (R/\lambda)^2$ with $dR/dx = 2^{1/2}\partial\sigma_y/\partial x$. Therefore $dM_2/ds = E_{pas}^{nf}$ leads to continuous spread rates for the far field.

$a_3 u' = \rho_a u_a [2^{1/2}\partial\sigma_y/\partial x]/\lambda$

HMP formulation for airborne plume (top-hat profile, no airborne drag)

The model by Hoot, Meroney and Peterka[95] is summarised in Section 15.43.3 in Lees[28]. A top-hat profile is assumed of a circular plume with radius R_{cld}, density ρ_{cld}, speed u_{cld}. Thus the cloud mass flow $M_{cld} = \pi R_{cld}^2 \rho_{cld} u_{cld}$. The adopted entrainment equation is $dM_{cld}/ds = E_{tot}$, with

$E_{tot} = E_{jet} + E_{cross}^{wind}$

$E_{jet} = [a_1/2] [2\pi R] \rho_{air} |u_{cld} - u_w \cos(\theta)|$, $a_1 = 0.09$ [$\alpha_1 = \pi^{0.5} a_1 = 0.16$]

$E_{cross} = [a_2/2] [2\pi R] \rho_{air} u_w |\sin(\theta)|$, $a_2 = 0.9$ [$\alpha_2 = a_2/2 = 0.45$]

Note that passive entrainment is not considered.

AEROPLUME formulation for airborne plume (top-hat profile, no airborne drag)

Also McFarlane[22] adopts a top-hat profile in AEROPLUME/HFPLUME in HGSYSTEM. His summation is as follows for an airborne plume[xcix]

$E_{tot} = E_{jet} + E_{cross}^{wind} + E_{pas}^{nf}$, airborne plume

where

$$E_{jet} = e_{jet} \frac{1 + (4/3)(\rho_{cld}/\rho_{air} - 1)}{1 + (5/3)(\rho_{cld}/\rho_{air} - 1)} P_{above} \rho_{air} |u_{cld} - u_w \cos\theta|, \; e_{jet} = 0.08$$

$$E_{wind}^{cross} = \alpha_2 \rho_{air} P_{abov} |u_w \sin\theta| \left[1 + \alpha_3 \max\left(0, \left(\frac{\rho_{cld}}{\rho_{air}} - 1\right)\right) \sin\theta\right] \sqrt{\frac{u_w}{u_{cld}}}, \; \alpha_2 = 0.6, \alpha_3 = 7.5$$

$$E_{pas}^{nf} = \left[1 - \frac{2W_{gnd}}{D}\right] \pi \rho_{air} e_{pas} \varepsilon^{1/3} \left(l_y^{4/3} + l_z^{4/3}\right)$$

[xcviii] Note that the term ρ_{air} was missing in the Emerson paper

[xcix] In AEROPLUME code: $E_{pas}^{nf} = [2\text{-(aspect ratio-1)}] \pi \rho_{air} e_{pas} \varepsilon^{1/3} [l_y^{4/3} + l_z^{4/3}]$

Here D is the plume diameter [$D = 2R_y = 2R_z$; area $A = \pi R_y R_z = \pi D^2/4$], the coefficient $e_{pas} = 1$; the turbulent (transverse horizontal, vertical) eddy length scales l_y, l_z, and the dissipation rate of kinetic energy ε are given by

$$l_y = \min\{0.5D,\ 0.88(z_c+z_0)L_y(\zeta)\},\ l_z = \min\{0.5D,\ 0.88(z_c+z_0)L_z(\zeta)\}$$
$$\varepsilon = E(z_c)\ u_*^3/[\kappa(z_c+z_o)]$$

where $\zeta = (z_c+z_o)/L$, z_c the centroid height, z_o the surface roughness length, L the Monin-Obukhov length L, u_* the friction velocity, κ the Von Karman constant. The functions $L_y(\zeta)$, $L_z(\zeta)$ and $E(\zeta)$ are defined as a function of stability class by

$L_y(\zeta) = L_z(\zeta) = (1-7.4\kappa\zeta)/E(\zeta)$, $E(\zeta) = 1 - 5\kappa\zeta$, stability class = A,B,C
$L_y(\zeta) = L_z(\zeta) = E(\zeta) = 1$ stability class = D
$L_y(\zeta) = 1 / (1+0.1\zeta)$, $L_z(\zeta) = 1/ E(\zeta)$, $E(\zeta) = 1 + 4\zeta$, stability class = E,F

Note that high-enough plumes $l_y = l_z = 0.5D = R_{pl}$, Chord=0 and the AEROPLUME formulation reduces to the Ooms formulation,

$$E_{pas}^{nf} = e_{pas}\,\rho_{air}[2\pi R_{pl}]\ (\varepsilon R_{pl})^{1/3}$$

Also the formula for ε is very similar [note that $E(z_) = \phi_m(z)$ for D, $E(z_) \approx \phi_m(z)$ for stable since $\beta \approx 5\ \kappa$, formulas more different for unstable].

AEROPLUME formulation during touchdown and slumping (top-hat profile)

The formulation during touchdown and slumping is (before transition to HEGADAS),

E_{tot} = $E_{jethvy} + E_{gspas}$, touchdown and slumping

Here E_{jethvy} represent the combined effect of jet entrainment E_{jet} and heavy-gas entrainment E_{hvy}, and E_{gspas} the combined effect of gravity-slumping entrainment E_{gs} and passive entrainment E_{pas},

E_{jethvy} = $[2W_{gnd}/P_{above}]\ \max(E_{jet},E_{hvy}) + [1 - 2W_{gnd}/P_{above}]\ E_{jet}$

$$= \frac{E_{jet}}{E_{jet}+E_{hvy}}E_{jethvy} + \frac{E_{hvy}}{E_{jet}+E_{hvy}}E_{jethvy} = E_{jethvy}^{jet} + E_{jethvy}^{hvy}$$

E_{gspas} = $\max(E_{gs},E_{pas})$

$$= \frac{E_{gs}}{E_{gs}+E_{pas}}E_{gspas} + \frac{E_{pas}}{E_{gs}+E_{pas}}E_{gspas} = E_{gspas}^{gs} + E_{gspas}^{pas}$$

where

$$E_{hvy} = P_{above}\rho_a \frac{\kappa\, u_*}{\Phi(Ri_*)}, \qquad Ri_* = 2\ g\ z_c \frac{\rho_{cld}-\rho_a}{\rho_a u_*^2}$$

$$E_{gs} = \left[1 - \frac{2z_c}{D\,|\cos\varphi|}\right]\rho_a\ e_{gs}\ z_{cld}\ u_{cld}\ |\cos\varphi|\ \frac{dD}{ds}\ ,\ e_{gs} = 0.85$$

Here Ri_* is the Richardson number, and $\Phi(Ri_*)$ the entrainment function

$\Phi(Ri_*)$ = $\{1 - 3Ri_*/5\}^{-0.5}$, $Ri_* < 0$
= 1 , $0 \le Ri_* < [189/90]$
= $\max\left\{\frac{Ri_*}{7}, \frac{10}{17}\sqrt{1+0.8Ri_*}\right\}$, $Ri_* > [189/90]$

Morton (crosswind extended)

The aim of this extension is to address the potential under-prediction of concentrations in the near-field. We have included the extension described below as (the default) "Morton (crosswind modified)" option in the UDM.

The formulation is based on a modifier to the Morton et al. model[32], which comprises

1. A near-field region where crosswind entrainment is suppressed.
2. A non-zero drag force in the near-field, acting normal to the trajectory.

Entrainment

The 'potential core' is the region where a solid central portion of the released plume remains unaffected by the crossflow. For its length, L_{core}, we use the Kamotani & Greber[96] expression as a function of source diameter D and velocity ratio R:

$$L_{core} = \frac{6.4D}{1 + (4.6/R)}$$

Crosswind entrainment is set to zero in this region. A floor of 0.5D has been applied to the L_{core} function at very low values of R as the function rapidly approaches zero.

Beyond this region, crosswind entrainment ramps up to its full value (as per Morton) over a distance L_{supp}. This is difficult to bound, but the papers of Kamatoni & Greber[97] and Yuan & Street[98] show broadly linear mass & volume flux relationships from 8-12D. A phase-in period of around 2-3L_{core}would therefore seem about the correct scale for the values of R they used. We also introduce a factor based on the density ratio to reflect a dense jet retaining integrity over a longer distance than a light jet.

The total distance over which entrainment is suppressed is therefore set to be

$$L_{supp} = \left(1 + \sqrt{\frac{\rho_0}{\rho_\infty}}\right) L_{core}$$

Crosswind entrainment is phased in linearly to achieve its unmodified value at L_{supp} according to:

$$E'_{cross} = 0 \qquad s \le L_{core}$$

$$E'_{cross} = \left(\frac{s - L_{core}}{L_{supp} - L_{core}}\right) E_{cross} \qquad L_{core} < s \le L_{supp}$$

Drag

The application of a crosswind drag force is also restricted to the near-field trajectory, but the distance over which the force acts is defined independently of the suppression lengths above. There is some slightly contradictory evidence on this: Yuan & Street[98] suggest drag is high initially and quickly phases out by 4D plume height, while Mahesh[99] indicates the force may occur over a longer distance, up to around 20D along the trajectory for their R=5.7 case.

We take the Mahesh approach here of a longer drag distance and define a drag length as a multiple of the suppression length. The density ratio Muppidi & Mahesh[100] used was 1.0, so it would give a broadly consistent drag length in this case to assume

$$L_{drag} = 3L_{supp}$$

We express this drag in terms of a coefficient C_d applied to the standard UDM air-drag model (Eq. 89). This starts at its maximum value and is phased out linearly with arc length s over L_{drag}

$$C_d = C_{drag}^{init}\left(1 - \max\left[\frac{s}{L_{drag}}, 1\right]\right)$$

An initial drag value of $C_{drag}^{init} = 0.39$ is proposed, three times the Ooms drag coefficient (in the UDM formulation). The entrainment coefficients α_1 and α_2 remain at 0.17 and 0.35 respectively.

Comparison of formulations

The table below summarises the formulations described above.

MODEL	cross-wind profile	α_1 (Mort./Spald.)	α_2	λ^2	C_D	E_{pas}^{ff}	Note
Ooms	Gaussian [c_0, u_{max}]	.2/λ M = 0.17	.5/λ = 0.43	1..35	0.15/λ = 0.13	Yes (from ε; formula not given)	Uses speed and concentration profiles cut-off profiles at $2^{1/2}$b, λ b = R_y = R_z Extra cos(θ) term in E_{cross} Total momentum
TECJET	Gaussian	.142 S	.17/λ = 0.16	1.1	0.1/λ = 0.095	Yes (from u')	Uses speed and concentration profiles No cut-off profiles; λ b = R_y = R_z Excess momentum $I_{x2}=M_2[u_{max}\cos\theta-u_a]$
UDM 5.2	'Drift' [u_{cld}]	.11 S	.26	1.4	0.15	No	Concentration profiles only with λ term Area in terms of R_y,R_z [=λb] Excess momentum $I_{x2}=M_{cld}[u_{cld}-u_a]$
UDM 6.0	'Drift' [u_{cld}]	.17 M	.35	n.a.	0	Yes (from ε; Disselhorst)	Concentration profiles only; no λ term Area in terms of R_y,R_z [=λb] Excess momentum $I_{x2}=M_{cld}[u_{cld}-u_a]$
HMP	top-hat	.16 M	.45	n.a.	0	No	Total momentum
AEROPLUME	top-hat	.282 M	.60	n.a.	0	Yes (from ε; Disselhorst)	No profiles; averaged top-hat conc./speed For max. values multipy c with 1.7 Excess momentum

Table 8. Comparison of integral plume models

Appendix C. Observer release times

Section 5.2.2 summarises the logic for observer release locations and observer release times in the case of time-varying dispersion. The current appendix provides more details regarding this logic.

C.1 Time-varying release without rainout

The observer release times are calculated by the Phast/Safeti discharge post-processing model TVAV. Input to TVAV are the time-varying discharge data (from GASPIPE, PIPEBREAK or TVDI calculations), and the number of 'release observers' n_{obs}^{rel}. These observers are released from the release location.

The release times for the release observers are based on $[n_{obs}^{rel}-1]$ equal release-mass segments[c], where the first release observer is released at the start of the first mass segment (at time t=0), and the last observer at the end of the last segment (at $t_{release}$); see Figure 12. The associated discharge data at these release times (release time, release rate, liquid fraction or temperature, droplet size, velocity) are input to the UDM model as observer release data.

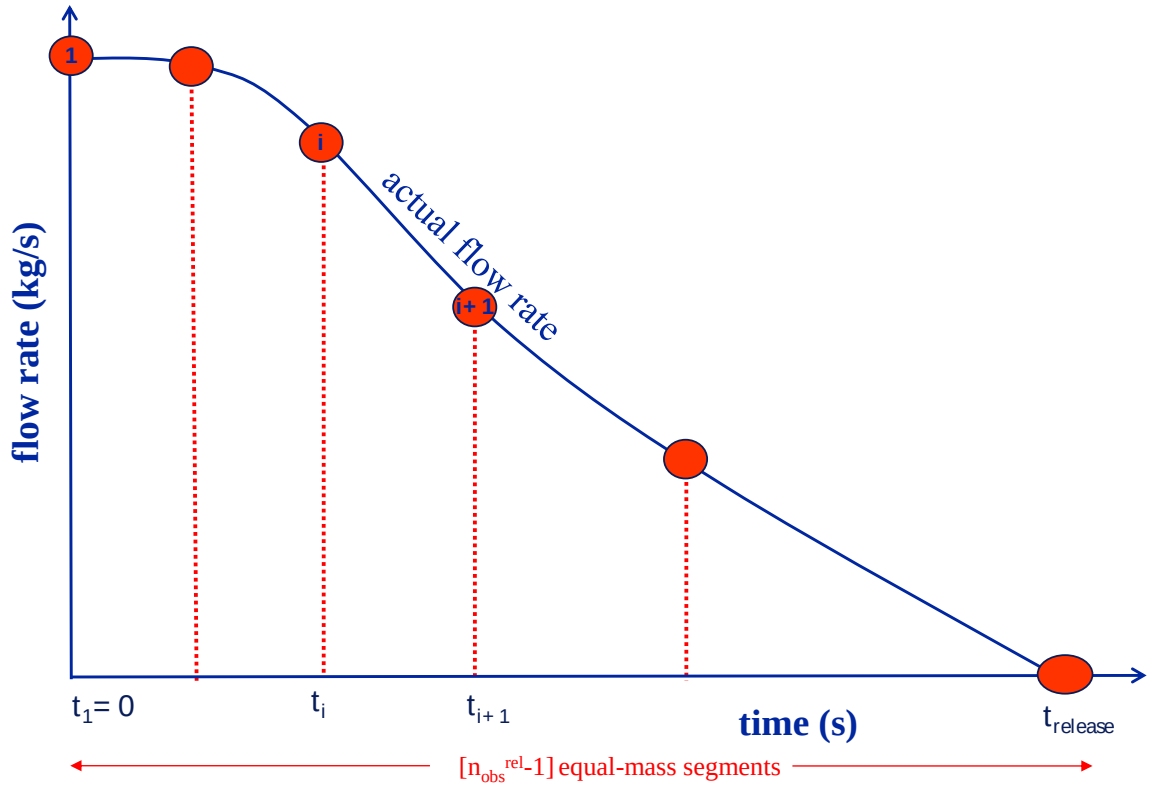

Figure 12. **Evaluation of 'release observer' data based on equal-mass release segments**
The figure illustrates the TVAV observer release algorithm for the case of n_{obs}^{rel}=6 release observers (5 equal mass segments).

[c] IMPROVE. This is appropriate in case of the absence of a pump or control valve. However in case of a long pipeline with a pump, the flow rate initially decreases very rapidly and subsequently is almost equal to the pump rate. Thus a reduced number of observers could be considered to be applied for the later times.

C.2 Liquid spill (immediate rainout)

This section discusses the logic of the observer release time in case of a liquid spil (immediate rainout), where no dispersion calculations need to be carried out prior to the pool calculations.
The cut-off evaporation rate $E_{vap,cut}$ is input to the PVAP pool evaporation model (Phast default: 0.1 kg/s for flammable, 0.001 kg/s for toxics). First PVAP pool calculations are carried out until the time t_{end} at which the pool evaporation rate reduces to $E_{vap,cut}$.

The first observer is released at the first time $t_{start,}$ at which the pool evaporation rate is larger than $E_{vap,cut}$. If t_{end} is the final time at which $E_{vap,cut}$ is exceeded, then the mass evaporated between these two times M_{evap} is calculated. The final observer is released after 99% of this mass has been released[ci]. The release times for the other pool observers are based on $[n_{obs}^{pool}-1]$ equal evaporated-mass segments between the first and last observers, where the number of pool observers, n_{obs}^{pool}, is input to the UDM model; see Figure 13. The observed pool evaporation data at these times (time, evaporation rate, temperature) are output by PVAP to the UDM model as part of the linking between the PVAP pool and the UDM cloud.[cii]

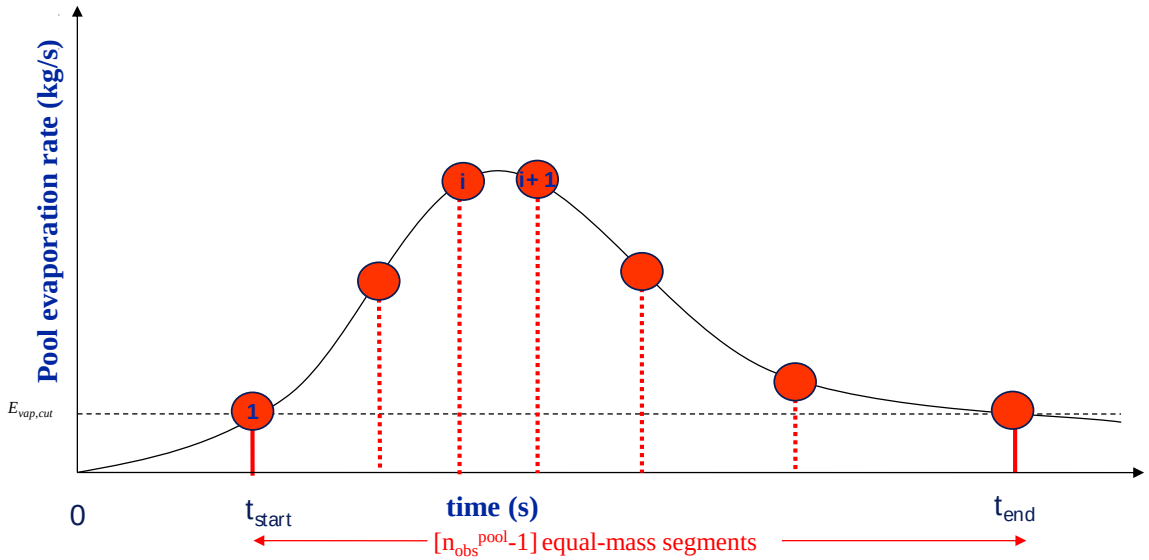

Figure 13. **Evaluation of 'pool observer' data based on equal-mass pool segments**
The figure illustrates the PVAP observer release algorithm for the case of $n_{obs}^{pool}=7$ release observers (6 equal mass segments).

[ci] D-11035. The 99% is so that there is time for the final observer to pick up some mass before the pool stops (as it will when vaporisation rate drops below the cut-off)

[cii] IMPROVE. Consider to further improve pool observer release logic:

(I) Need special logic for the end of the spill (where the pool evaporation rate may drop rapidly), as for the elevated with rainout case, i.e. construct observers in case of a rapid drop of observed total flow rate. Thus, add an additional pool observer when pool evaporation rate reaches its peak. This will result in more conservative predictions, particularly for flammable releases. The existing logic may be unconservative, and leads to rather random behaviour for the evaluation of the maximum observed pool evaporation rate (and therefore maximum observed concentrations, like relevant for short averaging times like relevant for PHMSA LNG validation.

(II) For long duration spills dispersion results for later pool observers are expected to be very close, since the pool evaporation rate would be approximately constant. In this case possibly the number of observers may be considered to be reduced (or release observers at earlier times), e.g. use logic like in Appendix **Error! Reference source not found.**.

C.3 Elevated release with rainout

1. The release times for the release observers (release duration $t_{release}$) are evaluated as for the case without rainout (see Appendix C.1), and calculations are carried out for all release observers until the point of rainout. For a finite-duration release with rainout two release observes are applied at the start and end of the release.

2. PVAP pool calculations are carried out and subsequently pool observer release times are evaluated as described for the case of liquid spill (see Appendix C.2; observer release times between t_{start} and t_{end}).

3. Two cases are considered, i.e. the cases where the upwind edge of the pool spreads or spreads not upwind of the release point. In the text below, modifications applicable for case when the pool spreads upwind are indicated by red font). Let t_{upw} be the time at when the pool spreads upwind ($t_{upw} = t_{release}$ in case the pool does not spread upwind).

    a. For each release time t_{obs} determined for pool observers with $t_{start} < t_{obs} < \min(t_{upw}, t_{release})$, release a new 'release observer' at the release location and run this observer until rainout[ciii].
    b. For all release observers with observer release time $t_{obs} < t_{upw}$ rewind the observer to when it first crosses the pool, and run to end point (including cloud/pool linking).
    c. Trail observer logic
        i. If $t_{upw} < t_{release}$, set time interval $\Delta t_{obs} = 0.05 \min(t_{release}, t_{end} - t_{start})$. Create two added pool observers that will reach the release point x=0 and times $t_{release} - \Delta t_{obs}/2$ and $t_{release} + \Delta t_{obs}/2$
        ii. Else, if the pool is still active when the downwind edge of the pool is left behind by the downwind edge of the original release[civ], let $t_{residual}$ be the time when the pool is left behind and set time interval $\Delta t_{obs} = 0.05 \min(t_{release}, t_{end} - t_{start})$. Add an additional 'pool observer' at the time $t_{residual} + \Delta t_{obs}/2$, which represents the start of the trailing cloud.
    d. For all pool observers with observer release times $\min(t_{upw}, t_{release}) < t_{obs} \leq t_{end}$; including the added trail observer), carry out observer calculations until end point.

C.4 Instantaneous release without or with rainout

In the case of an instantaneous release, a single instantaneous 'release' observer is released. In case of rainout additional 'pool' observers are released after the upwind edge of the instantaneous cloud passed the upwind pool edge; see Figure 9. As for the case of the liquid spill (See Appendix C.2), the pool observer release logic is again based on equal pool mass segments, where pool observers will only be released after the upwind edge of the instantaneous cloud has passed the upwind pool edge.

[ciii] This added release observer only applies for continuous releases. For time-varying releases no added release observer is released.

[civ] This is only applicable when the cloud does NOT spread upwind of the release point, in which case the momentum of the trail observers is often considerably smaller than those who see the original release. The actual discontinuity occurs when the upwind edge of the cloud passes over the upwind edge of the pool, but because of the high momentum it would normally be expected that the time for the original cloud to pass between the upwind and downwind edge of the pool to be relatively small.

- From the calculated value of N_{rates} (i.e. excluding the tail segment), divide the region spanning t_{start} and min(t_{tail}, $t_{cut\text{-}off}$, t_{end}) into equal mass[cv] segments. At the same time, obtain the time-averaged segment characteristics (i.e. duration, evaporation rate, pool radius and temperature) for each segment.
- Thereafter, obtain the time-averaged segment characteristics for the tail segment (i.e. if present/applicable).
- Combine adjacent segments with less than 10% difference in segment evaporation rates into single segments and update the value of N_{rates} accordingly.

[cv] By default, the segmentation logic in PVAP divides the non-tail portion of the PVAP results arrays into equal mass segments. However, the routine permits the division of non-tail segments based on equality in "vaporisation rate load". "Vaporisation rate load" is defined as the sum of the product of the vaporisation rate raised to a power "k" and elapsed time over a region of interest in the PVAP results arrays. When k = 1, the "Vaporisation rate load" equates to the total mass evaporated.

Appendix D. Cloud shape correction for downwind gravity spreading

D.1 Global cloud formulation (not implemented)

In low wind-speed releases of high-density materials, effects of gravitational spreading are relevant both in the crosswind and along-wind directions. However the UDM model allows for crosswind gravity spreading only and not along-wind gravity spreading; see Equation (87) or (154). This results in a cloud with too large crosswind dimensions and too small dimensions in the wind direction. Figure 14 depicts a 'cloud shape correction' which is applied to observer concentrations, to introduce downwind gravity spreading and reduce crosswind gravity spreading, such that downwind and crosswind gravity spreading are equal. This cloud shape correction is analogous to the cloud shape correction optionally applied in the HGSYSTEM heavy-gas dispersion program HEGADAS-T[cvi] as described by Witlox[70].

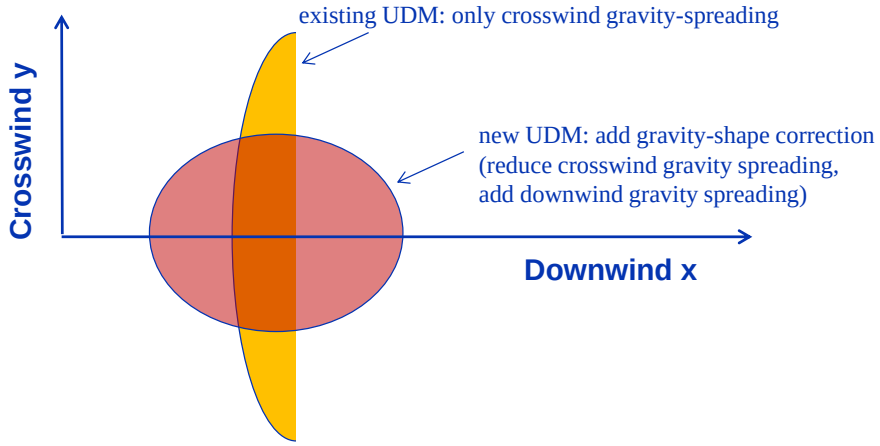

Figure 14. UDM modelling of crosswind and along-wind gravity spreading

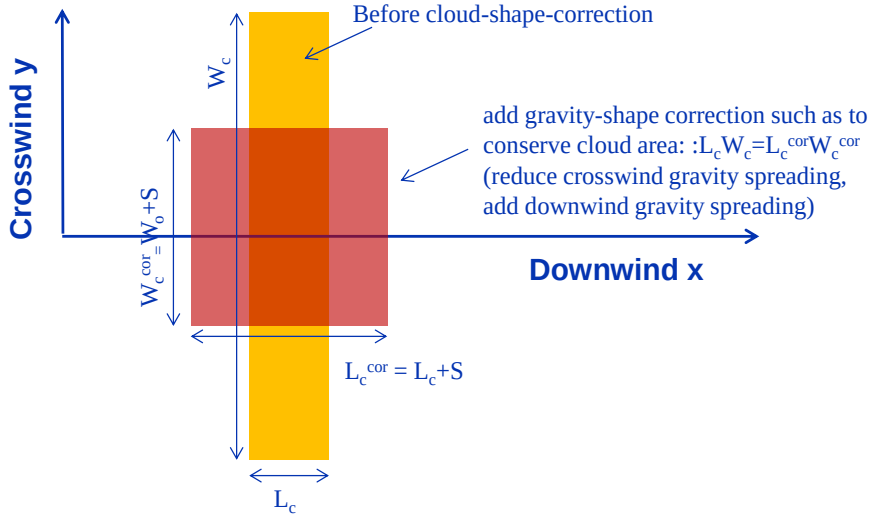

Figure 15. Cloud-shape gravity correction: conserve cloud area

Let L_c be the calculated cloud length and W_c be the calculated cloud width (prior to cloud shape correction), and let W_o be the initial cloud width at the onset of heavy-gas spreading. The corrected cloud length L_c^{cor} and the corrected cloud width W_c^{cor} are set in such a way that the amount of spreading S in the downwind direction of the cloud as a whole equals the amount of spreading S in the downwind direction (see Figure 15). Conservation of cloud area now requires

$$L_c^{cor} W_c^{cor} = L_c W_c \ , \ with \ L_c^{cor} = L_c + S \ \ and \ W_c^{cor} = W_o + S \qquad (194)$$

[cvi] In the heavy-gas dispersion model HEGADAS the correction can optionally always be applied. In the UDM it is only optionally applied when heavy-gas spreading is relevant (after the transition from jet to heavy-gas spreading, i.e. for a grounded dense plume).

The above quadratic equation in S can be solved for S,

$$S = -\frac{1}{2}(W_o + L_c) + \frac{1}{2}\sqrt{(W_o + L_c)^2 + 4L_c(W_c - W_o)} \quad (195)$$

Introducing dimensionless lengths $L_c^*=L_c/W_o$, $W_c^*=W_c/W_o$, $S^*=S/W_o$, the above equations become:

$$S^* = -\frac{1}{2}\left(1 + L_c^*\right) + \frac{1}{2}\sqrt{\left(1 + L_c^*\right)^2 + 4L_c^*\left(W_c^* - 1\right)} \quad (196)$$

$$L_c^{cor}/L_c = (L_c^* + S^*)/L_c^*, \; W_c^{cor}/W_c = (1 + S^*)/W_c^* \quad (197)$$

In HEGADAS the above gravity cloud shape correction (GSC) is applied to the entire cloud at each required output time ("global cloud formulation"). However this formulation has the problem for continuous releases that for increasing times the cloud length L_c increases and therefore the cloud shape correction at a given location reduces, while in reality this is not the case. In reality for ground-level unpressurised releases the cloud shape correction should be large and stay constant in the near-field, since the cloud centroid height z_c is low and therefore the windspeed $u_a(z_c)$ is low. The issue of the above correlation is that it depends on the overall cloud length L_c. As a result a modified GSC is implemented in the UDM based on an incremental cloud formulation[cvii], which is described in the following section.

D.2 Incremental cloud formulation (implemented in UDM)

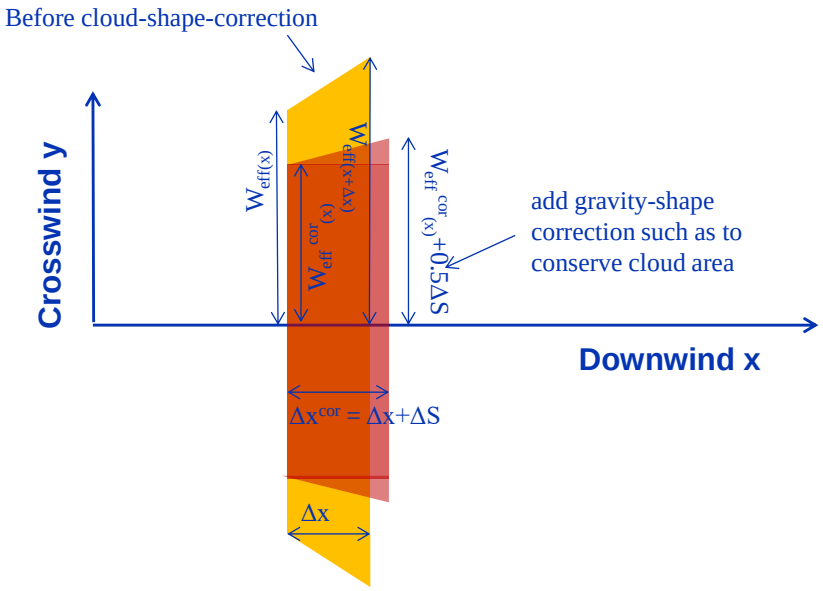

Figure 16. Cloud-shape gravity correction: conserve observer interval cloud area

Conservation of cloud area is applied to an incremental part of the cloud with uncorrected length $dx = u_{cld}\, dt$ and uncorrected cloud half-width W_{eff} (see Figure 16)

- Uncorrected cloud area = $2W_{eff}(x)\Delta x + [W_{eff}(x+\Delta x)-W_{eff}(x)]\Delta x$
- Corrected cloud area = $[2W_{eff}^{cor}(x)+ \Delta S][\, \Delta x+\Delta S]$

Equating corrected to uncorrected cloud area results in

[cvii] REFINE. Instead of an incremental formulation a more robust differential formulation can be considered.

$$\left[2W_{eff}{}^{cor}(x)+\Delta S\right]\left[\Delta x+\Delta S\right]=\left[W_{eff}(x)+W_{eff}(x+\Delta x)\right]\Delta x \qquad (198)$$

This square equation in ΔS can be solved as

$$\Delta S=-\frac{1}{2}\left(2W_{eff}{}^{cor}(x)+\Delta x\right)+\frac{1}{2}\sqrt{\left(2W_{eff}{}^{cor}(x)+\Delta x\right)^2+4\left[W_{eff}(x)+W_{eff}(x+\Delta x)-2W_{eff}{}^{cor}(x)\right](\Delta x)} \qquad (199)$$

The above incremental correction is applied starting from the downwind edge of the pool (ground-level area source) or downwind of the heavy to jet transition (whichever is most downwind). Thus using the above equations the following corrections are applied for a given observer to the downwind cloud distance x_{cld} and the effective half-width W_{eff} (i=1,2,….):

$$x_{cld,i}{}^{cor}=x_{cld,i-1}{}^{cor}+\Delta x_{cld,i}+\Delta S_i,\quad W_{eff,i}{}^{cor}=W_{eff,i-1}{}^{cor}+\Delta S_i \qquad (200)$$

The above correction is applied until the start of the passive transition. No correction is applied otherwise[cviii]. This ensures that gravity spreading is increased in the downwind direction and reduced in the crosswind direction such that the same amount of incremental spreading is applied. The above cloud shape correction applied at a specific location no longer diminishes with increasing overall cloud length L_c and it also modifies results for steady-state releases.

For validation against experimental data for the URA continuous Kit Fox experiments (see UDM verification manual), the above correction was found to apply a too strong correction. As a result by default a modified GSC has been implemented in the code, which only fully applies the gravity shape correction in case of 'excessive' downwind gravity spreading chosen to be defined by $dW_{eff}/dx > n\,S_{crit}$. No GSC is applied for $dW_{eff}/dx < S_{crit}/n$. In between a linear blending function f is used to gradually introduce GSC and to avoid a discontinuity. Thus:

$$\begin{aligned}
&x_{cld,i}{}^{cor}=x_{cld,i-1}{}^{cor}+\Delta x_{cld,i}+\Delta S_i,\quad W_{eff,i}{}^{cor}=W_{eff,i-1}{}^{cor}+\Delta S_i \quad if\ \Delta W_{eff,i}/\Delta x_{cld,i}>nS_{crit}\\
&x_{cld,i}{}^{cor}=x_{cld,i-1}{}^{cor}+\Delta x_{cld,i},\quad W_{eff,i}{}^{cor}=W_{eff,i-1}{}^{cor}+\Delta W_{eff,i} \quad if\ \Delta W_{eff,i}/\Delta x_{cld,i}<S_{crit}/n\\
&x_{cld,i}{}^{cor}=x_{cld,i-1}{}^{cor}+\Delta x_{cld,i}+f\Delta S_i,\quad W_{eff,i}{}^{cor}=W_{eff,i-1}{}^{cor}+f\Delta S_i+(1-f)\Delta W_{eff,i},\ otherwise\\
&with\\
&f=\frac{\Delta W_{eff,i}/\Delta x_{cld,i}-S_{crit}/n}{nS_{crit}-S_{crit}/n}
\end{aligned} \qquad (201)$$

Here the critical value S_{crit} = 1 is currently selected, and n=2. Above the pool, upwind of the heavy-gas regime, and downwind of the start of passive transition currently f is set = 0.

For time-varying releases (or cases with rainout), the above correction is applied for each observer in turn. Note that the correction is applied prior to the observer mass correction.

Note that the above GSC always moves the observers downwind. Therefore at a given downwind distance it will typically cause an increased concentration and a reduced cloud width.

[cviii] REFINE. This implies that cloud area is no longer conserved downwind of passive transition. A refinement of the GSC correction could possibly be considered upwind of the pool and along the passive transition regime, in order to also partially include here correction of gravity spreading.

Appendix E. Differential observer-velocity cloud mass correction

The observer-velocity cloud mass correction was described in Section 0. Appendix E.1 describes a time-shifting algorithm, which is applied prior to the observer mass correction to avoid observers approaching each other too close. Appendix E.2 describes a more rigorous implementation of the observer-velocity cloud mass correction for potential future implementation.

E.1 Time shifting for approaching observers

As observers disperse, they can do so at different speeds. Normally this will result in separation and concentrations will be adjusted downwards to conserve mass. However observers can also approach and this will lead to increased concentrations. If one observer overtakes another this will lead to infinitely high concentrations as $\Delta t \rightarrow 0$.

Therefore after the gravity-spreading correction (if applicable; see Appendix D) and prior to the observer mass correction being applied, an adjustment is made such that observers cannot approach each other too closely.[cix]

Assume we have two consecutive observers i and i-1. Let Δt_i^0 = the release interval between the two. Let Δt_i^x equal the difference in arrival time between the two observers at some distance x. The method can be represented by the following figure:

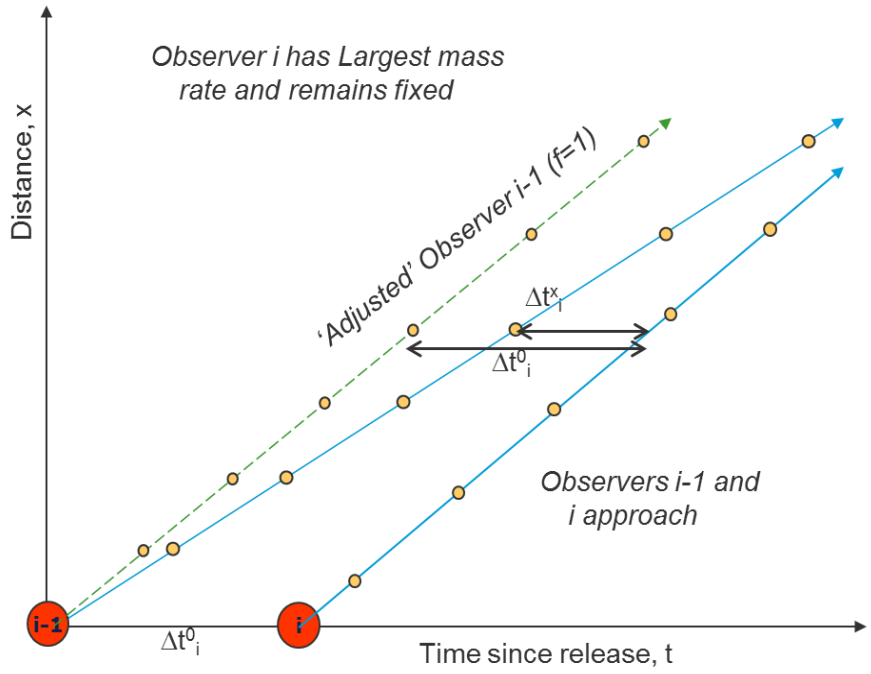

Figure 17. Observer time-shifting prior to Observer Mass Correction

As observer i-1 approaches observer i, then the time interval Δt_i^x reduces below its initial value Δt_i^0. We prescribe a minimum fraction f ($0 < f < 1$; f fixed at 0.75 in Phast) such that $\Delta t_i^x \geq f\,\Delta t_i^0$. If this condition does not hold true for any record at x in observer i-1, then we modify $t_{i-1}^x = t_i^x - f\Delta t_i^0$.

The factor f represents the degree of approach permitted: f = 1 implies observers cannot approach each other at all, whereas f = 0 allows observers to have an identical trajectory. Currently the method specifies a value f = 0.75.

[cix] A warning is provided by the model in case time-shifting of observers occurs.

For cases with many observers, the algorithm starts with the observer that has the highest final mass release rate, say for observer i_{max}. This observer remains unchanged. Each pair of observers released before or after observer i_{max} are then adjusted using his algorithm (*e.g.* observers i_{max} and i_{max}-1; observers i_{max}-1 and i_{max}-2;…)

E.2 Rigorous correction to observer variables stepping forward in time (not implemented)

Instead of the simplistic differential-velocity observer mass correction described in Section 0 (carried out by post-processing UDM steady-sates data), the method could be implemented by solving all observer equations simultaneously stepping forward in arc length s (and NOT with time t, which is now treated as a secondary variable). Here use is made of the additional mass-conservation Equation **Error! Reference source not found.** f or the material rate $Q_i(x)$, i=1,…N, which is now a secondary variable (as already currently in case of rainout or pool evaporation). Note that the change in material rate would also affect the thermodynamic data like liquid fraction and temperature.

Like for the simple observer correction, it would be again an issue if observers would become too close to each other, and therefore observer intervals would not be allowed to reduce with more than the ratio f = 0.75. Again a warning would need to be applied in case this would apply. Please note that the time-shifting algorithm and the observer mass correction may result in added or reduced momentum, which may not be realistic. Thus in this aspect also further improvement may be considered.

UDM solution algorithm for case of pools and rainout

In case of a pool source, the above correction may be relatively large in case of a large drop of pool evaporation rate, e.g. at the time when the pool thickness reduces to the minimum thickness and at the end of the spill.

The OMC is applied downwind of the downwind edge x_{dw}^{pool} of the pool, e.g. by presuming $M_i(x)= M_i(x_{dw})$, i=1,..N]. In case of a pressurised release including rainout, observer calculations are carried out separately to evaluate the pool. Subsequently all observer calculations are carried out (stepping forward in time) to the furthest pool distance x_{dw}^{pool}. Downwind of this again it is presumed that $M_{tot}(x)= M_{tot}(x_{dw})$. Thus the algorithmic steps are as follows:

1. In case of elevated two-phase release, first solve observer equations (stepping forward in s or time t) to determine rainout data (as currently); then call PVAP to set pool data and furthest distance x_{dw}^{pool} of downwind edge of pool
2. Subsequently redo all observer calculations (stepping forward in s or t) accounting for PVAP pool (including link cloud/pool, but ignoring any resulting modification of rainout data), until downwind distance x_{dw}^{pool}, and set arrival times $t_i(x_{dw}^{pool})$.
3. Carry observer calculations downwind of x_{dw}^{pool} as indicated above for case of no rainout, and presuming $M_{tot}(x)= M_{tot}(x_{dw})$.

Appendix F. Guidance on input and output for UDM dispersion model

F.1 Input data

In the UDM generic spreadsheet, the input for the outdoor dispersion model UDM is split into 'Input data' (always to be specified by the user; see Figure 18 and 'Input parameters' (input data to the changed by expert users only; see Figure 19). In the spreadsheet for each input parameter a brief description of the meaning of the parameter is given, its unit (SI units are used), and its lower and upper limits. The next column contains a complete list of input data corresponding to the base case. Subsequent columns need to include only those values that need to be changed to invoke other runs.

Inputs	DNV MODEL UDM								
Input Index	Description	Units	Limits Lower	Limits Upper	Continuous	Instantaneous	Poolsource	Spill	Timevarying
	GENERAL INPUT DATA								
1	Case Name				Continuous	Instantaneous	Poolsource	Spill	Timevarying
A	Use file <case name>.LTU file for input release data (0 = no, 1 = yes)		0	1	0				
A	Use file <case name>.OBS file for observer data (0 = no, 1 = yes)		0	1	0				
	RELEASE DATA								
	General inputs								
A	Flag: release type (instantaneous =1, continuous (old) = 2, time-varying =3)		1	3	2	1			3
N	Released material name (from material database)				PROPANE				AMMONIA
7	Released material stream handle		0		74986				
8	Number of observers = number of source term points (time varying only)		2	161	2				
	Release observer arrays								
10	State flag (1 - Temp, 7 = liquid fraction)								
A	Observer release time (time-varying) or duration (cont. old)	s	0		600		60		0,50.0
A	flowrate at observer time (non-instantaneous only)	kg/s	1.00E-06	1.00E+05	7		12	10	10.0,5.0
A	Initial mass flowrate of air mixed in (non-instantaneous only)	kg/s	0	1.00E+05	0				
A	State flag (1 - temperature, 6 = liquid fraction)		1	7	6		1	6	6,6
A	Temperature of release component	K	10	900	240		240		
A	Liquid mass fraction of release component	kg/kg	0	1	0.8			1	0.8,0.8
A	Droplet diameter (SMD)	m	0	0.01	1.00E-03			0.01	1E-3,1E-3
A	Droplet size distribution parameter arr	-	0	1	0.4				0.4,0.4
A	Droplet size distribution parameter brr	-	0	6	3.5				3.5,3.5
A	Release velocity (non-instnantaneous only)	m/s	0	500	50				50,50
A	Radius for pool source (≤ 0 not a pool source)	m		1000	0		10		
	Instantaneous only								
A	release mass (instantaneous only)	kg	1.00E-04	1.00E+09	4200	4200			
A	mass of air (instantaneous only)	kg	0	1.00E+09	0	0			
A	Expansion energy (instantaneous only)	(J/kg)	0	12500	0	0			
	Release height, angle and impingement								
A	Release height	m	0		1		0	0	
A	Release angle [0 = horizontal, pi/2 = vertical upwards; cont.only]	radians	-1.571	1.571	0				
A	Impingement flag (0 -horizontal, 1 - angled, 2 - vertical, 3 - along ground, 4 - impinged, 5 - angled from hori		0	5	1				
	AMBIENT DATA								
	Pasquill stability class (1-A,2-A/B,3-B,4-B/C,5-C,6-C/D,7-D,8-E,9-F,10-G); 0 = use								
A	Monin-Obukhov length	-	0	10	7				
A	Monin-Obukhov length (stable > 0, unstable < 0, neutral = 1E+5)	m	-1.00E+05	1.00E+05	1.00E+05				
A	Wind speed at reference height	m/s	0.1	50	5				
A	Reference height for windspeed	m	0.1	100	10				
A	Temperature at reference height	K	200	350	298				
A	Pressure at reference height	N/m2	50000	120000	101325				
A	Reference height for temperature and pressure	m	0	100	0				
A	Atmospheric humidity (fraction)	-	0	1	0.7				
	SUBSTRATE DATA								
A	Surface roughness length	m	0.0001	3	0.1				
A	Dispersing surface type (1-land,2-water)		1	2	1				2
A	Temperature of dispersing surface	K	200	500	298				
	POOL DATA								
A	Pool surface type (1-wet soil, 2-dry soil, 3 - concrete, 4 - insulated concrete, 5 - dee		1	9	2				
A	Temperature of pool surface	K	10	10000	298				
A	Bund diameter (<=0: no bund)	m	0		0				
A	Bund height (rainout when droplets hit bund & used if bund overspill = yes)	m	0	100	0				
	AVERAGING TIME								
A	Averaging time	s	1	3600	18.75				
	OBSERVER TERMINATION CRITERIA								
A	Minimum concentration of interest	mole fraction	0	100	0				
A	Maximum distance of interest	m	0	1.00E+08	1000				
	CLOUD OUTPUT CONTROL								
A	Required time	s	0		100				
A	Required downwind distance	m	0		1000				
A	Position for off-centre concentrations : crosswind distance y	m	0	1000	0				
A	Position for off-centre concentrations : height z above ground	m	0	1000	0				
	Raw observer data								
A	Output observer off-CL concentr.: 0=no, 1 = at req. distance, -1 = at req. time	-	-1	1	-1				
	Processed data after observer calculations (pre- and post-AWD)								
	Pre & AWD off-centreline results required vs time(<0) or distance x (>0): 0 = none,								
A	± 1 = width, ± 2 = height, ± 3 = max conc, ± 4 = max width, ± 5 = dose	-	-5	5	0				-5
A	Required concentration for width and height calculations	mole fraction	0	1	0.001				

Figure 18. UDM input data - Part I: input data always to be specified

The following five cases are include in the example spreadsheet:

- The base case corresponds to a horizontal continuous propane release (80% liquid fraction, 7 kg/s, jet release speed of 50 m/s) of 600s duration.
- The second case relates to an unpressurised instantaneous propane release of 4200kg.
- The third case refers to a ground-level continuous circular propane pool source with 10 m radius, source rate 12kg/s and duration 60s.
- The fourth case refers to the ground-level continuous spill of 10 kg/s of liquid propane at its boiling temperature (600s duration).
- The fifth case refers to a time-varying release of ammonia with two observers released at 0s (10 kg/s) and 50s (5 kg/s).Thus a release rate is applied of 0 kg/s before 0s and afer 50s and the release rate varies linearly between 10kg/s and 5kg/s between 0s and 50s.

Input data always to be specified by the user (see Figure 18)

The first part of the input data (general input data, release data, ambient data, substrate data, pool data, averaging time, termination criteria, and cloud output control) should always be specified by the user. The data can be further described as follows:

1. GENERAL INPUT DATA

1.1. *Case name*. The root name of input files used, or output files generated, by the model. See the next two input variables for details.

1.2. *Use file <case name>.LTU file for input release data (0 = no, 1 = yes)*.
- If set to 1, then the model will use the file <case name>.LTU generated by TVAV to set release data. Release inputs from the spreadsheet will be disregarded. If no such file exists an error will result.
- If set to 0, then the spreadsheet inputs will be used.

1.3. *Use file <case name>.OBS file for observer data (0 = no, 1 = yes)*
- 1: The model will use the file <case name>.obs to load in observer results already calculated from file and use these for AWD calculations. The observer dispersion calculations will not be run. If no such file exists then an error will result.[cx]
- 0: The observer dispersion calculations will be run.

2. RELEASE DATA

2.1. General inputs

2.1.1.*Flag:*
- *instantaneous (1):* a single instantaneous release observer is modelled (released from the source), with subsequent pool observers (released from upwind edge of pool) in case of rainout.

[cx] The purpose is to speed up calculations when observer dispersion results do not change between cases, but AWD options (such as output distance or time) do. Then for cases with the same case name the observer calculations need only be run once (setting = 0). This automatically writes a file <case name>.OBS which can be used by subsequent cases.

- *continuous (2)*: only to be used for finite-duration continuous releases, including continuous pool sources; a single continuous release observer is modelled, with subsequent pool observers in case of rainout
- *time-varying (3):* a number of release observers are modelled, with subsequent pool observers in case of rainout

2.1.2. *Released material name (from material database)*. All properties of the material are subsequently derived from the property file. The pollutant stream may consist of a pure component or a mixture. If a mixture is used, then an .xml file containing that mixture (exported from Phast) should be used.

2.1.3. *Number of release observers (time-varying only).* There must be a minimum of two release observers.

2.2. Release observer arrays (these data are not used in case of input data from a .LTU file)

2.2.1. Non-instantaneous releases only:

2.2.1.1. *Observer release time (time-varying), or release duration (continuous), s.* In case of time-varying, the first observer release time should be typically time t=0 (zero observer data are presumed at time t<0), and observer releases times should increase with subsequent observers (zero observer data are presumed after the last time).

2.2.1.2. *Mass flow rate at observer time, kg/s.* Mass release rate of material

2.2.1.3. *Initial mass flow rate of air mixed in, kg/s.* Mass release rate of air mixed in with the material. The initial air is assumed to be at the same temperature as the ambient air. If the air is required to be at the pollutant temperature, the air should be specified as part of the released pollutant

2.2.2. Initial thermodynamic state (in case of pressurised releases, they data correspond to post-expansion data, i.e. after depressurisation to ambient pressure)

2.2.2.1. *State flag (1 - Temp, 6 = liquid fraction).* Indicates how the state of the material is to be specified. If 1, then the temperature is used, if 6 the liquid fraction.

2.2.2.2. *Temperature of release component, K.* Used only if state flag = 1. Temperature is compared with normal boiling point to determine the phase of the released material (either pure liquid or vapour)[cxi].

2.2.2.3. *Liquid mass fraction of release component.* Used only if state flag = 6. Temperature is set to the normal boiling point, with the specified liquid fraction[cxii].

2.2.3. Droplet size data (initial post-expansion data; a_{rr}, b_{rr} only relevant for droplet parcels)

2.2.3.1. *Droplet diameter (SMD), m*

2.2.3.2. *Droplet size distribution parameter arr.* Rossin-Rammler 'a' coefficient for determining droplet size distribution (see droplet size theory manual for details)

2.2.3.3. *Droplet size distribution parameter brr.* Rossin-Rammler 'b' coefficient for determining droplet size distribution (see droplet size theory manual for details)

2.2.4. (non-instantaneous only; not used for pool sources) *Release velocity (m/s)*

2.2.5. *Pool source radius, m* (> 0 only, otherwise normal release) Pool sources specify radius instead of velocity; the latter is ignored.

2.3. *Instantaneous releases only:*

2.3.1. *Release mass, kg.* Total mass released.

[cxi] For MC cases a flash is done at the temperature and atmospheric pressure to determine the phase.

[cxii] IMPROVE Use of the MC multiple-aerosol thermodynamics requires specification of temperature rather than liquid fraction. This is due to limitations on the MA flash algorithm which as yet cannot iterate on temperature to find a given liquid fraction.

2.3.2. *Mass of air, kg.* Total mass of mixed-in air released. The initial air is assumed to be at the same temperature as the ambient air. If the air is required to be at the pollutant temperature, the air should be specified as part of the released pollutant.

2.3.3. *Expansion energy, J/kg*. For a user defined catastrophic rupture, the release velocity (U_{Rel}), is translated into an expansion energy (E_{exp}), whereby $Ee_{xp} = 0.5U_{Rel}^2$. The release velocity has a maximum value of 500 m/s and hence the expansion energy also has a maximum of 125,000 J/kg. For a modelled case, however, the expansion energy is provided directly from the discharge models.

2.4. Release height, angle and impingement

2.4.1. *Release height, m.* The release height is normally advised to be set at least 1 meter.

2.4.2. *(non-instantaneous releases only) Release angle θ_R [0 = horizontal, pi/2 = vertical upwards], radians.* Releases upwind are not allowed.

2.4.3. *Impingement flag*:

- 0: horizontal (release angle $\theta_R=0^o$). This angle overrides the angle given above.
- 1: angled (prescribed θ_R)
- 2: vertical ($\theta_R=90^o$). This angle overrides the angle given above.
- 3: along ground ($\theta_R=-90^o$). This corresponds to a vertical downward jet impinging onto the ground. By default this model over simplistically resets the elevation height to zero, modifies the release velocity with either a velocity factor (default 0.25) or reduces it to the velocity cap[cxiii] (if release velocity < cap), and sets the release direction to horizontal (see also footnote i for a further discussion).
- 4: horizontal impinged (prescribed $\theta_R=0$). This is a special case of option 5. This angle overrides the angle given above.
- 5: angled from horizontal impinged (prescribed θ_R). This option resets the release velocity as for option 3, but it does not reset the elevation height and release angle.

[cxiii] In Phast, parameters which refer to 'velocity cap' or 'velocity reduction factor' for impinged cases are disabled – impingement always reduces velocity by this factor.

Description	Time and Weather	Wind Speed *u*	Monin-Obukhov Length *L*	Pasquill-Gifford Stability Class
Very Stable	Clear night	<3 m/s	10 m	F
Stable	↓	2 to 4 m/s	50 m	E
Neutral	Cloudy or Windy	any	>l100 ml	D
Unstable	↓	2 to 6 m/s	–50 m	B or C
Very Unstable	Sunny	<3 m/s	–10 m	A

(a) Table 3.1 from CCPS guidelines[30]

	Daytime insolation			Nighttime Conditions		Anytime
Surface wind Speed, m/sec	Strong	Moderate	Slight	Thin overcast or >4/8 low cloud	≥3/8 cloudiness	Heavy Overcast
<2	A	A–B	B	F	F	D
2–3	A–B	B	C	E	F	D
3–4	B	B–C	C	D	E	D
4–6	C	C–D	D	D	D	D
>6	C	D	D	D	D	D

(b) From Gifford (1976) [101]

Table 9. Selection of stability class

3. AMBIENT DATA

3.1. *Pasquill stability class (1-A,2-A/B,3-B,4-B/C,5-C,6-C/D,7-D,8-E,9-F,10-G).* these can be selected to be A, A/B, B, B/C, C, C/D, D, E, F, G; see Table 9 on recommendations for selection of the stability class depending on the time (day/night), weather (cloud cover) and wind speed:
- By night time stable conditions occur (negative vertical temperature gradient) with stability reducing from F to D (neutral) with increasing cloud cover.
- By day time, unstable conditions occur with instability reducing from A to D with reducing cloud cover.
- For increasing wind speeds more neutral conditions are obtained.

3.2. *Wind speed at reference height (m)* and *Reference height for wind speed (m/s).* Wind speed u_a^o and corresponding reference height z_o. The vertical wind speed profile is determined from these data, and the specified surface roughness and stability class.

3.3. *Temperature* T_a^o (K) and *pressure* p_a^o (Pa) with corresponding *reference height* z_o^{Tp} (m)

3.4. *Atmospheric humidity, fraction.* The ambient relative humidity provides the amount of water in the amount of ambient wet air. A value of 1 corresponds to saturated conditions.

4. SUBSTRATE DATA

4.1. *Surface roughness length, m.* The surface roughness is related to the averaged obstacle height. A very detailed description of the evaluation of the correct value of the surface roughness length is provided by Hanna and Britter[102]. Table 10 includes recommended values by the EPA and the Purple Book.
4.2. *Substrate type (land or water).* In case the user selects water, water vapour pick-up from the substrate is accounted for.
4.3. *Substrate temperature, K*

5. POOL DATA

5.1. *Pool substrate type (1-wet soil, 2-dry soil, 3 - concrete, 4 - insulated concrete, 5 - deep open water, 6 - shallow open water, 7 - deep river of channel, 8 - shallow river or channel,9 - user-defined type).* In case of a user-defined pool surface, user-defined values are used for the roughness factor, conductivity, diffusivity, and minimum thickness (as specified in the parameters).
5.2. Temperature of pool substrate, K
5.3. *Bund diameter, m* (=0, if no bund).
5.4. *Bund height, m*. This is the height of the bund wall. Rainout is assumed to occur when the droplets hit the bund wall. If the parameter 'bund overspill' is set to yes (i.e. bund can fail), the bund is assumed to fail (allowing unlimited spreading) as soon as the pool liquid height exceeds the bund height.

6. AVERAGING TIME
6.1. *Averaging time, s*. This is the averaging time used following transition to passive dispersion to model wind meander. It is also used for the additional time-averaging of concentrations in case of time-varying concentrations resulting from time-varying releases and/or time-varying pools; see Section 3.7 for details.). Recommended values are 18.75 seconds for flammable materials (no averaging time), and 600 seconds for toxic materials (in line with TNO Yellow Book[65] and CCPS guidelines[66]).

7. OBSERVER TERMINATION CRITERIA

7.1. *Minimum concentration of interest (mole fraction)* and *Maximum distance of interest (m).* Observers will generally[cxiv] disperse until both these conditions have been met (i.e. centre-line concentration < minimum concentration c_{min} and downwind distance > maximum distance x_{max}. A value of zero for either condition will mean that the condition is ignored. We recommend for AWD calculations that a maximum distance of interest is used to prevent low mass observers terminating early, and concentration evaluations are only guaranteed be fully accurate up to a distance ½ or 1/3rd that distance. Alternatively, observers should be run to an order of magnitude lower concentration than is required for height or width calculations. See the detailed description of the termination criterion under the UDM parameter section below for full details on the termination criterion.

8. CLOUD OUTPUT CONTROL

Concentrations are output at a given off-centreline location (crosswind distance y_{int}, height above ground z_{int}). The output data are as follows:

- Optional output of raw observer off centre-line concentration data (pre-AWD data before interpolation) either at a given distance of interest x_{int} or at a given time of interest t_{int}.
- Output of pre-AWD and post-AWD concentrations both versus time (t at a given distance of interest x_{int}) and versus distance x (at at given time of interest t_{int}).
- Optional additional off-centreline result which may include cloud width and height to a given concentration of interest c_{int}, maximum concentrations and widths and (in case of toxics) toxic loads (doses).

Further details of the input data are as follows:

8.1. Required time and location

8.1.1. *Required time, s.* Time of interest, t_{int}. The spreadsheet reports off-centreline (at y_{int}, z_{int}) concentrations at the time t_{int} as a function of distance x downwind, typically with the upwind and downwind edges of the cloud defined by the concentration of interest c_{int} for width and height.

8.1.2. *Required distance, m.* Distance of interest, x_{int}. The spreadsheet reports off-centreline concentrations (at y_{int}, z_{int}) at this distance x_{int} downwind as a function of time t, typically with the leading and trailing edges of the cloud defined by the concentration of interest c_{int} for width and height.

8.1.3. *Position for off-centre concentration: crosswind distance y, m*. Crosswind distance of interest, y_{int}

8.1.4. *Position for off-centre concentration: vertical height z above ground, m*. Vertical height of interest, z_{int}

8.2. Output raw observer concentration:

- *0 = none*. No output of observer concentrations
- *1 = at required distance*. Output of observer concentrations at distance x_{int},
- *-1 = at required time*$_t$. Output of observer concentrations at tim t_{int},

8.3. Output processed data after observer calculations (pre- and post-AWD)

8.3.1. Pre & AWD off-centreline results required vs time (<0) or distance x (>0): 0 = none, ± 1 = width, ± 2 = height, ± 3 = max conc, ± 4 = max width, ± 5 = dose. This controls optional additional output of off-centreline results for a specified output variable both before and after inclusion of along-wind diffusion effects. In case of a specified positive value the variable is given as function of downwind distance, while in case of a negative value it is given as a function of time. The following variables can currently be output:

[cxiv] Depending on parameter settings.

- ± 1 = width: cloud half-width to specified concentration c_{int} at specified height z_{int}
- ± 2 = height: cloud height to specified conc. c_{int} at specified crosswind distance y_{int}
- 3 = maximum concentration over all times versus x at given y_{int}, z_{int}
- -3 = unused[cxv] maximum concentration (until time t) versus time t at given $x_{int}, y_{int}, z_{int}$
- 4 = maximum half-width to specified concentration c_{int} over all times versus distance x at given z_{int}
- -5 = toxic load (received until time t) versus time t at given $x_{int}, y_{int}, z_{int}$
- 5 = accumulated toxic load versus distance at given y_{int}, z_{int}.

8.3.2. *Required concentration for width and height calculations, mole fraction.* Concentration of interest c_{int} for width and height calculations. In general concentrations below this will not be reported, nor included in dose calculations. Te ensure accurate AWD and dose calculations, the user should ensure that the minimum concentration of interest c_{min} is significantly smaller than c_{int} (in the order of a factor of 10)

z_0 (m)	Typical Terrain	
1×10^{-4}	Calm open sea or snow-covered flat or rolling ground	Large expanse of water or desert.
1×10^{-3}	Off-sea wind in coastal areas	
2×10^{-3}	Natural snow over farmland	
3×10^{-3}	Frenchmen's Flats, NV test site	
5×10^{-3}	Cut grass (≅30cm)	Fairly level grassy plains
1×10^{-2}	Few trees, winter	
2.5×10^{-2}	Uncut grass, isolated trees	Airport runways
5×10^{-2}	Few trees, summer	Farmland
8×10^{-2}	Many hedges	
3×10^{-2}	**EPA rural cases**	
2×10^{-1}	Many trees, hedges, few buildings	
4×10^{-1}	Outskirts of town	Fairly level wooded country
5×10^{-1}	Centers of small towns	
1.0	Centers of large towns, cities. **EPA urban cases.** **Processing plants** (Peterson, 1990)	Forests
1.5–3.0	Centers of cities with very tall buildings	Very hilly and mountainous

(a) values recommended by EPA[66]

Class	Short description of terrain	z_0 (m)
1	open water, at least 5 km	0.0002
2	mud flats, snow; no vegetation, no obstacles	0.005
3	open flat terrain; grass, few isolated objects	0.03
4	low crops; occasional large obstacles, x/h > 20 (1)	0.10
5	high crops; scattered large obstacles, 15 < x/h < 20 (1)	0.25
6	parkland, bushes; numerous obstacles, x/h < 15 (1)	0.5
7	regular large obstacle coverage (suburb, forest)	(1.0) (2)
8	city centre with high- and low-rise buildings	(3.0) (2)

[cxv] Logically this would return the maximum concentration at a given time t over all x. This has not been implemented.

(1) *x* is a typical upwind obstacle distance and *h* the height of the corresponding major obstacles.
(2) Values are rough indications. The use of an aerodynamic roughness length, z_0, does not account for the effects of large obstacles.

(b) values recommended by Purple Book[73]

Table 10. Recommended values for surface roughness

Input parameters (input data to be changed by expert users only; see Figure 19)

For the parameters, we include here only a guide to those parameters directly relevant to the AWD cases, or those that are not disabled in this version of the model. A fuller description of remaining parameters can be found in the UDM Theory Manual.

1. MODEL CONTROL FLAGS

1.1. General flags

1.1.1.Impingement method (0 - use factor, 1 - use cap). This flag is relevant for impinged releases only, where either the velocity is reduced with a factor of 0.25 or a velocity cap is used.

1.1.2.*Pressurised instantaneous expansion model (0-Purple book, 1 - advanced)*. This defines the method adopted for modelling the intial phase of pressurised instantaneous expansion as described in Section 6. The advanced (default) option is always recommended for pure vapour pressurised instantaneous releases because it results in good agreement with experimental data. For two-phase pressurised instantaneous releases, no experimental data appear to exist, and there is a general feeling that the default method may produce sometimes too little rainout. However the underlying physics is felt to be overall better (except for the initial droplet size value and the initial droplet trajectory angle) than the over-simplified Purple Book method.

1.1.3.Jet model flag: 1 – Ricou-Spalding (Emerson), 2 – Morton et al. See Section 3.4.1 for details.

1.1.4.*Mixing height flag* (1 - yes, cloud rise is restrained by mixing layer, 2 - no, cloud rise is not restrained by mixing layer),

1.2. Thermodynamic / droplet flags (see UDM thermodynamic theory manual for further details)

1.2.1.*Thermodynamic model flag: -1 (no rainout, equilibrium), 1 (rainout, equilibrium), 2 (rainout, non-equilibrium).* No droplet equations are adopted for options -1 and droplet trajectories are calculated only for option 1.

1.2.2.*Multicomponent flag (0 - PC, 1 - Single aerosol, 2 - Multiple aerosol)*[cxvi]*:*

- *0:* pseudo-component method (PC): mixture approximated by pure component with averaged properties like boiling point and vapour pressure) with same composition of mixture liquid and mixture vapour. Use can be made of the non-equilibrium model including droplet modelling and rainout
- *1,2:* more rigorous multi-component method (MC): different composition of vapour and liquid (more volatile components in mixture evaporate more fast). Use is always made of the equilibrium two-phase model excluding droplet modelling and rainout. Single aerosol assumes that all components form simple droplet. More advanced multiple-aerosol algorithm presumes possible separate droplets for separate components, but presently this algorithm provides a numerical solution only for either one 2-component single aerosol or multiple one-component aerosols.

1.2.3.*Number of droplet parcels (0 - use SMD as specified).* If the value 0 is chosen, the specified value of SMD (Sauter Mean Diameter; always used for Phast) is adopted

[cxvi] FUTURE. An additional recommended option could be applied.

and droplet trajectories are calculated associated with this SMD. If a positive value is chosen, a range of droplet sizes is modeled.[cxvii]

1.2.4. *Flag for heat/water vapour transfer from substrate:* 1 – none, 2 – heat only, 3 – heat and water. If '3' is selected, the UDM model will include effects of heat transfer when the cloud moves over land and the effects of heat and water vapour transfer if the cloud moves over water.

1.2.5.Use DIPPR for ambient properties (1 - yes, 2 - no). See Appendix A to the UDM thermodynamics theory manual for details.[cxviii]

1.3. Pool modelling flags:

1.3.1.Method for cloud spreading over pool (1 - Van Ulden, 2 - Force to pool width, 3 - mass average (cloud mass), 4 - mass averaging (comp. mass)) [in product this is hard-coded as 4; option 2 is currently disabled in code]

1.4. Observer data post-processing flags

These input data control the optional post-processing following the observer calculations as described in Section 0:

1.4.1.Downwind gravity shape correction (1- no, 2 - yes). This correction is relevant for heavy-gas dispersion in case the crosswind gravity velocity is not significantly smaller than the ambient velocity. See Appendix D for details.

1.4.2.Differential observer-velocity mass-correction flag (1 - no, 2 - yes). This correction is relevant when observers move with significant different velocities, i.e. curves for observer downwind distance versus time are significantly different. This is particularly relevant for highly time-varying pressurised jet releases, and not for ground-level heavy-gas releases.

1.4.3.*Along-wind diffusion modelling (0 - none, 1 - QI, 2 - FDC, 3 - AWD)*.

- Option 0 will mean that no QI transition is permitted and no AWD modelling is carried out. 'AWD' results will be interpolated purely from observer data.
- Option 1 is as option 0 except that the QI transition is enabled (transition from continuous to instantaneous releases). This transition can only be enabled for continuous finite-duration releases without rainout.
- Option 2 uses the Finite Duration Correction method. No AWD results are generated. The FDC option can only be enabled for continuous cases without rainout (not for time-varying releases and instantaneous releases, but including pool sources). FDC is expected to produce more accurate results than QI in case of ground-level non-pressurised releases (with no rainout). For this case it produces results consistent with AWD. However it produces predictions of maximum concentrations only (no cloud width), and can therefore not be used in conjunction with risk calculations.
- Option 3 gives full AWD modelling.

1.4.4.*Time averaging for time-dependent concentrations (1 - no, 2 - yes).* Option 2 should be selected in case the user wishes to carry out time averaging using specified averaging time over time-dependent concentrations, with time-dependency resulting from either time-varying release of time-varying pool. See Section 3.7.2 for details.

2. MODEL ACCURACY, LIMITS, OUTPUT CONTROL

2.1. Model accuracy and stepping

2.1.1.*Solver tolerance for integration.* Reducing this numerical tolerance will increase CPU time and produce more accurate values. However it may lead more often to non-

[cxvii] FUTURE. Version does not fully work for multiple parcels; do not use, always use default = 0.

[cxviii] DIPPR not selected as default to avoid use of property system and therefore minimise CPU time

convergence since the required tolerance cannot be achieved. Caution should be exercised when modifying this value.

2.1.2. *Initial step size for cloud integration, s.* This is the initially reported step size for release observers, unless an earlier transition occurs. For pool observers this value is multiplied by 10.

2.1.3. *Maximum allowed step size for cloud integration, s*. Decreasing this will reduce the maximum gap between observer output steps, and thereby give improved interpolation in the far-field. However run times will be longer. Caution should be exercised when modifying this value.

2.1.4. *Maximum number of release observers* – not yet implemented

2.1.5. *Maximum number of pool observers.*

Two cases are considered:

- In case no release observers are present (e.g. pool source or direct spill), this is the number of pool observers released from the pool..
- In case release observers are present (e.g. elevated release), this there can be fewer or more depending on the type of case (see Section 0).

2.1.6. Control of output distances.

2.1.6.1. *Maximum number of fixed output steps*

2.1.6.2. *Multiplier for output step sizes*

The above data are applied for all observers. Ideally step sizes would only be increased after the observer has left the pool behind, and the user may wish to adapt the above data accordingly such that this applies for all observers.[cxix]

2.2. Limits

- *Minimum temperature* and *Maximum temperature*. These are used as lower and upper limits for the iterative solution of the temperature in the THRM thermodynamic calculations.
- *Minimum velocity (non-instantaneous and instantaneous)*. This value will overwrite the user-specified value in case the latter value is below this minimum value.
- *Maximum duration for a release.* This value will overwrite the user-specified value in case the latter value is above this maximum value.

2.3. Termination criterion

This includes termination parameters in addition to the termination input data described above (minimum concentration c_{min} and maximum distance x_{max}):

2.3.1. Input variables for stop criterion:

- *Absolute maximum distance* x_{max}^{abs} . The distance at which dispersion will stop, regardless of minimum concentration of interest or maximum distance of interest. This should be at least as large as the maximum distance of interest. If an observer stops due to this distance being exceeded before a requested minimum concentration is reached, then a warning (UDMA 1117) is reported. In this case AWD concentrations around the concentration of interest may underpredict.
- *Absolute maximum height* h_{max}^{abs} for dispersion. As with the absolute maximum distance, warning UDMA 1117 can be triggered.
- *Minimum probability of death* p_{min}[cxx].

2.3.2. *Stop flag* for UDM run:

[cxix] REFINE. As part of further work it may be considered to only increase the step size once an observer has become detached AND the maximum number of fixed output step sizes has been achieved.

[cxx] TODO. Not currently used – see footnote below.

- 1: Risk-based run. This option should be specified for continuous and/or instantaneous releases only; it can not be used for observer logic. Termination is based on material/result type:
    - if flammable, run stops when the maximum concentration at a downwind distance falls below the minimum concentration c_{min}
    - if toxic, run stops when the maximum concentration falls below the concentration corresponding to the minimum probability of death p_{min}. For toxic mixtures, the toxic calculation method specifies whether to use the probit functions provided for the mixture, to use the most toxic component, or to combine doses from components. This calculation is also dependent on the parameter 'maximum release duration'.
    - if both flammable and toxic, the run stops after both the minimum concentration c_{min} and the minimum probability of death p_{min} have passed
    - if inert, risk-based run is not allowed
- 2: Concentration and distance based run: run stops when both concentration is below c_{min} and maximum distance x_{max} have passed
- 3: Distance-based run: run stops when maximum distance x_{max} has passed
- 4: Concentration based run: run stops when concentration is below c_{min}

Note that the run will be terminated earlier in case either the absolute maximum distance x_{max}^{abs} has been passed, or the maximum centre-line height h_{max}^{abs} has been achieved. The results will not be reported to the spreadsheet (see Spreadsheet output control below) after the maximum number of output steps n_{max} has been achieved.

2.3.3. *Toxic calculation flag (used for toxic-load calculations for mixtures only)*. Applies only to termination of dispersion calculations. For AWD dose calculations the 'Most toxic material' (option 2) is always used.

- 1 - mixture probits. Probit coefficients for the entire mixture are used, and must be specified by the user
- 2 - most toxic material probits, The concentrations and probits of the most toxic component in the mixture are used.
- 3 - product of each toxic material. The probability of death is determined from the individual component lethalities, P^i_{death} i.e. $P_{death} = 1 - \Pi(1-P^i_{death})$

2.3.4. *User selected flammable/toxic flag*. Used to determine stop criterion for risk based runs:

- 1 – Flammable risk only considered for terminating dispersion (material must be flammable)
- 0 – Flammable and toxic risk both considered for terminating dispersion (material must be both)
- -1 – Toxic risk only considered for terminating dispersion results required
- -2 – Inert[cxxi].

2.3.5. *Probit Methodology*. Method of calculating probability of death, P_{death}:

- 1 - Prefer probit. Toxic probits are used to calculate a Pdeath between 0 and 1. If no probit coefficients exist for the material, the Dose method is used.
- 2 - Prefer Dose, The toxic dose is compared against the dangerous toxic load (DTL) for the material, and if exceeded Pdeath = 1, otherwise Pdeath = 0. If no DTL exists for the material the probit method is used
- 3 - Use Probit, As 'Prefer probit', but if the required data does not exist the model will not run
- 4 - Use Dose. As 'Prefer dose', but if the required data does not exist the model will not run

[cxxi] CHECK. How this affect stop criterion.

3. AMBIENT DATA:

These parameters affect the ambient data as described in Appendix A:

- *Wind profile flag* for vertical wind profile $u_a(z)$ [1 - constant, 2 - power-law fit of logarithmic profile]
- *Cut-off height for power-law wind profile*
- *vertical temperature/pressure profile* (1 - constant, 2 - linear, 3 - log)
- *Specific heat of dry air* (J/kg/K) and *atmospheric molecular weight* (kg/kmol)
- *height of mixing layer* (comma separated list of heights for all stability classes)

4. PHYSICAL MODEL PARAMETERS (see also Section 7 for an overview of UDM model coefficients):

4.1. Source and expansion zone:
- *Expansion length \ source diameter.* This is the ratio of the length L_{exp} of the expansion zone to the post-expansion release diameter D_{exp} as derived from the post-expansion release data as input to the UDM (continuous releases only). The UDM calculations are started from $x = \cos \alpha\, L_{exp}$, where α = release angle. Note that L_{exp} is typically very small, and this would therefore hardly affect the results.
- *Velocity multiplication factor for impinging releases*
- *Velocity cap for impinging releases*

4.2. Jet dispersion:
- *Jet entrainment coefficient* α_1; see Section 3.4.1 for details
- *Cross-wind entrainment coefficient* α_2: see Section 3.4.2 for details.
- *Plume/air drag coefficient* C_{Da}: see Section 3.5.1 for details.

4.3. Heavy gas dispersion:
- *Dense cloud edge-entrainment coefficient* γ (continuous or instantaneous); see Equation (63) for details.
- *Dense cloud spreading parameter* C_E (continuous or instantaneous); see Section 3.6.2 for details.

4.4. Passive dispersion:
- *Near-field passive entrainment parameter* e_{pas}; see Section 3.4.3 for details.
- *Ratio of instantaneous to continuous σ_y and σ_z.* Values of σ_y and σ_z for instantaneous releases are different from those for continuous releases. Insufficient data are available to derive good correlations for all stability classes over a wide range of distances, including the dependence on surface roughness. These ratio parameters are provided so that the values of σ_y and σ_z for continuous releases may be scaled up or down in magnitude to provide values for instantaneous releases.

4.5. Liquid component (droplet/rainout/pool):
- *Ratio drop to expansion velocity for instantaneous release*. For pressurised releases during the initial instantaneous expansion phase, droplet velocities are set to be this fraction of cloud expansion velocity.
- *Expansion energy for maximum droplet angle*. This is the expansion energy above which the initial droplet trajectory for pressurised instantaneous releases is a maximum. See Section 6.2.2 for details.
- *Critical droplet diameter for rainout*. Droplet diameter below which droplets are assumed to remain s uspended in the cloud and not rain out.

5. TRANSITION CONTROL

5.1. Transition to passive. See Section 3.3 for a detailed description of the transition from near-field dispersion to far-field passive dispersion. This is expressed in terms of the following input parameters:

- *Maximum cloud/ambient velocity difference*, r_u^{pas}: $|u_{cld}/u_a(z_c) - 1| < r_u^{pas}$
- *Maximum non-passive entrainment fraction*, r_E^{pas}: $[1-E_{pas}^{nf}/E_{tot} < r_E^{pas}]$ (for elevated plume, modified formulas otherwise: see Section 3.3)
- *Maximum Richardson number* Ri_*^{cr}: $Ri_* < Ri_*^{cr}$ (used for ground-level plume only)
- *Maximum cloud/ambient density difference*, r_ρ^{pas}: $|\rho_{cld}/\rho_a(z_{cld}) - 1| < r_\rho^{pas}$
- *Distance multiple for phasing in full passive entrainment*, r_{tr}^{pas}

5.2. Pool re-evaporation:

- *Cut-off for evaporation rate*. The PVAP calculation (after UDM rainout) will be terminated at the time when the evaporation rate reduces below this cut-off.

5.3. Other transitions:

- *Quasi-instantaneous transition parameter*, r_{quasi}. The transition from continuous to instantaneous will take place if the ratio of the cloud width to the cloud length exceeds r_{quasi}. Increasing the value of r_{quasi} will delay this transition. No along-wind diffusion effects are taken into account before the transition. This input parameter is only applicable when the QI transition criterion has been selected for finite-duration releases. See Section 4.1 for further details.
- *Richardson number for lift-off criterion* (default = -20). See Equation (79) for details.

6. POOL-MODEL PARAMETERS

These are additional parameters required by the pool model PVAP. See the PVAP theory manual for further details.

- *Solar radiation flux* Q_{rad}
- data used if user-defined bund surface type (type = 9): *thermal conductivity* k_s, *minimum pool thickness* H_{min}, *surface roughness factor* χ_s, *thermal diffusivity* α_s
- bund overspill switch: 0 (off), 1 (on). Allows bunds to 'fail' when liquid pool volume exceeds bund volume; for further details see description of input variable bund height.

7. SPREADSHEET OUTPUT CONTROL

7.1. *File output level*. This option controls the files that may be generated. In all cases the file name root is the case name specified in 1.1. Higher levels 3 and 4 generate many files and will be of interest only to expert users. Allowable levels are as follows:

- 0 - No files generated. As observer files are not written this option cannot be used to provide observer data for another run (See See 1.3).
- (default) 1 – Writes observer (.obs) and commentary (_comm.txt) files
- 2 - Writes observer (.obs) and enhanced commentary (_comm.csv) files.
- 3 - Writes Level 1 files and .csv containing cloud primary (_prim.csv), cloud secondary (_sec.csv), droplet (__drop.csv) and pool (_pool.csv) variables.
- 4 - Writes Level 1 files and additional files previously generated by the Phast 6.7 UDM version (.UDX, .UDM,. .ENT, etc.)

A complete list of file types which may be generated is given in the table below:

Name	Contents
.obs	Observer files contain data as function of time (x_{cld}, t, c_{cld}, R_y, R_z, m, n, θ, z_{cld}) for each observer.
_comm.txt	Commentary files contain a record of what transitions and when were made by each observer or the pool
_comm.csv	Extended commentary files contain a record of primary cloud variables as well as transitions made
_prim.csv	Cloud primary files contain the primary variables (cloud & droplet) + transition flags for each observer
_sec.csv	Cloud secondary files contain the secondary cloud variables
_pool.csv	Pool files contain pool primary and secondary variables
_drop.csv	Droplet files contain droplet primary and secondary variables. Mainly of interest for cases using droplet parcel logic
.ENT	Pre-AWD entrainment contributions for each observer
.UDM	Binary file used by Phast
.UDX	Text equivalent of .UDM file. Contains pre-AWD observer data. Superseded by Cloud primary and secondary files.
.obst / .obsx	Pre-AWD observer data calculated at a particular time (.obst) or distance (.obsx).

7.2. *Component of interest* (not yet implemented; now always entire mixture concentrations input). If the component of interest = 'Default', the entire mixture concentration/dose is output. Otherwise, concentration and dose results are produced for the component of interest. An error is given if the component of interest is not present in the database.

7.3. *Mass (=1) or mole (=0) for component of interest* (not yet implemented).

7.4. User-selected outputs. *(user output 1- 4).* This allows selection of three additional outputs on the spreadsheet. A large number of variables can be output and the list below includes only the most commonly-used variables :

- Cloud variables (<1000):
  - 4: effective cloud height H_{eff}, m
  - 8: effective cloud widthW_{eff}, m
  - 10: cloud centroid height z_c, m
  - 14: cloud mass (air + material) M_{cld}, kg/s (non-inst.) or kg (inst.)
  - 5: cloud-profile horizontal exponent m
  - 17: cloud-profile vertical exponent n
  - 18: Richardson number Ri, -
  - 19: angle to horizontal θ, radians
  - 28: ambient windspeed at centroid height, u_a, m/s
  - 29: air density ρ_{air}, kg/m^3
  - 30: cloud area A_{cld}, m^2 (non-instantaneous releases)
  - 34: cloud density ρ_{cld}, kg/m^3
  - 38: heat from substrate Q_{gnd}, J (inst.) or J/s (non-inst.)(
  - 39: cloud volume V_{cld}, m^3 (instantaneous release)
  - 75: wet air mass added to cloud, M_{wa}, kg (inst.) or kg/s (non-inst.)
  - 9: half-width of cloud touching down the ground, W_{gnd}, m (non-inst. release)
  - 1: area of cloud touching down the ground A_{gnd}, m^2 (inst. release)
  - 3: touchdown fraction h_d (0 – grounded, 1 – elevated)
- Droplet variables (>1000,<2000):
  - 1004: droplet mass m_d, m
  - 1001: droplet vertical velocity u_{dz}, m/s
  - 1005: droplet velocity u_z, m/s
  - 1006: droplet diameter D_d, m
  - 1007: droplet temperature T_d, K
- Pool variables (>2000):
  - 2004: mass dissolved in water M_{dis}, kg

- 2001: total mass spilt, kg
- 2011: pool effective radius R_{eff} (net area of evaporating pool; $R_{eff} \leq R_{actual}$), m
- 2012: pool depth, m
- 2013: pool temperature T_{pool}, K
- 2014: Q_{net} – net heat input into pool, W
- 2024: velocity of evaporating vapour, u_z^{pool}, m/s
- 2026: bubble point T_{bub}, K
- 2039: pool actual radius R_{actual} (total area covered by pool including 'blobs'), m

7.5. *Cloud half-width of interest* (see Appendix C of UDM validation manual for details)

- 1 - W_{eff} (UDM effective half-width; see Section 3.1 for details) This is the half-width of an equivalent top-hat profile with as top-hat concentration adopted the maximum centre-line concentration:

$$W_{eff} = \frac{1}{c(x,0,z)} \int_0^\infty c(x,y,z)dy$$

- 2 – W (Hanna's definition). This is the lateral distance at which the cloud concentration has fallen to a factor $e^{-0.5}$ times the centreline concentration.
- 3 – b (SMEDIS definition) with b determined from:

$$b^2 = \frac{\int_0^\infty y^2 c(x,y,z)dy}{\int_0^\infty c(x,y,z)dy}$$

7.6. *Number of output steps for AWD*. The number of output points in concentration and dose 'transects'. This also includes the number of points calculated along the concentration versus time curve used to calculate doses, so reducing this significantly while reducing run time will reduce the accuracy of dose calculations

Inputs		DNV MODEL UDM							
Input Index	Description	Units	Limits Lower	Limits Upper	Continuous	Instantaneous	Poolsource	Spill	Timevarying
	PARAMETERS (to be changed by expert users only)								
	MODEL CONTROL FLAGS								
	General flags								
A	Impingement method (0 - use factor, 1 - use cap)		0	1	0				
A	Pressurised instantaneous expansion model (0-Purple book, 1 - advanced)	-	0	1	1				
A	Jet Model Flag (1 - Emerson, 2 - Morton et al)		1	2	2				
A	Mixing height flag (1-yes,2-no)		1	2	1				
	Thermodynamic / droplet flags								
A	Thermodynamic model flag: , -1 (no rainout, equilibrium), 1(rainout, equil.), 2 (raino		-1	2	2				
A	Multicomponent flag (0 - PC, 1 - Single aerosol, 2 - Multiple aerosol)	-	0	2	0				
A	Number of droplet parcels (0 - use SMD as specified)		0	10	0				
A	Flag for heat/water vapour transfer (1 - none, 2 - heat only, 3 - heat and water)		1	3	3				
A	Use DIPPR for ambient properties (1 - yes, 2 - no)		1	2	2				
	Pool modelling flags								
A	Pool sources: spreading over pool (1 - Van Ulden, 2 - Force to pool width, 3 - mass average (cloud mass),		1	4	4				
	Observer data post-processing flags								
A	Downwind gravity shape correction (1- no, 2 - yes)		1	2	1				
A	Differential observer-velocity mass-correction flag (1 - no, 2 - yes)		1	2	1				
A	Along-wind diffusion modelling (0 - none, 1 - QI, 2 - FDC, 3 - AWD)		0	3	3	0			
A	Time averaging for time-dependent concentrations (1 - no, 2 - yes)		1	2	1				
	MODEL ACCURACY, LIMITS, OUTPUT CONTROL								
	Model accuracy and stepping								
A	Solver tolerance for integration		1.00E-06	1	1.00E-03				
A	Initial step size for cloud integration	s	0	10	0.01				
A	Maximum allowed step size for cloud integration	s	1	1000	1000				
A	Maximum number of release observers	-	1	100	10				
A	Maximum number of pool observers	-	1	100	5				
A	Core averaging time (TEMPORARY ONLY FOR TESTING PURPOSES)	s	0	1.00E+05	18.75				
A	Maximum number of fixed output step sizes	-	0	1000	20				
A	Multiplier for output step sizes	-	0	10	1.2				
	Limits								
A	Minimum temperature	K	0	300	9.999				
A	Maximum temperature	K	300	5000	900				
A	Minimum release height for continuous and time-varying horizontal release	m	0		0				
A	Minimum velocity (non-instantaneous and instantaneous)	m/s	0.01	100	0.1				
A	Maximum duration for a release	s	0	1.00E+08	3600				
	Termination criterion								
A	Absolute maximum distance for dispersion	m	1	1.00E+06	50000				
A	Absolute maximum height for dispersion	m	10	10000	1000				
A	Stop flag(1-Risk based, 2-Conc/Dist based, 3-Dist based, 4-Conc risk based)	-	1	2	2				
A	Minimum probability of death	-	0	1	0.001				
A	Toxic calculation flag (used for toxic-load calculations for mixtures only)		1	4	1				
A	User selected flammable/ toxic flag (1-flam,0-both,-1-toxic, -2 - inert)	-	-2	1	1				
A	Probit Methodology (1-Prefer Probit, 2-Prefer Dose, 3-Use Probit, 4-Use Dose		1	4	3				
	AMBIENT								
A	Wind profile flag (1-const,2-log)		1	2	2				
A	Cut-off height for power-law wind profile	m	0.1	1	1				
A	Atm.temperature/pressure profile (1-const,2-lin,3-log)		1	3	3				
A	Specific heat of dry air	J/kg/K	800	1200	1004				
A	Molecular weight of dry air	kg/kmol	10	100	28.9505				
A	Height of mixing layer for each stability class	m	0	5000	1300,1080,920,880,840,820,800,400,100,100				

(a) First part of UDM input parameters

Inputs	DNV MODEL UDM								
Input Index	Description	Units	Limits Lower	Limits Upper	Continuous	Instantaneous	Poolsource	Spill	Timevarying
	PARAMETERS (to be changed by expert users only)								
	PHYSICAL MODEL PARAMETERS								
	Source and expansion zone								
A	Expansion length \ source diameter	-	0.01	100	0.01				
A	Velocity multiplication factor for impinging releases	-	0	1	0.25				
A	Velocity cap for impinging releases	m/s	0	2000	500				
	Jet dispersion								
A	Jet entrainment coefficient ALPHA1	-	0.01	2	0.17				
A	Cross-wind entrainment coefficient ALPHA2	-	0.01	2	0.35				
A	Plume\air drag coefficient	-	0	1	0				
	Heavy dispersion								
A	Dense cloud side entrainment parameter GAMMA (continuous)	-	0	2	0				
A	Dense cloud side entrainment parameter GAMMA (instantaneous)	-	0	2	0.3				
A	Dense cloud spreading parameter CE (continuous)	-	0	2	1.15				
A	Dense cloud spreading parameter CE (instantaneous)	-	0	2	1.15				
	Passive dispersion								
A	near-field passive entrainment parameter		0.00	1.00	1.00				
A	Ratio of instantaneous \continuous sigma y	-	0.10	10.00	1.00				
A	Ratio of instantaneous \continuous sigma z	-	0.10	10.00	1.00				
	Liquid component (droplets/rainout/pool)								
A	Ratio drop to expansion velocity for instantaneous release	-	0	1	0.8				
A	Expansion energy for maximum droplet angle	J/m2	0	100000	690				
A	Pool vaporisation entrainment parameter	-	0	2	1.5				
A	Critical droplet diameter for rainout	m	1.00E-05	1	1.00E-05				
	TRANSITION CONTROL								
	Transition to passive								
A	Maximum cloud/ambient velocity difference, RU [|ucld/ua - 1|<RU]		0		0.1				
A	Maximum non-passive entrainment fraction, RE [1-Epas/Etot< RE]		0	1	0.3				
A	Maximum Richardson number RICR [Ri < RICR]		0		15				
A	Maximum cloud/ambient density difference, RR [rhocld/rhoa-1<RR]		0		0.015				
A	Distance multiple for phasing in full passive entrainment		0.00		2.00				
	Pool re-evaporation								
A	Cut-off for evaporation rate	kg/s	0	100	0.1				
	Other transitions (quasi-instantaneous, lift-off, rainout)								
A	Quasi-instantaneous transition parameter		0.1	10	0.8				
A	Richardson number for lift-off criterion			0	-20				
	POOL-MODEL PARAMETERS								
A	Solar radiation flux	W/m2	0	1200	500				
A	User defined thermal conductivity [used in pool model, only if user-defined bund s	W/m/K	0		2.21				
A	User defined minimum pool thickness	m	0.001	0.3	0.005				
A	User defined surface roughness factor	-	1	5	2.634				
A	User defined thermal diffusivity	m2/s	1.00E-08	1.00E-06	9.48E-07				
A	Bund overspill switch (0-Off, 1-On)		0	1	0				
	SPREADSHEET OUTPUT CONTROL								
	General output								
A	File output level (0 - none, 1 - commentary, 2 - plus cloud primaries, 3 - detailed, 4 - all)		0	4	1				
11	Component of interest				Default				
A	Mass (=1) or mole (=0) output for component of interest		0	1	0				
12	Maximum number of output steps reported	-	2	10000	1000				
	User-selected outputs								
	See doc for full list (4 = H_eff, 8 = W_eff, 10 = zc, 14 = M_cld, 5 = m, 17 = n, 19 = theta, 34 = rho_cld, 29 = rho_air, 30 = A_cld, 39 = V_cld, 1004 = M_d, 1005 = u_d, 1006 = D_d, 1007 = T_d, 2004 = M_diss, 2012 =D, 2014 = Q_net)								
A	User output 1		0		4				
A	User output 2		0		8				
A	User output 3		0		2012				
A	User output 4				19				
N	Cloud half-width of interest [1 - Weff (effective half-width), 2 - Hanna's definition, 3		1	3	1				
13	Number of output steps for AWD		2	1000	100				

(b) Second part of UDM input parameters

Figure 19. UDM input data - Part II: input parameters

This second part of the input data correspond to the values of the input parameters, which should be changed by expert users only

F.2 Model run and output data

Following initialisation of data, dispersion calculations are carried out. The output data are listed in Figure 20.

Outputs					Continuous	Instantaneous	Poolsource	Spill	Timevarying
Output Index	Description	Units							
	ERROR STATUS				*OK*	*WARN*	*OK*	*OK*	*WARN*
	Ambient Conditions								
A	Friction velocity	m/s			0.433358131	0.433358131	0.433358131	0.433358131	0.433358131
A	Exponent in the wind speed profile	-			0.17280417	0.17280417	0.17280417	0.17280417	0.17280417
A	Temperature at ground level	K			298	298	298	298	298
	Transitions								
A	Time to quasi-instantaneous transition	s			Undefined	Undefined	Undefined	Undefined	Undefined
A	Distance to quasi-instantaneous transition	m			Undefined	Undefined	Undefined	Undefined	Undefined
A	End time for instantaneous energetic expansion	s			Undefined	Undefined	Undefined	Undefined	Undefined
	Miscellaneous								
A	Droplet lag distance (instantaneous only)	m			Undefined	Undefined	Undefined	Undefined	Undefined
A	Rainout flag (0 - no rainout, 1 - rainout)				1	1	0	1	1
A	Bund status flag (0 - no bund, 1 - not hit, 2 - hit, 3 - overspilled)				0	0	0	0	0
	Raw Observer data								
43	Number of observers	-			0	0	0	0	0
3	Observer rainout fraction	fraction							
4	Distance to observer rainout	m							
5	Observer time (to a specified distance) or observer distance (to a specified time)	s or m							
6	Observer off-centreline concentration (at specified time or distance)	mole fraction							
	Dispersion data								
7	Number of output steps				415	353	60	259	445
	Independent variable								
8	Time from start of release	s							
	Observer data								
	Cloud position and speed								
9	Downwind distance or pool centre	m							
10	Centreline height	m							
11	Velocity	m/s							
	Mass and concentration								
12	Component mass (flowrate)	kg or kg/s							
13	Centre-line concentration - wind meander averaged - no FDC/AWD effects	mole fraction							
14	Liquid mass fraction	kg/kg							
15	Wet air entrainment rate	kg/s or kg/m/s							
	Profile and geometry								
16	Cloud cross-wind radius RADY - wind meander averaged - no FDC/AWD effects	m							
17	Cloud vertical radius RADZ	m							
	Cloud state								
18	Touchdown flag (1 - elevated, 2 - touching down, 3 - grounded, 10 - capped)								
19	Dispersion phase (1 - inst exp, 2 - jet, 3 - heavy, 4 - passive)								
20	Thermodynamics flag (-1 - no drop, 1 - equil drop, 2 - non-equil drop)								
21	Instantaneous/continuous flag (1 - instantaneous, 2 - continuous)								
22	Over pool? (0 - upwind pool or no pool, 1 - above pool, 2 - downwind of pool)								
	Thermodynamic properties								
23	Cloud vapour temperature	K							
	Droplets								
24	Droplet height	m							
	Pool data								
25	Spill rate	kg/s							
25	Pool mass	kg							
26	Pool radius	m							
28	Pool temperature	K							
27	Evaporated mass	kg							
28	Evaporation rate	kg/s							
	Optional outputs								
29	User output 1	various							
30	User output 2	various							
31	User output 3	various							
32	User output 4	various							
	Short duration results (FDC, AWD, time averaging for time dependent concentrations)								
33	Finite-duration concentration (FDC)	mole fraction							
34	AWD output times for concentration	s							
35	Pre-AWD off-centreline concentration at distance as a function of time	mole fraction							
36	AWD off-centreline concentration at distance as a function of time	mole fraction							
38	AWD output distances for concentration	m							
39	Pre-AWD off-centreline concentration at time as a function of distance	mole fraction							
40	AWD off-centreline concentration at time as a function of distance	mole fraction							
37	AWD output time or distance for off-centreline results	s or m							
41	Pre-AWD off-centreline result at time(distance) as a function of distance(time)	various							
42	AWD off-centreline result at time(distance) as a function of distance (time)	various							

Figure 20. UDM output data

The above output data are derived from the generic spreadsheet for the UDM. The values of the runs in columns correspond to the input values included in Figure 18 and Figure 19. Output data for the dispersion array data are not included in this figure.

AMBIENT CONDITIONS, TRANSITIONS, MISCELLANEOUS

These output data are related to:

- Ambient data (see Appendix A for details)
  - friction velocity u_* (m/s)
  - exponent p in vertical wind-speed power-law profile $u_a(z)$
  - ground-level temperature $T_a(z=0)$

- Transitions:
  - QI transition for continuous finite-duration releases: time (s) and downwind distance (m) to transition
  - End time of initial phase of instantaneous energetic expansion for pressurised instantaneous releases

- Miscellaneous
  - Droplet lag distance (instantaneous cases only)
  - Rainout flag (0 - no rainout, 1 – rainout)
  - Bund status flag (0 – no bund, 1 – not hit, 2 – hit, 3 – hit and overspilled)

RAW OBSERVER DATA

This includes scalar raw (non-interpolated) data for each observer i:

- Number of observers. This is the total number of observers, including both release observers and pool observers.
- Observer rainout data:
  - Observer rainout mass fraction η_{ro} (kg/kg)
  - Downwind distance x_{ro}^i to observer rainout (m)
- Optional output:
  - Observer time t to user-specified downwind distance x_{int}, or observer distance x to user-specified time t_{int}
  - Observer off-centreline concentration C (at y_{int}, z_{int}; at specified time t_{int} or distance x_{int})

DISPERSION DATA

1. Observer data. Data are reported successively for each observer. For each observer, dispersion data (Outputs 9 through 24) are reported as function of time (Output 8) with successive rows including data. A blank row is included between data of two successive observers. Of most interest are the following dispersion data: time t (8), downwind distance x (9), component mass m_c (12), and centreline concentration (13). A discontinuity will occur in observer data at the point of rainout. Further information on the observer data is as follows:
   1.1. *Time from start of release, t (s)*
   1.2. Cloud position and speed
      1.2.1. *Downwind distance, x (m)*
      1.2.2. *Centreline height, z_{cld} (m)*
      1.2.3. *Centroid velocity, u_{cld} (m*/s*);* for sufficiently elevated release the centroid height z_c will equal the centre-line height z_{cld} , but otherwise it will be higher than the centre-line height (see Section 3.1 for details on evaluation of the centroid height)
   1.3. Mass and concentration
      1.3.1. *Component mass, m_c (instantaneous, kg) or component flow rate (else, kg/s)*
      1.3.2. *Cloud centre-line molar (volume) concentration (mole fraction)*. This includes effects of time-averaging because of wind-meander, and excludes FDC/AWD effects and any other effects of time averaging.
      1.3.3. *Liquid mass fraction, η_{cL} (kg of liquid component / kg of total component)*

1.3.4. *Wet air entrainment rate [instantaneous dm_{wa}/dt (kg /s), or continuous dm_{wa}/ds, kg/s/m]*

1.4. Profile and geometry

1.4.1. *Cloud cross-wind radius R_y, m.* This includes effects of time-averaging because of wind-meander, and excludes FDC/AWD effects and any other effects of time averaging.

1.4.2. *Cloud vertical radius R_z, m*

1.5. Cloud state

1.5.1. *Touchdown flag*: 1 (elevated or lifted off), 2 (touching down or lifting off), 3 (grounded; centre-line height z_{cld}=0), 10 (capped)

1.5.2. *Dispersion phase:*1 (initial phase of pressurised instantaneous expansion), 2 (jet dispersion), 3 (heavy-gas dispersion), 4 (passive dispersion)

1.5.3. *Instantaneous / continuous flag*: 2 (continuous), 1 (instantaneous). The flag will change from 2 to 1 following a QI transition

1.5.4. *Over pool?* : 0 - upwind pool or no pool, 1 - above pool, 2 - downwind of pool

1.6. *Cloud vapour temperature, K*

1.7. *Droplet height, m*. It is noted that the downwind droplet distance does not match the observer downwind distance in case of a pressurised instantaneous release (lag)[lxviii].

2. Pool data. Data (Output 9, Output 25 through Output 28) are reported at successive times (Output 8). Of most interest are 'spill rate' (Output 25) and 'pool evaporation rate' (Output 28). Output 9 is the 'downwind distance of the pool centre'.

3. Optional outputs. These are additional four user-selected outputs as defined in the 'Spreadsheet output control' parameters.

4. Short duration results

4.1. FDC concentrations (Output 33) are only calculated for continuous releases without rainout, when the AWD modelling flag is set = 2.

4.2. The short duration results (other than FDC) combine observer results into a time-dependent representation of the cloud. They include 3 types of results:

4.2.1. Concentration at specified distance x_{int} as a function of time . Uses the specified required AWD output distance x_{int} (a user-supplied input) to calculate concentration at that distance as a function of time t:

4.2.1.1. *AWD output times*. The times at which the concentrations are reported. The start and end times are chosen by the model such that the concentration equals the user-specified concentration of interest c_{int} for height and width calculations.

4.2.1.2. *Pre-AWD off-centreline concentration at distance as a function of time.* Concentrations derived purely from interpolating observer concentrations. No AWD effects included.

4.2.1.3. *AWD off-centreline concentration at distance as a function of time*. AWD concentrations, based on Gaussian integration over distance of pre-AWD concentrations.

4.2.2. Concentration at specified time t_{int} as a function of distance. Uses the specified required AWD output time t_{int} (a user-supplied input) to calculate concentration at that time as a function of distance x.

4.2.2.1. *AWD output distances*. The distances at which the concentrations are reported. The upwind and downwind distances are chosen by the model such that the concentration equals the user-specified concentration of interest c_{int} for height and width calculations.

4.2.2.2. *Pre-AWD off-centreline concentration at time as a function of distance*. Concentrations derived purely from interpolating observer concentrations. No AWD effects included.

4.2.2.3. *AWD off-centreline concentration at time as a function of distance.* AWD concentrations, based on Gaussian integration over distance of pre-AWD concentrations.

4.2.3. Optional additional off-centreline result. Depending on the user-specified cloud output control flag, this either specifies the additional off-centreline result at either a specified distance x_{int} as a function of time, or at a specified time t_{int} as function of distance. The additional result can be width or height to concentration of interest c_{int}, maximum concentration, maximum width or dose.

4.2.3.1. *AWD output time or distance for off-centreline result*

4.2.3.2. *Pre-AWD off-centreline result at time(distance) as a function of distance(time)*

4.2.3.3. *AWD off-centreline result at time(distance) as a function of distance(time)*

F.3 Detailed information on UDM errors and warnings

Below information on errors/warnings/messages are given, which can currently be produced by the UDM model. Other errors and warnings can occur, but these are either self-explanatory or no general guidance can be given on correcting them.

Error messages

	UDM Errors (UDM Version 3)
UDM3 39	Initial dilution of the cloud is not allowed when using Hydrogen Fluoride thermodynamics The UDM is provided with an estimate for the initial dilution of the cloud for such discharge scenarios as vent from vapor spaces or in-building releases. The complex HF thermodynamics algorithm cannot handle the presence of an initial mass of air in the plume. As a result the UDM does not allow for HF releases that are in buildings.
UDM3 42	Pool sources and spills are not allowed when using Hydrogen Fluoride thermodynamics As for UDM3 39 above – pool source require initial dilution with air.
UDM3 122 UDM3 127	Unable to converge on consistent state for cloud Failed to calculate a convergent centroid height The UDM technical reference manual provides full details of the equations governing the calculation of the plume dimensions. These calculations are straightforward when the cloud is elevated or grounded, but involves an iterative technique during cloud touchdown due to the interdependence of the cloud vertical radius (R_Z) and the touchdown fraction parameter (h_d). Under extreme circumstances the iterative technique may not converge.
UDM3 164	Failed during solver step The solution has run into numerical problems. Often this is caused by low momentum, vertical or near vertical cases, in which case reducing the release angle (or increasing the release height) can be effective. Alternatively increasing the relative tolerance (2.1.1) to 0.01 (or even 0.1) can sometimes remove this error.
UDM3 160 UDM3 170	Illegal primary variable for the cloud Exception caught during call to IDASolve This usually indicates the model solver has failed unexpectedly. Try the approaches described for UDMA 164.
UDM3 180	Case has rained out but only for one observer. Rerun this case with more observers For non-instantaneous releases the model requires at least two observers to rain out, so that a spill term for the pool can be determined. If this error is encountered, try using more source observers, or use a continuous release
UDM3 187	Gravity spreading: incremental areas not matched The application of the gravity spreading correction (GSC) to this case has failed. Try re-running the case with GSC switched off. See Appendix D.

	UDM Warnings (model UDM3)
UDM3 1015	Cloud centre has hit the ground while liquid remains. Strongly consider running this case under pseudo-component logic MC cases cannot rainout, and furthermore are run using equilibrium thermodynamics (where droplet will evaporate quickly). This suggests that if liquid exists when the cloud centreline hits the ground, then in reality significant rainout could have occurred. It might be advisable in such cases to run under PC logic which will allow rainout.
UDM3 1107	Solid formation is likely, but not handled. Results will be inaccurate, and case may fail due to convergence or thermodynamic problems In the UDM version 6.54 there are no extensions to handle solid phase. The model has detected that solid effects are likely in this case, and therefore thermodynamic calculations (e.g. temperature and liquid fraction) will be inaccurate, as may other dependent cloud properties. Note that for mixtures this warning is never issued as there is no simple way to determine whether solid formation is likely
UDM3 1122 of 1124	Case has rained out but only for one observer. Pool calculations won't be carried out Non-instantaneous releases require at least 2 observers to rain out before an input to the pool model can be defined. If this occurs you can try rerunning the case with more observers
UDM3 1135	Minimum duration of <Time> applied for a continuous release. Release rate lowered to ensure mass conserved. Consider using a catastrophic rupture scenario. Dispersing observers can move relative to each other, and where these observers are initially close together this can magnify mass conservation problems.
UDM3 1136	Evaporated mass from the pool not accounted for is significant (<fraction> of the dispersing mass). Consider reducing the pool evaporation cut-off rate. Evaporated mass from the pool below the cut-off rate is not added back to the dispersing cloud. However in this case that mass is significant when compared to the mass in the cloud. Consider reducing the cut-off rate. Mainly this will be a problem for very small, flammable only releases where almost everything rains out.
UDM3 1139	Dispersion stopped at <Distance> downwind. Results beyond this should not be used, and far-field concentrations upwind of this may be under-estimated. Dispersion calculations have terminated early due to either maximum distance or height being exceeded. Far-field concentrations - especially beyond this distance - will be under-estimated. Try increasing the limits in dispersion parameters.
	Post-Processing Warnings (CVIEW)
CVIEW 1019	Finite Duration Correction selected but disabled for time varying releases and continuous releases with rainout, switching to AWD mode FDC can only be used for finite duration releases that do not rain out. AWD is now the preferred method and does not suffer from the same limitations as FDC.

Appendix G. SUNDIALS Differential-Algebraic Solver Licensing

The UDM dispersion equations are solved using the package IDA, part of the Sundials[10] suite of solvers developed at Lawrence Livermore National Laboratory.

Copyright (c) 2002, The Regents of the University of California.
Produced at the Lawrence Livermore National Laboratory.
Written by S.D. Cohen, A.C. Hindmarsh, R. Serban, D. Shumaker, and A.G. Taylor.

UCRL-CODE-155951 (CVODE)
UCRL-CODE-155950 (CVODES)
UCRL-CODE-155952 (IDA)
UCRL-CODE-155953 (KINSOL)

All rights reserved.

This file is part of SUNDIALS.

Redistribution and use in source and binary forms, with or without modification, are permitted provided that the following conditions are met:

1. Redistributions of source code must retain the above copyright notice, this list of conditions and the disclaimer below.

2. Redistributions in binary form must reproduce the above copyright notice, this list of conditions and the disclaimer (as noted below) in the documentation and/or other materials provided with the distribution.

3. Neither the name of the UC/LLNL nor the names of its contributors may be used to endorse or promote products derived from this software without specific prior written permission.

THIS SOFTWARE IS PROVIDED BY THE COPYRIGHT HOLDERS AND CONTRIBUTORS "AS IS" AND ANY EXPRESS OR IMPLIED WARRANTIES, INCLUDING, BUT NOT LIMITED TO, THE IMPLIED WARRANTIES OF MERCHANTABILITY AND FITNESS FOR A PARTICULAR PURPOSE ARE DISCLAIMED. IN NO EVENT SHALL THE REGENTS OF THE UNIVERSITY OF CALIFORNIA, THE U.S. DEPARTMENT OF ENERGY OR CONTRIBUTORS BE LIABLE FOR ANY DIRECT, INDIRECT, INCIDENTAL, SPECIAL, EXEMPLARY, OR CONSEQUENTIAL DAMAGES (INCLUDING, BUT NOT LIMITED TO, PROCUREMENT OF SUBSTITUTE GOODS OR SERVICES; LOSS OF USE, DATA, OR PROFITS; OR BUSINESS INTERRUPTION) HOWEVER CAUSED AND ON ANY THEORY OF LIABILITY, WHETHER IN CONTRACT, STRICT LIABILITY, OR TORT (INCLUDING NEGLIGENCE OR OTHERWISE) ARISING. IN ANY WAY OUT OF THE USE OF THIS SOFTWARE, EVEN IF ADVISED OF THE POSSIBILITY OF SUCH DAMAGE.

FIGURES

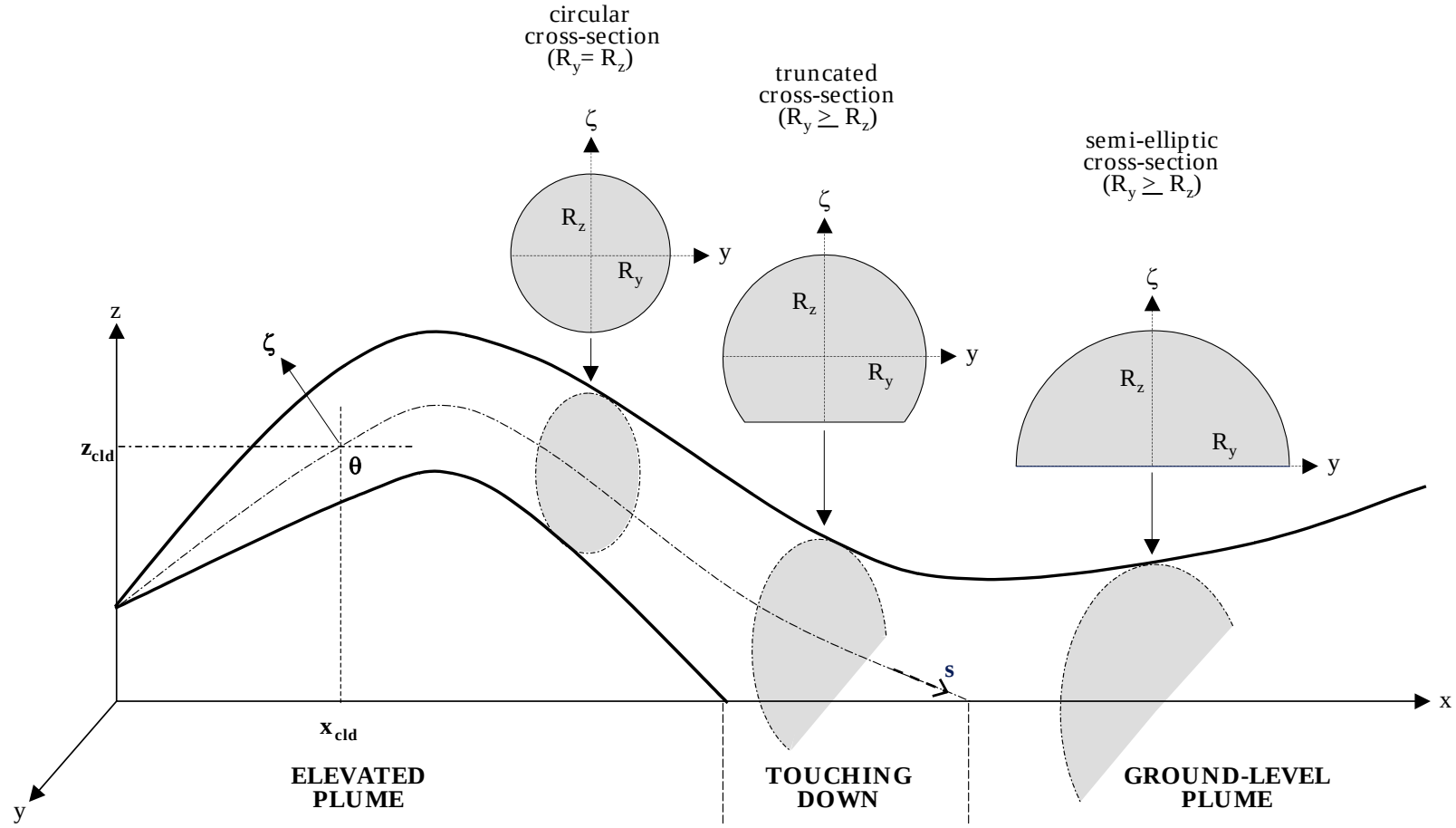

Figure 21. UDM plume geometry for continuous release (notation, stages of dispersion)

Cartesian co-ordinates [horizontal, cross-wind, vertical distances x,y,z] and plume co-ordinates [plume arclength s, perpendicular distance ζ to plume centre-line]
Plume position: centre-line height $z=z_{cld}(s)$ of plume and angle $\theta=\theta(s)$ to horizontal plane [$z = z_{cld} + \zeta \cos\theta$]
Plume cross-section: $(y/R_y)^m+(\zeta/R_z)^n=1$ with cross-wind radius $R_y=R_y(s)$ and ζ-radius $R_z=R_z(s)$
circular during jet dispersion, truncated circle during touching down, semi-elliptical during ground-level dense and passive dispersion

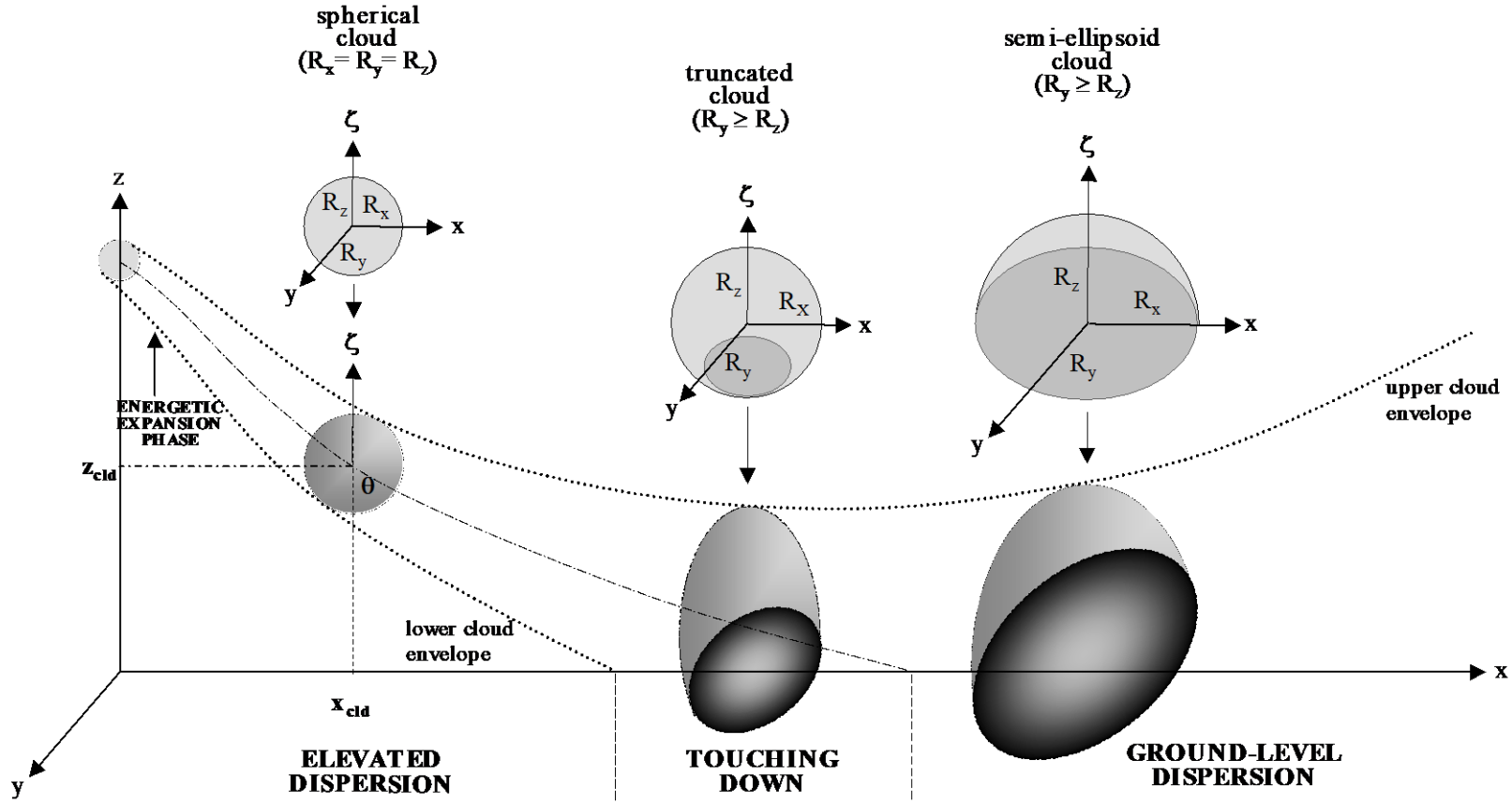

Figure 22. UDM cloud geometry for instantaneous release (notation, stages of dispersion)

Cartesian co-ordinates [horizontal, cross-wind, vertical distances x,y,z] and plume co-ordinates [plume arclength s, vertical distance ζ to cloud centre-line]

Cloud position: height z_{cld}= z_{cld} (s) of cloud centre and angle θ=θ(s) to horizontal plane [z = z_{cld} +ζ]

Cloud profile { $[(x/R_x)^2+(y/R_y)^2]^{m/2}$ +$(\zeta/R_z)^n$=1 with down-wind, cross-wind and vertical radii R_x=R_y(s), R_y=R_y(s) and R_z=R_z(s)

Cloud shape at core averaging time t_{av}^{core} (R_x=R_y is assumed): spherical during jet dispersion, truncation by ground during touching down, semi-ellipsoid during ground-level dense and passive dispersion. After onset of touching down, the cloud ground surface area is circular.

Increasing averaging time increases effects of wind meander. This leads to increasing R_y downwind of passive transition [more wide (elliptic) cloud].

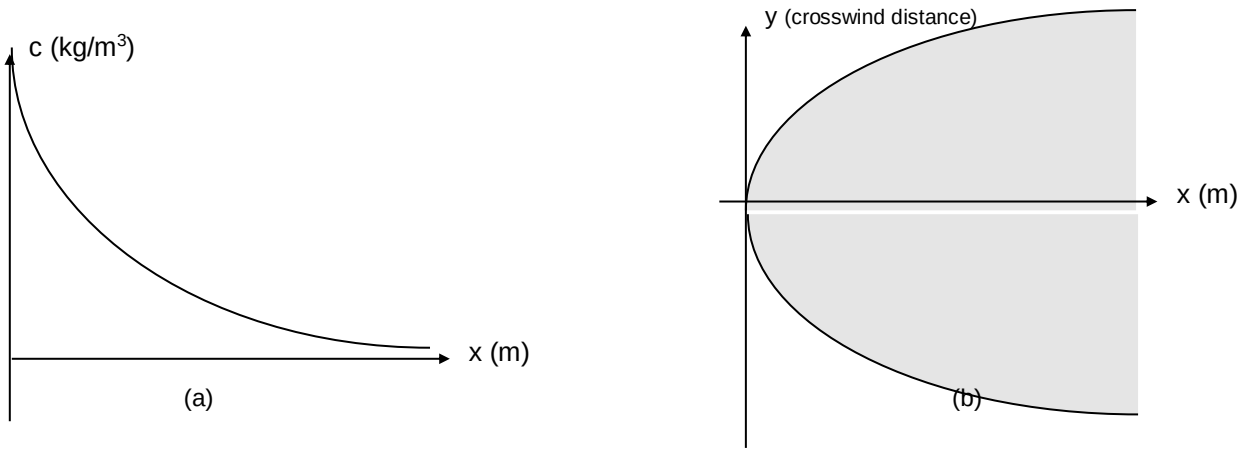

Figure 23. **Steady-state source**
Source assumed to be located at ground level at x=0; (a) centre-line ground-level concentration, (b) cloud foot print as function of downwind distance x

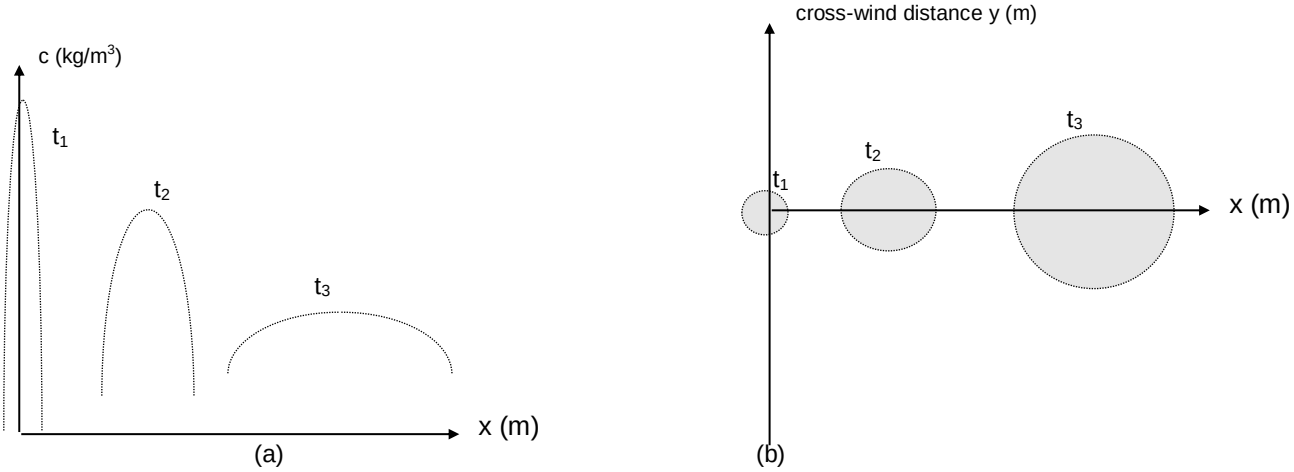

Figure 24. **Instantaneous source**
Source assumed to be present at ground level at x=0; location of UDM cloud at successive times t_1, t_2, t_3; (a) centre-line ground-level concentration c, (b)cloud foot print (circular) as function of downwind distance x

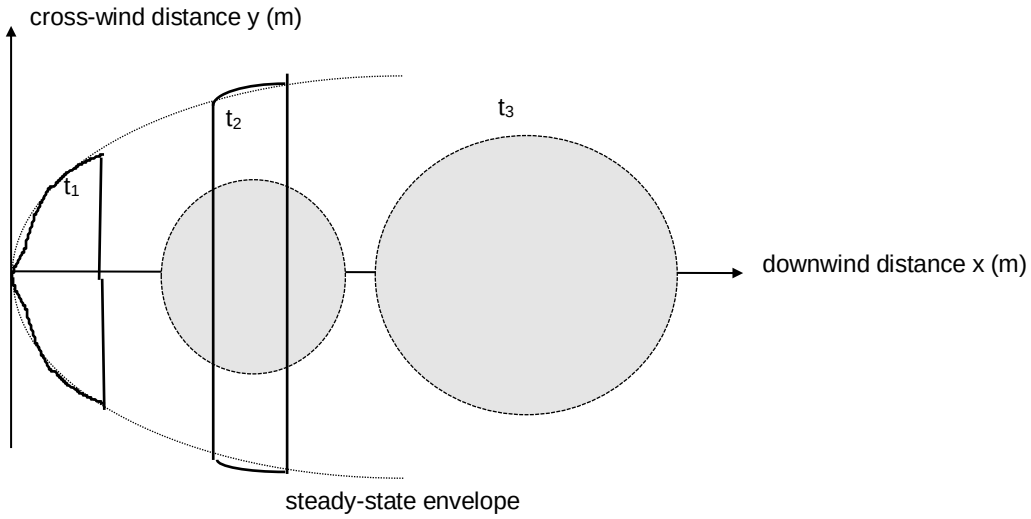

(a) Quasi-instantaneous model
[replace steady plume with circular instantaneous cloud, if width/length ratio becomes large]

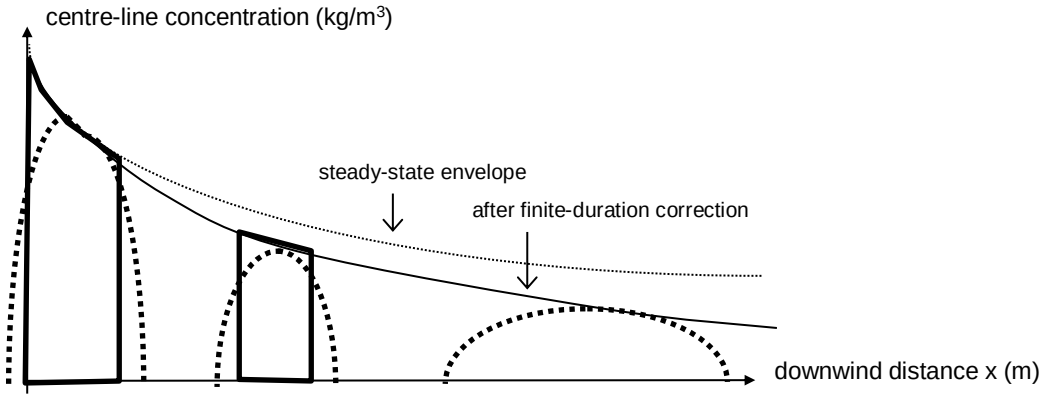

(b) Finite-duration correction
[adjustment to steady-state centre-line ground-level concentration]

Figure 25 **UDM models for finite-duration release**
Source assumed to be present at ground level at x=0; location of UDM cloud at successive times t_1, t_2, t_3

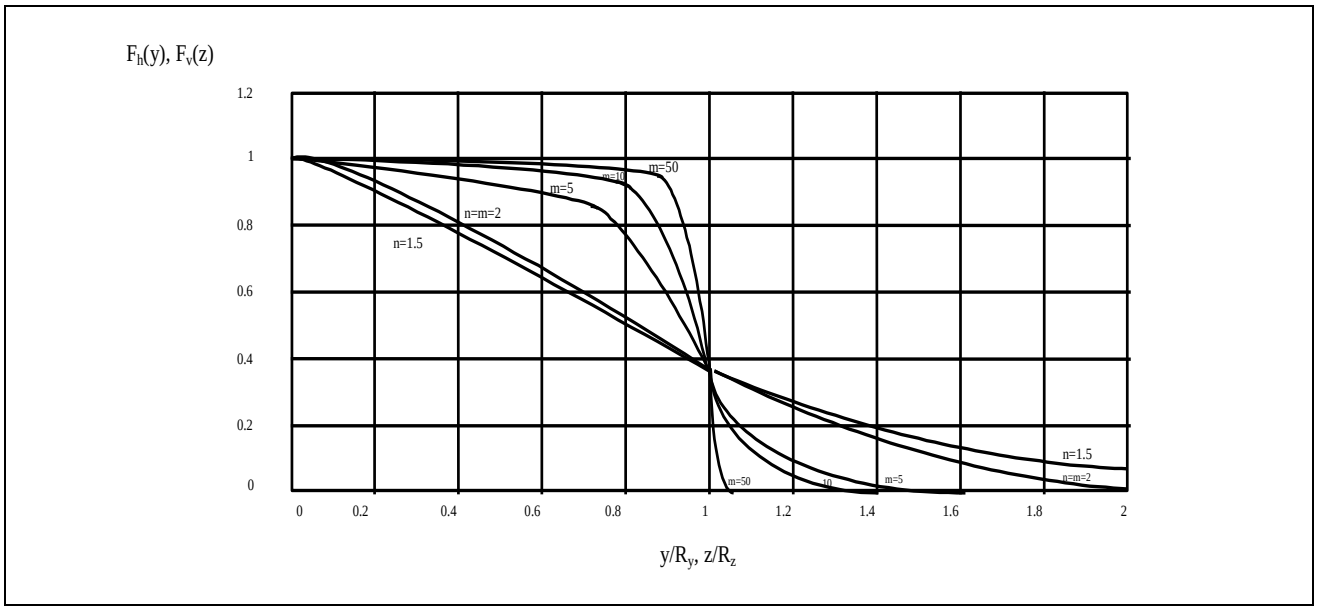

Figure 26. Vertical and horizontal concentration profiles

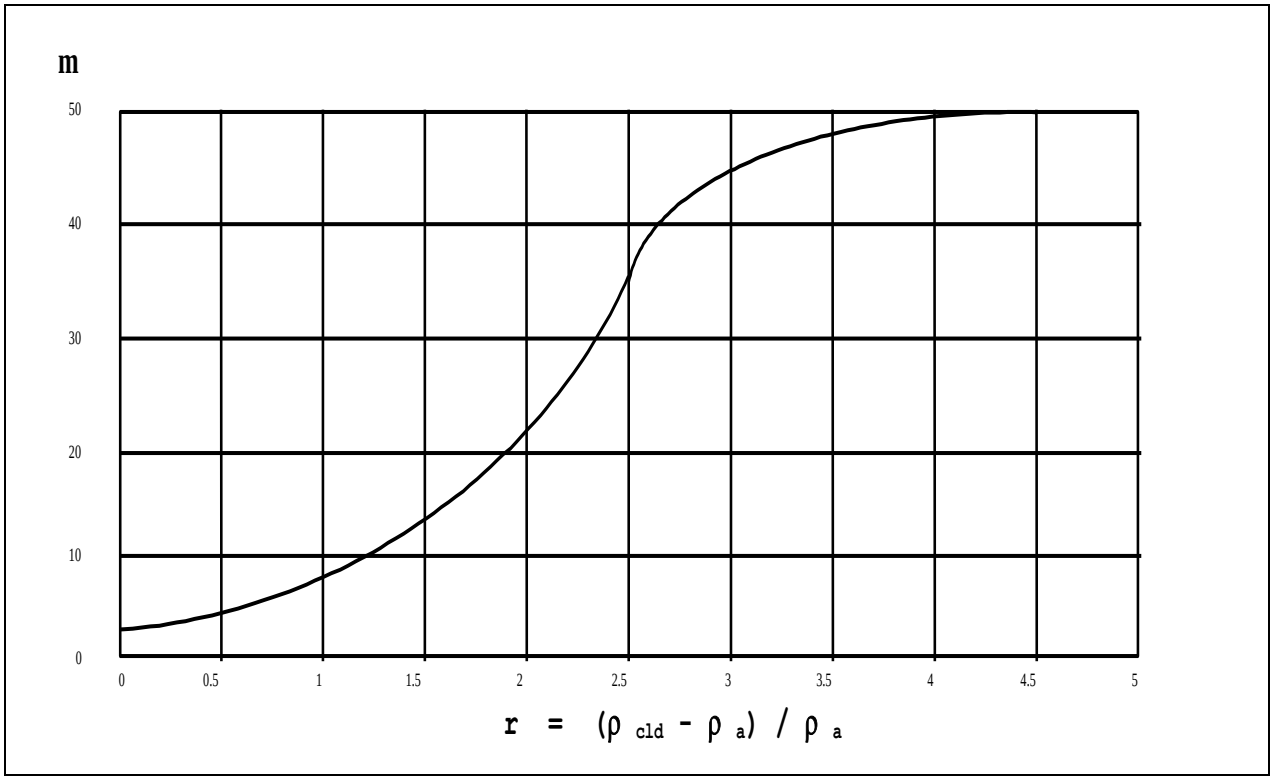

Figure 27. Correlation for the exponent m used in the horizontal profile

The adopted correlation is: $m = 2.0 + \left[\frac{12.0\, r}{\frac{2}{r} + 0.25\, r - 0.5} \right]$, *with* $r = \frac{\rho_{cld} - \rho_a}{\rho_a}$

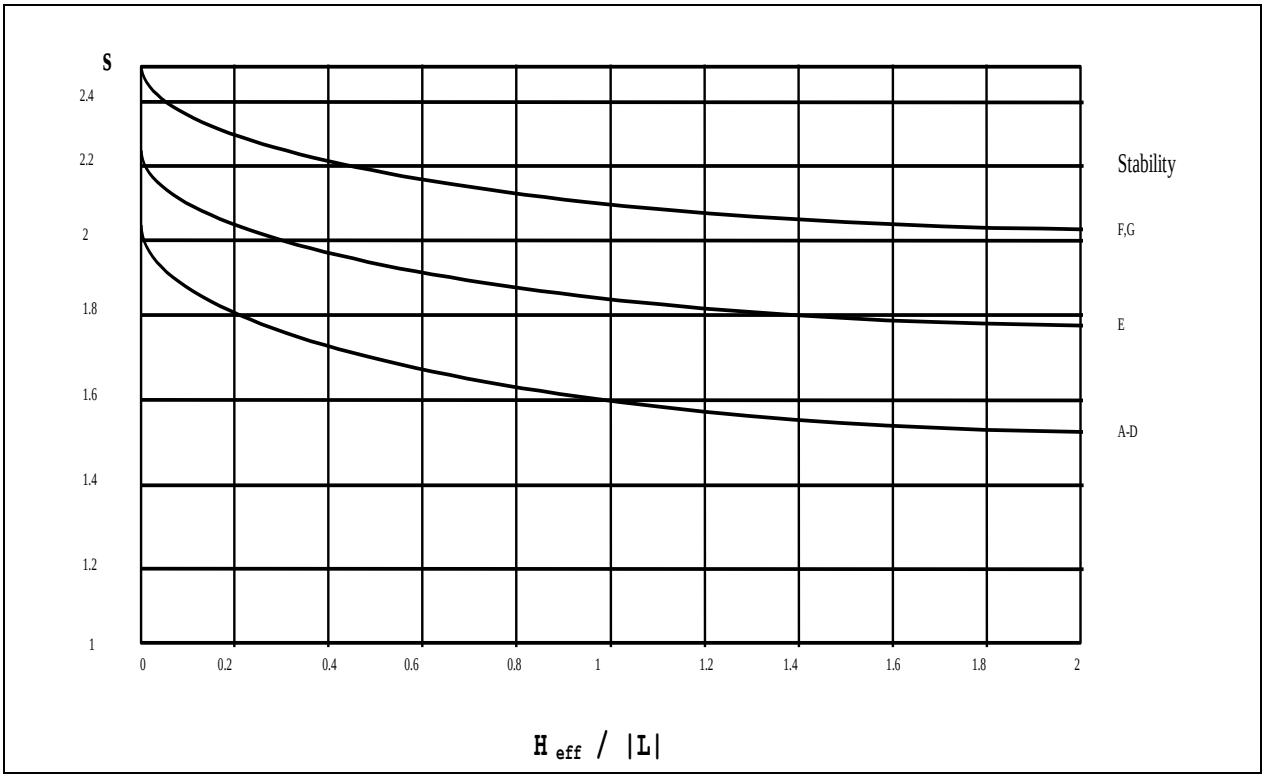

Figure 28. **Correlation for the exponent n used in the vertical profile**

The adopted correlation is: $$n = Max\left[n_{base} - \frac{4.5\frac{H_{eff}}{L}}{1.0 + 9.0\frac{H_{eff}}{L}}, 1.0 \right]$$

where n_{base} = 2 for stability classes A-D, 2.25 for stability class E, and 2.5 for F,G.

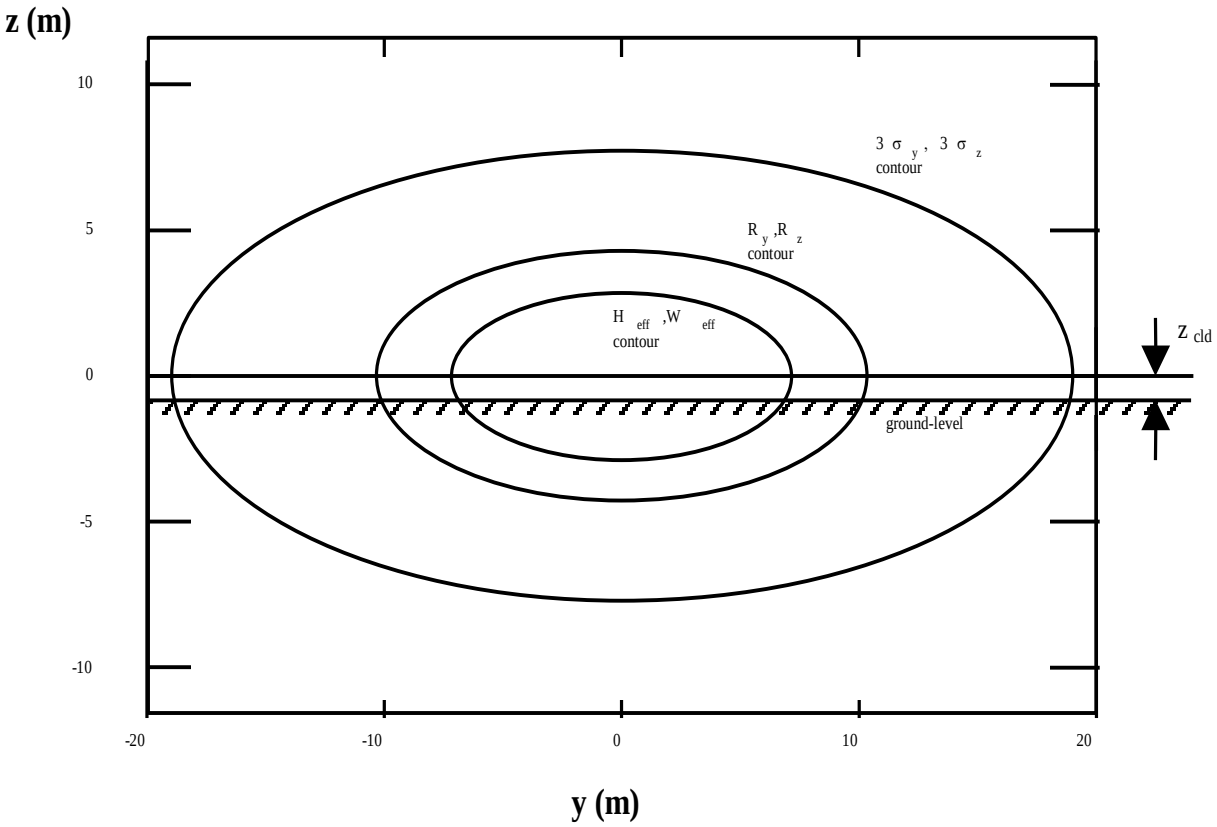

Figure 29. Cloud profile during touching down

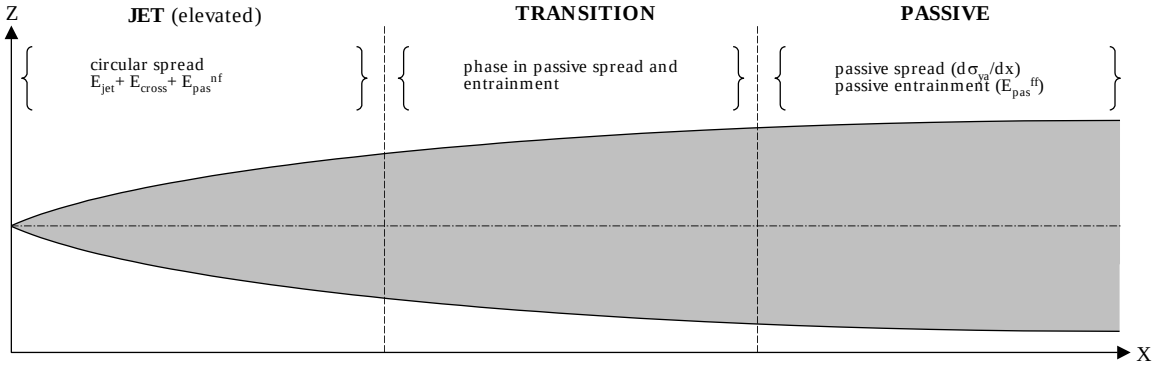

(a) elevated jet/plume (no touching down, no capping)

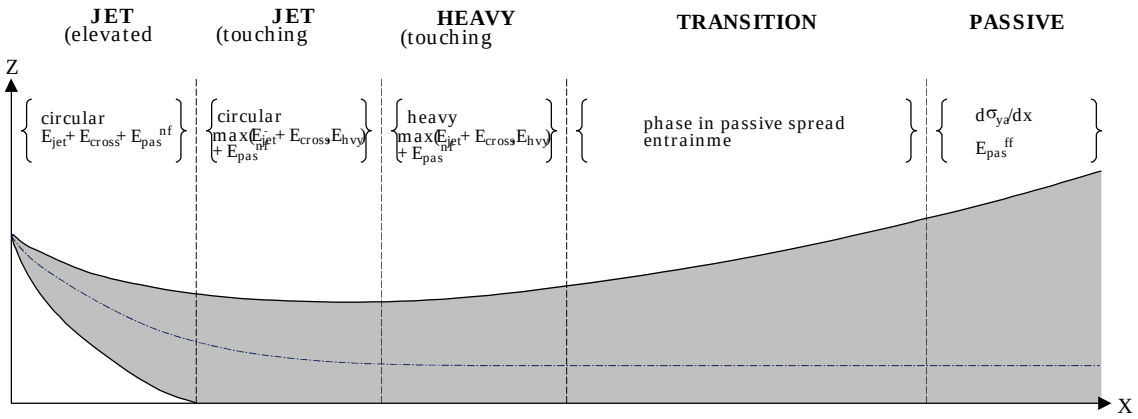

(b) jet/plume becomes passive during touching

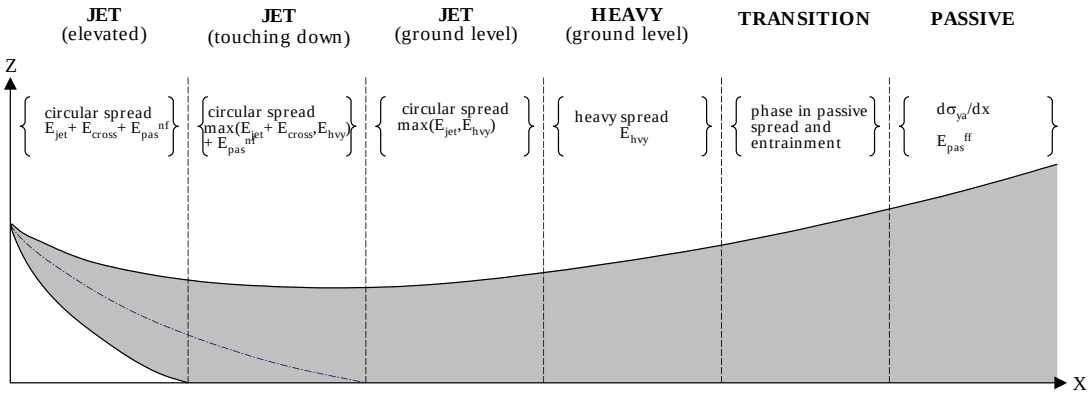

(c) jet/plume become passive after touch down

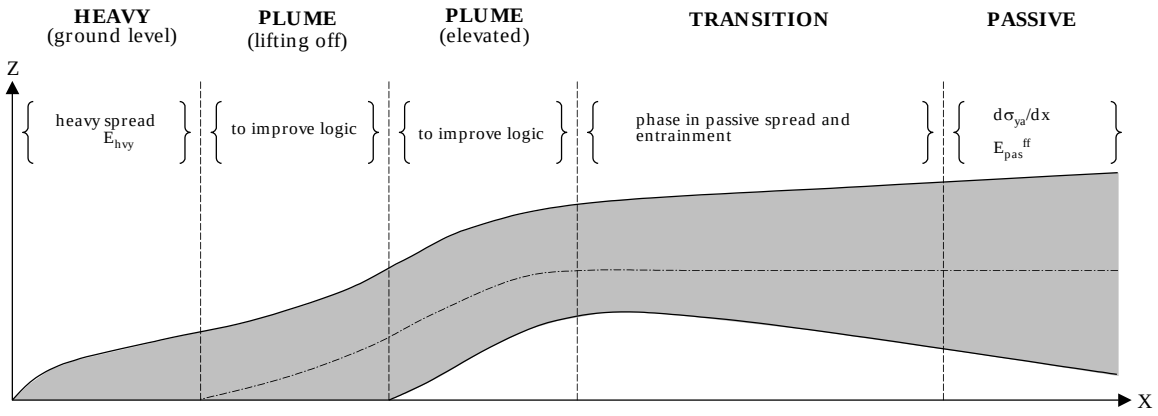

(d) ground level plume lifts off

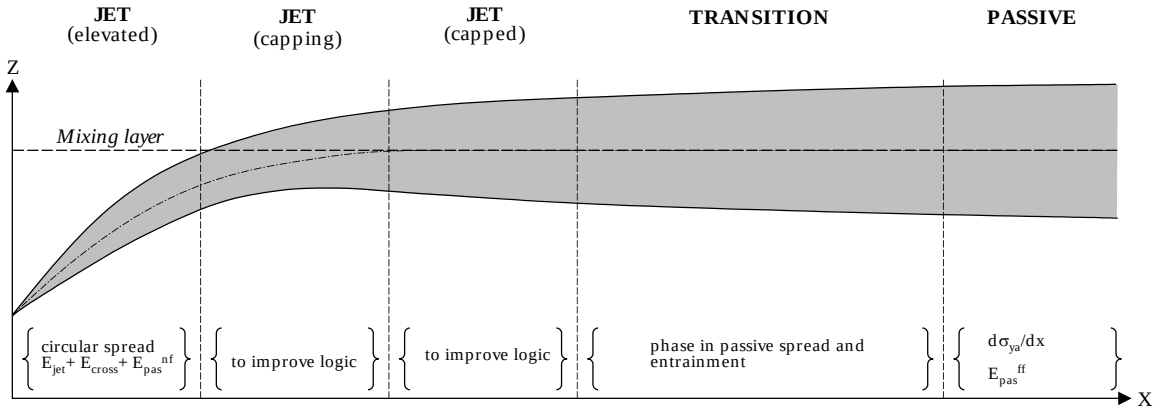

(e) jet/plume hits mixing layer

Figure 30. **Phases in UDM cloud dispersion for range of scenarios**
Figures include scenarios: (a) no touching down, (b) touching down only, (c) full touchdown, (d) lift-off, (e) capping by mixing layer. The figures indicate for each phase the type of spreading (circular jet, heavy or passive) and the mechanism of entrainment (E_{jet} = jet; E_{cross} = cross-wind; E_{pas}^{nf} = near-field elevated passive , E_{hvy} = ground-level heavy, E_{pas}^{ff} = far-field passive). Along the transition zone the near-field spread/entrainment are phased out and the far-field spread/entrainment are phased in.

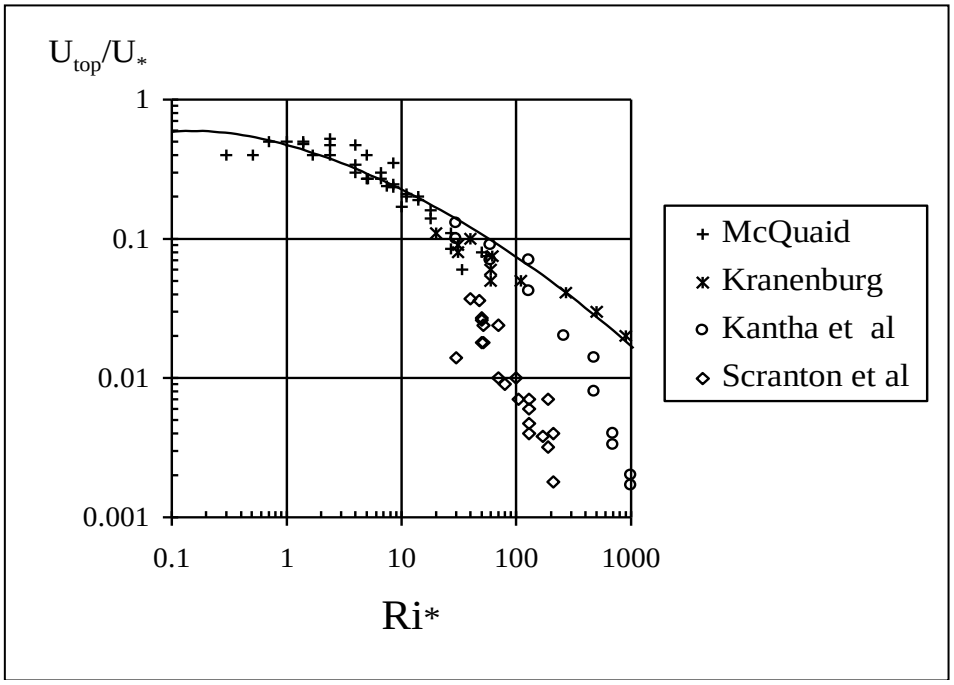

(a) old UDM 5.2 fit to experimental data;
data by McQuaid (1976)[44] and Kranenburg (1976)[45]obtained using a straight water channel; data by Kantha et al. (1977)[47] and Scranton and Lindberg (1983) [46] obtained using an annular water channel

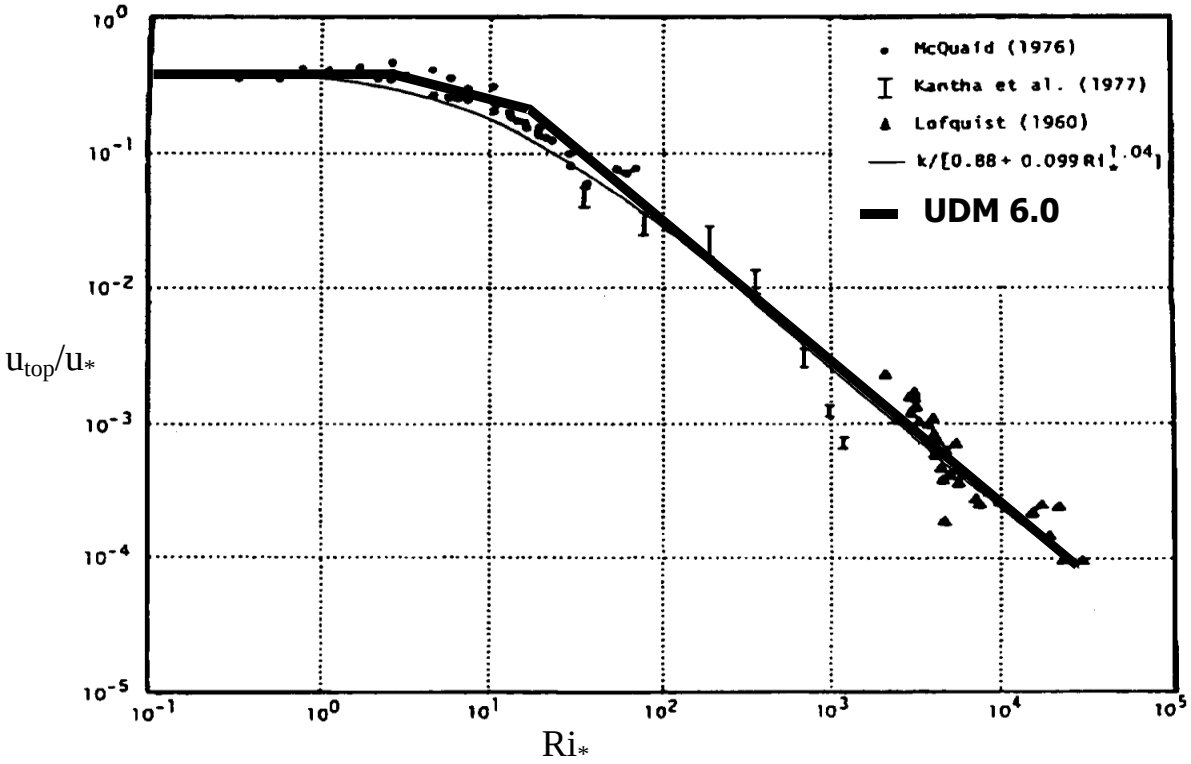

(b) new UDM 6.0 fit
data McQuaid (1976)[44], Kantha et al. (1977)[47] and Lofquist (1960)[50]. The figure also includes the DEGADIS fit $u_{top}/u_* = 0.4/(0.88 + 0.099\ Ri_*^{1.04})$

Figure 31. Normalised entrainment velocities
[The figure plots the normalised entrainment velocity u_{top}/u_* against the Richardson number Ri_*]

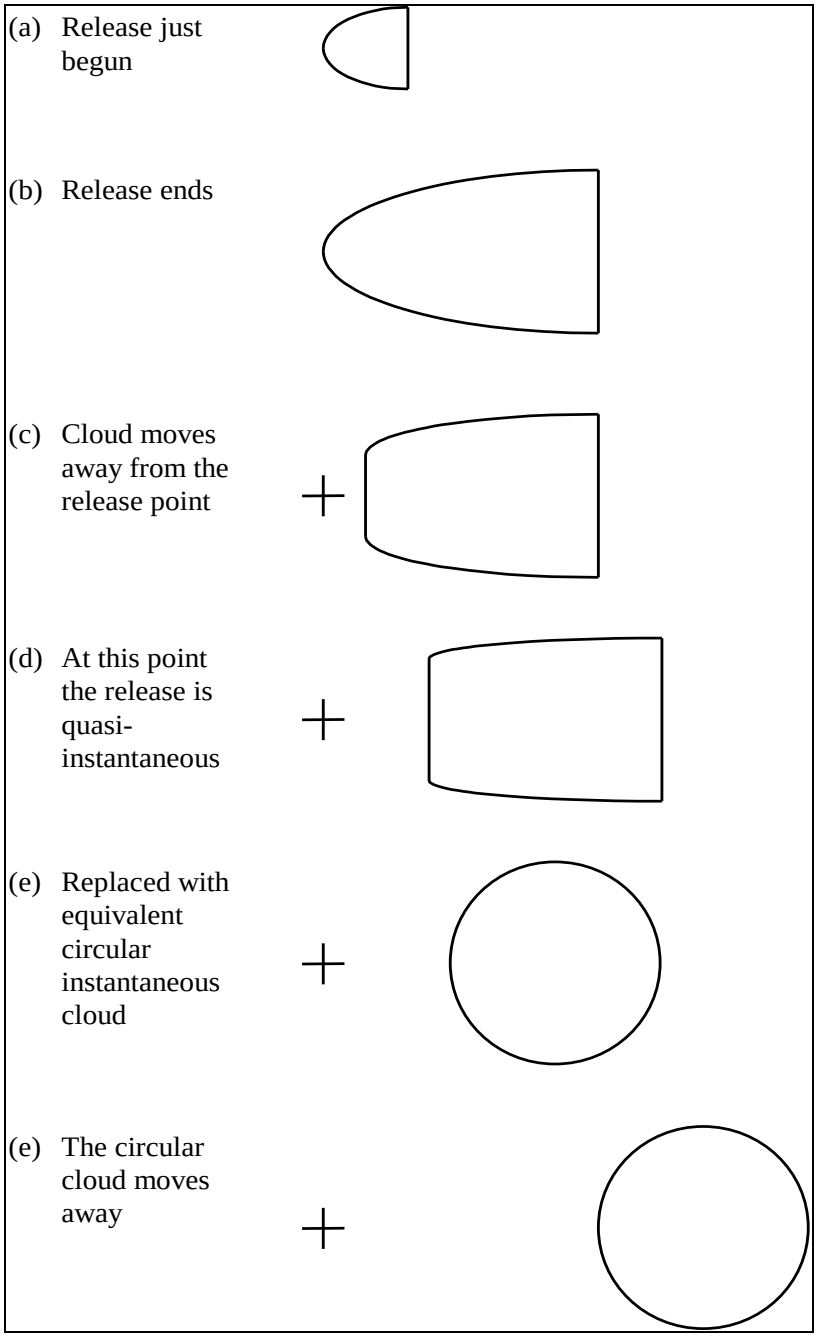

Figure 32. The development of a quasi-instantaneous release

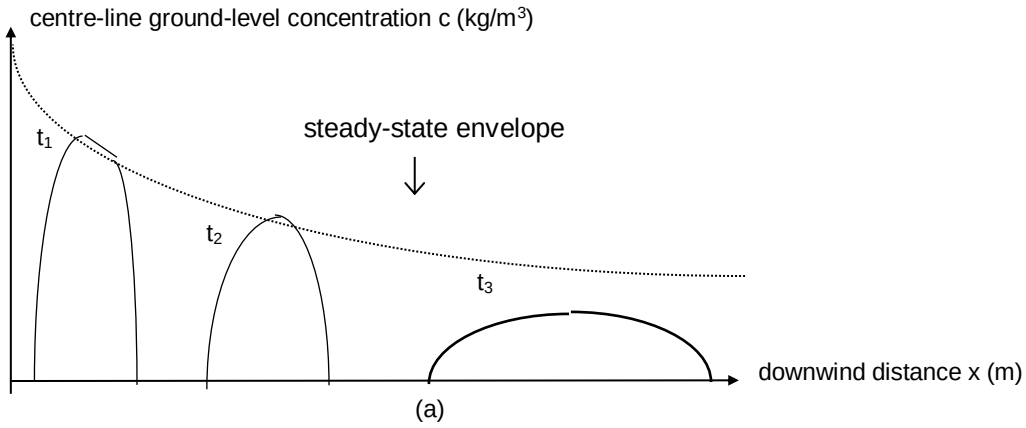

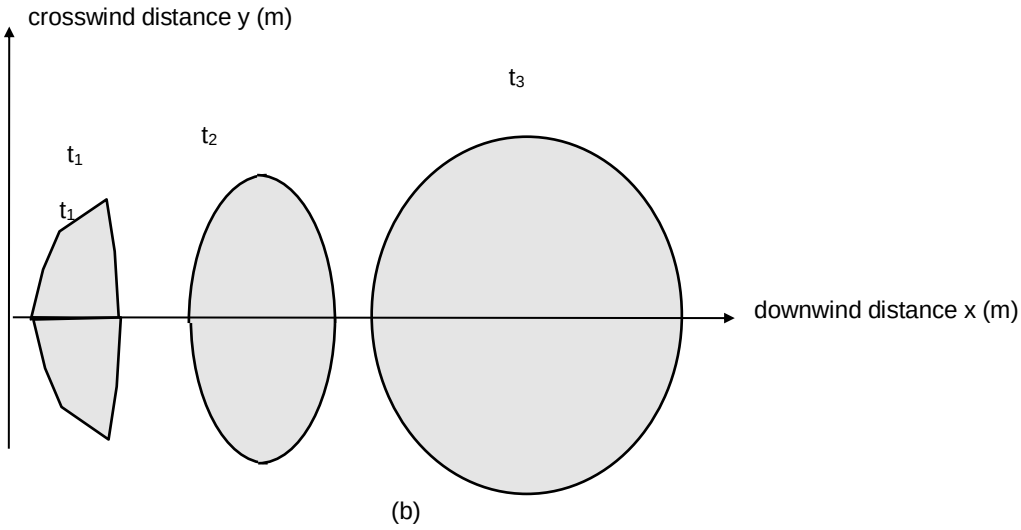

Figure 33. **Finite-duration source**
Source is assumed to be to be present at ground level at x=0); location of cloud at successive times t_1, t_2, t_3; (a) centre-line ground-level concentration c, (b) cloud foot print as function of downwind distance x

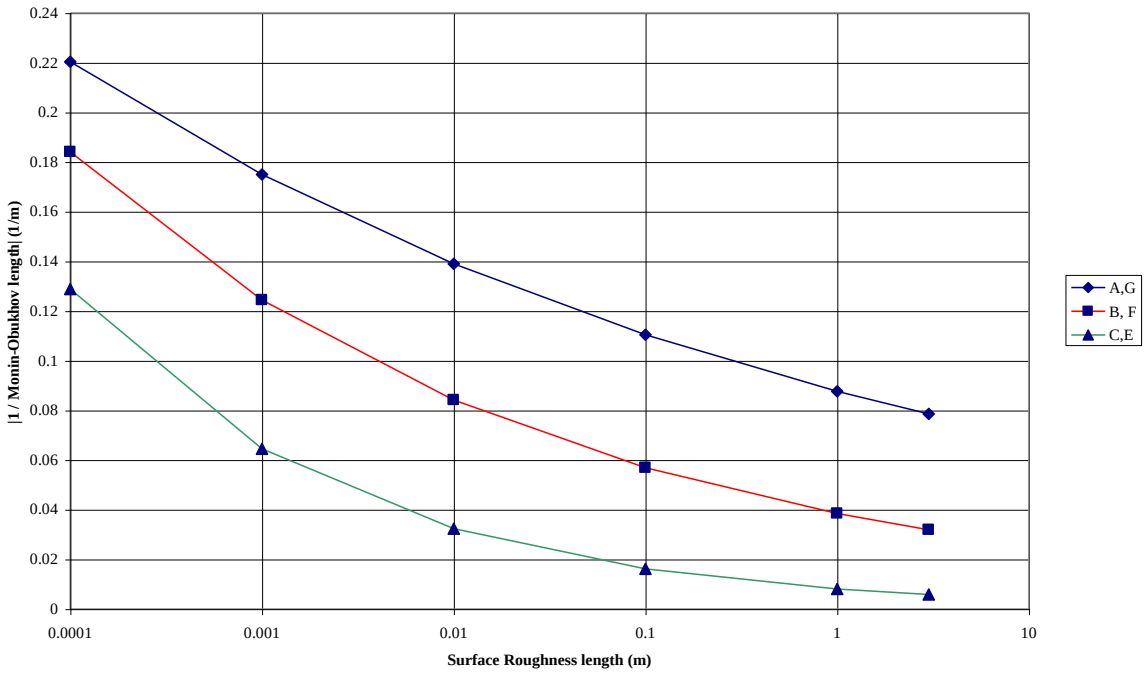

Figure 34. Monin-Obukhov length

The figure plots the modulus of the inverse of the Monin-Obukhov Length as a function of surface roughness length for the different stability classes. The Monin-Obukhov length is negative for stability classes A to C, and positive for stability classes E to G (see section A.1 for further details).

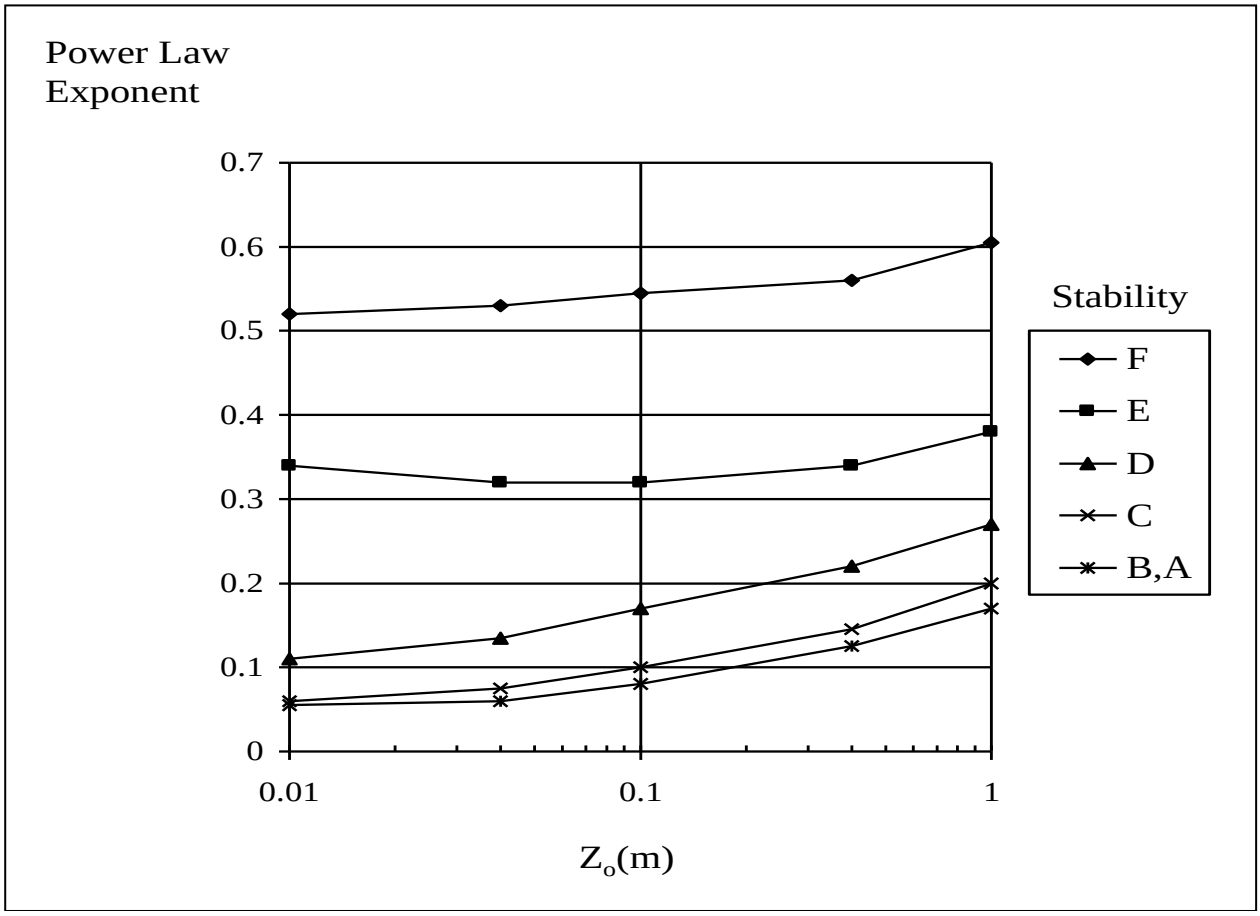

Figure 35. Wind power-law exponent

The figure plots the average exponent in the wind power law from 10 to 100m as a function of surface roughness length and stability class. The curves are from Irwin (1979)[89].

NOMENCLATURE

A_{cld}	cross sectional area of continuous cloud, m^2
A_{side}	effective side area of instantaneous plume, m^2
A_{top}	effective top area of instantaneous plume, m^2
c	concentration, kg of component /m^3
c_o	centre-line concentration, kg of component / m^3
C_{Da}	drag coefficient of plume in air (-)
C_E	parameter in gravity-spreading law (-)
C_p^{cld}	vapour heat capacity of cloud mixture, J/kg/K
C_m	conversion factor between cloud half-widths, $C_m = W_{eff}/R_y$
C_n	conversion factor between cloud half-depths, $C_n = H_{eff}/R_z$
D_{ac}	diffusivity of the released material (component) into the surrounding air, m^2/s
E_{cross}	cross-wind entrainment rate, kg/s or kg/m/s
E_{hvy}	dense gas entrainment rate, kg/s or kg/m/s
E_{jet}	jet (high-momentum) entrainment rate, kg/s or kg/m/s
E_{pas}^{nf}	near-field passive dispersion entrainment rate, kg/s or kg/m/s
E_{pas}^{ff}	far-field passive dispersion entrainment rate, kg/s or kg/m/s
E_{tot}	total dispersion entrainment rate, kg/s or kg/m/s
F_{drag}^{air}	airborne drag force, N/m or N
F_{drag}^{ground}	ground drag force, N/m or N
$F_h(x)$	horizontal distribution function for concentration (-)
$F_v(\zeta)$	vertical distribution function for concentration (-)
g	gravitational acceleration m/s^2
h_d	fraction of bottom half of cloud which is above ground (-)
H_{eff}	effective height of cloud after full touchdown, m [height prior to full touchdown = $H_{eff}(1+h_d)$]
I	plume momentum [$I=m_{cld}\,u_{cld}=(I_x^2 + I_z^2)^{1/2}$], kg m/s or kg/m/$s^2$
I_{x2}	downwind horizontal plume momentum in excess to ambient momentum [$I_{x2}= I_x - m_{cld}u_a$], kg m/s or kg/m/s^2
I_x	downwind component of plume momentum [$I_x= m_{cld}u_x$], kg m/s or kg/m/s^2
I_z	vertical component of plume momentum, kg m/s or kg/m/s^2
L	Monin-Obukhov length, m
m	exponent of horizontal distribution function for concentration (-)
m_c	component released mass (instantaneous release, kg) or mass rate continuous release, kg/s)

m_{cld}	mass in plume (instantaneous release, kg) or mass rate in plume (continuous release, kg/s)
m_{wv}^{gnd}	water-vapour added from the substrate, kg or kg/s
n	exponent of vertical distribution function for concentration (-)
p	exponent in power-law for wind-speed profile
P_a	atmospheric pressure, Pa
P_{abov}	perimeter length of jet, m
$P_v^{\alpha}(T)$	saturated vapour pressure as function of temperature T (K) for compound α, Pa [α = c (released component), w (water)]
q_{gnd}	heat transfer rate from ground to cloud, J or J/s
R_y	term in cross-wind concentration profile, m [$R_y = R_y(x) = 2^{1/2}\sigma_y(x)$]
R_z	term in vertical concentration profile, m [$R_z = R_z(x)\ 2^{1/2}\sigma_z(x)$]
Ri_*	layer Richardson number, (-)
s	arclength along centre-line of the plume, m
S_{gnd}	footprint area for instantaneous plume, m^2
t	time since onset of release, s
t_{av}	averaging time, s
t_{av}^{core}	averaging time for which UDM core calculations are being carried out, s
T_a	ambient temperature, K
T_{gnd}	substrate temperature, K
T_{vap}	temperature of vapour phase of the cloud, K
u_*	friction velocity for cloud, m/s
u_a	ambient wind-speed, $u_a = u_a(z)$, m/s
u_{cld}	total cloud speed, m/s
u_{ref}	value of ambient windspeed u_a at reference height $z = z_{ref}$, m/s
u_{side}	entrainment velocity through sides of plume, m/s
u_{top}	entrainment velocity through top of plume, m/s
u_x, u_z	horizontal and vertical component of cloud speed u_{cld}, m/s
V_{cld}	volume of cloud, m^3
W_{eff}	effective half width of plume, m
W_{gnd}	footprint half-width for continuous plume, m
x	horizontal downwind distance, m
x_{cld}	horizontal downwind position of center of cloud, m
y	crosswind distance, m

z vertical height above ground, m

z_o surface roughness length, m

z_c height above ground of cloud centroid, m

z_{cld} height abouve ground of cloud centre-line, m

z_R release height above ground, m

z_{ref} reference height above ground, m

Greek letters

α_1, α_2 'jet' and cross-wind entrainment coefficients (-)

γ heavy-gas side-entrainment coefficient (-)

η_{cL} liquid mass fraction of released component in the cloud

Γ Gamma function (-)

θ angle to horizontal of plume, rad; $\theta = 0$ corresponds to a horizontal plume (in downwind x-direction), while $\theta = \pi/2$ corresponds to a vertical upwards plume (in z-direction)

ζ distance from plume centre-line, m

κ Von Karman constant, $\kappa = 0.4$ (-)

μ_{ac} dynamic vapour viscosity of material in air, kg/m/s

ρ_{cld} density of plume, kg/m^3

ρ_a density of ambient air, kg/m^3

σ_y standard deviation of horizontal profile of cloud concentration, m

σ_z standard deviation of vertical profile of cloud concentration, m

σ_{ya} standard empirical correlation for passive crosswind dispersion coefficient, m
[used to calculate σ_y in passive regime]

σ_{za} standard empirical correlation for vertical crosswind dispersion coefficient, m
[used to calculate σ_z in passive regime]

About DNV

We are the independent expert in risk management and quality assurance. Driven by our purpose, to safeguard life, property and the environment, we empower our customers and their stakeholders with facts and reliable insights so that critical decisions can be made with confidence. As a trusted voice for many of the world's most successful organizations, we use our knowledge to advance safety and performance, set industry benchmarks, and inspire and invent solutions to tackle global transformations.

Digital Solutions

DNV is a world-leading provider of digital solutions and software applications with focus on the energy, maritime and healthcare markets. Our solutions are used worldwide to manage risk and performance for wind turbines, electric grids, pipelines, processing plants, offshore structures, ships, and more. Supported by our domain knowledge and Veracity assurance platform, we enable companies to digitize and manage business critical activities in a sustainable, cost-efficient, safe and secure way.

DNV | digital@dnv.com | dnv.com/digital

REFERENCES

[1] Johnson, D.W., "Prediction of aerosol formation from the releaes of pressurised, superheated liquids to the atmosphere", Intern. Proc. Int. Conf. and Workshop on Modelling and Mitigating the Consequences of Accidental Releases of Hazardous Materials, May 20-24, Fairmont Hotel, New Orleans, Louisiana, AIChE/CCPS, pp. 1-34 (1991)
[2] Woodward, J.L, and Papadourakis, A., "Reassessment and reevaluation of rainout and drop size correlation for an aerosol jet", Journal of hazardous materials 44, pp. 209-230 (1995)
[3] Woodward, J.L., "Aerosol drop size correlation and corrected rainout data using models of drop evaporation", International Conference and workshop on modelling and mitigating the accidental releases of hazardous materials, AIChE, CCPS, New Orleans, LA, September 26-29, pp. 117-148 (1995)
[4] Woodward, J.L, Cook, J., and Papadourakis, A., "Modelling and validation of a dispersing aerosol jet", Journal of hazardous materials 44, pp. 185-207 (1995)
[5] Cook, J. and Woodward, J.L., "Further development of the Unified Dispersion Model", Symposium on Loss prevention in the Process Industry, Brussels, Belgium (1995)
[6] Woodward, J.L. and Cook, J., "Modelling of dispersion with seamless transitions in entrainment mechanism, edge profile and touchdown with the Unifed Dispersion Model", AIChE meeting, Seattle, WA, August 14-19 (1993)
[7] Cook, J. and Woodward, J.L., "A new unified model for jet, dense, passive and buoyant dispersion including droplet evaporation and pool modelling", International Conference and Exhibition on Safety, Health and loss prevention in the Oil, Chemical and Process Industries, Singapore, February 15-19 (1993)
[8] Witlox, H.W.M. and Harper, M., "Two-phase jet releases, droplet dispersion and rainout, I. Overview and model validation", Journal of Loss Prevention in the Process Industries 26 (3), pp. 453-461 (2013)
[9] "UDM pool evaporation/spreading model (PVAP)" and "UDM thermodynamics model", Version 7.1, DNV (2013). The UDM Technical Reference Manual as well as documentation for the discharge models and droplet size validation forms part of the Phast (Risk) Technical Reference Documentation included on the Phast 7.1 installation CD.
[10] Hindmarsh, A.C., Brown, P.N., Grant, K.E., Lee, S.L., Serban, R., Shumaker, D.E.e, Woodward, C.S. "Sundials: suite of nonlinear and differential/algebraic equation solvers," in ACM Transactions on Mathematical Software, Vol. 31, No. 3, September 2005, Pages 363–396.
[11] Ooms, G., Mahieu, A. P. and Zelis, F., "The plume path of vent gases heavier than air", 1st Intl. Symp. Loss Prevention and Safety Promotion in the Process Industries, The Hague, Delft, pp. 211-219 (1974)
[12] Webber, D.M., S.J. Jones, G.A. Tickle and T. Wren, "A model of a dispersing dense gas cloud and the computer implementation D*R*I*F*T. I: Near instantaneous release." SRD Report SRD/HSE R586 April 1992, and ". . . II: Steady continuous releases.", SRD Report SRD/HSE R587 (1992)
[13] Businger, J.A., J.C. Wyngaard, Y. Izumi, and E.F. Bradley, "Flux-profile relationships in the atmospheric surface layer", J Atmos. Sci, 28, pp. 181-189 (1971)
[14] Dyer, A.J. and B.B. Hicks, "Flux-gradient relationships in the constant flux layer", Quart. J. Roy. Meteor. Soc, 96, pp. 715-721 (1970)
[15] Lo, A.K. and G.A. McBean, 1978, "On the relative errors in methods of flux calculation", J Applied Meteorology, 17, pp. 1704-1711 (1978)
[16] Abramowitz, M., and Stegun, I.A., "Handbook of mathematical functions", Dover Publications, New York (1972)
[17] Press, W.H., Teukolsky, S.A., Vetterling, W.T., Flannery, B.P., "Numerical recipes in Fortran", Second Edition, Cambridge University Press, Cambridge (1992)
[18] Ooms, G., "A new method for the calculation of the plume path of gases emitted by a stack", Atm. Environment 6 , pp. 899-909 (1972)
[19] Emerson, M. C., "Dense cloud behaviour in momentum jet dispersion", IMA Conference on Mathematics in Major Accident Risk Assessment, Oxford, July (1986)
[20] Emerson, M. C., "A new unbounded jet dispersion model", 5th Intl. Symp. Loss Prevention and Safety Promotion in the Process Industries, Cannes, September (1986)
[21] Emerson, M.C., "A model of pressurized releases with aerosol effects", paper presented at the International Conference on Vapor Cloud Modeling, Cambridge, MA, November 2-4 (1987)
[22] McFarlane, K., "Development of plume and jet release models", International Conference and workshop on modelling and mitigating the accidental releases of hazardous materials, AIChE, CCPS, New Orleans, LA, May 20-24, pp. 657-688 (1991)
[23] McAdams, W.H., "Heat Transmission", McGraw-Hill (1954)
[24] Holman, J.I., "Heat transfer", 5th Ed., McGrawHill (1981)
[25] Witlox, H.W.M., "Technical description of the heavy-gas-dispersion program HEGADAS", External Report TNER.93.032 (non-confidential), Thornton Research Centre, Shell Research, Chester, England (1993)
[26] Van Ulden, A.P., "A new bulk model for dense gas dispersion: two-dimensional spread in still air, in "Atmospheric dispersion of heavy gases and small particles" (Ooms, G. and Tennekes, H., eds.), pp. 419-440, Springer-Verlag, Berlin (1984)
[27] Witlox, H.W.M. and McFarlane, K., "Interfacing dispersion models in the HGSYSTEM hazard-assessment package", Atmospheric Environment, Vol. 28, No. 18, pp. 2947-2962 (1994)
[28] Lees, F.P., "Loss Prevention in the process industries: hazard identification, assessment and control", Volume 1, Second Edition, Butterworth-Heinemann, Oxford (1996)
[29] Bakkum, E.A., and Duijm, N.J., "Vapour cloud dispersion", Chapter 4 in "Methods for the calculation of physical effects – Yellow Book", CPR14E (Part I), SDU, Third Edition (1997)
[30] "Guidelines for use of vapor cloud dispersion models", Second Edition, CCPS, New York (1996)
[31] Ricou, F.P. and Spalding, D.B., "Measurements of entrainment by aximsymmetrical turbulent jets", J. Fluid Mech. 11 (1), pp. 21-31 (1961)
[32] Morton, B.R., Taylor, G.I., and Turner, J.S.,"Turbulent gravitational convection from maintained and instantaneous sources", Proc. R.Soc., Series A, 234, 1 (1956)
[33] Wheatley, C.J., "Model for a two-phase jet of liquefied ammonnia", Report SRD R410, SRD, UK (1987)
[34] Webber, D.M., and Kukkonen, J.S., "Modelling of two-phase jets for hazard analysis", J. Haz. Materials 16, pp. 357 (1990)
[35] Post, L., "Validation of the AEROPLUME model for the simulation of pressurised releases of vapour or two-phase mixtures", Shell External Report TNER.94.014, Thornton Research Centre (1994)

[36] Briggs, G.A., "Plume rise and buoyancy effects", Ch. 8 (pp. 327-366) in Randerson, D. (ed.), "Atmospheric Science and Power Production", Technical Information Center, US Department of Energy, Report DOE/TIC-27601 (1984)
[37] Kamotani, Y. and Greber, I., "Experiments on a Turbulent Jet in a Cross Flow,"Rept.FTAS/TR-71-62,1971, Div. of Fluid, Thermal, and Aerospace Sciences, Case Western Reserve Univ., Cleveland, Ohio; also CR-72893, 1971, NASA.
[38] Yuan, L.L. and Street, R.L. "Trajectory and entrainment of a round jet in crossflow," Physics of Fluids, vol. 10, p. 2323–2335, 9 1998.
[39] Disselhorst, J.H.M., "The incorporation of atmospheric turbulence in the KSLA Plumepath program", Shell Internationale Research Maatschappij B.V., The Hague, AMGR.84.059 (1984)
[40] Havens, J., and Spicer, T.O.,"Development of an atmospheric dispersion model for heavier-than-air mixtures" (DEGADIS model), Vols. 1- 3, University of Arkansas (1985)
[41] Witlox, H.W.M., "Evaluation of the dense gas dispersion program HEGADAS against 2-D wind tunnel experiments", Shell Report TNGR.89.108, Thornton Research Centre (1989)
[42] Britter, R.E., "A review of mixing experiments relevant to dense gas dispersion", IMA Conference on stably stratified flow and dense gase dispersion, April 1986, Chester, Oxford University Press (1988)
[43] McFarlane, K., Prothero, A., Puttock, J.S., Roberts, P.T., and Witlox, H.W.M., "Development and validation of atmospheric dispersion models for ideal gases and hydrogen fluoride", Part I: Technical Reference Manual, Shell Report TNER.90.015, Thornton Research Centre (1990)
[44] McQuaid, J., "Some experiments on the structure of stably-stratified shear flows", Tech. Paper p. 21, Safety in Mines Research Establishment, Sheffield, UK (1976)
[45] Kranenburg, C., "Wind-induced entrainment in a stably stratified fluid", J. Fluid Mech. 145, pp. 253-273 (1984)
[46] Scranton, D.R. and W.R. Lindberg, "An experimental study of entraining, stress-driven, stratified flow in an annulus", Physics Fluids, 26 (5), pp. 1198-1205, May 1983; McQuaid, ed, p. 273 (1985)
[47] Kantha, L.H., O.M. Phillips, and R.S. Azad, "On turbulent entrainment at a stable density interface", J Fluid Mech. 79, 753-768 (1977)
[48] Kato, H. and O.M. Phillips, "On the penetration of a turbulent layer into stratified fluid", J. Fluid Mech., 37, pp. 643-656 (1969)
[49] Deardorf, J.W. and G.E. Willis, "Dependence of mixed-layer entrainment on shear stress and velocity jump", J. Fluid Mech. 115, pp. 122-150 (1982)
[50] Lofquist, K., "Flow and stress near an interface between stratified liquids", Physics of fluids 3 (1960)
[51] Havens, J.A. and T. Spicer, "LNG vapor dispersion prediction with the DEGADIS dense gas dispersion model", Gas Research Institute Topical Report, September (1990)
[52] Cox, R. A. and Carpenter, R. J., "Further development of a dense vapour cloud model for hazard analysis", in "Heavy Gas and Risk Assessment", S. Hartwig ed., (1980)
CRC Press, "CRC Handbook of Chemistry and Physics", 66th edition (1986)
[53] McMullen, R. W., "The change of concentration standard deviations with distance", J. Air Pollution Control Assoc. of America 25, pp. 1057-1058 (1975)
[54] Hosker, R. P., "Estimates of dry deposition and plume depletion over forests and grassland", Physical Behaviour of Radioactive Contaminants in the Atmosphere Symposium, Vienna (1973)
[55] McElroy, J.L. and F. Pooler, "St. Louis dispersion study, Vol. II-analysis", USEPA, NAPCA Publication No. AP-53 (1968)
[56] Turner, D.B., "Workbook of atmospheric dispersion estimates", Public Health Service Publication 999-AP-26, National Air Pollution Control Assoc., Cincinnati, Ohio (1969)
[57] Smith, M., ed., "Recommended guide for the prediction of the dispersion of airborne effluents", Am. Soc. of Mech. Eng., NY (1968)
[58] Hanna, S.R., Briggs, G.A., and Hosker,R.P., "Handbook on atmospheric dispersion", DoE/TIC-11223 (1982)
[59] Pasquill, F., and Smith, F.B., "Atmospheric diffusion", 3nd ed., Ellis Horwood Ltd., Chichester (1983)
[60] Briggs, G.A., "Diffusion estimates for small emissions", ATDL Contribution File No. 79, National Oceanbic and Atmospheric Administration, Atmospheric Turbulence and Diffusion Laboratory, ATDL Contribution File No. 87 (draft), National Oceanic and Atmospheric Administration, Oak Ridge
[61] Li, X.Y, Leijdens, H., and Ooms, G., "An experimental verification of a theoretical model for the dispersion of a stack plume heavier than air", Atmospheric Environment 20 (1986)
[62] Havens, J., "A dispersion model for elevated dense gas jet chemical releases". Volume 1. Theory Guide, US Environmental Protection Agency, Research Triangle Park, North Carolina, PB88-20239, April (1988)
[63] Linden, P.F. and Simpson, J. E., "Modulated mixing and frontogenesis in shallow seas and estuaries," Continental Shelf Research, vol. 8, no. 10, pp. 1107–1127, Oct. 1988, doi: 10.1016/0278-4343(88)90015-5.
[64] Witlox, H.W.M. "Technical description of the HEGADAS model," Chapter 7A in HGSYSTEM 3.0 Technical Reference Manual, http://www.hgsystem.com/tech_ref/Contents.htm
[65] "TNO Yellow book", 2nd edition, TNO, The Netherlands (1992)
[66] EPA, "RMP consequence analysis guidance" (1996)
[67] Ermak, D.L., "Unpublished notes on downwind spreading formulation in finite-duration release version of SLAB", Lawrence Livermore National Laboratory, California (1986)
[68] Ermak, D.L., "User's Manual for SLAB: an atmospheric dispersion model for denser-than-air releases, Lawrence Livermore National Laboratory, Livermore, California, February 1989
[69] Witlox, H.W.M., McFarlane, K., Rees, F.J., and Puttock, J.S., "Development and validation of atmospheric dispersion models for ideal gases and hydrogen fluoride", Part II: HGSYSTEM program user's manual, External Report RKER.90.016 (non-confidential), Thornton Research Centre, Shell Research, Chester, England (1990)
[70] Witlox, H.W.M., "The HEGADAS model for ground-level heavy-gas dispersion, II. Time-dependent model", Atmospheric Environment 28 (18), pp. 2933-2946 (1994)
[71] Chatwin, P.C., "The dispersion of a puff of passive contaminant in the constant stress region", Quart. J. Royal Meteor. Soc. 94, pp. 350-360 (1968)
[72] Witlox, H.W.M. and Harper, M., "Improved link between pool evaporation model PVAP and dispersion model UDM", Report C2, Contract 96501233/98505400, Phase III of droplet-modelling joint industry project, DNV, London (2008)
[73] Committee for the Prevention of Disasters. "Guidelines for Quantitative Risk Assessment. – Purple Book, CPR 18E, Den Haag, SDU (1999)
[74]Witlox, H.W.M., "UDM model for pressurised instantaneous releases", Part of Phast 8.0 technical documentation, DNV (2016)
[75] Pattison, M.J., "E.C. Cloud Project – Initial stages of release", Draft note, Department of Chemical Engineering and Chemical Technology, Imperial College, London (1994)

[76] Schmidli, J., The initial phase of sudden releases of superheated liquid, Ph.D. Thesis, ETH, Zurich (1993)
[77] Landis, J.G., R.E. Linney, B.F. Hanley, "Dispersion of Unsteady State Jets", J. Loss Prev., submitted July 1993
[78] Maurer, B., H.Schneider, K.Hess and W.Leuckel, "Modellversuche zur flash-entspannung, atmosphärischen vermischung und deflagration von flüssigassen nach deren freisetzung bei behälterzerknall." International seminar on extreme load conditions and limit analysis procedures for structural reactor safeguards and containment structures (ELCALAP), Berlin, 8-11 September 1976
[79] Maurer, B., Schneider, H., Hess, K. and Leuckel, W., "Modelling of vapour cloud dispersion and deflagration after bursting of tanks filled with liquefied Gas", Int. Loss Prevention Symposium, Heidelberg, 1977
[80] Opschoor, G., "Methods for the calculation of the physical effects of the escape of dangerous material", Chapter 5, TNO (1979)
[81] Eisenklam, P., Arunachalam, S.A., Weston J.A., "Evaporation rates and drag resistence of burning drops", Eleventh Symposium on Combustion at Combustion Institute, Pittsburgh, PA, pp. 715-728 (1967)
[82] Kunsch, J.P. and Fanneløp, T.K., "Unsteady heat-transfer effects on the spreading and dilution of dense cold clouds", J. of Haz. Materials 43, pp. 169-193 (1995)
[83] Wilson, D.J., "Concentration fluctuations and averaging time in vapor clouds", CCPS, New York (1995)
[84] Crabol, B., "Dispersion Atmospherique methodes de calcul developpees a l'IPSN" (1995)
[85] L. Post (editor), "HGSYSTEM 3.0 Technical Reference Manual", External Report TNER.94.059 (non-confidential), Thornton Research Centre, Shell Research, Chester, England (1994)
[86] J. M. Morris, "Experimentation and Modeling of the Effects of Along-Wind Dispersion on Cloud Characteristics of Finite-Duration Contaminant Releases in the Atmosphere," University of Arkansas, 2018.
[87] Roberts, P.T. and Hall, D.J., "Wind-tunnel simulation. Boundary layer effects in dense gas dispersion experiments", J. Loss. Prev. Process Ind., Volume 7, No. 2 (1994)
[88] Webber, D.M., Jones, S.J. and Martin, D., "Modelling the effects of obtstacles on the dispersion of hazardous materials", Proceedings of Int. Conf. on modeling and mitigating the consequences of accidental releases of hazardous materials, pp. 379-404 (1995)
[89] Irwin, J. S., "A Theoretical Variation of the Wind Profile Power Law Exponent as a Function of Surface Roughness and Stability", Atmos. Environment 13, pp. 191-194 (1979)
[90] Crutcher, H. L., "Monitoring, Sampling and Managing Meteorological Data", in D. Randerson (ed), "Atmospheric Science and Power Production", US Dept. of Energy, DOE/TIC-27601 (1984)
[91] Randerson, D., "Atmospheric Boundary Layer", in D. Randerson (ed), "Atmospheric Science and Power Production", US Dept. of Energy, DOE/TIC-27601 (1984)
[92] Pasquill, F., and F. B. Smith, "Atmospheric Diffusion", 3rd ed., Ellis Horwood (1983)
[93] Panofsky, H. A., and J. A. Dutton, "Atmospheric Turbulence: Models And Methods For Engineering Applications", John Wiley & Sons (1984)
[94] Clarke, R. H., "A Model for Short and Medium Range Dispersion of Radionuclides Released to the Atmosphere", National Radiological Protection Board report NRPB-R91, Sept 1979
[95] Hoot, T.G., Meroney, R.N. and Peterka, J.A., "Wind tunnel tests of negatively buoyant plumes, Rep. CER73-74TGH-RNM-JAP-13, Colorade State Univ., Fort Collins, CO (1973)
[96] Kamotani, Y. and Greber, I., "Experiments on a Turbulent Jet in a Cross Flow,"Rept.FTAS/TR-71-62,1971, Div. of Fluid, Thermal, and Aerospace Sciences, Case Western Reserve Univ., Cleveland, Ohio; also CR-72893, 1971, NASA.
[97] Kamotani, Y. and Greber, I., "Experiments on a Turbulent Jet in a Cross Flow," AIAA Journal, vol. 10, p. 1425–1429, 11 1972
[98] Yuan, L.L. and Street, R.L. "Trajectory and entrainment of a round jet in crossflow," Physics of Fluids, vol. 10, p. 2323–2335, 9 1998.
[99] Mahesh, K. "The Interaction of Jets with Crossflow," Annual Review of Fluid Mechanics, vol. 45, p. 379–407, 1 2013.
[100] Muppidi, S. and Mahesh, K. "Direct numerical simulation of passive scalar transport in transverse jets," Journal of Fluid Mechanics, vol. 598, p. 335, 2008
[101]Gifford, F.A., "Turbulent diffusion typing schemes: a review", Nuclear Safety, Vol. 17, No. 1 (1976)
[102] Hanna, S.R., and Britter, R.E., "Wind flow and vapour cloud dispersion at industrial and urban sites", CCPS, New York (2002)